Solar Variability and Planetary Alignments

Philippa Anne Mary Berry

Submitted for the degree of Doctor of Philosophy

The University of Aston in Birmingham

May 1984

Acknowledgements

I wish to thank Dr. C.J. Brookes for his supervision and guidance. Of the many others who have helped me, my especial thanks go to Dr. D. Wilson of the Mathematics Department, and Dr. A. Sinclair of The Royal Greenwich Observatory, for their advice and encouragement.

I also wish to thank the staff of The Royal Greenwich Observatory for the provision of planetary coordinates and the staffs of Cambridge Observatory and R.A.E. Farnborough for the use of library facilities. I am grateful to Mrs. S. Puar for typing this thesis.

This work was supported by a research studentship funded by The University of Aston in Birmingham.

To my family and friends.

List of Contents

List of Tables and Figures

INTRODUCTION

Many years after 'blemishes' were first observed on the solar disc by Galileo, Fabricius and Scheiner in 1610, it was realised that the number of such 'sunspots' was not constant, but varied in a cyclic manner with a mean period of about eleven years (Schwabe, 1844). In addition it was established that, in each hemisphere, the average latitude of the groups of sunspots was found to exhibit a linked periodic variation. Modern techniques have revealed the existence of intense local magnetic fields, of which the sunspots are but one manifestation (e.g. Lust, 1965; White, 1977); these and other related features are now monitored regularly.

A major constraint on research in this field is the finite length of the sunspot records. In 1848, Wolf devised a formula for estimating the fraction of the sun's disc obscured by spots at any time, the relative sunspot number, R. Following this, a careful correlation of all available sunspot data by Wolf (1868) and more recently by Waldmeier (1961) has yielded a systematic index of solar activity from 1700 onwards. The low early counts, and the long interval between the discovery of sunspots and the identification of their cyclic pattern of activity, have been attributed by Maunder (1907) to a real dearth of sunspots between 1645 and 1715. The existence of this 'Maunder Minimum' is at present under debate (Eddy, Gilman, and Trotter, 1976; 1977; Eddy, 1977; Hindley, 1977; Ding and Chang, 1978; Weiss and Weiss, 1979; Cullen, 1980).

Because of the paucity of early sunspot records (Wittmann, 1978) there is much interest in connecting the cycle with other Earth based recorded

events (Cole, 1975; Willis, 1976; Pittock, 1978) ranging from aurorae (Schove, 1955; Link, 1977; 1978) to tree rings (Fritts, 1972; 1976; Epstein and Yapp, 1976; Mitchell, Stockton and Meko, 1978; Sonett and Suess, 1984), glacial deposits (Agterber, 1969; Fairbridge and Hillaire-Marcel, 1977; Hibler, 1979) and others (Mock, 1976; Povinets, 1977; Lo and Li, 1978). The most widely accepted correlation is with records of aurorae, but there are conflicting interpretations of the data; Schove (1955) and others find support for the existence of the Maunder Minimum whereas Ding and Chang (1978) and Schroder (1979) do not.

The most comprehensive series of solar observations presently available is that of Waldmeier (1961). Many statistical analyses of these numbers have been undertaken (e.g. Yule, 1927; Cohen and Lintz, 1974; Lomb and Anderson, 1980). Periodicities other than the eleven year variation have been identified in the Waldmeier sunspot series by most of the more recent analyses (e.g. Cole, 1973; Lomb and Anderson, 1980) although the resulting estimates of these periods vary considerably.

There is intense controversy over possible mechanisms governing the variation. Simple dynamo models first developed for magnetic 'A' stars (Babcock and Babcock, 1955; Babcock, 1961) and refined into sophisticated models of the solar interior (e.g. Leighton, 1969; Parker, 1964) still do not adequately predict solar activity (Stix, 1981; de Csada, 1981). With an increase in number and type of solar observations, new problems associated with the use of existing dynamo theories have arisen; this has led to the development of 'flux tube models' as an alternative explanation of solar magnetism (e.g. Meyer et al., 1974; Balligooijen, 1982).

Because of the importance of predicting the sunspot cycle, statisticians have evolved several empirical approaches to the problem in an attempt to forecast sunspot behaviour and, by finding a good

numerical approach,to cast light on the physical cause of the sunspot cycle. Some authors have favoured a model in which no true periodic variation is present, each cycle being regarded as a fresh outburst starting at a time T_0 of the order of eleven years, and described by one member of a specified family of curves $f(t)$, $t \leq T_0$ (e.g. Stewart and Eggleston, 1940; Morris, 1977); the resulting impulse model consists of the superposition of independent pulses. Examination of the sunspot cycle by Dicke (1978; 1979) did not reveal the large random walk predicted on the basis of an outburst model; hence the possibility was suggested of an 'internal clock' within the sun, correcting at intervals the free-running solar cycle (Dicke, 1977; 1979; Lomb and Anderson, 1980; Bray 1980). Autoregressive models basing future activity on functions of past behaviour are also often considered by those favouring a true cycle (e.g. Yule, 1927; Morris, 1977). Limited forecasting success results from these several approaches; to date, statistical forecasting of the sunspot cycle does not accurately predict the variation (de Meyer, 1981).

Because of the fairly close period match of Jupiter (11.86 years) to that of the solar cycle (~ 11.1 years) there has been interest in connecting parameters of motion of the giant planets with sunspot activity for some time (e.g. Brown, 1900; Anderson, 1954; Ferns, 1969; Kozhevnikov, 1976A; B; C). Sets of periodicities detected in the sunspot cycle by statistical analyses are frequently used for comparison, and good correlations have been obtained with various synodic periods of the outer planets. The motion of the centre of mass of the solar system with respect to the sun has also been investigated (e.g. José, 1965; Dauvillier 1976) and a periodicity of about 180 years is generally reported and identified with a similar long sunspot period (e.g. José, 1965; Cole, 1973).

Another possibility which has been considered is the contribution of the inner planets by means of tidal action at the sun surface, with tidal force envisaged as a trigger to sunspot activity (e.g. Schuster, 1911; Smythe and Eddy, 1977; Hantzche, 1978). Among the several approaches to this problem, tidal effects at sequences of planetary conjunctions have yielded very close period matches with the eleven year cycle (Wood, 1972; Wood, 1975). The magnitude of tidal forces at the sun surface caused by three or four planets have also correlated well with sunspot and flare appearance (e.g. Blizard, 1968; Ambroz, 1971). The Maunder Minimum is also suggested as a test for planetary theories, with the cessation of solar activity in this period seen as refuting the possibility of a connection (e.g. Smythe and Eddy, 1976).

A number of problems thus exist with respect to the sunspot cycle itself. Before being able to investigate possible planetary influence on the sunspot cycle, it is necessary to establish the reliability of the various sunspot and auroral databases. Of particular interest is the time around the Maunder Minimum; it must be determined whether there is sufficient evidence of activity during this period to regard the cycle as continuous throughout this time. If this were so, then the possibility of long term effects (not necessarily periodic in character) modulating in amplitude the eleven year cycle could not be excluded.

Because the only direct indicator of solar activity available for a considerable timespan is the Waldmeier sunspot series, the reliability of this index must be assessed, with particular reference to the early sunspot counts. A number of statistical analyses have reported the existence of periodicities in the Waldmeier sunspot records other than the eleven year variation; however, comparison of source literature reveals that different statistical techniques often yield conflicting

values. One common factor is the use by researchers of smoothed sunspot numbers, with the precision of the output data often quoted as greater than the accuracy of the input information. It will thus be necessary critically to assess existing research, and if possible conduct a more rigorous statistical examination of the available data than has previously been undertaken, using spectral analysis techniques. The results of such an analysis could then be used to evaluate the significance of research connecting frequencies of planetary motion to short period sunspot variations.

Existing research concerning a possible planetary origin for the sunspot cycle has generally been restricted to the three or four planets with greatest effect; Jupiter, Earth, Venus and Mercury for tidal work, and the giant planets for motion of the solar system centre of gravity. As, particularly in the case of tidal motion, other planets can exert an appreciable effect, it must be determined what level of precision can be associated with existing approaches to the problem. One direction of improvement is the use of an accurate nine planet solar system model, removing the common assumptions of coplanar motion, and improving on the first order approximations universally applied in existing work to the tidal equations. Since in some of the existing research it is difficult to assess the sensitivity of generated patterns to the actual parameters of planetary motion, and hence to determine the likelihood of a 'real' connection with the sunspot cycle, it may be useful to introduce a control system with a similar but not identical planetary configuration. It is intended to consider several different approaches, particularly those positive results outlined previously. Because researchers in this field have generally employed subjective criteria for evaluation of results, it is also intended to develop statistical analysis techniques to avoid the possibility of

unconscious bias.

If a possible connection is established, it must be considered in what way such a mechanism could operate on the birth and development of sunspots. Of interest in this context might be the recently detected solar oscillations, with their implications for the traditional dynamo theories of a quiet sun and the alternative flux tube theories. Finally, comprehensive comparison tests of any planetary theory against observation are necessary to complete such an investigation, although it is realised that such a large task may be outside the scope of this research project.

SECTION 1

INVESTIGATION OF LONG-TERM SUNSPOT AND AURORAL RECORDS

Before proceeding to examine the detailed sunspot records of Waldmeier (1961), it was thought necessary to establish the reliability of the various databases available, and if practicable to utilise suitable methods of analysis to search for periodic effects in the long - running auroral and sunspot records.

I.I Sunspot Databases

Since the first compilation of sunspot records (Wolf, 1868) there has been interest in detecting patterns in the data other than the clearly visible eleven year 'sunspot cycle'. Gleissberg, in 1944, proposed that the eleven year variation was governed by an eighty year cycle, and numerous subsequent papers have supported the existence of such an effect (Gleissberg, 1962; 1973; Brown, 1976; Vitinsky, 1978; Kopecky, 1978; Gleissberg and Damboldt, 1979).

More recently, detailed analyses of the Waldmeier sunspot numbers have indicated the presence of a number of different periodicities which are suggested to have modulated the amplitude of the eleven year cycle; for example application of Time Series Analysis (Cole, 1973) indicated that the 'seven cycle variation' was in reality a composite of an 88 and a 59 year periodicity. This conclusion was supported by Berdichevskaya (1976) and Lomb and Anderson (1980) who found ninety and fifty-five year cycles using a similar technique.

The small amount of sunspot data available limits the detection of longer period variations. Nevertheless, Jose (1965) proposed a 179 year period, subsequently found by Cohen and Lintz (1974). With the addition to the sunspot records of auroral and other data, other researchers have suggested the existence of an 180 to 200 year cycle (Bonov, 1973; Bray, 1980). Also, an 'ultralong cycle' of about a thousand years, first proposed by Gleissberg (1962) as modulating the eighty to ninety year cycle, has been found by Henkel (1972) as a periodicity of nine hundred years, and by Vitinsky (1978) as a six hundred year cycle.

Several other indices of sunspot activity exist. Heliographic observations at the Royal Greenwich Observatory have yielded estimates of that area of the solar disc covered by spots, from 1874 to 1976. Other related solar phenomena such as flares and prominences are now monitored daily, but such information is only available over the last few cycles (Legrand and Simon, 1981).

Comparison of the Waldmeier series with these more detailed observations indicates that it is quite a good indicator of the level of solar activity (Xanthakis, 1973; Mayaud, 1977; Vitinsky, 1979; Kopecky and Kuklin, 1980), although peak numbers may be underestimated (Xanthakis, 1973). However, inhomogeneities are found to exist between the various series examined (Vitinsky, 1979; Kopecky and Kuklin, 1980). Mayaud (1977) advises caution in estimating long term periodicities using Waldmeier's early data. This conclusion is supported by Vitinsky (1979).

Clearly, the most reliable long term record of the level of solar activity is the Waldmeier sunspot series. Whilst the Greenwich data is more comprehensive, the limited timespan curtails its usefulness in investigating the long-term behaviour of the sunspot cycle. However, it is evidently worth examining the auroral and giant sunspot records for additional information about possible long period variations in solar activity.

1.2 Auroral Databases

Due to the highly significant correlation known to exist between solar activity and auroral frequency (Xanthakis, 1965; Eddy, 1978) it is possible to use the latter for the determination of solar cycles. Whilst solar observations were until recently restricted to a limited number of astronomers, auroral observations were accessible to a large part of the population of Europe and the Orient, and consequently were reported in numerous publications (Link, 1962; 1964). Various catalogues have been compiled (Fritz , 1928; Kanda, 1933; Seydl, 1954) the most comprehensive and widely used being that of Schove (1955). Combining auroral records with 'naked-eye' sunspot observations and the Waldmeier sunspot tables he produced a list of projected maxima and minima dates and estimated intensities, from 649 BC to the present day. His main assumptions in deducing the pattern of sunspot activity on the basis of Waldmeier's records over $2\frac{1}{2}$ centuries, were that the time between successive maxima lay always in the interval of 8 to 16 years, and that there were nine maxima in every hundred years. Of neccessity, many dates of minima were interpolated, according to the strength of the neighbouring maxima, using characteristics of sunspot curves deduced from Waldmeier's sunspot series.

From this data Schove inferred a number of empirical formulae for the loose prediction of the long term behaviour of solar activity. Further, the existence of the 80 year period postulated by Gleissberg (1944) was confirmed by him as a 78 year cycle, and a longer cycle of 160 to 170 years was suggested to have been affecting activity for the years since 1510. The mean length of the principal sunspot cycle was determined by Schove as 11.1 years.

This work is widely referenced as a database for many aspects of the solar variation. However, it is often not appreciated that many assumptions were made prior to the compilation of the tables, affecting the

validity of Schove's conclusions. In particular, the estimate of an 11.1 year period, whilst possibly correct, arises inevitably from the assumption of nine cycles per century; and whilst an effect modulating the intensity of maxima over seven cycles may tentatively be traced in the data, evidence for the existence of a longer term periodicity of 160 to 170 years must be regarded as slight.

Recently, further work has been undertaken in this area. Bray (1980) has published a 'Solar Index' from 522 BC to AD 1968, a compilation of several earlier papers, recombining the sunspot and auroral data of Schove (1955; 1962) to give an estimate similar to the 'sunspot-relative' number of Waldmeier. This is compared with data from other sources, including the recently completed oriental catalogue of Keimatsu (1976). The results of this study support the hypothesis of an 'internal clock' (Dicke, 1978; 1979), and indicate the persistence of solar activity through the Maunder Minimum, and the earlier minima indicated by Eddy (1977).

Considerable research into 16th and 17th century records of sunspots and aurora by Link (1962; 1964; 1977A; 1977B; 1978) has led to a comprehensive index of solar activity in this period. Over 400 auroral observations are tabled (Link, 1962; 1964; 1977A; 1977B), indicating, in contrast to Eddy et al. (1976; 1977), that reports of aurora persisted throughout the period AD 1550 to AD 1700. This conclusion is strengthened by the sunspot records collected by Wolf between 1856 and 1883, which include series of observations of the 'newly discovered phenomenon' by Galileo and Hevelius. Whilst cautious interpretation of such early records is necessary (Eddy, 1977; Link, 1978), the sources collated by Wolf (1868; 1883) do indicate intermittent observations of sunspots throughout the 17th century (c.f. Weiss and Weiss, 1979).

1.3 Giant Sunspots and Other Databases

Using several hundred observations (mainly Chinese) of giant sunspots, Wittmann (1978) has traced the phase of the 11 year sunspot cycle back to 466 BC, deducing a mean period of 11.135 years. Auroral observations are discarded as 'uncertain,' and the results are noted to disagree with those of Schove, being 180^{o} out of phase around the epochs AD 1300 and AD 1080. However, it is known that giant sunspots occur occasionally near to sunspot minima, and frequently in the years surrounding dates of maxima (Smith and Smith, 1963; Lust, 1965) . This limits the effectiveness of the method in determining dates for 'ancient' sunspot cycles. This, together with the limited amount of data involved,reduces the accuracy of the giant sunspot database.

As has previously been mentioned, many other earth-based phenomena have been cited as linked to the sunspot cycle. Several such 'indicators' have been used to trace epochs of high and low activity for thousands of years, in geological (Fairbridge et al., 1977), climatological (Mitchell et al.,1978) and biological (Epstein and Yapp, 1976) data. All such correlations involve many assumptions about the links between sunspots and atmospheric weather conditions, which are known to be complex (Roberts, 1978; Larson and Kelly, 1978). Disparities exist between these various 'sunspot epoch' studies (Eddy, 1977; Pittock, 1978),even those utilizing similar techniques, for example in tree ring analysis (Fritts, 1976; Epstein and Yapp, 1976; Eddy, 1977). In addition, at present such research is only able to indicate parameters of the solar activity sustained over hundreds of years. Because of the tenuous nature of such indices, it does not appear possible at present to deduce useful information about the solar cycle. Future work may enable such methods to be used, which would allow the solar activity to be traced back reliably over a far longer timespan than is possible at present.

1.4 Investigation of the Maunder Minimum

A good period for the comparison of various data sources is that immediately preceding the start of Waldmeier's tables and bracketing the Maunder Minimum, i.e. the 17th century. Here, we have not only the long-running sunspot and auroral series (e.g. Schove, 1955; Wittmann, 1978; Bray, 1980), naturally more comprehensive in this comparatively modern period, but also results of work specifically undertaken to explore the existence of the Maunder minimum (Eddy, 1976 ; 1977; Link, 1978; Gleissberg, 1979; Weiss and Weiss, 1979) together with the first telescopic sunspot observations (Waldmeier, 1961).

Figure 1.41 shows a comparison of 5 such sources for the period AD 1500 to AD 1700.

a) Schove's auroral series, with his estimates of time and level of maximum activity in each cycle, and his times of minima.

b) Link's auroral series, with his 'Spectral Index' normalized to the Wolf Sunspot No. R (S.I. = 1 at R = 50, S.I. = 2 at R= 100, etc.).

c) Bray's combined sunspot and auroral series, using the 'mean times of maxima' rather than his original S.I. dates, which were adopted from Schove (1955).

d) Waldmeier dates of maxima and minima from 1600 onwards.

e) Wittmann dates of maxima.

Note that the dates of maxima given by Bray and Waldmeier are linearly interpolated from accompanying minima dates, also that from AD 1600 Wittmann has adopted the results of Waldmeier, slightly smoothed.

The most comprehensive source of auroral data is clearly that of Link (1978). If a 'missing cycle' is assumed to exist with maximum around AD 1590-1595, following the general pattern of sunspot cycle duration of 8 to 16 years (Schove, 1955; Waldmeier, 1961) then the mean period present is 10.54 years (c.f. 11.1 years assumed by Schove). Figure 1.41. shows the effect of

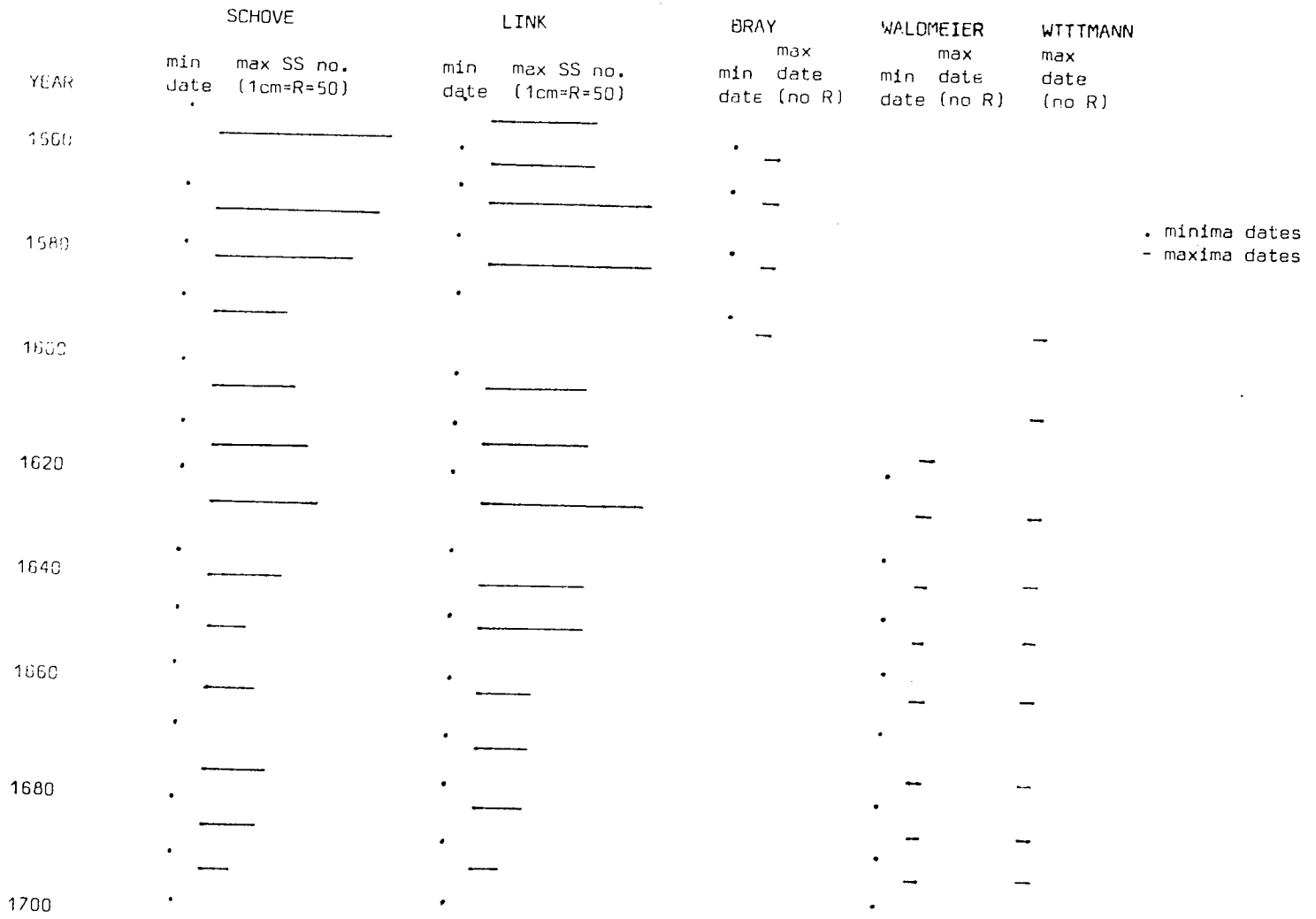

Figure 1.41 Sunspot and auroral sources for period AD 1550 to AD 1700

this assumption, as cycles (a) and (b) shift into phase at AD 1580 - AD 1660. Link has not made any *a priori* assumptions about existing periodicities, and uses a wide pool of data, thus his series must be regarded as more reliable than that of Schove for this period. The postulated existence of an 80 year periodicity, however, is not well supported by the data.

It is evident from figure 1.41 that there is disparity between the auroral series of Link (1978) and the sunspot number series since AD 1675. It is suggested (Eddy, 1977; Link, 1978) that a low level of solar activity combined with a lack of systematic observations of the sun renders the early sunspot records unreliable. Whilst this is evidently so, it should also be noted that the relationship between the sunspot and the incidence of aurora is complex. In particular, it is generally understood that the cycles of activity may not be in phase, and that a lag of 2-4 years can occur between the dates of sunspot and auroral maxima (Smith and Smith, 1963; Xanthakis, 1965; Eddy, 1978). It would thus appear best to regard the mean cycle length as relevant, rather than actual times of maxima, in all auroral records. Similarly, the records of giant sunspots, assigning dates of sunspot maxima to times of greatest incidence of giant spots, must be interpreted with care, as previously mentioned.

The hypothesis that the Maunder minimum represents a cessation of the sunspot cycle rather than a period of fairly low activity rests on the absence of auroral and sunspot observations during the years AD 1645 - 1715 (Maunder, 1907; Eddy et al., 1976; 1977; Weiss and Weiss, 1979). Whilst the conflicting data renders it difficult to define epochs of high and low activity with any precision, there is sufficient data available to show continued sunspot activity through the period of the Maunder minimum, and to establish that the sunspot cycle continued uninterrupted, probably at a fairly low level. Hence the possibility must be investigated that long-term effects (not necessarily periodic) are modulating the overall level

of activity.

1.5 Methods of Analysis for long-term databases

For an initial examination of such records, a graph similar to figure 1.41 was drawn for

a) Schove auroral data

b) Bray original S.I. and mean dates of maxima

c) Wittmann dates of maxima.

The results are presented in figure 1.51, and it is clear that the series are not in agreement. Whilst the eye tentatively superimposes long-term variations on the data within each series, no overall pattern is clear. For better examination and comparison there is recourse to statistical methods.

The difficulty in applying statistical methods to data of this type is that the function 'R' is sampled at irregular intervals. Techniques such as spectral analysis assume regular sampling. In many cases, the data can be interpolated by various techniques (Percy, 1977; Meisel, 1978) to equidistant time points for analysis. The alternatives are folding and sorting analyses, cumbersome procedures for use when searching for an unknown periodicity (Jenkins and Watts, 1978).

As the character of individual sunspot cycles is not known for this data, interpolation is not feasible. Hence, previous examinations of the data of Schove (1955) have used only simple techniques, often with subjective criteria (Henkel, 1972; Gleissberg, 1973). Recently, however, a technique has been developed for fitting Fourier components to randomly spaced data, for use in x-ray astronomy where regular sampling is not easily achieved (Ponman, 1981; 1982A; 1982B). Several approximations are made in this approach, with only one frequency fitted at a time and the components themselves being fitted separately. However, the effect of this is minimal except at very low frequencies. As the spectral estimate is produced

Figure 1.51 Sources for long-period auroral and sunspot data AD 0-600

piecewise, it is not a fit as a whole to the data, and so cannot be used to reconstruct input information.

Consider a set in time t of N stationary data points f(t), of zero mean, comprising a random noise term N(t) plus a periodic signal of frequency ν':

$$f(t) = \mathcal{N}(t) + \sum_{m=1}^{\infty} \left[\alpha_m c^{(m)}(t) + \beta_m s^{(m)}(t) \right] \qquad 1.5(I)$$

where $c^{(m)}(t) = \cos(2\pi \nu^{(m)}(t))$

$s^{(m)}(t) = \sin(2\pi \nu^{(m)}(t))$

and the α_m, β_m, $(m = 1 \ldots \infty)$ are constants.

Consider also, the function $A(\nu) = \sum_n f_n c_n / \sum_n c_n^2$; 1.5(II)

if N is large and $1/\nu \ll t_n - t$ then $\sum_n c_n^2 \simeq N/2$.

Terms in $A(\nu)$ of the form $\Sigma \sin(a) \cos(b)$ and $\Sigma \cos(a) \cos(b)$ will be small when compared with N/2, as will the noise term. Thus, $A(\nu)$ will be small unless the frequency ν is present in the data, when a large term $\sum_n \alpha_m c_n^{(m)} c_n^{(m)}$ occurs, and $A_\nu \simeq \alpha_m$. Thus $A(\nu)$ may be used to estimate the cosine amplitude. Similarly, a function $B(\nu) = \sum_n f_n s_n / \sum_n s_n^2$ will approximately estimate the sine amplitude.

How closely the resulting power spectrum $P(\nu) = A^2(\nu) + B^2(\nu)$ approximates the true spectrum will depend on the data spacing and nature of the power spectrum.

The standard deviation of $P(\nu)$ due to noise from data weighted by factor $1/\sigma_n^2$ may be found from

$$\tilde{\varepsilon}(\nu) = 2\sqrt{\frac{A^2(\nu)}{C_\nu} + \frac{B^2(\nu)}{S_\nu} - \frac{1}{2C_\nu^2} - \frac{1}{2S_\nu^2}} \qquad 1.5(III)$$

where $C_\nu = \sum_n c_n^2/\sigma_n^2$, $S_\nu = \sum_n s_n^2/\sigma_n^2$.

However, the bias b and variance σ_p introduced into the spectral estimate by imperfect cancellation of cross terms are given by

$$b = \frac{4\sum_n 1/\sigma_n^4}{(\sum_n 1/\sigma_n^2)^2}\,\sigma_f^2 \;;\; \sigma_p^2 \leqslant \frac{16\sum_n 1/\sigma_n^4\,\sigma_f^2.P(\nu)}{(\sum_n 1/\sigma_n^2)^2} \qquad 1.5(IV)$$

which for randomly spaced data may be greater than the error introduced in (III).

Ponman (1981; 1982A; 1982B) indicates that, for semi-regular sampling interval Δt the bias and variance of(IV) are reduced by a factor of ~N/4, and thus $\tilde{\varepsilon}(\nu)$ is the greater, if certain conditions are fulfilled, i.e. if $N >> \frac{8\sigma_f^2 \sum_n 1/\sigma_n^4}{\sum_n 1/\sigma_n^2}$ where $\sigma_f^2 = \frac{1}{N}\sum_n f_n^2$.
The main problem with any such method is aliasing. However, whilst reflection about the Nyquist frequency occurs as for conventional Fourier analysis, the height of the reflected peak is reduced. Similarly, smaller satellite peaks may still be observed around a major peak in the spectrum, but their heights will be diminished more than in a 'normal' Fourier spectrum. Peaks will have a finite width, as a frequency close to ν' may still give quite a good fit to the data. All these point must be considered in the application of such an analyzing tool.

1.6 Analysis of Schove Auroral Data

Initially, data was selected from 220BC, at which point the series is fairly continuous and most maxima have an estimated R, to AD 1700 after which time Schove adopted data from Waldmeier (1961), thus giving about 1920 years of data. Hence the longest period which could realistically be detected (Ponman, 1981) is 480 years. For a reliable estimate, the limit was set at ν_L = .003c/yr, a period of just over 300 years, as it was considered that, given uncertainties in the early data, summing over only four cycles was insufficient. A typical sampling interval was effectively imposed by Schove (1955) as 11.1 years, thus the Nyquist frequency ν_n = .045c/yr. Accordingly, the high frequency limit was set at .040c/yr. Peak width 1/T

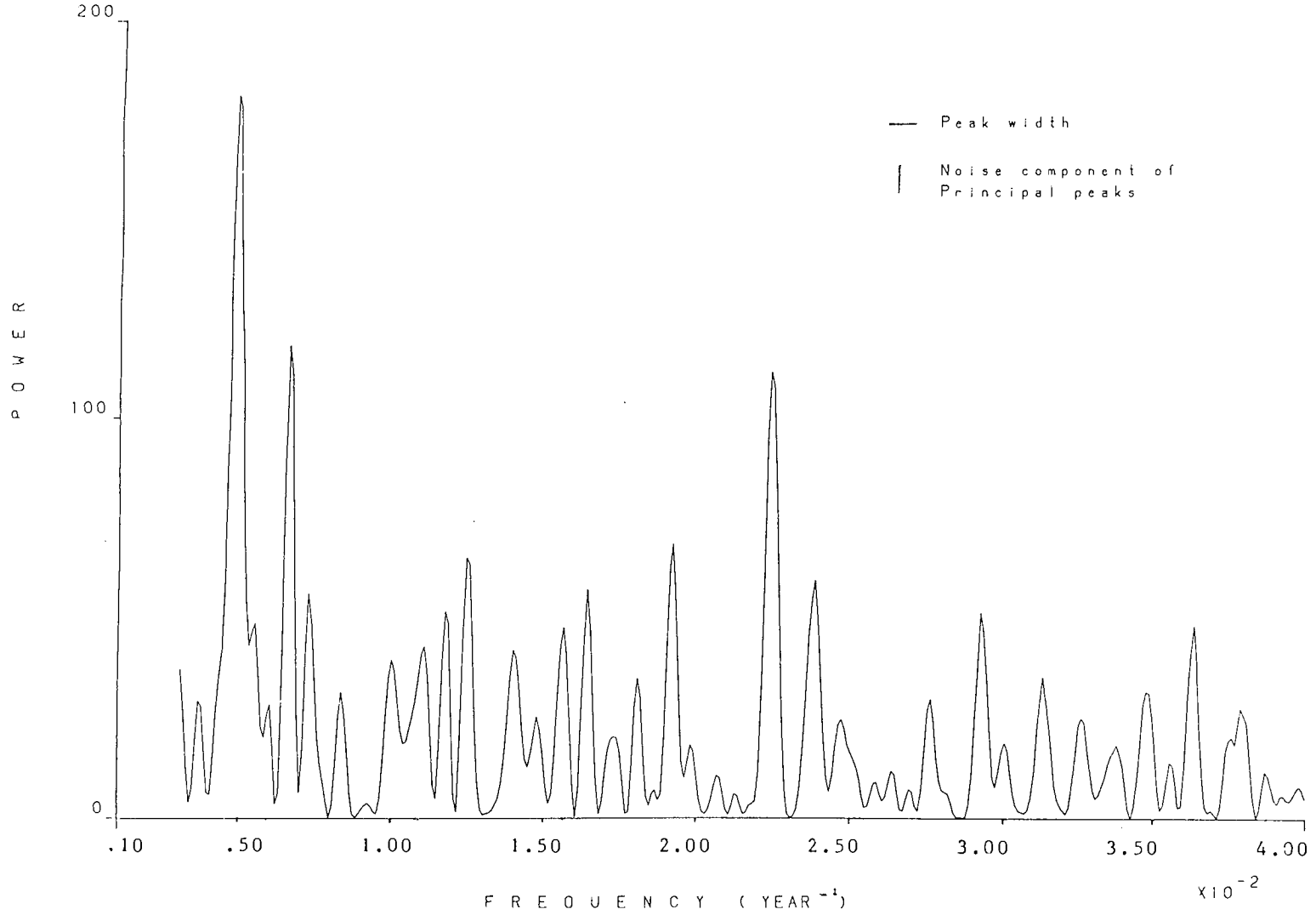

Figure 1.61 Spectrum of Schove Data 220BC - AD1700

Figure 1.62 Alias Peaks for Schove data

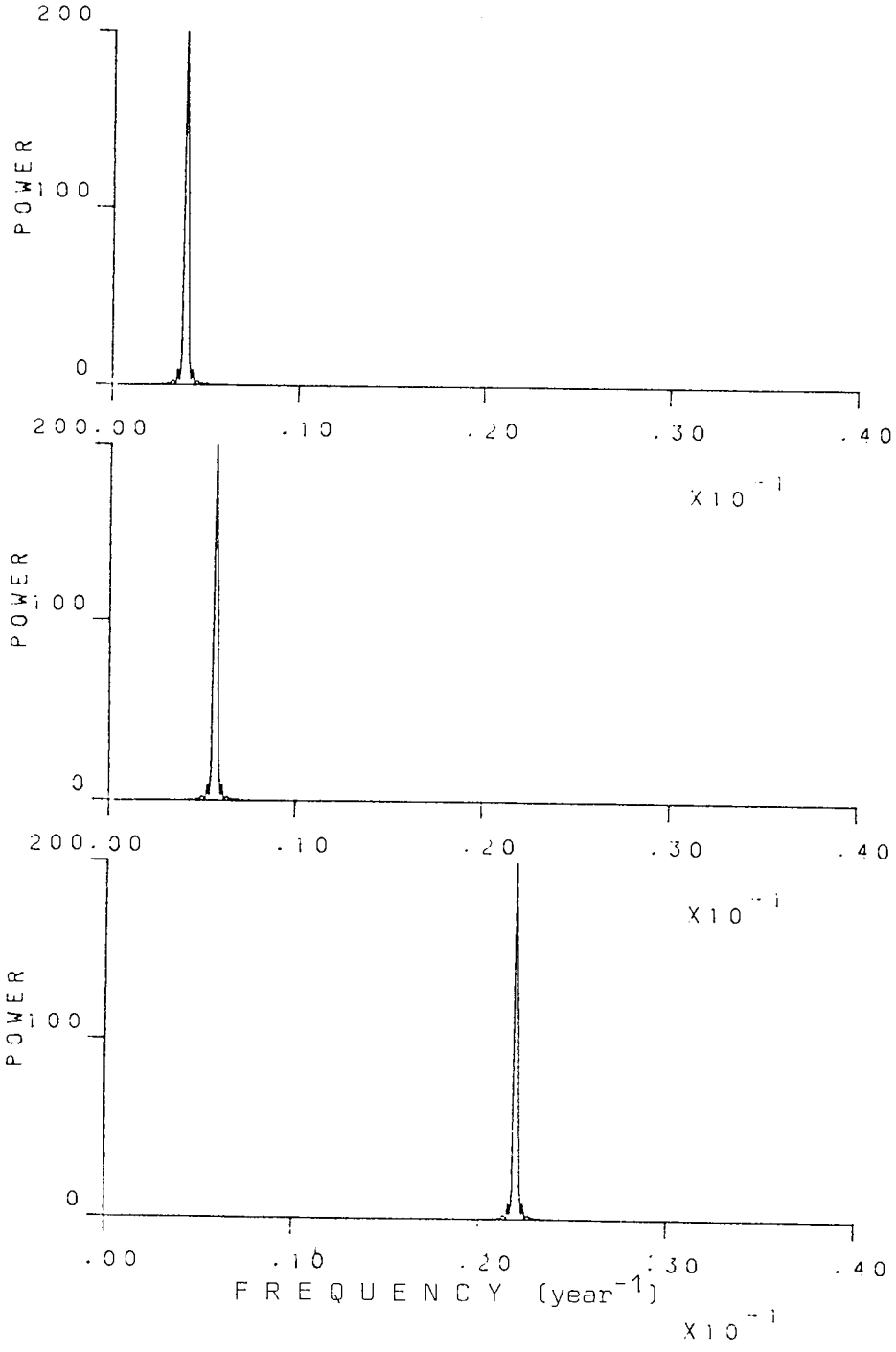

is .0005c/yr, and consequently the frequency interval was chosen to be .0001c/yr.

The resulting power spectrum for Schove auroral data is shown in figure 1.61. A pronounced peak is observed at $\nu \simeq \cdot 005$c/yr, with lesser peaks at ν = .0067c/yr, ν = .023c/yr, and periodicities of about 200 years, 150 years and 44 years respectively. As nine cycles of 200 year duration are included in the data, this peak is well within the theoretical limits and thus must be considered actually to be present in the spectrum, rather than an artefact of the analysis. However, the neighbouring peak at .0067c/yr could be due to aliasing. There is no significant power present at or around .0125c/yr, corresponding to the 80 year cycle.

To estimate the effects of aliasing, it was decided to input a pure cosine wave at the frequencies of interest, and to sample and weight it in the same way as was the original data. This is advisable as the pattern of aliases produced at a single frequency is not frequency invariant as for conventional Fourier analysis (Ponman, 1981; 1982A; 1982B). With an input wave $S_G(t) = \cos(2\pi\nu' t)$, the spectrum $P_G(\nu) = A^2{}_G(\nu) + B^2{}_G(\nu)$ may be estimated from

$$A_G(\nu) = \frac{\sum_n \cos(2\pi\nu' t_n)\, c_n\, \mathrm{sinc}(\nu'\tau_n)/\sigma_n{}^2}{\sum_n c_n{}^2/\sigma_n{}^2}$$

and

$$B_G(\nu) = \frac{\sum_n \cos(2\pi\nu' t_n)\, s_n \mathrm{sinc}\,(\nu'\tau_n)/\sigma_n{}^2}{\sum_n s_n{}^2/\sigma_n{}^2}$$

where $\mathrm{sinc}(x) = \sin(\pi x)/\pi x$;

τ_n is integration time of data.

In this case, data is effectively 'integrated' over one year. As a typical sampling interval Δt is 11.11 years, $\tau \ll \Delta t$ and may be set to zero, thereby simplifying the equations.

Power spectra were calculated for the frequencies of interest, but in

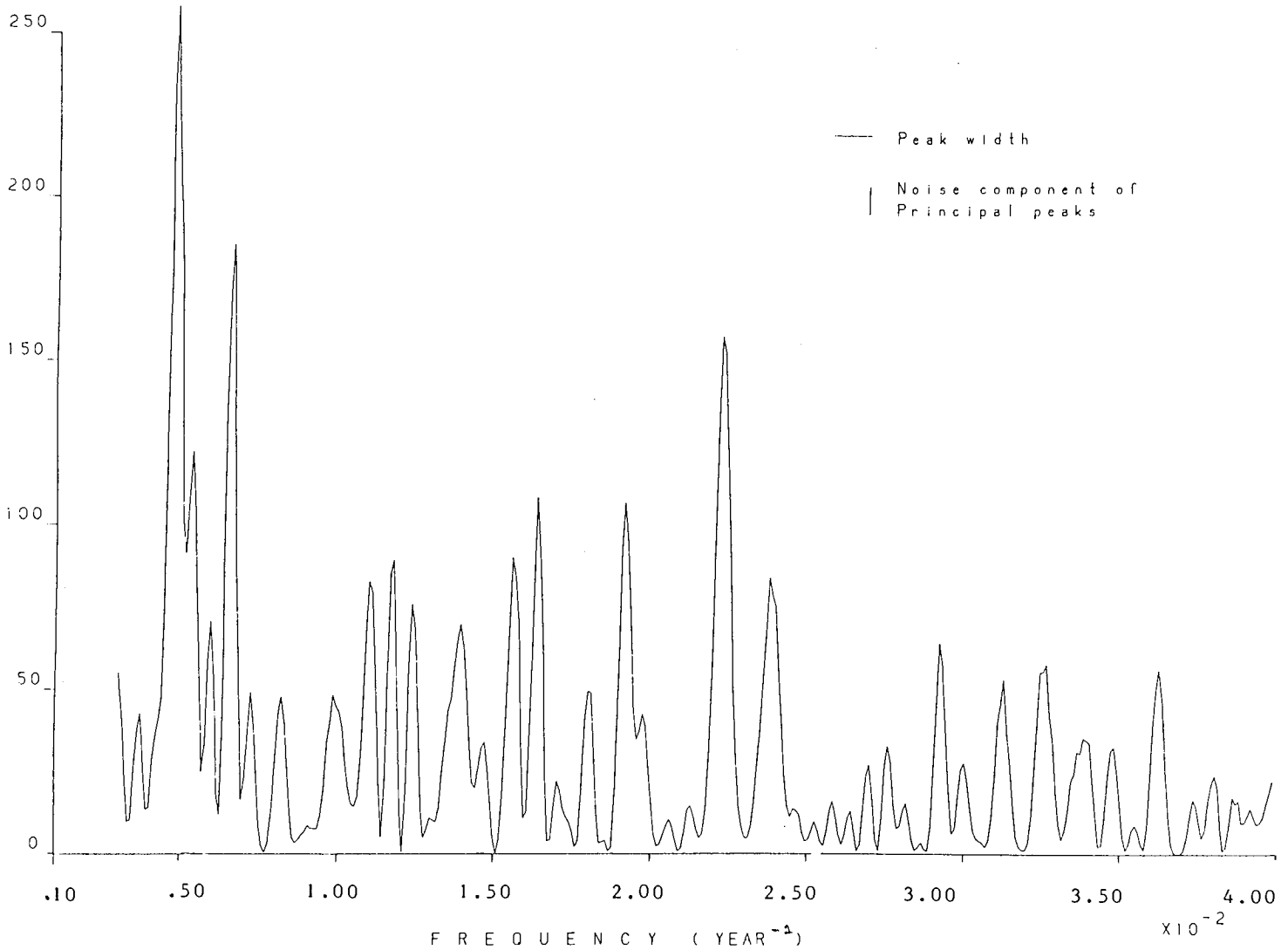

Figure 1.63 Spectrum of Schove data (weighted) 220BC - AD1700

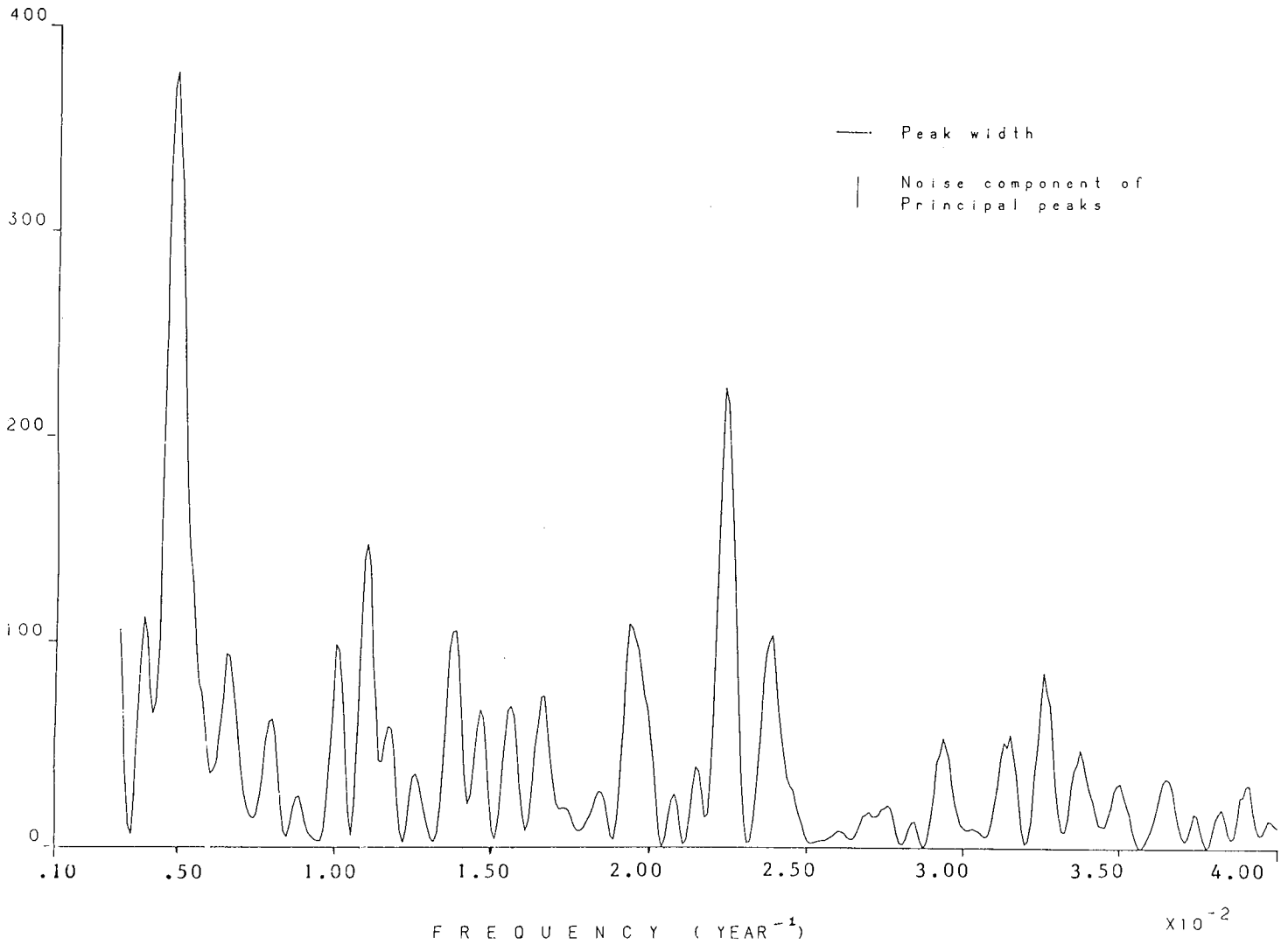

Figure 1.64 Spectrum of Schove data (weighted) AD290 - AD1705

all cases almost all the power was found to be concentrated in the peak (figure 1.62). To determine the significance of the peaks, a 'noise' spectrum was calculated. It was found that use of formula 1.5(III) was not really necessary, as the errors approximated well to

$$\tilde{\varepsilon}_p^{\,2} = \frac{8\,P(\nu)}{\sum_n 1/\sigma_n^{\,2}} \qquad \text{(see Appendix 4/1)}$$

The application of criteria for errors due to the imperfect cancellation of cross-terms indicated that there would be some bias and variance in the spectrum from this cause. The bias was computed, but unfortunately no formula is presently available for computation of variance in this case, the only procedure possible being to set an upper bound on possible variance using the full relation

$$0 \leq \frac{\sigma_p^{\,2}}{P(\nu)} \leq \frac{16}{N^*}\left(\sigma_f^{\,2} - \tfrac{1}{4}P_n\right)$$

where $N^* = \dfrac{(\sum_n 1/\sigma_n^{\,2})^2}{\sum_n 1/\sigma_n^{\,4}}$ (see Appendix 4/2)

This gives a variance so great that no spectral peak could be significant unless it contained most of the power in the spectrum. Use was therefore made of the semi-regular sampling, which reduces this bias and variance by a factor $\geq N/4$ (Ponman, 1981; 1982A; 1982B). Using this criterion, the peak at .005c/yr is seen to be significant by a small margin, and therefore is probably real.

As categories, rather than actual sunspot numbers, are associated with times of maxima in Schove's data, it was decided to rework his tables, associating a level of uncertainty with each data point according to the width of the category, rather than simply adopting the median values suggested by Schove (1955). The spectrum was then recalculated for weighted data (figure 1.63).

The general noise in the spectrum is increased, with the peak at .005c/yr a little more prominent, and that at .0067c/yr still present. The overall characteristics of the spectrum are as before, and

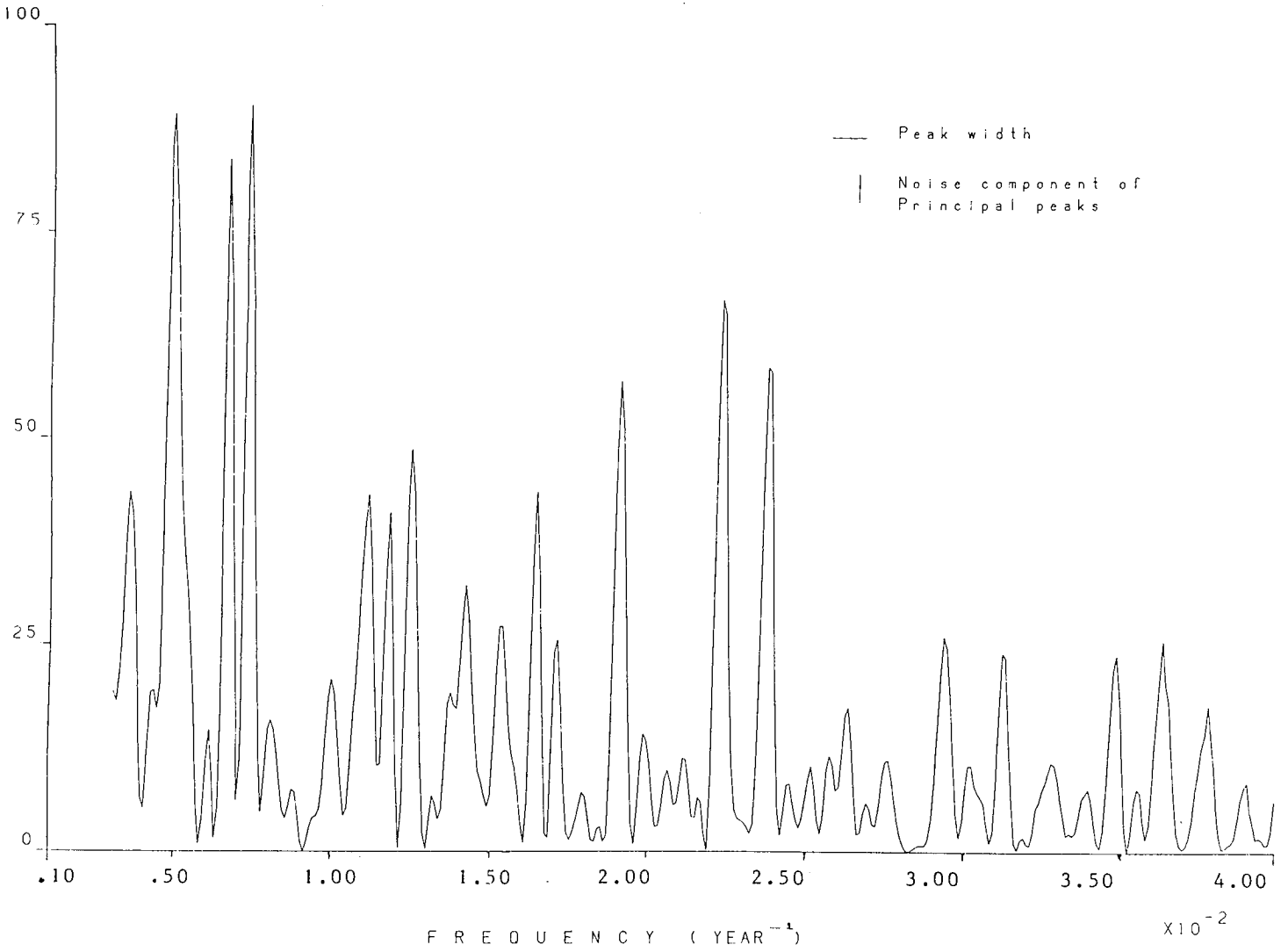

Figure 1.71 Spectrum of Bray data 522BC - AD1600

Figure 1.72 Alias peaks for Bray data

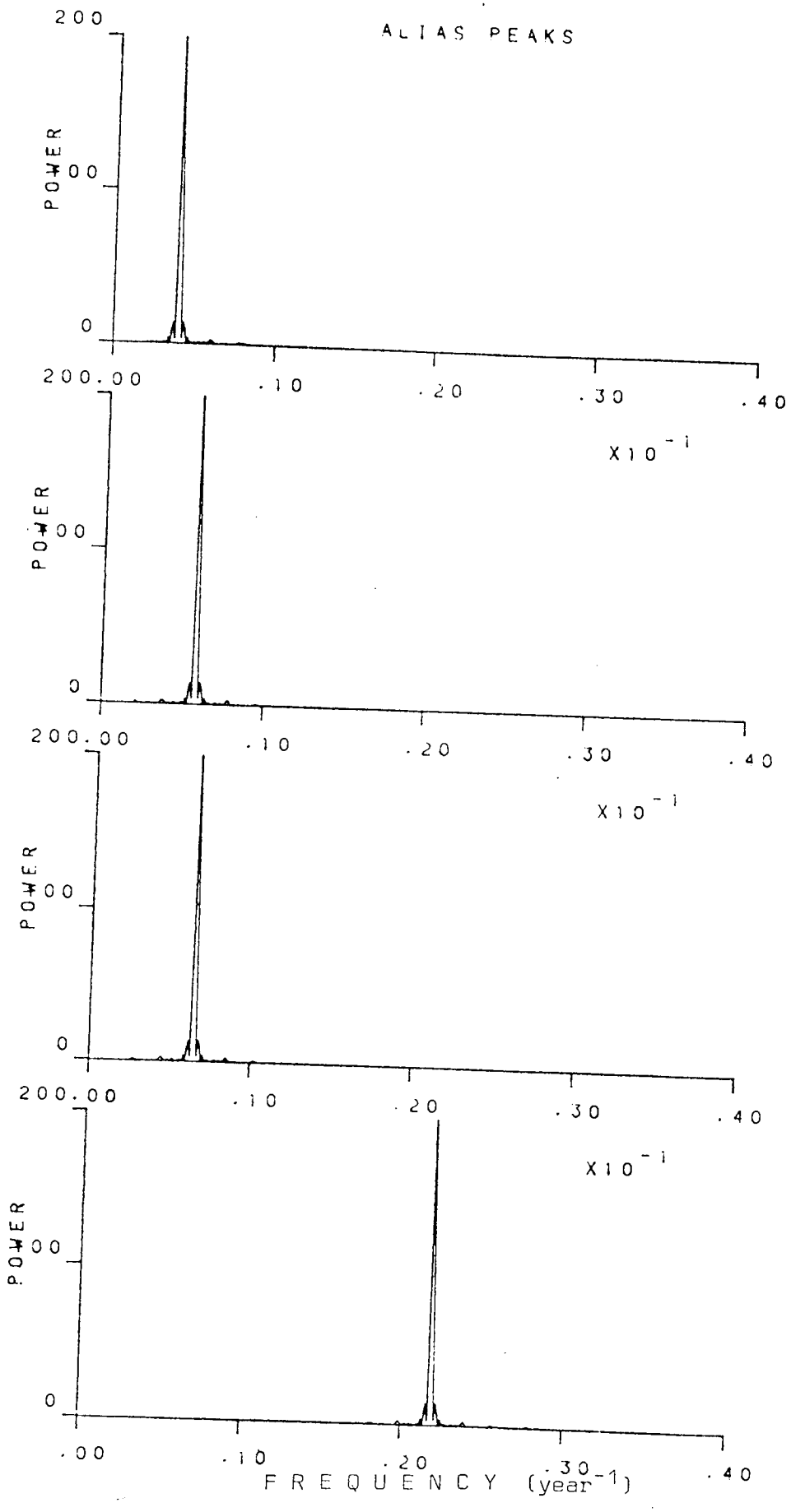

recalculation of error terms yields similar results; the 200 year periodicity is probably real, but other peaks are too low to be considered significant.

As the early Schove data contains several 'unknown' peaks, the data interval was restricted to AD290 - 1700 and the spectrum for weighted data was recalculated (figure 1.64). This spectrum was seen to display marked differences from the previous two; note the disappearance of a peak at .0067c/yr, and the clear peak at .023c/yr. Calculation of error terms indicated that the smaller sample size increased the probable variance such that the large 200 year peak was only marginally significant. For frequencies of interest, aliasing was estimated as before, the chief effect of weighted data being to increase the 'noise' around the critical frequency.

Overall, the only peak shown to be of significance in the spectra of Schove weighted and unweighted data is that at ~.005c/yr. It is concluded that a periodicity of ~200 ± 20 years exists in Schove's data.

1.7 Analysis of Bray auroral data

Bray (1980) gave precise estimates of R, with no indication of possible error. The number of observations used in the determination of each cycle is, however, listed. The heights of the maxima listed were therefore checked against the numbers of observations, but the resulting distribution was found to be random.

The data in the period 522BC - AD1600 was then analysed in the same way as in section 1.6. Peak width was found to be .00047 c/y, and so the same frequency interval as before was employed, and the same restrictions were imposed on frequency range. The resulting spectrum is shown in figure 1.71 with alias estimates (figure 1.72). A group of peaks is observed in the region .005 - .008 c/yr, but the noise present is evidently too high.

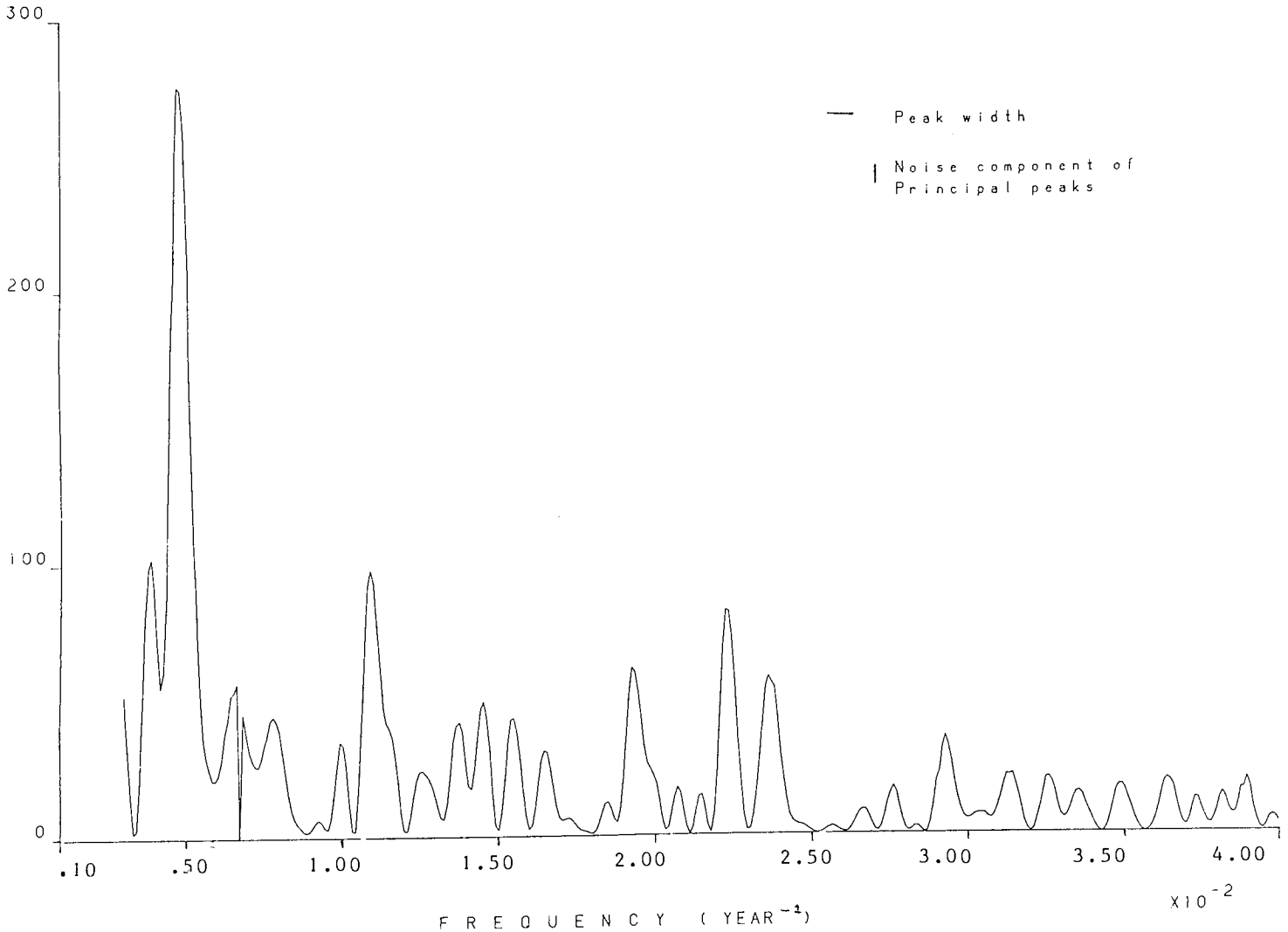

Figure 1.73 Spectrum of Bray data (restricted range) 290AD - AD1705

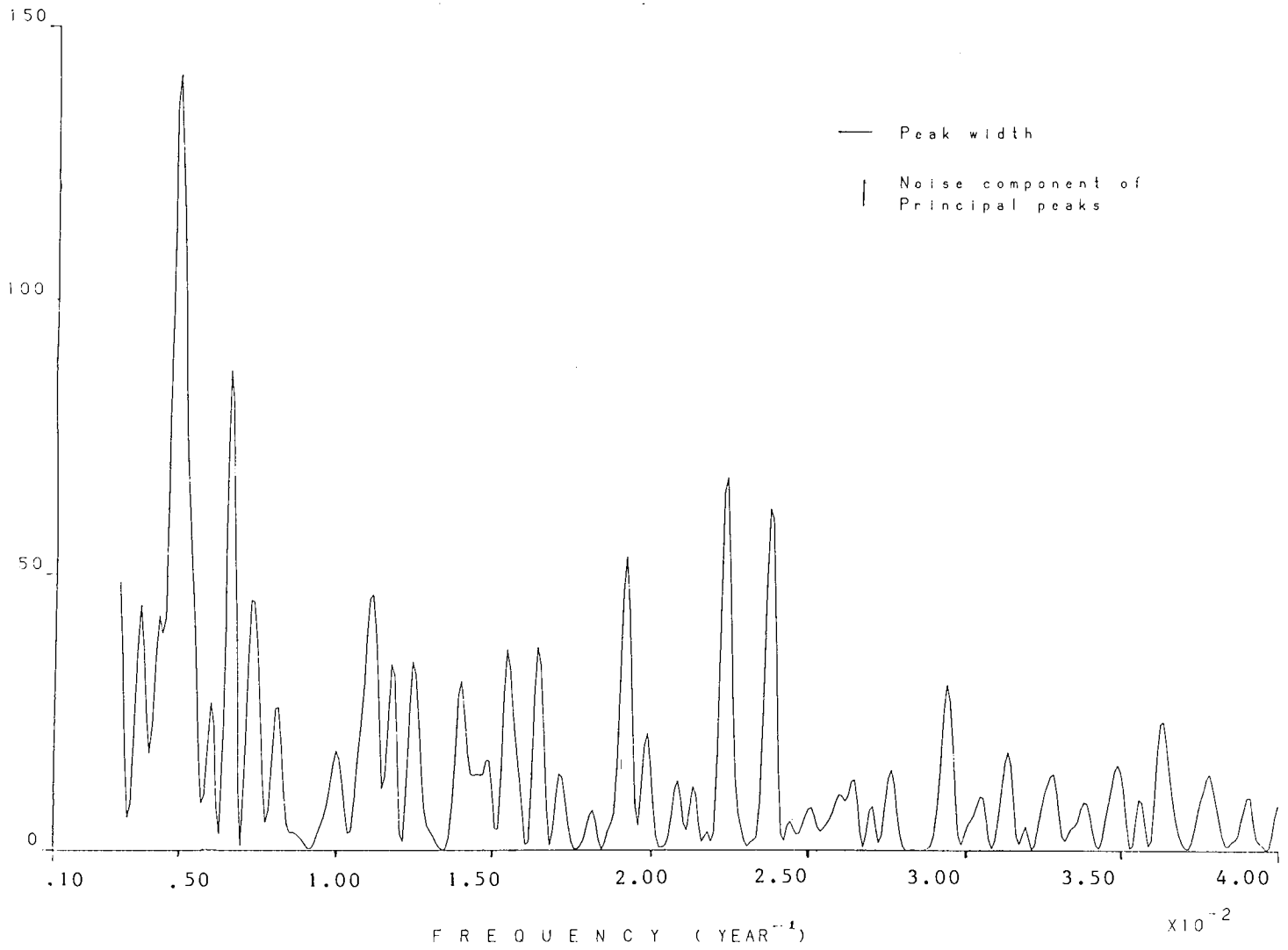

Figure 1.74 Spectrum of Bray data (full range) 522BC - AD1700

to distinguish any period present. The data range was thus restricted from AD 290, and extended after AD 1600,(previously determined as a suitable end-point,as several of Bray's source auroral catalogues terminate at this date.), to AD 1700 where his 'Solar Index' ends.

Spectra were then calculated for the restricted range AD 290 - AD 1700 (figure 1.73),and for the full range 522 BC - AD 1700 (figure 1.74). The latter shows a pronounced peak at ~ .005 c/y, with numerous lesser peaks. Although this spectrum displays considerable noise, calculation of the contribution to peak height of noise gave a value of ~.1P(ν). Again, the probable variance is close to the peak height, thus the 200 year peak is only marginally significant. Figure 1.73 shows a very large peak at ~ .005c/y, with minor activity elsewhere. However, the reduced data sample increases the probable error, so that again this peak is only just significant.

From this analysis, it is evident that a 200 year periodicity exists in the data. It must be noted, however, that much of the data utilized by Bray (1980) was derived from that of Schove (1955), and thus the two estimates of solar activity are not independent; in fact the similar characters of the power spectra indicate considerable similarities between the two data-bases.

1.8 Discussion

The reality of the 'Maunder Minimum' as an extended interval of low solar activity is clearly established. However, examination of sunspot and auroral data from the period 1650 to 1715 reveals the existence of both phenomena throughout the interval in question. Whilst the sporadic sunspot observations are not sufficient in themselves to show the presence of periodic variations in the solar activity, when combined with the more extensive auroral records it is clear that a cycle of activity was present, operating at a fairly low level. It appears likely that the widely accepted

supposition of the cessation of the solar cycle during this time (Eddy et al., 1976; 1977; Weiss and Weiss, 1979) results from limitations in the data sources used, together with the assumption of a mean cycle length of just over eleven years. It is thought that a value of about 10.5 years is more appropriate.

The auroral records indicate that the present century has an unusually high level of solar activity, and there is evidence of earlier epochs of high and low activity (Kanda, 1933; Seydl, 1954; Henkel, 1972; Pittock, 1978). Hence it appears that the overall level of activity is changing on a longer timescale than eleven years. It is here suggested that the mean length of a solar cycle may also not be constant, but may vary in a non-random manner, with a period of about 10.5 years associated with very low activity, and a period of about 11.1 years, with comparably high activity. The interpretation of this result may require knowledge of the short period variations variously reported within the eleven year sunspot cycle (Currie, 1973; Wolff, 1976; de Meyer, 1981).

Whilst a previously unknown periodic variation of about two hundred years is identified using statistical techniques, in the sunspot and auroral databases of Schove (1955) and Bray (1980), no evidence is found for the presence in this data of the eighty year 'Gleissberg period' generally reported (Gleissberg, 1962; 1973; Brown, 1976; Vitinsky, 1978; Gleissberg and Damboldt, 1979).

The existence of this effect as a long-term periodic modulation of the sunspot cycle cannot, therefore, be accepted. However, as a similar periodicity has been detected in the Waldmeier sunspot numbers (Cole, 1973; Wolff, 1976; Kopecky, 1978), the possibility cannot be excluded that it may be operating as a quasi-periodic effect over a few hundred years.

Section 2

Analysis of the Waldmeier Sunspot Series

A number of previous publications have reported the existence of periodicities in the Waldmeier sunspot numbers other than the 11 year variation. These papers are often subsequently referenced as the starting point for investigations into planetary influence on sunspots. It is argued that, to prove a connection between the two phenomena, periodicities inherent in various planetary configurations must match precisely those determined from sunspot analysis. However, comparison of source literature reveals that different statistical techniques often yield conflicting results for the value of sunspot periods involved.

One factor common to much research in this area is the use of yearly averaged data; the precision to which periodicities are quoted is often greater than the accuracy of the input information. Thus it was thought necessary to perform a critical evaluation of existing research, and if possible to conduct a more rigorous statistical examination of the sunspot data then has previously been undertaken. It was also considered desirable to examine the character of the 11 year variation itself; there is controversy over whether early recorded sunspot cycles display the same statistical structure as more recent data. Differences between these data sets would indicate that the nature of the 11 year sunspot cycle is changing with time, possibly reflecting long period variations modulating this 'sunspot cycle'.

2.1 Choice of Method of Analysis

Detailed statistical analyses of the sunspot records have been performed by several researchers (Cole, 1973; Currie, 1973; Cohen and Lintz, 1974; Hill, 1977; Wittmann, 1978; Lomb and Anderson, 1980; de Meyer, 1981), and many periodicities other than that of the eleven year cycle have been detected in the data. Both the statistical techniques adopted and the periodicities obtained vary considerably.

Methods of power spectrum analysis (taken from Blackman and Tukey, 1959) have been applied (Cole, 1973) to the Waldmeier yearly mean sunspot numbers from AD 1700 to AD 1969, yielding a spectrum from which were identified periodicities at 88, 10.45 and 5.75 years. Extending the sunspot database with the addition of information from Schove (1955), re-analysis yielded periodicities of 196, 94.5 and 78.5 years.

Techniques of maximum entropy spectral analysis (MESA) have also been applied to the Waldmeier sunspot numbers (Currie, 1973; Cohen and Lintz, 1974; Wittmann, 1978). This method estimates the spectrum of a time series based on an autoregressive description of the data to be analysed. Applied to monthly sunspot numbers from AD 1749 to AD 1957, this method revealed 18 periodicities in the sunspot data (Currie, 1973). Analyzing annual sunspot numbers in the interval AD 1750 to AD 1963, Cohen and Lintz (1974) reported the presence of periodicities of 11.0, 9.8 and 8.3 years, and combined these results with figures from Cole (1973) to identify a longer term variation of 160 - 190 years. Wittmann, in 1978, computed a MESA spectrum of yearly sunspot data from the period AD 1701 to AD 1970. The results obtained were compared with these of Cohen and Lintz (1974) and were found to be somewhat similar, with periods of 92.42, 54.91, 11.11 and 9.96 years identified in the spectrum. However, these 'quasi-periodic variations' were

regarded with some sceptiscism by the author (Wittmann, 1978).

Both Cole (1973) and Cohen and Lintz (1974) were cited in a short paper (Hill, 1977) on the application of Fourier Analysis techniques to the Vitinsky (1962) sunspot numbers, with the numbers adjusted to display alternate positive and negative signs for the assumed reversal of magnetic polarity. No details of method or results were given, but 40 spectral 'lines' were used to construct a model indicated as giving a good fit to the sunspot data.

Frequency analysis has been applied to the Waldmeier yearly mean sunspot numbers in the interval AD 1700 to AD 1964 (Lomb and Anderson, 1980). This relatively slow method involves repeated least squares fitting of sine waves to the data, plotting the reduction in the sum of squares of the residuals as a function of frequency. The greatest power in the sunspot data was identified in peaks at 11.00, 10.74, 9.96, 90.3, 11.9 and 55.4 years, with a total of 14 peaks identified, and a model was presented to explain these periodicities as a modulation in amplitude and phase of the 11 year cycle by two cycles of 55 and 90 years.

Application of periodogram analysis (de Meyer, 1981) to the annual sunspot numbers from AD 1749 to AD 1977 has also yielded a series of periodicities, in very good agreement with those of Cole (1973).

Of the methods previously applied to the sunspot data, the relative insensitivity of MESA techniques has been indicated by several researchers (Wittmann, 1978; Lomb and Anderson, 1980; de Meyer, 1981). The comparatively sophisticated analysis of Cole (1973) based on statistical methods widely used in communications engineering (Blackmann and Tukey, 1959; Anderson, 1971) employed a basic weighting function, since superseded by a range of more intricate smoothing techniques. Periodogram analysis, though straightforward, is liable to give

unstable estimates of the true power spectrum of input data (Anderson, 1971), and the avowedly simple method of Lomb and Anderson (1980) is very slow; only one frequency is subtracted at each stage of calculation and the repeated prewhitening of the data set may cause difficulties (Box and Jenkins, 1970). Thus none of the methods previously employed is ideal for the purpose.

It is evident that the records of sunspot counts, particularly those early values which were assigned retrospectively, will be subject to random fluctuations resulting both from observer errors and from incorrect transcription (Izenman, 1982). This element may be compounded by random convection effects within the photosphere (de Meyer, 1974; Piddington, 1982) affecting the precise time of appearance of sunspots on the solar surface.

Accordingly, it is necessary that the statistical method utilized for analysis of the Wolf numbers is able to provide criteria for distinguishing between 'real' periodicities and transitory effects resulting from random components in the data set. The finite length of the Wolf sunspot series is clearly a further restriction on the determination of short term periodicities.

As the quantity and quality of the sunspot data available for analysis is very limited, a powerful statistical technique is required. A very effective method for the examination of such noisy data is that of spectral analysis (Wilson, pers. comm.) an early version of which was employed in Cole (1973).

2.2 Spectral Analysis

Before proceeding to apply the methods of spectral analysis to a data set such as the sunspot series, it is necessary to examine the theoretical background; it is essential that the techniques are used with an appreciation of the inbuilt constraints of this powerful statistical tool. In particular, it will be seen that the importance of the distinction between deterministic and stochastic processes, cannot be too greatly stressed.

The following section contains a brief outline of techniques of spectral analysis; more detailed information is given in Appendix 5.

The Autocovariance Function

Of the moments used to describe the dependence between values $X(t_1)$, $X(t_2)$ of an infinite continuous time series at time points t_1 and t_2, the most widely used is the autocovariance function

$$\gamma_{XX}(t_1, t_2) = E\left[\{X(t_1) - \mu(t_1)\}\{X(t_2) - \mu(t_2)\}\right] \quad \text{(see Appendix 5/1)}$$

where $E[\ ]$ denotes the expectation value, and $\mu(t)$ the mean value at time t. As this function is dependent on the scale of measurement of X(t), the normalised 'autocorrelation coefficient'

$$\rho_{XX}(t_1, t_2) = \frac{\gamma_{XX}(t_1, t_2)}{\sigma(t_1)\,\sigma(t_2)}$$

is defined, where $\sigma^2(t_1)$ and $\sigma^2(t_2)$ are the variances of $X(t_1)$ and $X(t_2)$ respectively.

If process X(t) is in a state of equilibrium the mean and variance of X(t) will be constant; then $\gamma_{XX}(t_1, t_2)$ will be a function of lag $u = t_2 - t_1$ only;

$$\gamma_{XX}(u) = E\left[(X(t) - \mu)(X(t + u) - \mu)\right] = \mathrm{cov}\,(X(t), X(t + u)).$$

Thus $\rho_{XX}(u) = \gamma_{XX}(u)/\gamma_{XX}(o)$

is a function only of lag u for stationary processes. In practice, only records x(t) of finite length T are available, and so the theoretical autocovariance function $\gamma_{XX}(u)$ must be estimated. The most generally accepted estimator $c_{XX}(u)$ is given by

$$c_{XX}(u) = \frac{1}{T} \int_0^{T-|u|} (x(t) - \bar{x})(x(t + |u|) - \bar{x})\, dt \qquad 0 \leq |\ | \leq T$$

$$= 0 \qquad |u| > T$$

where $\bar{x}$ denotes the mean value of series x(t).

If the observations $x_1, x_2, \ldots x_N$ are taken from a discrete time series, the corresponding discrete estimator $c_{XX}(k)$ will be given by

$$c_{XX}(k) = \frac{1}{N} \sum_{t=1}^{N-k} (x_t - \bar{x})(x_{t+k} - \bar{x}) \qquad k = 0, 1, \ldots N - 1$$

where $\bar{x} = \frac{1}{N} \sum_{t=1}^{N} x_t$ is the sample mean.

The stationarity conditions will, in general, be fulfilled over a limited timespan. In practise, therefore, the mean and variance are only required to be constant over the period of interest. In the case of sunspot activity, the series is stationary over many centuries.

Sample Spectrum

The variance or average power of a signal $x(t), -T/2 \leq t \leq T/2$ can be decomposed into contributions at harmonics $f_m = m/T$, m integer, of fundamental frequency $f_1 = 1/T$ according to

$$S_T^2 = \frac{1}{T} \int_{-T/2}^{T/2} x^2(t)dt = \sum_{m=-\infty}^{\infty} |\mathcal{X}_m|^2$$

where $\mathcal{X}_m$ is the complex amplitude at frequency $f_m = m/T$,

$$\mathcal{X}_m = \frac{1}{T} \int_{-T/2}^{T/2} x(t)\, e^{-i2\pi mt/T}\, dt \qquad \text{where } i = \sqrt{-1}.$$

Similarly, for a discrete signal observed at times $t = -n\Delta, -(n-1)\Delta, \ldots, 0, \ldots, (n-1)\Delta$, the average power can be split into contributions

at a finite number of harmonics of the fundamental frequency

$f_1 = 1/n\Delta$ $\quad (N = 2n)$ and

$$S_T^2 = \frac{1}{N} \sum_{t=-n}^{n-1} x_t^2 = \sum_{m=-n}^{n-1} |\mathcal{X}_m|^2$$

where $\mathcal{X}_m = \frac{1}{N} \sum_{t=-n}^{n-1} x_t \, e^{-i2\pi mt/N}$,

the contribution $|\mathcal{X}_m|^2$ being the intensity at frequency f_m.

The variance of the infinite record is

$$\sigma^2 = \lim_{T\to\infty} \frac{1}{T} \int_{-T/2}^{T/2} x^2(t)\, dt = \lim_{T\to\infty} \sum_{m=-\infty}^{\infty} (T|\mathcal{X}_m|^2)\frac{1}{T}$$

$$= \int_{-\infty}^{\infty} \Gamma(f)\, df.$$

where $\Gamma(f)$ is the Fourier 'power spectrum'.

$$T\,|\mathcal{X}_m|^2 = C_{xx}(f) = \frac{1}{T}\left|\int_{-T/2}^{T/2} x(t)e^{-i2\pi ft}dt\right|^2 \qquad 2.2(I)$$

$C_{xx}(f)$ will usually tend to a well-defined limit $\Gamma(f)$. For deterministic signals, the convergence of $C_{xx}(f)$ to $\Gamma(f)$ is smooth; function $C'_{xx}(f)$ obtained by increasing record length T to new length T' will be a smoother version of function $C_{xx}(f)$ based on a record of length T.

However, for a stochastic process, it is found that the plot of $C'_{xx}(f)$ obtained from a record of length $T' > T$ is just as erratic as that obtained from a record of length T ie. $C_{xx}(f)$ does not converge in any statistical sense to a limiting value as $T \to \infty$.

Using equation 2.2(I) transformation $u = t - t'$, $v = t'$ and definition of $c_{xx}(u)$ yields

$$C_{xx}(f) = \int_{-T}^{T} c_{xx}(u)e^{-i2\pi fu}du \qquad -\infty \le f \le \infty \quad \text{(see Appendix 5/2)}$$

i.e. the sample spectrum is the Fourier transform of the sample auto-covariance function.

Thus $c_{xx}(u) = \int_{-\infty}^{\infty} C_{xx}(f)e^{+i2\pi fu}df \qquad -T \le u \le T$

For $u = 0$, $c_{XX}(0) = S_T^2 = \int_{-\infty}^{\infty} C_{XX}(f)\, df$,

and so the sample spectrum describes how the variance of $x(t)$ is distributed over frequency.

For discrete processes, $C_{XX}(f) = \Delta \sum_{k=-(N-1)}^{N-1} c_{XX}(k) e^{-i2\pi fk\Delta}$

$$-1/2\Delta \leqslant f < 1/2\Delta$$

The mean of $C_{XX}(f)$, $E[\, C_{XX}(f)\,]$ is given by

$$E[\, C_{XX}(f)\,] = \int_{-T}^{T} E[\, c_{XX}(u)\,] e^{-i2\pi fu}\, du$$

$$= \int_{-T}^{T} \gamma_{XX}(u) \left(1 - \frac{|u|}{T}\right) e^{-i2\pi fu}\, du \,. \qquad 2.2(II)$$

Now, $\Gamma_{XX}(f) = \lim_{T\to\infty} E[\, C_{XX}(f)\,] = \int_{-\infty}^{\infty} \gamma_{XX}(u) e^{-i2\pi fu}\, du$ (see Appendix 5/2)

It is often argued that, since $c_{XX}(u)$ tends to $\gamma_{XX}(u)$ as $T\to\infty$ then

$$\lim_{T\to\infty} C_{XX}(f) = \int_{-T}^{T} \lim_{T\to\infty} c_{XX}(u) e^{-i2\pi fu} du$$

$$= \int_{-\infty}^{\infty} \gamma_{XX}(u) e^{-i2\pi fu}\, du = \Gamma_{XX}(f)$$

Whilst it is true that the mean square error of $c_{XX}(u)$ is of order $1/T$ and hence its distribution clusters around $\gamma_{XX}(u)$ as $T \to \infty$, rendering $c_{XX}(u)$ a consistent estimator of $\gamma_{XX}(u)$, this does not imply that the same is true of the Fourier transform of $c_{XX}(u)$.

From 2.2(II) it is seen that the mean of the sample spectrum estimator is the Fourier transform of the product of $\gamma_{XX}(u)$ and the function

$$w(u) = \begin{cases} 1-|u|/T & |u| \leqslant T \\ 0 & |u| > T \end{cases}$$

Hence $E[\, C_{XX}(f)\,] = \int_{-\infty}^{\infty} T\left(\frac{\sin\pi Tg}{\pi Tg}\right)^2 \Gamma_{XX}(f-g)\, dg$.

So the sample spectrum estimator has an expected value corresponding to looking at the theoretical spectrum $\gamma_{XX}(f)$ through a 'spectral window'

$$W(f) = T\left[\frac{\sin\pi Tf}{\pi Tf}\right]^2 \quad \text{(Blackman and Tukey, 1959)}.$$

Spectral Windows

Now $\lim_{T\to\infty} E\left[C_{XX}(f)\right] = \Gamma_{XX}(f)$,

so $C_{XX}(f)$ is an asymptotically unbiased estimator of $\Gamma_{XX}(f)$. But for finite record length, $C_{XX}(f)$ is biased, with bias $B(f) = E\left[C_{XX}(f)\right] - \Gamma_{XX}(f)$. For large T, as w(f) is a slit of width ~ 1/T, it may be assumed that $\Gamma_{XX}(f)$ is constant over the slit. Then

$$E\left[C_{XX}(f)\right] \approx \Gamma_{XX}(f)$$

and thus bias will be small if T is large.

Dividing the time series into k sub-series each of length M yields estimates

$$C_{XX}^{(j)}(f) = \int_{-M}^{M} c_{XX}^{(j)}(u) e^{-i2\pi fu} du \qquad j = 1, 2, .. k$$

Hence the smoothed estimator

$$\bar{C}_{XX}(f) = \frac{1}{K}\sum_{j=1}^{k} C_{XX}^{(j)}(f) = \int_{-M}^{M} \bar{c}_{XX}(u)\, e^{-i2\pi fu} du$$

where $\bar{c}_{XX}(u) = \frac{1}{k}\sum_{j=1}^{k}\left\{\frac{1}{M}\int_{(j-1)M}^{jM-u} X(t)X(t+u)dt\right\} \qquad u \geq 0.$

Taking expectation values:

$$E\left[\bar{C}_{XX}(f)\right] = \int_{-\infty}^{\infty} \Gamma_{XX}(f-g)M\left[\frac{\sin\pi gM}{\pi gM}\right]^2 dg.$$

Thus subdividing the record of length T into k sections of length M = T/k and forming a smoothed spectral estimate is equivalent to smoothing the sample spectrum by window

$$W(f) = M\left[\frac{\sin\pi fM}{\pi fM}\right]^2.$$

The base width of the spectal window is 2/M; thus, by controlling the length M of the sub-series it is possible to regulate the base width of the spectral window. By reducing M, it will later be shown that

the variance is reduced. However, this corresponds to increasing the base width, and so smoothing over a wide range of frequencies, so that bias B(f) may be large. Hence the necessary smoothing of a spectral estimator to yield an approximation to the true spectrum $\gamma_{XX}(f)$ renders necessary a compromise between variance and bias.

Many different smoothing procedures have been suggested (Bartlett, 1953; Blackman and Tukey, 1958; Parzen, 1961) of the form

$$\bar{C}_{XX}(f) = \int_{-\infty}^{\infty} w(u) c_{XX}(u).e^{-i2\pi fu} du$$
$$= \int_{-\infty}^{\infty} \bar{c}_{XX}(u).e^{-i2\pi fu} du$$

for continuous data, with similar expressions for discrete data. Those lag windows most widely used in spectral analysis (Bartlett, 1966; Anderson, 1971; Jenkins and Watts, 1978) are given in Table 2.20.

Variance and Bias

As the requirements for base width of a window with small variance and low bias are diametrically opposed, it is necessary to derive expressions for both variance and bias for all spectral windows of interest. Now bias

$$B(f) = E\left[\int_{-\infty}^{\infty} \omega(u) c_{XX}(u) e^{-i2\pi fu} \, du\right] - \int_{-\infty}^{\infty} \gamma_{XX}(u) e^{-i2\pi fu} du$$
$$\approx \int_{-\infty}^{\infty} (\omega(u) - 1)\, \gamma_{XX}(u).e^{-i2\pi fu} du$$

and so it is possible to obtain the following approximate expressions for the bias of a spectral window: (see Appendix 5/.)

$$B_B(f) \approx \frac{1}{M} \int_{-\infty}^{\infty} - |u|\, \gamma_{XX}(u).\, e^{-i2\pi fu} du,$$

$$B_T(f) \approx \frac{\pi^2}{4M^2} \int_{-\infty}^{\infty} -u^2 \gamma_{XX}(u) e^{-i2\pi fu} du + O(1/M^4)$$
$$= \frac{.063}{M^2}\ \Gamma''_{XX}(f) + O(1/M^4)$$

Description	Lag window	Spectral window
rectangular	$w_R(u) = \begin{cases} 1, & \lvert u\rvert \leq M \\ 0, & \lvert u\rvert > M \end{cases}$	$W_R(f) = 2M\left(\frac{\sin 2\pi fM}{2\pi fM}\right), \quad -\infty \leq f \leq \infty$
Bartlett	$w_B(u) = \begin{cases} 1 - \frac{\lvert u\rvert}{M}, & \lvert u\rvert \leq M \\ 0, & \lvert u\rvert > M \end{cases}$	$W_B(f) = M\left(\frac{\sin \pi fM}{\pi fM}\right)^2, \quad -\infty \leq f \leq \infty$
Tukey	$w_T(u) = \begin{cases} \frac{1}{2}\left(1 + \cos\frac{\pi u}{M}\right), & \lvert u\rvert \leq M \\ 0, & \lvert u\rvert > M \end{cases}$	$W_T(f) = M\left\{\frac{\sin 2\pi fM}{2\pi fM} + \frac{1}{2}\frac{\sin 2\pi M(f + \frac{1}{2}M)}{2\pi M(f + \frac{1}{2}M)} + \frac{1}{2}\frac{\sin 2\pi M(f - \frac{1}{2}M)}{2\pi M(f - \frac{1}{2}M)}\right\}$ $= M\left(\frac{\sin 2\pi fM}{2\pi fM}\right)\left(\frac{1}{1 - (2fM)^2}\right), \quad -\infty \leq f \leq \infty$
Parzen	$w_P(u) = \begin{cases} 1 - 6\left(\frac{u}{M}\right)^2 + 6\left(\frac{\lvert u\rvert}{M}\right)^3, & \lvert u\rvert \leq \frac{M}{2} \\ 2\left(1 - \frac{\lvert u\rvert}{M}\right)^3, & \frac{M}{2} < \lvert u\rvert \leq M \\ 0, & \lvert u\rvert > M \end{cases}$	$W_P(f) = \frac{3}{4}M\left(\frac{\sin \pi fM/2}{\pi fM/2}\right)^4, \quad -\infty \leq f \leq \infty$

Table 2.20 Parameters for spectral windows.

where $\Gamma''_{XX}(f)$ denotes the second derivative of the spectrum at frequency f.

$$B_p(f) \approx \frac{6}{M^2} \int_{-\infty}^{\infty} -u^2 \gamma_{XX}(u).e^{-i2\pi fu} du + O(1/M^3)$$

$$= \frac{.0152}{M^2} . \Gamma''_{XX}(f) + O(1/M^3).$$

The above equations indicate that peak heights will generally be underestimated, and troughs overestimated due to bias; also, narrow peaks will have large bias. For the same truncation point M, the Tukey window will have the smallest bias, and the Bartlett window, the greatest bias. The rectangular window included in Table 2.20 compares so poorly with the other windows available that it is excluded from further consideration here.

The calculations for esimation of variance are tedious. It may be shown (Jenkins and Watts, 1978) that the covariance between two estimators at a sufficiently wide frequency spacing is almost zero; hence independent confidence intervals may be constructed at this frequency separation. For any normal stochastic process X(t) it is found that

$$\text{Cov}\,(C_{XX}(f_1),\ C_{XX}(f_2)) \text{ is of order } (1/T^2) \qquad f_1 \neq f_2$$

and $\text{Var}\,(C_{XX}(f)) \approx \Gamma^2_{XX}(f)$

For smoothed spectral estimators, the equivalent result is:

$$\text{Cov}\,(\bar{C}_{XX}(f_1), \bar{C}_{XX}(f_2)) \approx \frac{1}{T} \int_{\infty}^{\infty} \Gamma^2_{XX}(g)\, W(f_1 - g).\,(W(f_2 + g) + W(f_2 - g))\, dg$$

where W(f) denotes the Fourier transform of spectral window $\omega(u)$. Thus, for $f_1 = f_2 = f$:

$$\text{Var}\,(\bar{C}_{XX}(f)) \approx \frac{\Gamma^2_{XX}(f)}{T} \int_{-\infty}^{\infty} W^2(g)\, dg$$

$$= \frac{\Gamma^2_{XX}(f)}{T} \int_{-\infty}^{\infty} w^2(u)\, du = \Gamma^2_{XX}(f).\frac{I}{T}$$

where $I = \int_{-\infty}^{\infty} w^2(u)du$

Thus it is possible to derive equations for the variance of different spectral windows (Appendix 5/3). Clearly, the variance of the smoothed spectral estimator may be reduced by making truncation point M of the lag window small, as previously indicated; the correct choice of M is thus of critical importance.

Confidence Limits

The sample $C_{XX}(f)$ is the Fourier Transform of covariance function estimator $c_{XX}(u)$, which is assumed zero outside the interval $-T \leq u \leq T$. If $c_{XX}(u)$ is represented over this interval by periodic function

$c^P_{XX}(u)$ $(= c^P_{XX}(u + 2T))$ then $c^P_{XX}(u)$ has a Fourier series representation:

$$c^P_{XX}(u) = \sum_{\ell=-\infty}^{\infty} C^P_{XX}\left[\frac{\ell}{2T}\right] e^{+i(2\pi\ell u/2T)}.$$

Since $w(u) = 0 \quad |u| \geq M$, functions $\bar{c}_{XX}(u) = c_{XX}(u).\ w(u)$ and $\bar{c}_{XX}(u) = c^P_{XX}(u).\ w(u)$ are identical over all u, so that

$$\bar{C}_{XX}(f) = \int_{-\infty}^{\infty} W(f - g)\ C_{XX}(g)dg$$

and $$\bar{C}_{XX}(f) = \sum_{\ell=-\infty}^{\infty} W(f - \tfrac{\ell}{2T})\ \ C^P_{XX}(\ell/2T).$$

But

$$\frac{C_{XX}(\ell/2T)}{2T} = C^P_{XX}(\ell/2T) \text{ and hence}$$

$$\bar{C}_{XX}(f) = \frac{1}{2T} \sum_{\ell=-\infty}^{\infty} C_{XX}(\ell/2T)\ \ W(f - \ell/2T)\ .$$

Thus $\bar{C}_{XX}(f)$ is a weighted sum of random variables $C_{XX}(\ell/2T)$ at subharmonic frequencies $\ell/2T$. These r.v.'s will be distributed as a χ_2^2, hence distribution of $\bar{C}_{XX}(f)$ may be approximated by $a\chi_\nu^2$, with

$$\nu \approx \frac{2(E[\bar{C}_{XX}(f)])^2}{Var[\bar{C}_{XX}(f)]} \text{ and } a \approx E\ [\bar{C}_{XX}(f)]/\nu. \qquad 2.2(IV)$$

If the spectrum is smooth with respect to the window,

$$E\left[\bar{C}_{XX}(f)\right] \approx \Gamma_{XX}(f)$$

and Var $\left[\bar{C}_{XX}(f)\right] \approx \frac{\Gamma^2_{XX}(f)}{T} \int_{-\infty}^{\infty} \omega^2(u)\, du$

Hence $\nu \approx \frac{2T}{I}$, $a \approx \frac{\Gamma_{XX}(f)}{\nu}$, from equation 2.2(IV).

Thus the random variable '$\nu\bar{C}_{XX}(f)/\Gamma_{XX}(f)$'

is distributed as a χ_ν^2 with degrees of freedom ν; the degrees of freedom of the smoothed spectral estimator depend on the window $\omega(u)$.

So probability $Pr\left\{x_\nu\left(\frac{\alpha}{2}\right) < \nu \frac{\bar{C}_{XX}(f)}{\Gamma_{XX}(f)} \leq x_\nu\left(1 - \frac{\alpha}{2}\right)\right\} = 1 - \alpha$

where $Pr\{\chi_\nu^2 \leq x_\nu(\alpha/2)\} = \alpha/2$.

Thus the interval between $\frac{\nu\bar{C}_{XX}(f)}{x_\nu(1-(\alpha/2))}, \frac{\nu\bar{C}_{XX}(f)}{x_\nu(\alpha/2)}$

is a $100(1 - \alpha)\%$ confidence interval for $\Gamma_{XX}(f)$.

The confidence interval is frequency dependent; thus it may be convenient to plot the spectral estimates on a logarithmic scale, when the confidence interval for the spectrum is simply represented by a constant interval on the graph.

It is found that, to obtain a good estimate of a peak in a spectrum, the 'width' of the spectral window must be of the same order as the 'width' of the peak. This 'width' is defined by considering the bandpass spectral window

$$\omega(f) = \frac{1}{h} \quad -\frac{h}{2} \leq f \leq \frac{h}{2}$$

which is rectangular in the frequency domain and has unique width h. The variance of the corresponding smoothed spectral estimator is

$$\text{Var}\left[\bar{C}_{XX}(f)\right] \approx \frac{\Gamma^2_{XX}(f)}{T.b}$$

where b denotes bandwidth. The bandwidth of a given spectral window is then defined as the width of a rectangular window yielding the same variance i.e.

$$\text{Var } \bar{C}_{XX}(f) \simeq \frac{\Gamma^2_{XX}(f)}{T} \int_{-\infty}^{\infty} w^2(u)\, du .$$

$$\text{Thus } b = \frac{1}{I} = \frac{1}{\int_{\infty}^{\infty} W^2(f)df} .$$

Values of corresponding bandwidths for the Parzen, Tukey and Bartlett spectral windows are given in Appendix 5/3.

With formulae for the autocovariance function and a smoothed spectral estimator, it is now possible to apply spectral analysis to a time series. It is clearly imperative that estimates of variance and bandwidth accompany every analysis, and that the nature of the series in question, deterministic or stochastic, is known.

Practical Procedure

In general, it is not possible to compute $c_{XX}(u)$ for all lags u; thus a cut-off point must be adopted beyond which it may be assumed that $c_{XX}(u) = 0$, $u \leq u_{LIMIT}$. In practice, a limiting value of $u \leq N/4$ is adequate. It is also necessary to determine a suitable spectral window; then the smoothing of an estimator is completely determined by the shape and the bandwidth (or truncation point) of the window used. Normal procedure is to compute a series of smoothed spectral estimates, progressively reducing the initially high bandwidth. This 'window closing' process should, ideally, be continued until the window width is less than the width of the narrowest significant detail in the spectrum. However, at some stage the instability of the record will prevent more detail being revealed; the amount of information accessible will depend on to what degree it is possible to discriminate between 'real' detail and sampling fluctuations due to instability.

2.3 Choice of Parameters of Sunspot Analysis

From prior knowledge of the sunspot cycle, the presence of an approximately eleven year periodicity is suspected; this may be expected to produce a narrow peak in the spectrum of the spectral windows available (Table 2.20). W_{rect} has very large sidelobes i.e. it permits values of $\Gamma_{XX}(g)$ at frequencies g distant from frequency f to make large contributions to the bias at f, an effect known as leakage (Blackman and Tukey, 1959). This may be troublesome if a narrow peak is present in the spectrum. $W_{BART}(f)$ also has quite high leakage; thus $W_p(f)$ or $W_T(f)$ are more suitable spectral windows for an analysis of this type. As, for a given bandwidth, the Parzen window requires ~40% more lags than the Tukey window, the latter spectral window was chosen for initial analysis of the sunspot data.

With regard to the sunspot database itself, it will be necessary to select the most appropriate of the several sets of Wolf sunspot numbers. Additional smoothing is often introduced in statistical modelling of the sunspot numbers, by the use of averaged sunspot data from Waldmeier (1961). These 'smoothed monthly sunspot numbers' are obtained by fitting a six month running mean through the unsmoothed data. Whilst this is of considerable use for modelling techniques such as autoregression analysis, because it reduces short-term and random fluctuations, it may lead to the suppression of information useful for the method outlined in section 2.2. Thus for power spectral analysis of the sunspot numbers it is more appropriate to use values derived from unsmoothed data.

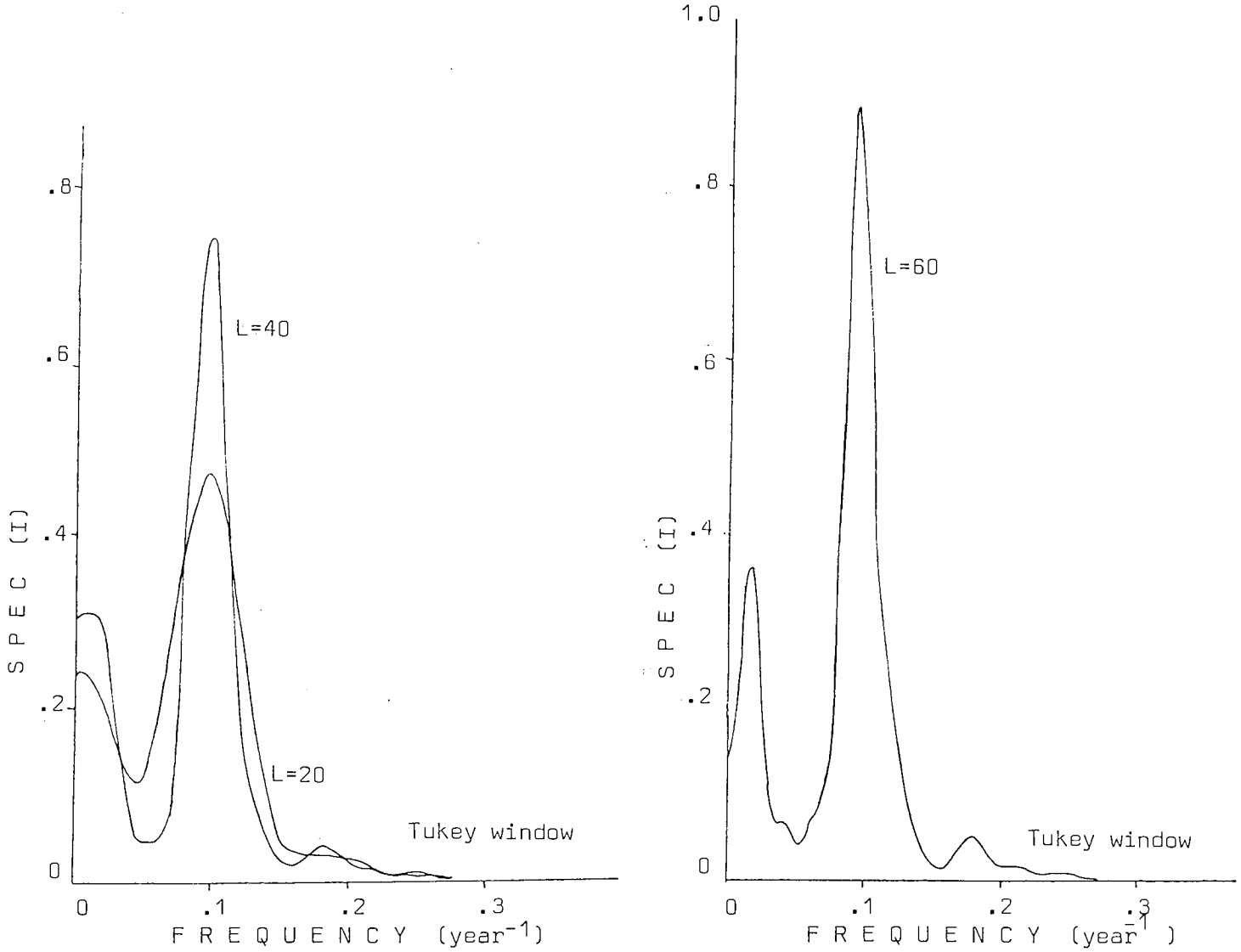

Figure 2.31 Test spectrum of annual mean sunspot numbers 1750-1950 using Tukey window

The maximum data spacing permissible is $\Delta = 1/2f_0$ where f_0 is the Nyquist frequency; the spectrum may be estimated for $\Delta \leq f \leq f_0$, and thus the use of yearly sunspot data will permit detection, theoretically, of any periodicities of greater length than two years. However, very little prior knowledge of $\Gamma_{XX}(f)$ is available; it is not known that $\Gamma_{XX}(f)$ is zero for $f > 1/2\Delta$. It must therefore be assumed that f_0 is much less than that frequency beyond which $\Gamma_{XX}(f)$ is zero, and so it may be necessary to sample much more frequently than the Nyquist condition requires.

Using the yearly averaged sunspot numbers (Waldmeier, 1961) from 1750 to 1950, the correlation coefficient $c_{XX}(u)$ was calculated for lags $u \leq 90$. The result, similar to that in Craddock (1967), confirms that a truncation point of $U \sim N/4$ is suitable for this data set; thus a limiting lag value of $u = 60$ was adopted. With a frequency spacing of .01 c/yr and lags $L = 20$, 40, and 60, a pilot spectrum was calculated for the frequency range $0.001 \leq f \leq 0.500$ c/yr (figure 2.31). It is evident that, for $L = 20$, the spectrum is oversmoothed. As window closing is applied at $L = 40$, a peak is apparent which is more prominent at $L = 60$. However, a side-lobe of this peak is also apparent at $L = 60$. Because of this, the analysis was repeated using the Parzen window, which has very low leakage.

The Parzen window proved to be the optimal window for analyses of the sunspot data, with low leakage and variance. Because W_p is a wider window than W_T, when window closing is applied the estimate requires more lags to settle down to a steady value; hence greater computing time is required when using the Parzen window. However, analyses using this smoothing technique show no appreciable leakage, and the slightly greater bias is not of critical importance.

2.4 Initial Analysis

It was intially intended that the work of Cole (1973) should be investigated and possibly extended with the use of more data, and the better smoothing techniques now available. Accordingly, six-month mean sunspot numbers were calculated from the unsmoothed monthly sunspot numbers (Waldmeier, 1961) for the period 1749 to 1960 inclusive. The autocorrelation coefficient was initially obtained for lags up to L = 150, and a series of spectra computed for varying lags L from L = 20 to L = 100. Figure 2.41 shows power spectra for lags 50 and 100. Using results from Table 2.20 bandwidths and 80% confidence limits were calculated. It is seen that very smooth spectra are obtained for these lag values, but that the 80% confidence limit is already close to the peak height at L = 100.

These spectra are dissimilar to those obtained by Cole (1973); there is no indication in his work of calculations of variance or bias, and it would appear that the importance of distinguishing between stochastic and deterministic processes was not then well understood. To investigate this possibility, after recalculating the autocorrelation function for lags up to 350, spectra were obtained for lags L = 200 (figure 2.42) and L = 350 (figure 2.43) with corresponding estimates of bandwidth and variance. It is seen that, as smoothing is reduced, the spectrum becomes more similar to that of Cole (1973), and it is clear that a further reduction in width of the spectral window beyond L = 350 would yield a spectrum virtually identical to that of Cole (1973). The 80% confidence limit for L = 200 at peak frequency .085 c/yr is 37.6 c.f. peak height 23.2, and for L = 350 the 80% C.I. is 48.1, c.f. peak height 31.3.

Thus, it is apparent that the numerous peaks observed in figure 2.43 may not be assumed to indicate the existence of periodicities

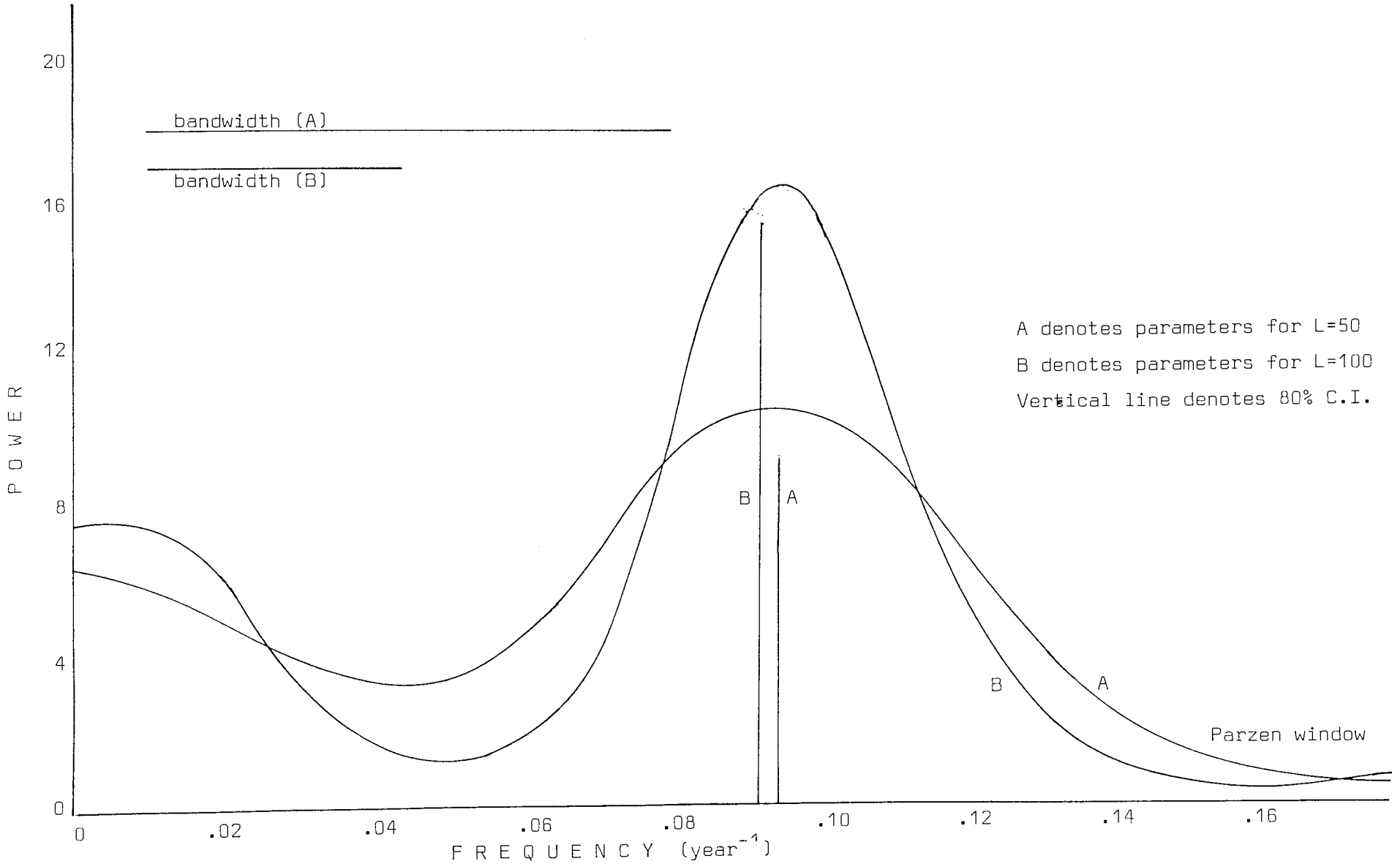

Figure 2.41 Power Spectrum of 424 six-month mean Sunspot numbers in Interval AD 1749-1960

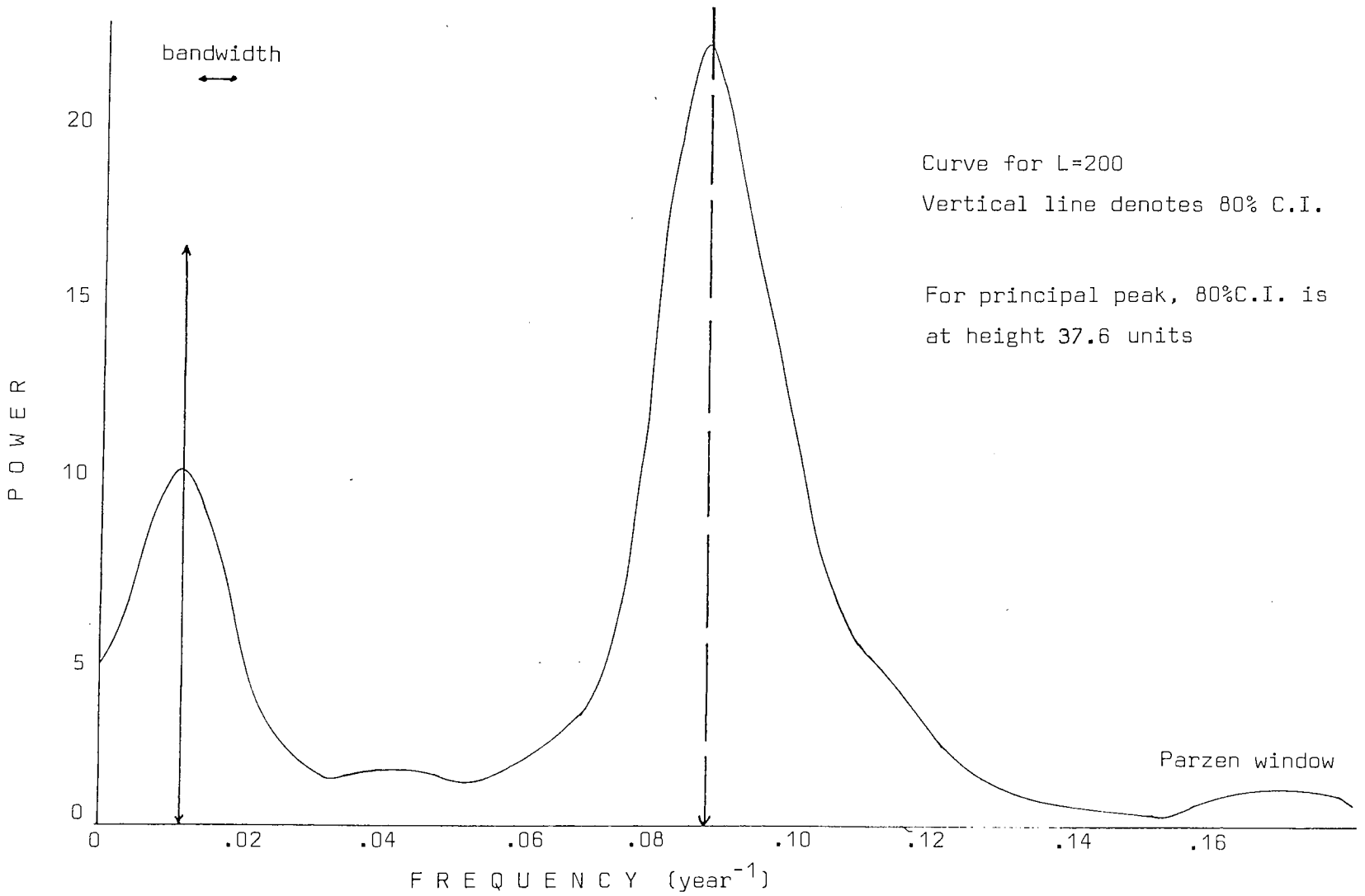

Figure 2.42 Power Spectrum of 424 Six-Month Mean Sunspot Numbers AD 1749-1960

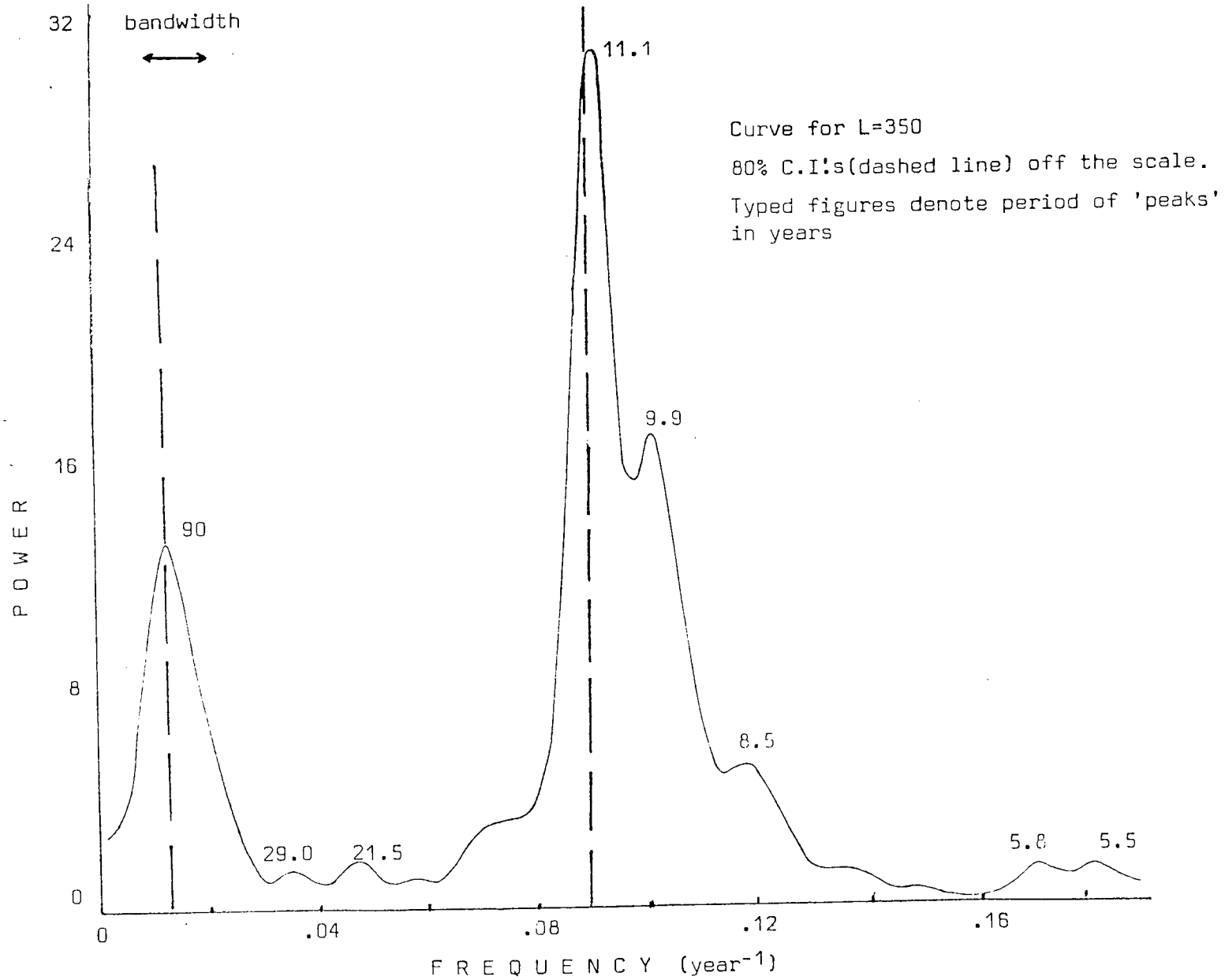

Figure 2.43 Power Spectrum of 424 Six-Month Mean Sunspot Numbers AD 1749 - 1960

in the data at these frequencies. With the limited amount of data presently available for analysis, to discriminate at this level between 'real' peaks and sampling fluctuations due to instability is not possible.

2.5 Further Analysis of the Waldmeier Sunspot Series

It was decided to conduct a detailed analysis of the Waldmeier sunspot numbers in order to obtain the greatest possible amount of information about the eleven year sunspot cycle. Previous statistical analyses of the sunspot series have utilized yearly averaged sunspot data (Cole, 1973; Cohen and Lintz, 1974; Wittmann, 1978; Lomb and Anderson, 1980; de Meyer, 1981). As this involves considerable smoothing of the data, reducing the information originally present, it was considered useful to ascertain the effect on an output power spectrum of such alterations to the input sunspot numbers.

Most statistical analysis of the Waldmeier sunspot series has been performed using the yearly mean sunspot numbers, i.e. using smoothed data. This can be regarded as filtering the initial 'raw' data before use. If we denote the actual unsmoothed data by an input process $\{U_T\}$ to a filter with transfer function $\psi(B)$, then output $\{X_T\}$ is related to $\{U_T\}$ by $\{X_T\} = \psi(B).\{U_T\}$

We can express the transformation $\{X_T\} \rightarrow \{U_T\}$ in terms of its effect on the autocovariance generating function $c_{XX}(z)$:

$$c_{XX}(z) = \psi(z).\ \psi(z^{-1}).\ c_{uu}(z)$$

The power spectra of $\{X_T\}$ and $\{U_T\}$ are clearly not identical; they are related by $G_{XX}(\omega) = F(\omega).\ G_{uu}(\omega)$

where $F(\omega) = \psi(e^{i\omega}).\psi(e^{-i\omega})$.

This 'filter factor' $F(\omega)$ summarises the information on how a particular filter changes the distribution of variance over the frequency range.

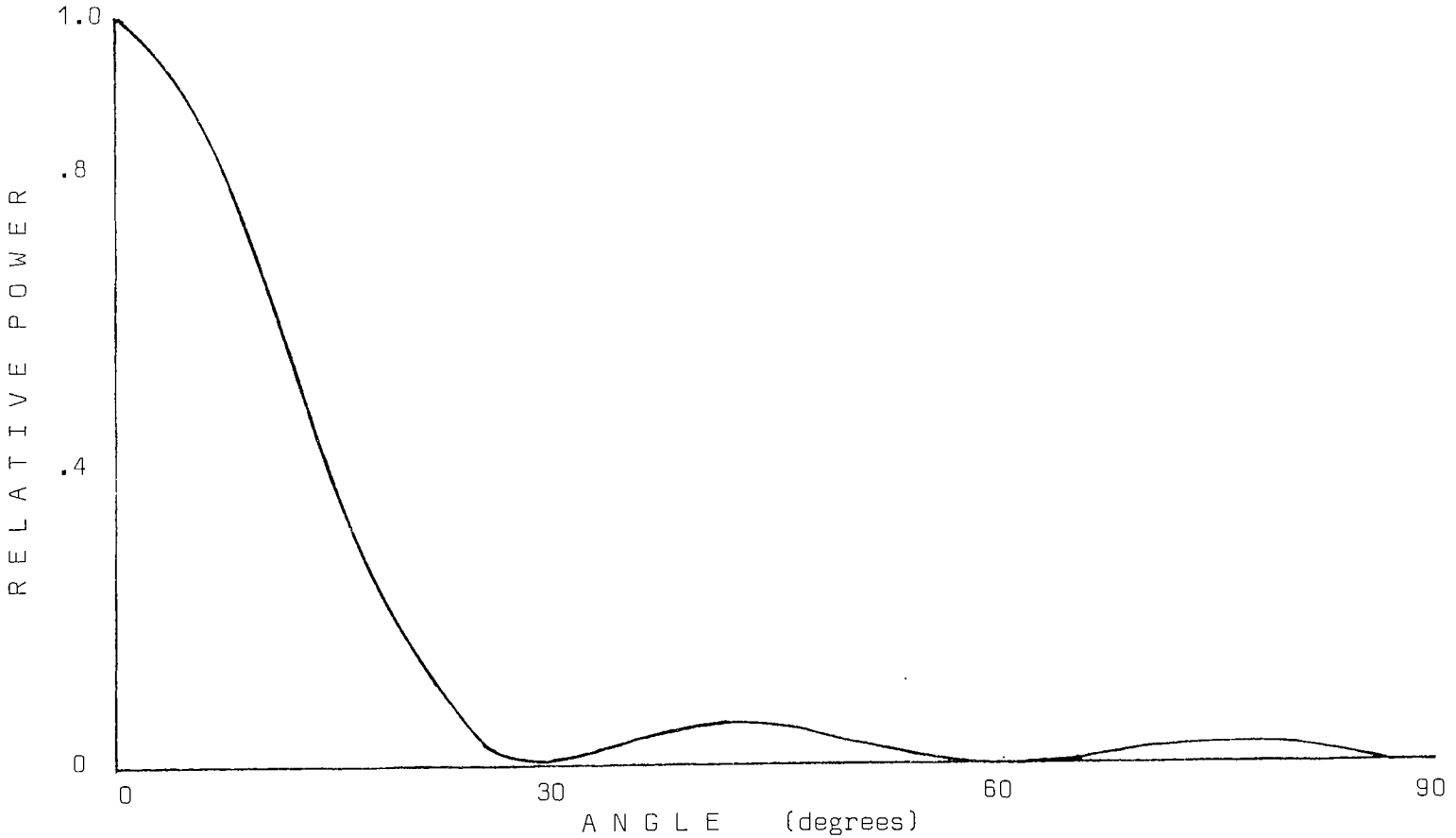

Figure 2.51 Filter Factor for 12 Point Moving Average Process

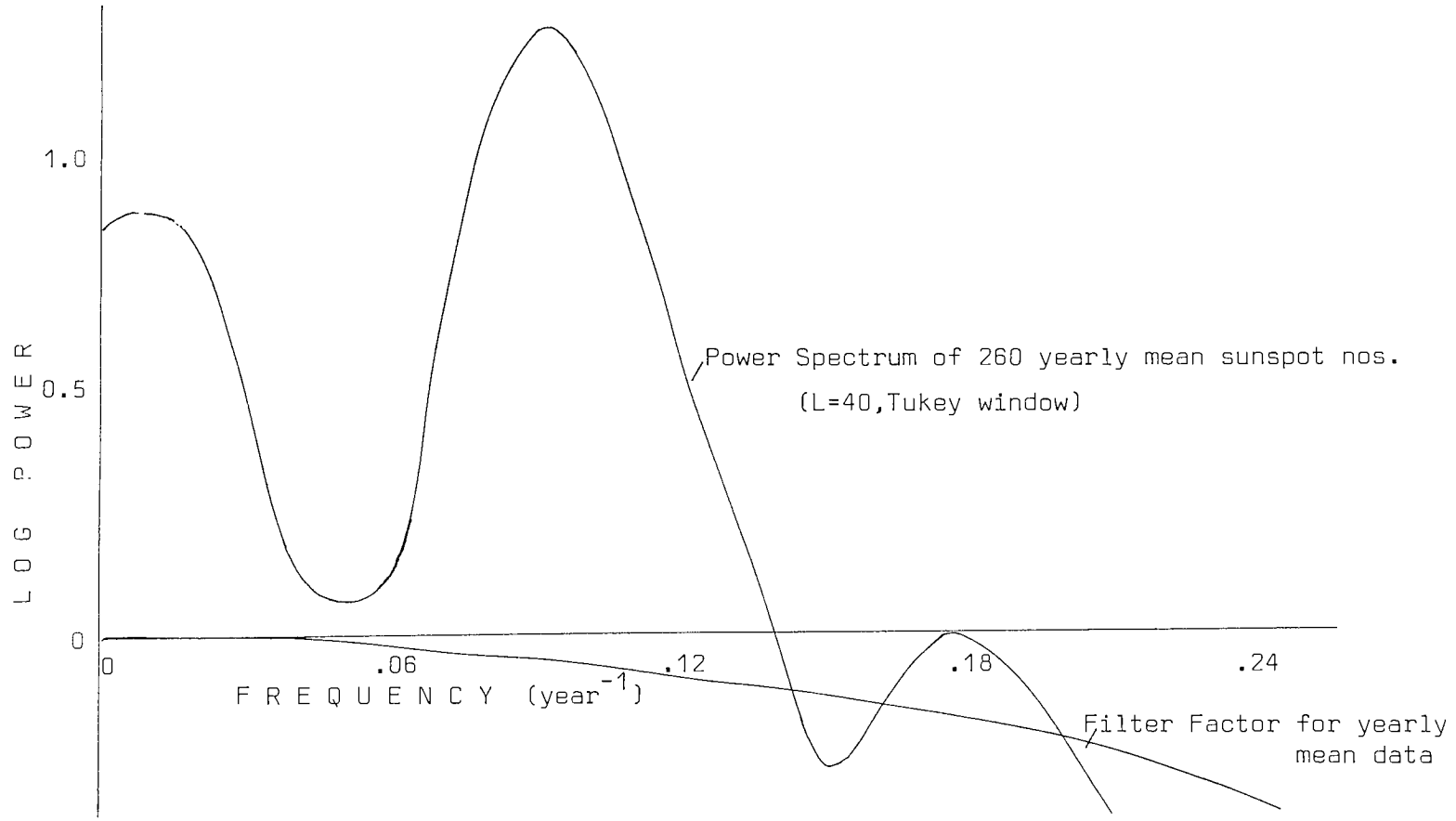

Figure 2.52 Effect of Filter Factor (figure 2.51) on Typical Sample of Yearly Mean Sunspot Numbers

Thus, filtering data can create or remove peaks and troughs from an input spectrum.

Consider the effect of averaging the monthly sunspot data to obtain the widely used yearly mean numbers. The operator $\psi(z)$ will be given by

$$\psi(z) = \frac{1}{12} \sum_{n=0}^{11} z^n$$

which yields a filter factor $F(\omega)$:

$$F(\omega) = \frac{1}{12}\left[6 + 11\cos\omega + 10\cos 2\omega + 9\cos 3\omega + 8\cos 4\omega + 7\cos 5\omega + 6\cos 6\omega + 5\cos 7\omega + 4\cos 8\omega + 3\cos 9\omega + 2\cos 10\omega + \cos 11\omega \right]$$

shown in Figure 2.51. Clearly this filter factor 'boosts' the low frequencies with respect to the high frequencies, which are virtually eliminated as one would expect, but the effect is not uniform. Hence, it is important to be aware that the inevitable level of prefiltering with the sunspot data (daily numbers are subject to large random errors necessitating some level of smoothing) affects the resulting power spectrum in a non-uniform manner, and it is important to ensure that periodicities detected are much greater than the smoothing interval.

Figure 2.52 shows a typical power spectrum of 260 yearly sunspot numbers, with log power versus frequency. As $\ell n(G_{xx}) = \ell n(F) + \ell n(G_{uu})$ the use of logarithmic plots enables the effect of the filter factor to be subtracted from the spectrum of the smoothed data. At frequencies as low as .1 c/year there is clearly a significant loss of power due to the effect of prefiltering, an effect which is appreciable at frequencies as low as .07 c/year. This effect is particularly important in series such as the sunspot series, where the accuracy of the technique is pushed as far as possible to gain the maximum amount of information with very limited data and where, as shown, the height required for a peak to be considered real (here to 80% confidence) is only just attained.

2.6 Detailed Analysis

Much statistical work modelling the sunspot cycle is done using the smoothed monthly sunspot number tabulated by Waldmeier (1961). Because of the 'Filter Factor' effect, these figures are of limited use for time series analysis, as they are calculated using a 6 month running mean. Thus it is best to use the unsmoothed monthly sunspot numbers (Waldmeier, 1961),and construct an appropriate level of smoothing as required.

Accordingly, 3-month-mean sunspot numbers were calculated for the interval 1790-1960, as it was considered that this was the highest level of data pre-smoothing compatible with the above conditions. As the sunspot numbers prior to 1800 are known to be approximate, involving appreciable amounts of interpolation (Eddy, 1977; Morris, 1977),this early data was excluded from the analysis. The remaining data set, estimated as fairly reliable (Eddy, 1977) was then divided into two groups of 80 years, to see if any statistical differences could be detected between early and more recent sunspot cycles.

After computing the autocovariance function and checking for convergence, power spectra were calculated for the 3-month-mean sunspot numbers 1799-1878, for lag windows at L = 40 and L = 80 (figure 2.61),and for frequency range $.001 \leq f \leq .3$ c/yr. Intermediate spectra were then produced for L = 60 and L = 70 (figure 2.62), as lag value L = 80 was found to be the highest lag value yielding meaningful results. All the curves obtained are of necessity considerably smoothed, with only one significant peak at ~ .09 c/yr. Considerable power is present at low frequencies and on the peak, with very little present towards the high-frequency end of the spectrum; this lack of power can not be ascribed to the filter factor effect.

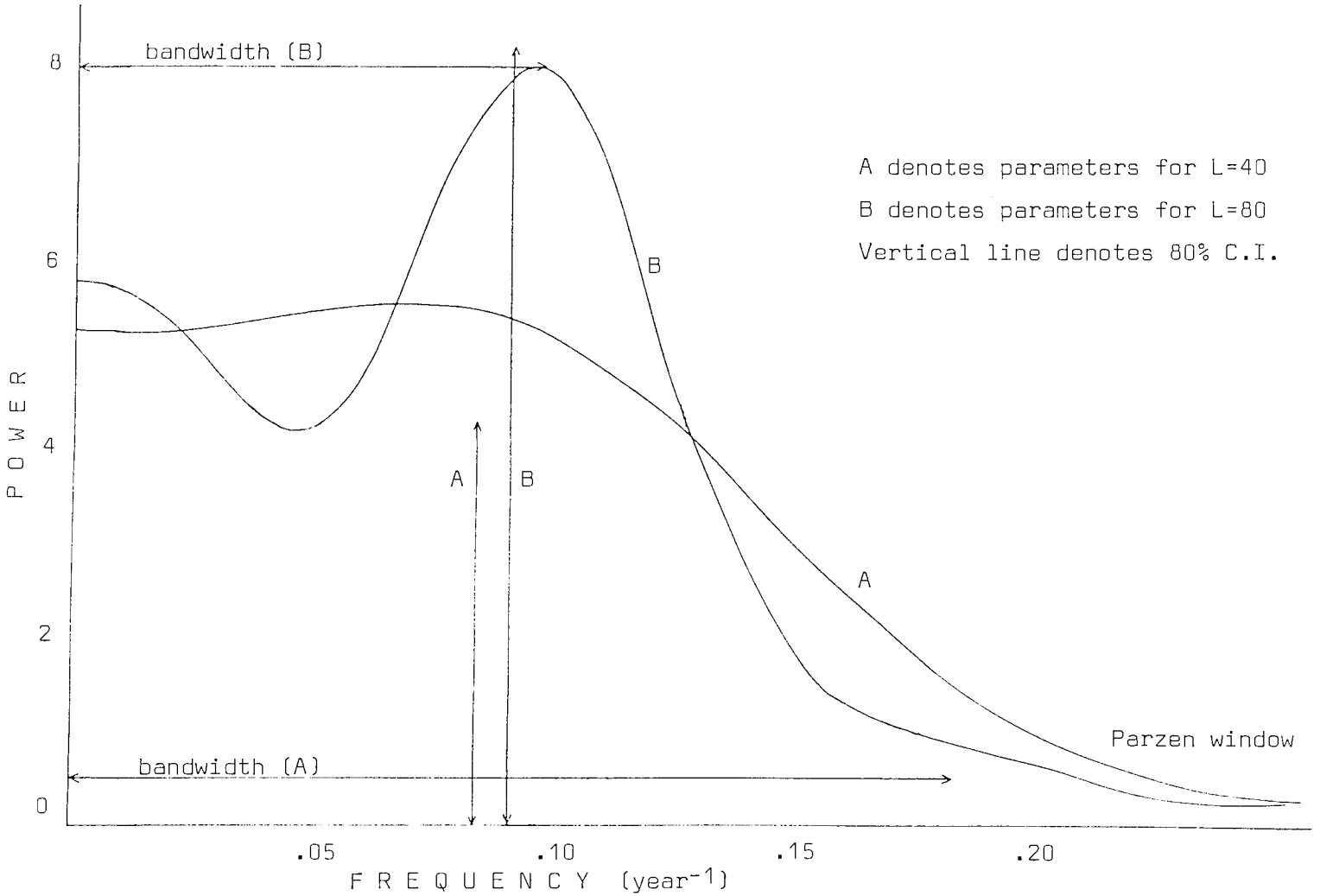

Figure 2.61 Power Spectrum of Three-Month Mean Sunspot Numbers in Interval 1799-1878

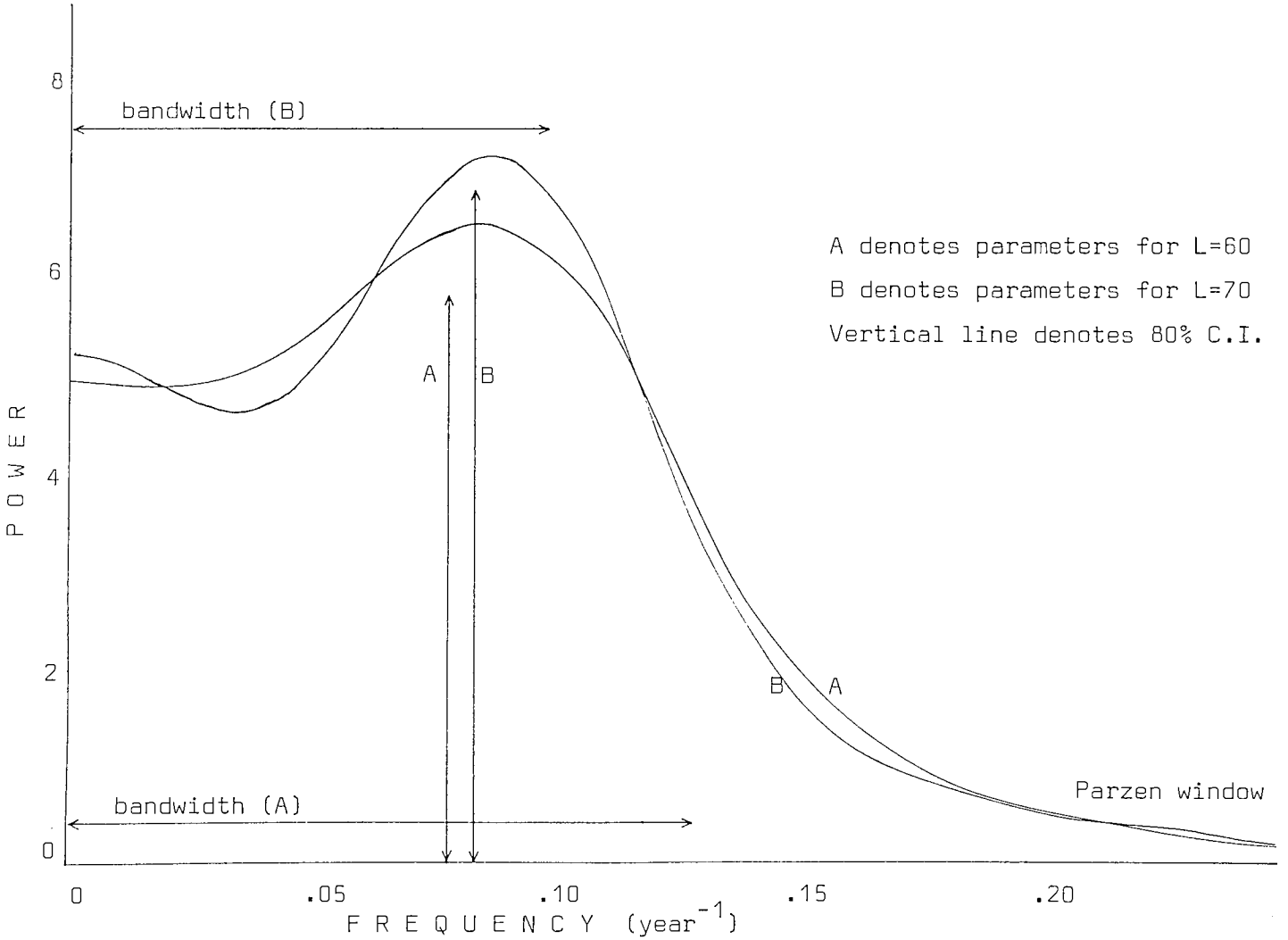

Figure 2.62 Power Spectrum of Three-Month Mean Sunspot Numbers in Interval 1799-1878

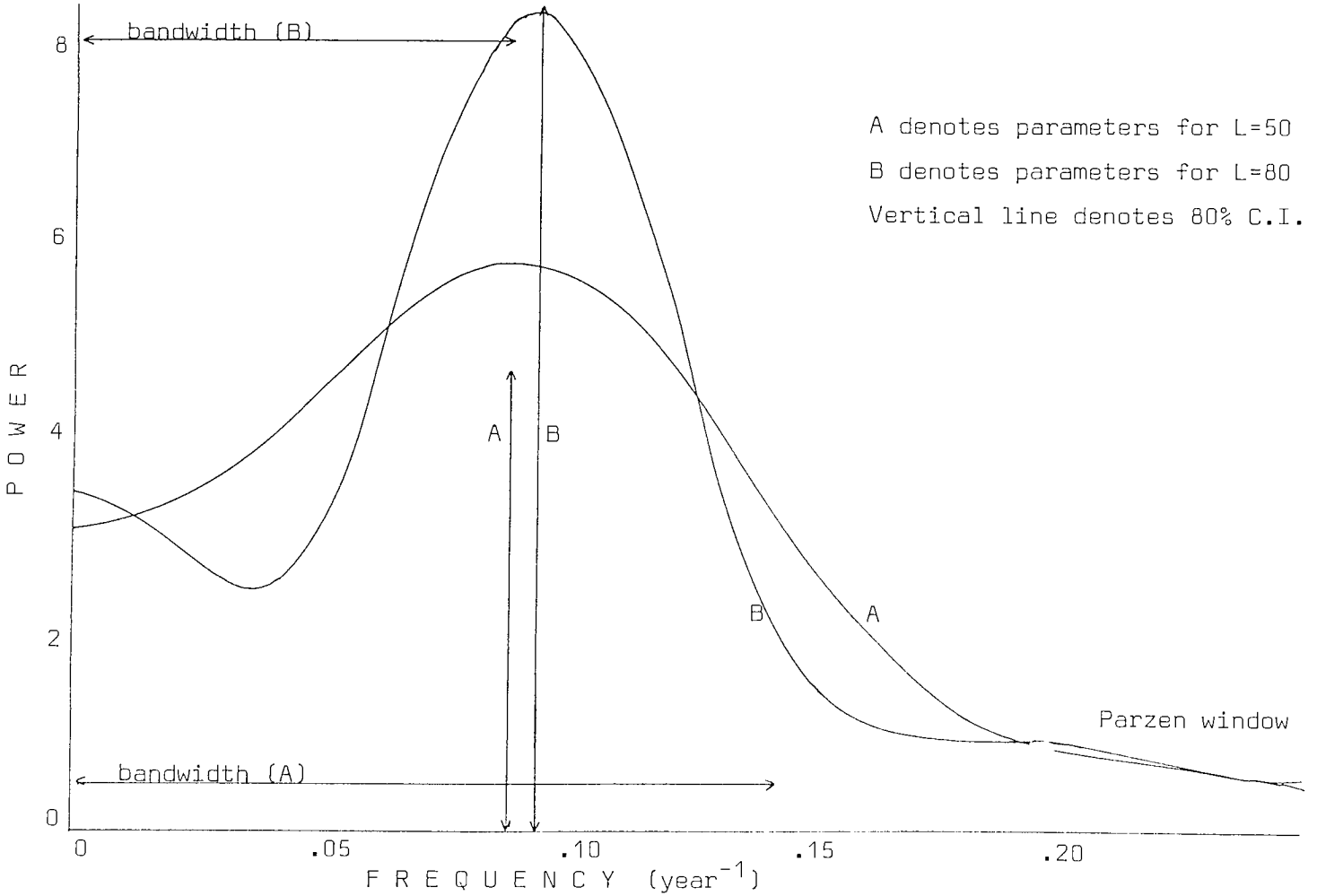

Figure 2.63 Power Spectrum of Three-Month Mean Sunspot Numbers in Interval 1878-1957

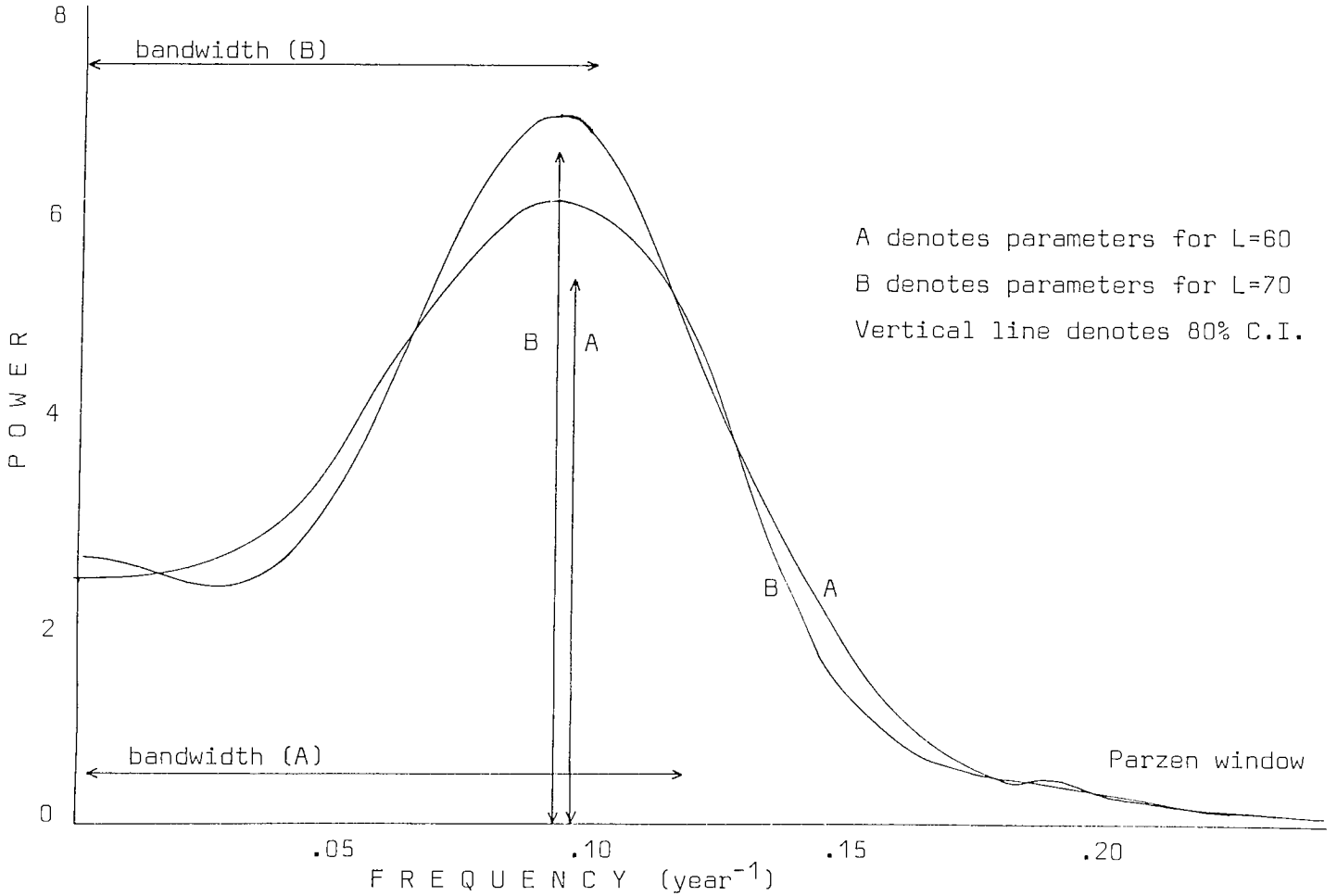

Figure 2.64 Power Spectrum of Three-Month Mean Sunspot Numbers in Interval 1878-1957

Plots were then drawn of log (power) vs frequency, so that the confidence interval could be simply represented for all frequencies, but these were not found to be helpful for such smooth power spectra.

In a similar manner, the sunspot data from 1878-1957 was analysed, and spectra calculated for a range of window widths, over the same frequency interval as before (figures 2.63, 2.64). These spectra have little power at low frequencies, with the majority of the power in the spectra contained in the large peak at ~.10 cy/yr. Again, activity at high frequencies is not apparent.

Comparison of the two sets of spectra indicates significant differences between the curve shapes and power distributions, with the 'early' data showing considerable power at low frequencies, and a broader peak. However, the difference in the frequency of peak power is not significant.

In order to use the greatest amount of available information it was decided to repeat the entire analysis using less smoothed data. Because of the large random fluctuations inherent in daily sunspot numbers, and the enormous amount of data involved, it was not considered practicable to analyse this sunspot data in raw form. It was found that a smoothing interval of one month was sufficient to average out these random effects, and so analyses were performed on the monthly sunspot numbers from 1799-1878 and 1878-1957, for a frequency interval $0.03 \leq f \leq 0.40$ c/yr, and a range of lag windows from L = 150 to L = 200.

Spectra from the 'early' data are plotted in figures 2.65 and 2.66. The greater precision of the data used is seen to result in better definition of the peak at ~ .09 c/yr; the overall structure is similar to that previously obtained, with considerable power contained at low frequencies. The spectra of the 'recent' sunspot

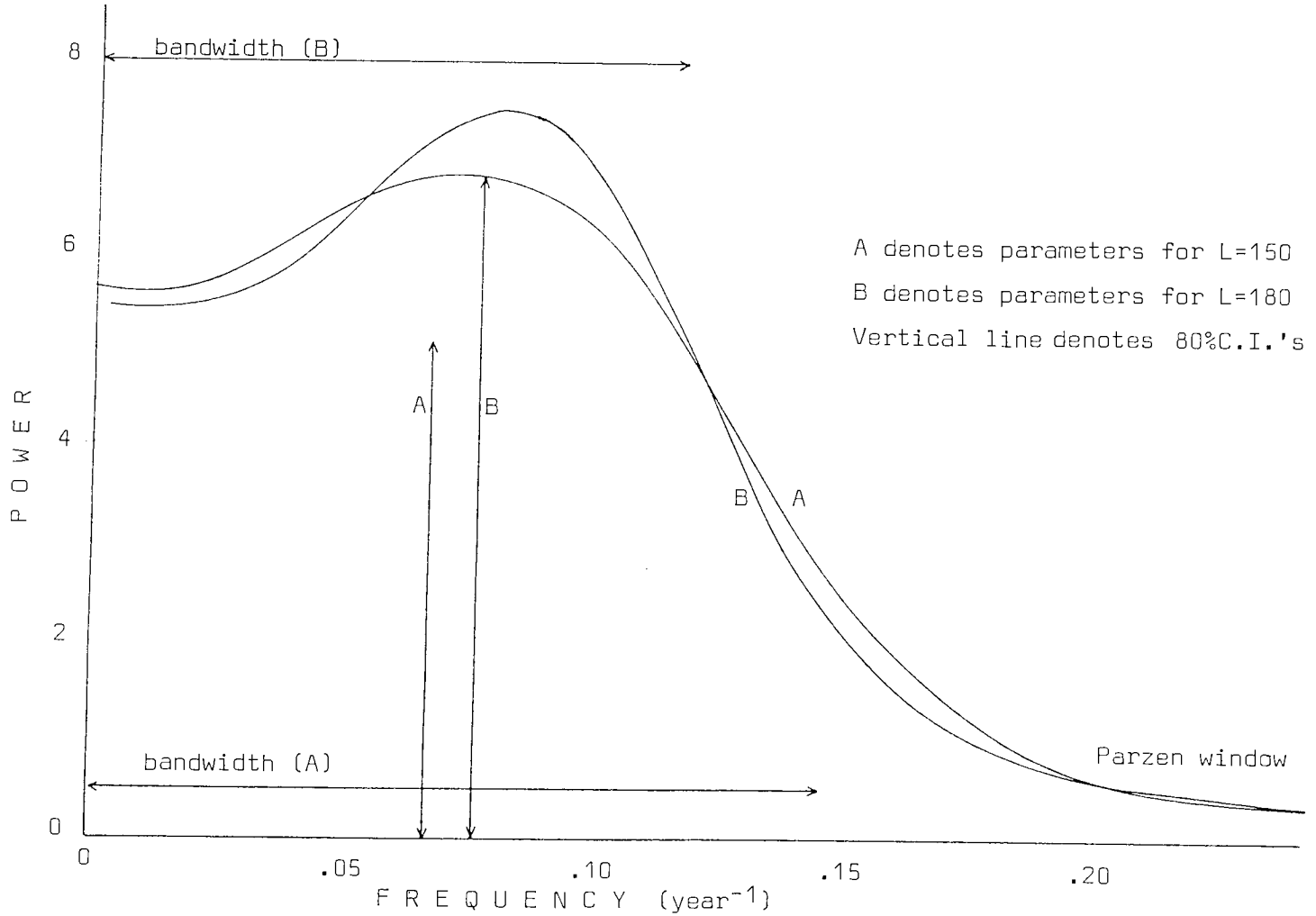

Figure 2.65 Power Spectrum of 960 One-Month Mean Sunspot Numbers in Interval 1799-1878

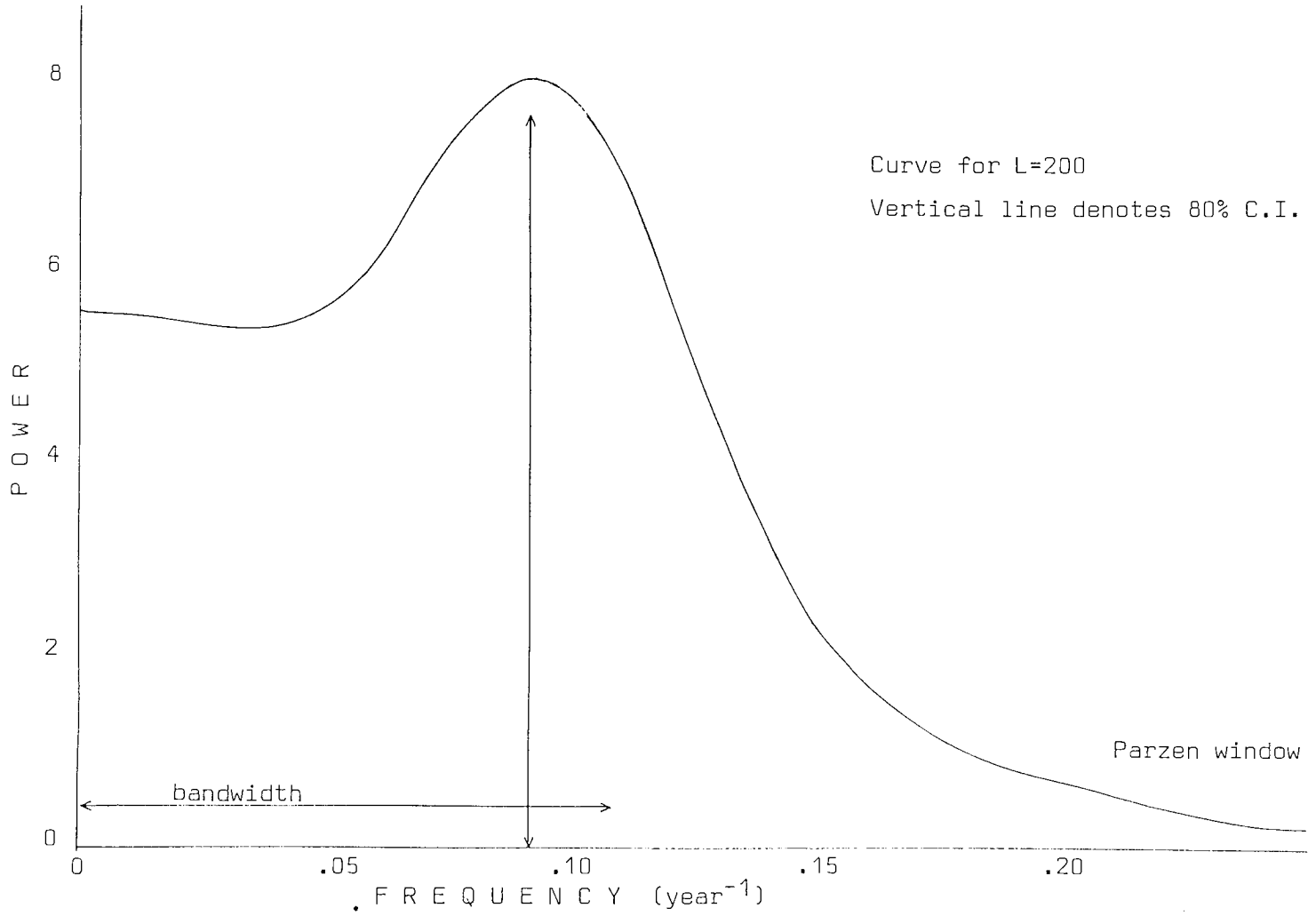

Figure 2.66 Power Spectrum of 960 One-Month Mean Sunspot Numbers in Interval 1799-1878

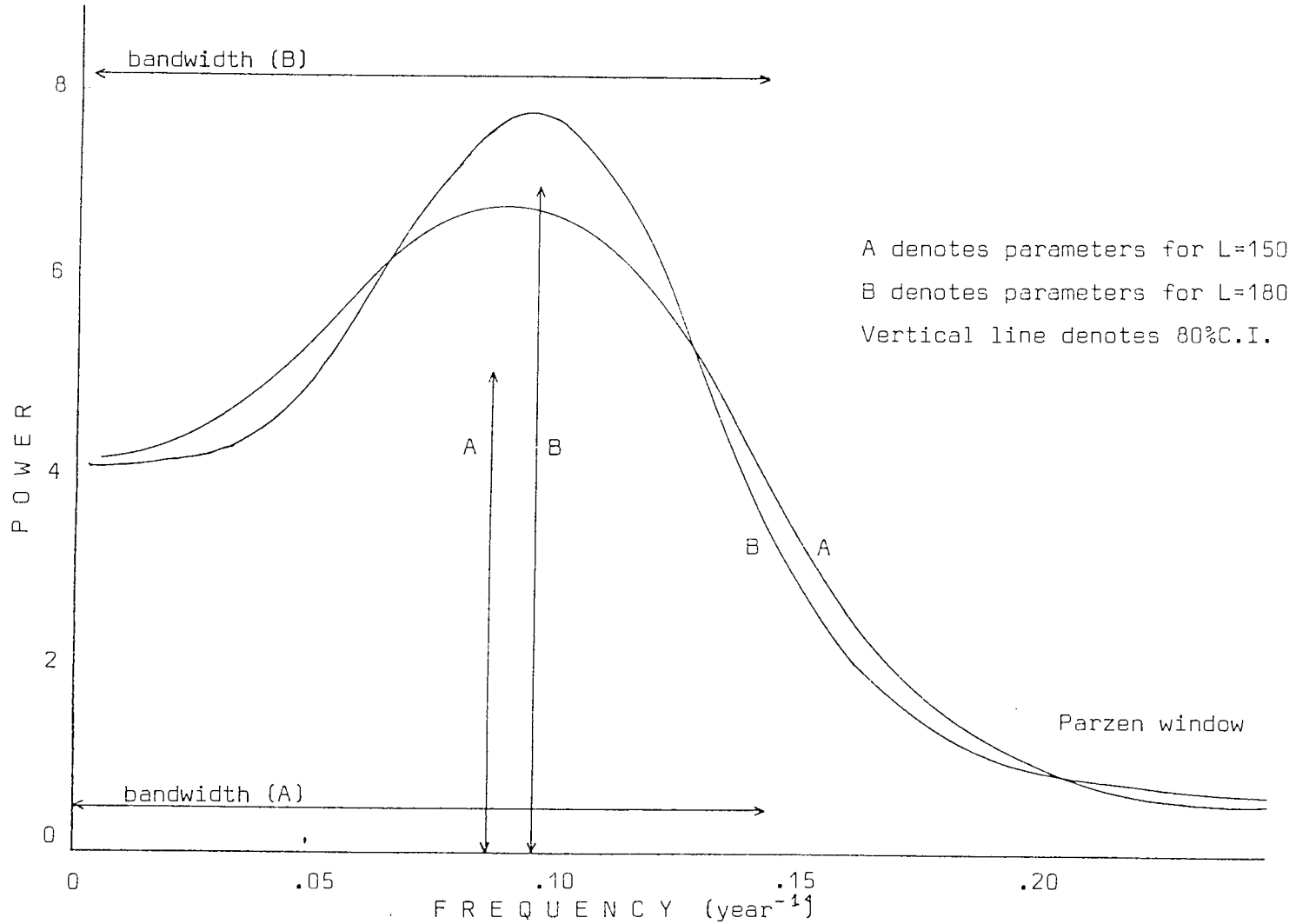

Figure 2.67 Power Spectrum of 960 One-Month Mean Sunspot Numbers in Interval 1878-1957

numbers are also similar to those previously obtained (figures 2.67, 2.68); comparison of the two series of spectra calculated from monthly sunspot numbers indicates that the differences observed from analysis of the 3 month mean sunspot numbers are still present.

The autocorrelation function was then computed for the entire data interval 1800-1960 for the monthly sunspot numbers, and several series of spectra were obtained; very little additional information was gained, the resulting graphs being an amalgam of the previous results. A better definition of the peak was evident (figure 2.69) but, for all lag windows considered, there was no indication of any peak in the spectrum at any frequency other than .01 c/yr.

2.7 Discussion

The results of this study of the Waldmeier sunspot numbers call into question the reality of 'periodicities' previously reported within the eleven year sunspot cycle (Cole, 1973; Currie, 1973; Cohen and Lintz, 1974; Hill, 1977; Wittmann, 1978;Lomb and Anderson, 1980; de Meyer, 1981) particularly as the results obtained by Cole (1973) formed a basis for subsequent research (e.g. Cohen and Lintz, 1974; Wolff, 1976; Lomb and Anderson, 1980; de Meyer, 1981). Results obtained using the method of Maximum Entropy Spectral Analysis (Currie, 1973; Cohen and Lintz, 1974; Wittmann, 1978) are weakened by the observed dependence of periodicities detected on the sample size used (Smythe and Eddy, 1977; Wittmann, 1978; de Meyer, 1981). This observation may be explained if the 'peaks' are caused by random components in the sunspot data. The negative results from an analysis of Russian sunspot numbers by Hill (1977) support this hypothesis.

In the work of Lomb and Anderson (1980) the fitting of high order sine waves results in the identification of ten closely spaced peaks around the frequency 0.1 cycles/year, an effect easily

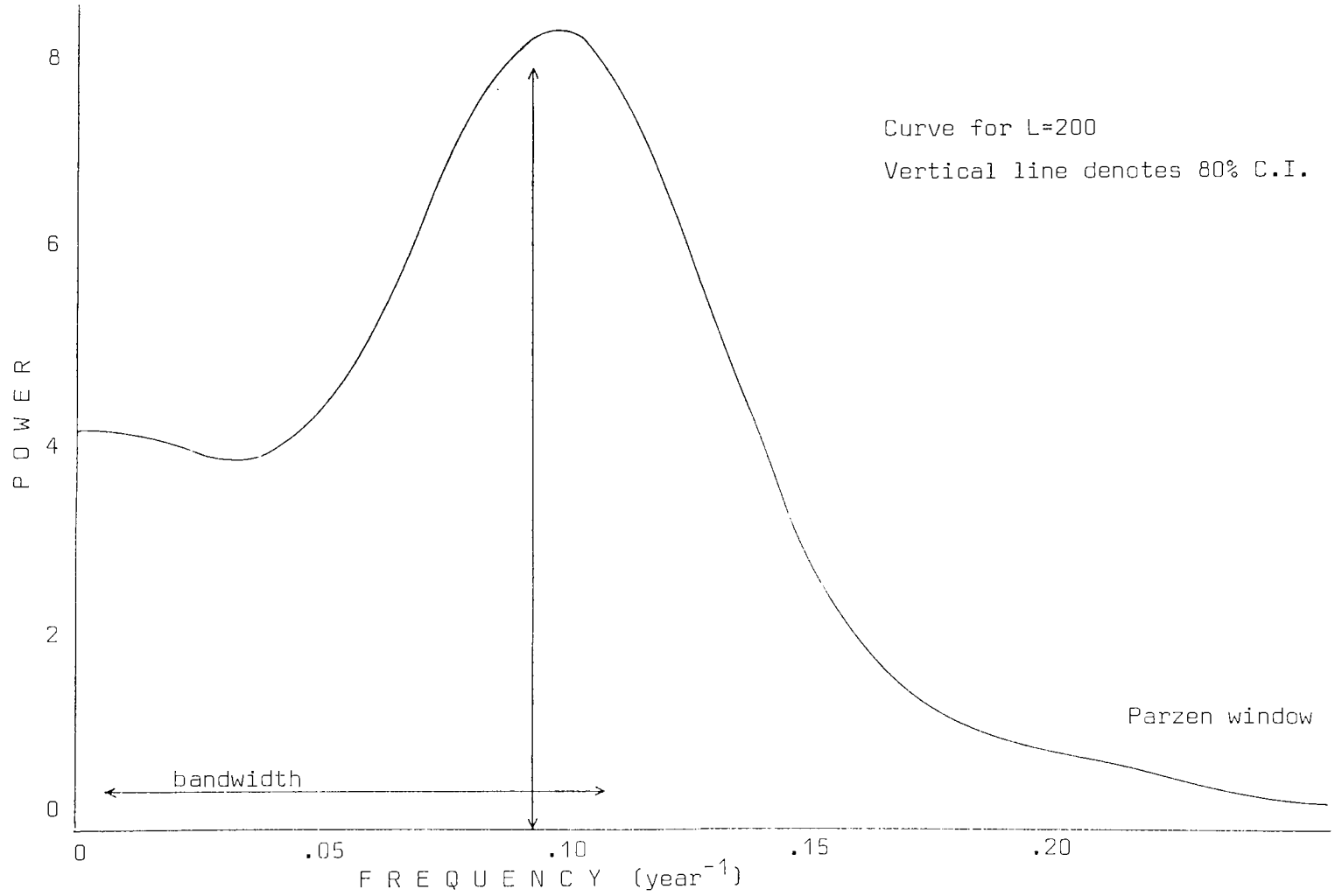

Figure 2.68 Power Spectrum of 960 One-Month Mean Sunspot Numbers in Interval 1878-1957

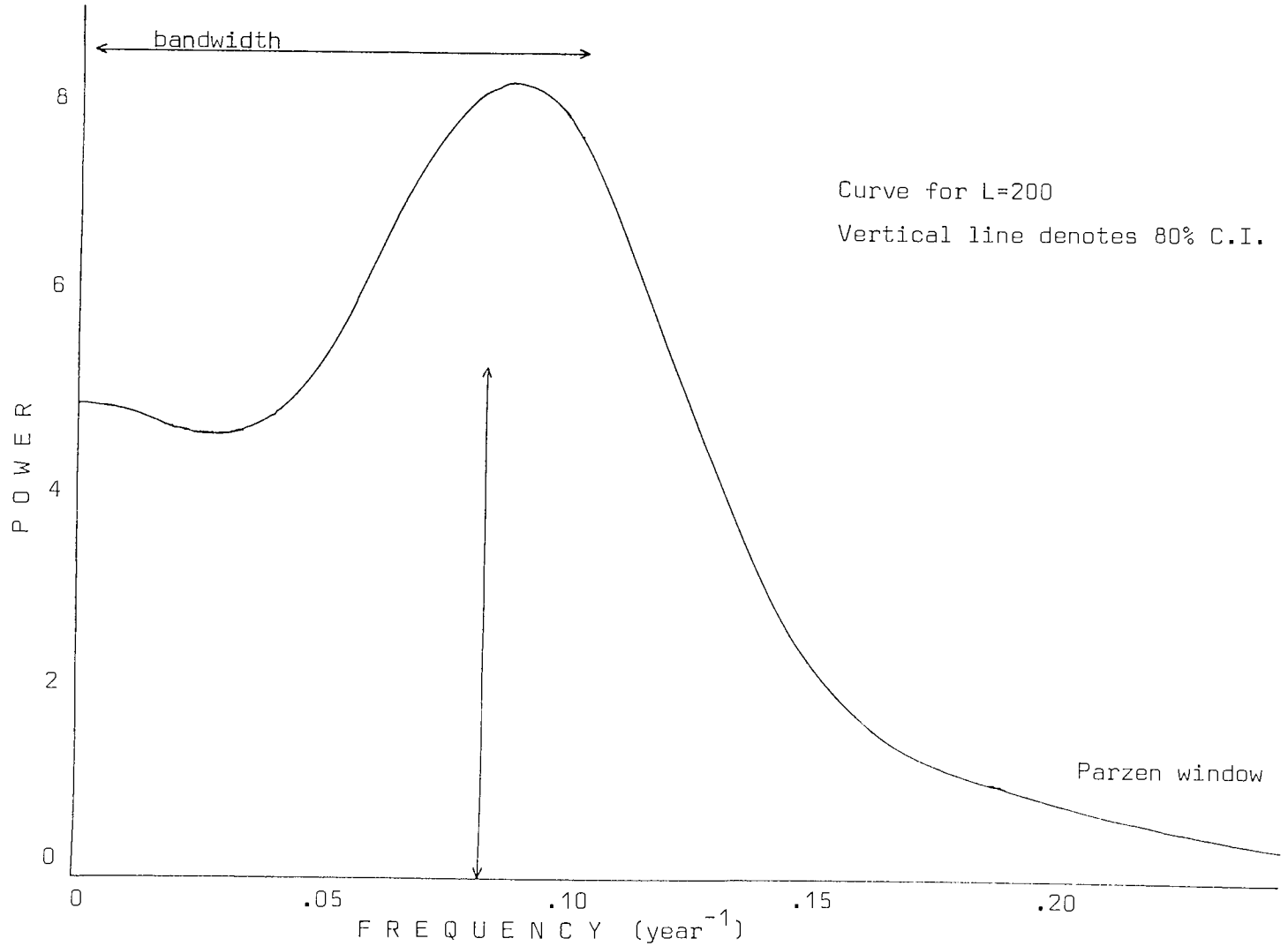

Figure 2.69 Power Spectrum of 1920 One-Month Mean Sunspot Numbers in Interval 1800-1960

produced by this method when the 'true' power is, in reality, spread over a wide frequency interval, generating a broad peak in the actual power spectrum. It is also noted that in the analysis of Lomb and Anderson (1980) the spectrum of 'residual power' remaining after the removal of all 'significant' periodicities contains peaks of a height comparable to peak heights assigned to 'real' effects. It is thus difficult to attribute real significance to most of the features in the spectra obtained, and, as no calculations for the considerable effects of aliasing (Bracewell, 1965) are reported, further work in this area is required before the existence of any of the periodicities reported can be accepted. It is here suggested that all the many short 'periodicities' detected to date within the eleven year variation are illusory, and can be attributed to the often cursory and conflicting interpretation of the results obtained, the lack of proper statistical tests for significance throughout, and the use of unsuitable highly smoothed sunspot numbers. To analyse such data effectively requires both a critical evaluation of 'peaks' in the power spectra, and an awareness that the use of any mathematical algorithm to derive hidden periodicities from data invokes the possibility that the generated periodicities are introduced either by the particular numerical method used or by the time interval analysed.

It is clear that the limiting factor in statistical analysis of the Waldmeier sunspot numbers is the restricted amount of 'noisy' data avaiable. However, the detailed examination of 160 years of monthly unsmoothed sunspot numbers does reveal differences between 'early' and 'recent' data, evidence which supports the general arguments of McNish and Lincoln (1949) and Slutz (1970), and is in agreement with the results in Section 1. The results of this section thus support the hypothesis that long term effects are modulating the sunspot cycle.

One interpretation of the variation in mean period discussed in Section 1 is to assume the existence of two discrete solar cycles of 11.1 yr and 10.5 yr. Simple sinusoidal models of the form

$$R^* = A\cos(2n\omega_1 t) + B\cos(2\pi\omega_2)$$

with $\left.\begin{aligned}\omega_1 &= 11.08 \text{ years} \\ \omega_2 &= 10.05 \text{ years}\end{aligned}\right\}$ and various values of A and B

give quite a good facsimile of the sunspot cycle for ratio A : B of $\sim$10 : 4, and the sunspot 'number' R* normalized to the scale of the Wolf number. The beat period of R* is then about 200 years, in agreement with the periodicity detected in auroral data in Section 1. Clearly, a more complex and realistic model is required in this area; with the limited amount of noisy data available, it is difficult to test such a model against observation adequately; however, it is possible that the 'sunspot cycle' consists in reality of two discrete cycles, at $\sim$11.1 years and $\sim$10.5 years.

SECTION 3

Databases for Planetary Motion

In order to evaluate possible connections between the planets and the sunspot cycle, it is essential to have access to accurate planetary coordinates, which may be required over an extended period of time. Such information is readily available for only a limited period, for example in magnetic tape form from 1800 AD to 2000 AD (Greenwich Observatory).

For the inner planets, over a few hundred years analytic techniques are accurate to well within one degree (Sinclair, pers. comm). Use of a numerical integration process for the inner planets necessitates a short step-length, rendering the computing time required prohibitive, especially if Mercury is included in the calculation (Schubart and Stumpff, 1966). Whilst an algorithm for the positions of Jupiter and Saturn is presently available which is accurate to 1' in angle and .001 AU in distance over a period of a few hundred years (Emerson,1981), a requirement for the co-ordinates of all the giant planets necessitates the use of another method.

It was thus decided to consider methods for numerical integration of the differential equations of planetary motion both to provide an extended database of planet positions if required, and to enable the construction of an 'alternate solar system' with slightly different orbital elements. This database could then be used as a 'control system' to help assess the validity of any correlations found between sunspots and parameters of planetary motion.

It was not expected that Pluto would exert sufficient effect on any such parameters to justify its inclusion; whilst numerical integration of

the equations of motion for the planets Jupiter, Saturn, Uranus and Neptune excluding the effect of Pluto would produce errors in the resulting coordinates, these errors should be small over the timescale considered (Schubart and Stumpff, 1966).

As preliminary calculation indicated that Mars would not make a significant contribution to the solar system models under consideration, it was decided to omit Mars from the initial calculations, with the option of including the planet at a later stage if required.

To integrate the differential equations of motion for the outer planets, a predictor-corrector method was chosen because of the small number of derivative evaluations required at each step; the restrictions on variation of step length being unimportant in this context (Merson, 1975; Johnson, 1982). The Gauss-Jackson eighth order method (Jackson, 1924; Herrick, 1972; Merson, 1975) was chosen because other applications of the method indicated that it would be efficient at integrating orbital equations of this type (Merson, 1975; Sinclair, pers.comm.).

3.1 The Gauss-Jackson Integrator

In order to use an 8th order predictor-corrector method for integrating the system of equations

$$\ddot{y}_i = f_i(t, y_1, y_2, \ldots y_n, \dot{y}_1, \dot{y}_2, \ldots \dot{y}_n) \quad i = 1, 2, \ldots n$$

where t is time,

the starting values $y_{i,k}$, $\dot{y}_{i,k}$, $\ddot{y}_{i,k}$ $\quad k = 0, 1, \ldots 8$

must be available and a difference table obtained to 8th order.

From the starting values, it is first necessary to determine the first and second sums of the f_i at the first point at which they may be calculated to 8th order.

Since $D\,\dot{y}_{i,k} = f_{i,k}$ and $D^2 y_{i,k} = f_{i,k}$

where $D = d/dt$ then (assuming integration constants zero)

$$\nabla^{-1} f_{i,k} = h^{-1} y_{i,k} + (\nabla^{-1} - (hD)^{-1}) f_{i,k} \qquad 3.1(I)$$

and

$$\nabla^{-2} f_{i,k-1} = \delta^{-2} f_{i,k}$$
$$= h^{-2} y_{i,k} + (\delta^{-2} - (hD)^{-2}) f_{i,k} \qquad 3.1(II)$$

where ∇ is the backward difference operator,

δ is the central difference operator

and $h = t_{k+1} - t_k$ is the tabular interval.

Substituting to obtain the above relations in terms of central difference δ using the relations

$\nabla^{-1} = \frac{1}{2} + \mu\delta^{-1}$, $\mu = (1 + \frac{1}{4}\delta^2)^{\frac{1}{2}}$, $hD = 2\sinh^{-1}(\delta/2)$

yields $\nabla^{-1} f_{i,k} = h^{-1} y_{i,k} + \frac{1}{2} f_{i,k} + \mu \left\{ \delta^{-1} - \frac{1}{2}(1 + \frac{1}{4}\delta^2)^{-\frac{1}{2}} (\sinh^{-1}\delta/2)^{-1} \right\} f_{i,k}$

and

$$\nabla^{-2} f_{i,k-1} = h^{-2} y_{i,k} + \left\{ \delta^{-2} - \tfrac{1}{4} (\sinh^{-1}\delta/2)^{-2} \right\} f_{i,k} .$$

Consider the expansion $\sinh^{-1}\delta/2 = \delta/2 \left(1 - \frac{\delta^2}{3.8} + \frac{3\delta^4}{4.5.32} - \ldots \right)$.

Now $(\sinh^{-1}\delta/2)^{-2} = 4\delta^{-2} (1 + 2x + 3x^2 + \ldots)$

where $x = \frac{\delta^2}{3.8} - \frac{3\delta^4}{4.5.32} + \ldots$.

Hence $\frac{1}{4} (\sinh^{-1} \delta/2)^{-2} = \delta^{-2} \left(1 + \frac{\delta^2}{12} - \frac{\delta^4}{240} + \frac{31\delta^6}{60480} - \frac{289}{3628800} \delta^8 + \frac{317}{22809600} \delta^{10} \ldots \right)$

Thus $\nabla^{-2} f_{i,k-1} = h^{-2} y_{i,k} + \left(-\frac{1}{12} + \frac{1}{240} \delta^2 \ldots \right) f_{i,k}$. $\qquad 3.1(III)$

Similarly, $(\sinh^{-1} \delta/2)^{-1} = \left(1 + \frac{\delta^2}{24} - \frac{17\delta^4}{5760} + \ldots \right) .2\delta^{-1}$

and hence

$$\nabla^{-1} f_{i,k} = h^{-1} y_{i,k} + \left(\frac{1}{2} + \frac{1}{12} \mu\delta - \frac{11}{720} \mu\delta^3 + \ldots \right) f_{i,k} . \qquad 3.1(IV)$$

For convenience, the above relations are often expressed in terms of backward differences, so that 3.1(IV) becomes

$$\nabla^{-1} f_{i,k} = h^{-1} \dot{y}_{i,k} - A_0 f_{i,k} - A_1 \nabla f_{i,k+1} - A_2 \nabla^2 f_{i,k+1} - A_3 \nabla^3 f_{i,k+2}$$
$$- A_4 \nabla^4 f_{i,k+2} - \ldots\ldots \qquad 3.1(V)$$

where coefficients A_0 to A_8 are tabled in Table 3.11. 3.1(VI)

Similarly 3.1(III) may be written

$$\nabla^{-2} f_{i,k-1} = h^{-2} y_{i,k} - B_0 f_{i,k} - B_2 \nabla^2 f_{i,k+1} - B_4 \nabla^4 f_{i,k+2} - B_6 \nabla^6 f_{i,k+3}$$
$$- B_8 \nabla^8 f_{i,k+4}$$

where coefficients B_0 to B_8 are given in Table 3.11.

The pattern for this 8th order process is shown in Table 3.12. It is clearly possible to use equations 3.1(V), 31.(VI) to calculate the first and second sums $\nabla^{-1} f_{i,j}$, $\nabla^{-2} f_{i,j}$.

To continue the table, a predictor of y_i is required. Rewriting equation 3.1(I) for $f_{i,k}$ yields

$$\dot{y}_{i,k+1} = h \nabla^{-1} f_{i,k} + h \left[(hD)^{-1} E - \nabla^{-1}\right] f_{i,k} \qquad 3.1(VII)$$

and from equation 3.1(II), the relation

$$\nabla^{-2} f_{i,k} = h^{-2} y_{i,k+1} + (\delta^{-2} - (hD)^{-2}) E f_{i,k} .$$

Hence, $y_{i,k+1} = h^2 \nabla^{-2} f_{i,k} + h^2 \left[(hD)^{-2} - \delta^{-2}\right] E f_{i,k}$. 3.1(VIII)

Transforming to backward differences

$$\dot{y}_{i,k+1} = h\nabla^{-1} f_{i,k} + h\left[(-\ell n(1 - \nabla))^{-1} (1 - \nabla)^{-1} - \nabla^{-1}\right] f_{i,k} \qquad 3.1(IX)$$

$$y_{i,k+1} = h^2 \nabla^{-2} f_{i,k} + h^2 \left[(- \ell n(1 - \nabla))^{-2} (1 - \nabla)^{-1} - \nabla^{-2}\right] f_{i,k} \qquad 3.1(X)$$

Now $\dfrac{-1}{\ln (1 - \nabla)} = \nabla^{-1} - \frac{1}{2} - \dfrac{\nabla}{12} - \dfrac{\nabla^2}{24} - \ldots\ldots$

and $(1 - \nabla)^{-1} = 1 + \nabla + \nabla^2 + \ldots$

Thus expanding equation 3.1(IX) yields

$$\dot{y}_{i,k+1} = h\nabla^{-1} f_{i,k} + h\left(\tfrac{1}{2} + \frac{5}{12} \nabla + \frac{9}{24} \nabla^2 + \frac{251}{720} \nabla^3 + \ldots . \right)$$

ie $$\dot{y}_{i,k+1} = h\left(\nabla^{-1} f_{i,k} + F_0 f_{i,k} + \sum_{j=1}^{8} f_j \nabla^j f_{i,k}\right) \qquad 3.1(XI)$$

Table 3.11

Coefficients for an eighth order Gauss-Jackson process

j	A_j	B_j	F_j
0	- 1/2	1/12	1/2
1	- 1/12	0	5/12
2	1/24	- 1/240	3/8
3	11/720	0	251/720
4	- 11/1440	31/60480	95/288
5	- 191/60480	0	19087/60480
6	191/120960	- 289/3628800	5257/17280
7	2497/3628800	0	1070017/3628800
8	- 2497/7257600	317/22809600	25713/89600

where the coefficients F_i are given in Table 3.11. Similarly, expanding

$$(-\ell n\ (1 - \nabla))^{-2} = \nabla^{-2}\left[1 - \nabla + \frac{\nabla^2}{12} - \frac{1}{240}\nabla^4 + \ldots\right]$$

and substituting expansions into equation 3.1(XI) yields, after reduction,

$$y_{i,k+1} = h^2\,\nabla^{-2} f_{i,k} + h^2\left[\frac{1}{12} + \frac{\nabla}{12} + \frac{19}{240}\nabla^2 + \frac{18}{240}\nabla^3 + \frac{4315}{60480}\nabla^4 + \frac{4125}{60480}\nabla^5 + \frac{237671}{3628800}\nabla^6 + \frac{229124}{3628800}\nabla^7 + \frac{9751299}{159667200}\nabla^8\right] f_{i,k}$$

ie. $$y_{i,k+1} = h^2\left[\nabla^{-2}{}_{i,k} + C_0 f_{i,k} + \sum_{j=1}^{8} C_j \nabla^j{}_{i,k}\right] \qquad 3.1(XII)$$

where coefficients C_j are given in Table 3.13.

Thus, using $\nabla^s f_{i,8}$, $i = -2, \ldots 8$, $y_{i,9}$ and $\dot{y}_{i,9}$ may be found; substitution in the acceleration formulae then yields $f_{i,9}$. A new row of differences $\nabla^s f_{i,9}$, $s = -2, \ldots 8$ are then calculated.

In many applications, the accuracy and stability of this sytem may be improved by the use of a corrector formula for $\dot{y}_{i,k+1}$ and $y_{i,k+1}$. From equation 3.1(VII),

$$\dot{y}_{i,k+1} = h\nabla^{-1} f_{i,k} + h\left[(hD)^{-1} - \nabla^{-1}E^{-1}\right] f_{i,k+1}$$

$$= h\nabla^{-1} f_{i,k} + h\left[(-\ell n\ (1 - \nabla))^{-1} - \nabla^{-1} + 1\right] f_{i,k+1} \cdot$$

This after expansion yields

$$\dot{y}_{i,k+1} = h(\nabla^{-1} f_{i,k} + \tfrac{1}{2} f_{i,k+1} - \frac{\nabla}{12} f_{i,k+1} - \frac{\nabla^2}{24} f_{i,k+1} \ldots\ .)$$

$$= h(\nabla^{-1} f_{i,k} + E_0 f_{i,k+1} + \sum_{j=1}^{8} E_j \nabla^j f_{i,k+1}) \qquad 3.1(XIII)$$

where coefficients E_j are given in Table 3.13.

Similarly, from equation 3.1(VIII)

$$y_{i,k+1} = h^2\,\nabla^{-1} f_{i,k} + h^2\left[(-\ell n\ (1 - \nabla))^{-2} - \nabla^{-2} + \nabla^{-1}\right] f_{i,k+1}$$

which after expansion yields

$$y_{i,k+1} = h^2\nabla^{-1} f_{i,k} + \left(\tfrac{1}{2} - \frac{1}{240}\nabla^2 - \frac{1}{240}\nabla^3 - \frac{221}{60480}\nabla^4 - \frac{190}{60480}\nabla^5 - \frac{9829}{3628800}\nabla^6 - \frac{8547}{3628800}\nabla^7 - \frac{330157}{159667200}\nabla^8 \ldots\right) f_{i,k+1}$$

Table 3.12

Pattern of Differences for an Eighth Order Gauss-Jackson Process

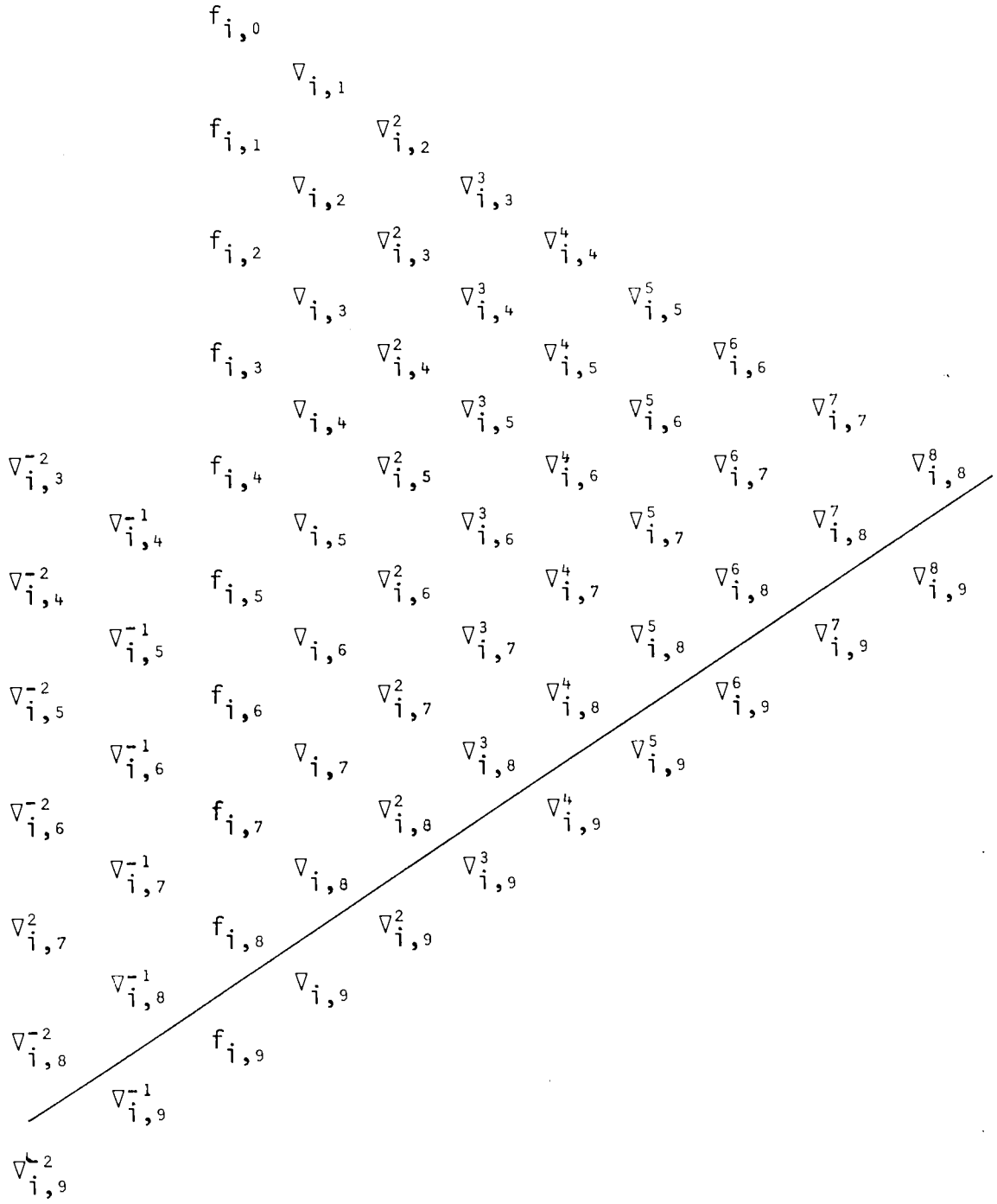

Table 3.13

Coefficients for an eighth order Gauss-Jackson process

j	C_j	E_j	G_j
0	1/12	1/2	1/12
1	1/12	- 1/12	0
2	19/240	- 1/24	- 1/240
3	3/40	- 19/720	- 1/240
4	863/12096	- 3/160	- 221/60480
5	275/4032	- 863/60480	- 19/6048
6	33953/518400	- 275/24192	- 9829/3628800
7	8183/129600	- 33953/3628800	- 407/172800
8	3250433/53222400	- 8183/1036800	- 330157/159667200
9	-	-	- 24377/13305600

or

$$y_{i,k+1} = h^2(\nabla^{-2} f_{i,k} + G_0\, f_{i,k+1} + \sum_{j=1}^{8} G_j\, \nabla^j f_{i,k+1}) \,, \qquad 3.1(XIV)$$

where constants G_i are given in table 3.12 and the term of ninth order (not calculated here) is retained for error estimation.

At this stage, it is often of use (Merson, 1975; Johnson, 1981) to reapply the corrector formulae 3.1(XIII), 3.1(XIV) to the output values of $y_{i,k+1}$ and $\dot{y}_{i,k+1}$. For the purpose of further integration, however, the once-corrected values are used. It should be noted that Herrick (1972) recommends a modification to the system which effectively dispenses with the corrector altogether.

3.2 Program Development

As a preliminary stage of development, it was decided to apply the Gauss-Jackson method to a system with known solution, both as a check on the numerical integrator itself and to enable estimation of the stability of the numerical solution. Calculation of the first few coefficients of each series and comparison with Merson (1975) had revealed a typing error in the sign for coefficient E_0, with the possibility (Merson, pers. comm.) of other trivial errors in the higher order terms. An independent calculation of all coefficients required for an eighth order process yielded fractions which reduced to those of Merson (1975); however, this additional check was considered useful.

The system chosen was of one 'planet' in undisturbed circular motion. Since this numerical process was to be applied to the outer planets only, the interval of integration required for Jupiter would determine the step-length required for the system; thus the hypothetical planet was given a mass and distance from the sun similar to those of Jupiter. For this simple model, the integrator was started directly, as analytic calculation of position and velocity components was easily achieved. Thus the Gauss-Jackson

process was initially set to solve the 3 equations

$$\frac{d^2y_i}{dt^2} = -\frac{\mu y_i}{r^3}, \quad i = 1, 2, 3, \quad r = (\Sigma y_i^2)^{\frac{1}{2}}, \quad \mu \text{ constant of gravitation.}$$

Circular motion was established by specifying the relationship

$\underset{\sim}{r}_i \dot{\underset{\sim}{r}}_i = 0$ where $\dot{r}_i = \frac{dr_i}{dt}$ between initial values.

The system was run for varying numbers of iterations and step lengths. Good agreement was found with the theoretical solution, and with the orbit modified to an ellipse, a value for h of 40 days was confirmed as easily adequate for this simple case. As numerical solutions using predictor-corrector methods eventually spin away from the theoretical solution, the system was run for a period of 50 years. No such effect was discernable. It was thus decided to proceed to integrate the equations of motion of a system of planets.

For this procedure, a starting table is required; it is necessary to use another numerical technique to generate data y_i, $\dot{y}_i$, $i = 1, 2, \ldots 8$, $j = 1, 2, \ldots n$ from initial conditions $y_{i,0}$ $\dot{y}_{i,0}$. It was decided initially to use a 4th order Runge-Kutta process, and to modify this later if necessary either to a non-standard R-K process (Merson, 1972) or to a linear multistep method (Johnson et al., 1982). To integrate a system of n first order equations

$$\frac{dy_i}{dt} = f_i(y_1, y_2, \ldots y_n) \quad i = 1, 2, \ldots n$$

the function evaluations for a 4th order R-K process may be written

$$K_{i1} = hf_i\ (y_{i,\ell} \cdots y_{n,\ell}),$$

$$K_{i2} = hf_i\ (\ldots., y_{j,\ell} + a_{21}\ K_{j1}, \ldots),$$

$$K_{i3} = hf_i\ (\ldots., y_{j,\ell} + a_{31}\ K_{j1} + a_{32}K_{j2} \ldots),$$

$$K_{i4} = hf_i\ (\ldots., y_{j,\ell} + a_{41}\ K_{j1} + a_{42}\ K_{j2} + a_{43}\ K_{j3}, \ldots),$$

and $y_{i,\ell+1} = y_{i,\ell} + \sum_s W_s K_{is}$,

Table 3.21

Coefficients for Fourth Order Runge-Kutta Processes

Using Butcher notation

0					
C_2	a_{21}				
C_3	a_{31}	a_{32}			
C_4	a_{41}	a_{42}	a_{43}		
:	:	:			
C_n	a_{n1}	a_{n2}	a_{n3}	..	a_{nm-1}
	ω_1	ω_2			ω_n

the classical 4th order R-K is denoted by

0				
$\frac{1}{2}$	$\frac{1}{2}$			
$\frac{1}{2}$	0	$\frac{1}{2}$		
1	0	0	1	
	$\frac{1}{6}$	$\frac{1}{3}$	$\frac{1}{3}$	$\frac{1}{6}$

c.f. the Merson 4th order R-K

0.22524	0.22524			
0.35201	0.17174	0.18026		
1	1.63559	-5.93444	5.29884	
	0.33761	-1.11494	1.58366	0.19366

where a_{ij}, ω_i are constants and $h = t_{\ell+1} - t_\ell$ is the constant tabular interval. Coefficients for a standard 4th order process are given in Table 3.21. The x component of acceleration of a planet of mass m at heliocentric coordinates (x, y, z), relative to the centre of mass of the 'sun and inner planets' mass m_s, is given by

$$\ddot{x} = -k^2(m_s + m)\frac{x}{r^3} + \sum_{j=1}^{4} k^2 m_j \left(\frac{x_j - x}{\rho_j^3} - \frac{x_j}{r_j^3}\right)$$

where $r^2 = x^2 + y^2 + z^2$, $r_j^2 = x_j^2 + y_j^2 + z_j^2$

$m_s = 1.00000597682\ m_{sun}$,

k^2 is the gravitational constant

and $\rho_j^2 = (x_j - x)^2 + (y_j - y)^2 + (z_j - z)^2$

with heliocentric coordinates of the j^{th} planet denoted by (x_j, y_j, z_j). Similar equations exist for the y and z components of acceleration. The values for planet masses used are given in Appendix I.

3.3 Generation of Data

Having rewritten each set of three equations as six first order equations, a program was constructed to evaluate position and velocity components for planets Jupiter to Neptune, in double precision. A table of positions and velocities was generated for each planet, using a step length of one day, and initial data from Oesterwinter and Cohen (1972). This information was output in machine form for 10 day intervals, to form the database for the Gauss-Jackson program, which was then run to evaluate the above equations, in double precision, using a 10 day integration interval. Integrating over various periods from 1 year to 50 years, final values of position were output, and the generated results compared with Eckert et al. (1953). Minor differences were observed in some coordinates.

The program was then run from JD 2420000.5 to JD 2441200.5. The output coordinates were checked with Oesterwinter and Cohen (1975) and very good agreement was obtained. It was thus decided that the minor differences

previously observed in comparisons with A.P.A.E. XI could be attributed to the slightly different input information.

3.4 Choice of Starter Procedure

For a Runge-Kutta process of even order ν and integration interval h, truncation errors in position have linear growth components proportional to $h^{\nu}t$, and quadratic growth components proportional to $h^{\nu+1}\ t^2$. If the Runge-Kutta process is to be used only as a starting procedure, the low order error terms will predominate; thus Merson (1972) has calculated a non-standard 4th order Runge-Kutta process to minimise the linear error term. A trial run of the sytem was thus carried out using this starting procedure; however, no significant improvement was observed over the limited timescale considered.

For integration over a long period of time, it was decided to replace the starter with a 6th order Runge-Kutta process (Butcher, 1964; Merson, 1972) to improve the precision of the starting table, and it was thought that should a greatly extended database be required, consideration must be given to the use of a multistep starting procedure, (e.g. Johnson, 1982).

3.5 Further Evaluation

The Gauss-Jackson numerical integrator showed no appreciable loss of accuracy through the timespan considered, the accuracy of the starting table being of prime importance. Thus it was decided that, with an improved set of initial data, this program was adequate to integrate the planetary equations of motion over a considerably longer time if required. However, it was thought that the modification suggested by Herrick (1972) was not appropriate in this situation, since its use could increase the accuracy required of the starting table (Merson, 1972).

Further runs checking the values of predictor and corrector supported this view, and confirmed that a step-length of 40 days was adequate for this sytem. The integration interval was altered accordingly, and the system set to provide an extended database of Jupiter, Saturn, Uranus and Neptune coordinates if required.

For the purpose of constructing an 'alternate' solar system, the step-length of 10 days in the Gauss-Jackson program and 1 day in the Runge-Kutta program was retained.

3.6 An Alternate Solar System

Following numerical integration of simulated planetary systems, Ovenden (1972) proposed a hypothesis of 'Least Interaction Action' which, applied to the satellite systems of Jupiter and Saturn, gave good results for the satellite orbits. Applying this criterion to the solar system, the author deduced a model for a previous configuration of planets, with a planet mass of about 90 M_{earth} at the present distance of the asteroid belt, this mass to have dissipated suddenly 1.6×10^7 years ago.

As an alternate solar system was required, it was decided to adopt this possible past configuration of the solar system. Whilst the author indicates the possibility of the existence of a ring of matter at 2.79 AU from the sun, the sudden dispersal of matter required by the model seems more difficult to explain on the basis of a ring than of a single mass (Ovenden, 1972). Thus it was decided to model the system under the latter assumption, calculating initial position and velocity components from the approximate figures suggested by Ovenden (1972), reproduced in Table 3.61.

3.7 Initial Conditions

In order to calculate the motion of a system of bodies by the Gauss-Jackson technique, a set of starting values is required. Whilst, following

Table 3.61

Orbital Parameters for Ovenden System

Planet	a	Planet	a
Mercury	0.394 A.U.	Jupiter	5.201 A.U.
Venus	0.719 A.U.	Saturn	9.509 A.U.
Earth	1.00	Uranus	19.46 A.U.
Mars	1.49	Neptune	29.71 A.U.
A	2.794		

where 'a' denotes the semi-major axis of orbit

Ovenden (1972) the calculations could initially be made on the basis of circular coplanar orbits, this is of limited value in constructing a 'realistic' model; however, it is clearly not feasible to form a definitive set of orbital elements for the Ovenden system. Consequently, the planets Jupiter, Saturn, Uranus and Neptune (JSUN) were arbitrarily given the orbital elements of epoch 1900.0, and were each placed at the perihelion distance calculated from Table 3.61. This configuration allows considerable angular separation between the planets, and thus it may reasonably be assumed that the mutual perturbing forces are not too great. Thus, if planet A is initially given a suitable position, with values of $\tilde{\omega}$ (longitude of perhelion) of about 230^{o}, Ω (longitude of the ascending node) of about 90^{o}, and inclination $i = 0$, then initial velocity components may reasonably be calculated on the basis of undisturbed elliptic motion. Because of the considerable perturbing force of Jupiter, planet A was initially given a low value of eccentricity, similar to that of Venus. Velocity V will thus be given for each planet by

$$V^2 = \mu \left(\frac{2}{r} - \frac{1}{a}\right) \qquad \text{where a is semi-major axis of orbit}$$

and r is the instantaneous radius of the orbit.

The normal to the orbit plane, $\underset{\sim}{n}$, will be given by

$$\hat{\underset{\sim}{n}} = (\sin\ell \ \sin\Omega, \ -\sin\ell \ \cos\Omega, \cos\ell)$$

and $\hat{\underset{\sim}{r}} = (x, y, z)/\sqrt{x^2 + y^2 + z^2}$.

Thus $\underset{\sim}{V} = (\hat{\underset{\sim}{n}} \times \hat{\underset{\sim}{r}})\ V$

where heliocentric ecliptic coordinates (x, y, z) for each planet are obtained from

$$x = r\left[\cos\Omega \ \cos(\omega + \nu) - \sin\Omega \ \sin(\omega + \nu)\cos i\right] ,$$

$$y = r\left[\sin\Omega \ \cos(\omega + \nu) + \cos\Omega \ \sin(\omega + \nu)\cos i\right] ,$$

$$z = r \sin(\omega + \nu)\sin i$$

where $\omega = \tilde{\omega} - \Omega$.

For this case, $|\underset{\sim}{r}| = a(1 - e)$.

3.8 Generation of Data for an 'Ovenden' System.

Position and velocity components were calculated (Table 3.61). Using the standard 4th order Runge-Kutta program modified for this program, a starting table was generated using a step-length of 1 day. The Gauss-Jackson program modified for this system was then run using an integration time of 10 days, initially for a period of 1 year. It was found that, as expected, a 10 day step-length was adequate. The Runge-Kutta program was then run over the same period, but with a step-length of 1 day, and a random selection of coordinates was output. These were found to be in perfect agreement with the results of the Gauss-Jackson program, to the accuracy of the input data, indicating the internal consistency of the model. Several comparison runs over longer timescales yielded similar results.

The Gauss-Jackson program was then run for the maximum number of iterations permitted by constraints on computer time. Random sampling of the output gave expected results. However, over a long period of time it was observed that the radius of Neptune's orbit was oscillating below the perihelion limit, to 29.44 AU c.f. 29.45 AU from theory. Restarting the integration using the final sets of difference tables, positions and velocity components, gave coordinates for a total of 110 years, with the possibility of further integration, the practical limit on the system being the stability of the integrating program. Checks on aphelion and perihelion distances, on planet periods and on random selections of output coordinates showed no evidence of spiralling of the numerical solution; as before, the predominate factor determining the accuracy of the output data appeared to be the accuracy of input conditions.

The numerical integration was then repeated for differing initial configurations of all planets at aphelion. The resulting coordinates showed, in the first 1000 iterations, variations in R larger than expected; however, this did not appear to be due to a limitation in stability of the numerical integrator. It is suggested that this behaviour is due to non-optimal

starting conditions, and it seems likely that the set of starting values with all planets at perihelion lies closer to the optimal solution for this particular system. Rerunning the system with starting conditions based on this assumption, all distances set to the minimum of the distance interval suggested by Ovenden, reduced the amount of oscillation considerably. Initial conditions are given in Appendix III.

Starting data for the runs were then stored, and calculations were made of various parameters of motion. The results are given in Section 4.

For these trial runs of an 'Ovenden' system, values for parameters of elliptic orbits have been assumed. These may not be the optimal choices, but do provide 'realistic' sets of data, with the additional bonus that they may indeed represent a past configuration of the solar system. Integration over a somewhat longer timescale is possible for this sytem, with the reduced accuracy that is associated with the method of calculation of the input data.

It was expected that coordinates for the inner planets would be generated analytically, should they be required in later sections.

3.9 Discussion

The Gauss-Jackson numerical integration procedure is found to be highly efficient and accurate for integration of planetary equations of motion, no appreciable loss of accuracy being observed over 4000 iterations. However, the critical importance of accurate starting conditions is very clearly demonstrated; thus the use of a high order Runge-Kutta or multistep method as a starting procedure is appropriate for long-period integration, and will be used if an extended database is required. The model for an alternate solar system based on a possible past configuration of planets (Ovenden, 1972) is, with an appropriate set of initial conditions, generating a suitable 'control system' database. Thus the planetary coordinates generated for

this Ovenden system can be retained for the investigation into possible links between the sunspot cycle and parameters of planetary motion.

SECTION 4

Motion of the Solar System Centre of Mass

Because the orbital period of Jupiter (11.862 years) is close to that attributed to the sunspot cycle (~11.1 years) there has been interest in linking one with the other for a considerable time (e.g. Brown, 1900; Pocock, 1918; José, 1965; Prokudina, 1978). The significant difference between the two values has led to consideration being given to possible modulating influences of the other outer planets, particularly Saturn (Romanchuk, 1975A; 1976; 1977). Good correlations have been obtained (Bureau and Craine, 1970; Sleeper, 1972; Morth and Schlamminger, 1979; de Meyer, 1980) between various synodic periods of the four giant planets and sets of periodicities detected in the sunspot cycle by other researchers (e.g. Anderson, 1954; Cohen and Lintz, 1974; de Meyer, 1980).

Due to the importance of the outer planets in determining the motion of the mass centre of the solar system, several authors have sought to relate the sunspot cycle to parameters of this motion (José, 1965; Wood and Wood, 1965; Dauvillier, 1970; 1975; 1976; 1977; 1978; Petrova, 1979). Whilst few connections are made with the 11 year solar cycle (c.f. Wood and Wood, 1965) a long term periodicity in the motion of the centre of gravity of 160-180 years is generally reported (eg. José, 1965; Dauvillier, 1976; 1977; Petrova, 1979) and identified with a long-term sunspot period.

The extent of the support given by several of the above papers (José, 1965; Bureau and Craine, 1970; Sleeper, 1972; Morth and Schlamminger, 1979; Petrova, 1979; de Meyer, 1980) to the hypothesis of a connection between planetary motion and the sunspot cycle, is reduced by their employing for

comparison periodicities in the sunspot cycle whose existence is not proven (see Sections 1 and 2). Similarly, the results obtained by Dauvillier (1976; 1977; 1978) are limited by the small sample size used (Meeus, 1978). However, interesting preliminary curves of motion are obtained by José (1965) and an 11 year period is reported by Wood and Wood (1965). Hence it was decided to investigate parameters of the motion of the solar system centre of gravity around the sun, initially repeating the study of José (1965). The intention was to broaden the scope of the analysis by using an accurate model of the solar system; to remove the approximation of planar motion imposed by the author; and to employ statistical analysis of generated data in place of the more subjective criteria utilized by previous researchers (e.g. José, 1965; Wood and Wood, 1965; Dauvillier, 1970; 1976; 1977; Petrova, 1979). It was intended further to use this more comprehensive system to examine other parameters of motion, and to investigate the results of other authors, particularly Wood and Wood (1965).

4.1 Planetary Database

In order to investigate parameters of the motion of the sun with respect to the centre of gravity of the solar system, an accurate database of planet positions is required. For the initial research, magnetic tapes of planet coordinates supplied by B.D. Yallop (Greenwich Observatory) were utilized; these tapes contain the heliocentric equatorial rectangular coordinates of the planets referred to epoch 1950.0. Data for the 5 outer planets is taken from Astronomical Papers vol. XII, tabled at 40 day intervals from JD 2378500.5 to JD 2451880.5. For Venus, Mars, and the centre of mass of the Earth-Moon system, data is tabled at 10 day intervals over the same period; for Mercury, data is supplied at 2 day intervals from JD 2415416.5 to JD 2452048.5. Values for planetary masses are adopted from Astronomical Papers vol. XIII, part II.

Simple calculation of the relative contributions of the planets yields the result in table 4.11. As the relative contribution of the inner planets is small, it was decided that initially, only the five outer planets should be included in the calculations; thus the motion studied was that of the centre of mass of the 'sun and inner planets' with respect to the solar system centre of gravity.

4.2 Choice of Reference Plane

Let the masses of the outer planets be denoted by m_i, $i = 1, 2, \ldots 5$; their heliocentric rectangular equatorial co-ordinates by x_i, y_i, z_i, $i = 1, \ldots 5$ and let the sum of the masses of the inner planets be m_0.

Then the X co-ordinate of the centre of the solar system is given by

$$X_{EQ} = \sum_{i=1}^{5} \frac{m_i x_i}{1+m_0+\sum_{i=1}^{5} m_i} \quad \text{with similar equations for } Y_{EQ},\ Z_{EQ}.$$

For a set of n planets, radius vectors R_i from an unaccelerated point O, and mutual radius vectors $r_{ij} = R_j - R_i$

$$m_i \ddot{\underset{\sim}{R}}_i = G \sum_{j=1}^{n} \frac{m_i m_j}{r_{ij}^3} \underset{\sim}{r}_{ij} \qquad j \neq i$$

where G is the gravitational constant.

Hence $\sum_{i=1}^{n} m_i \underset{\sim}{R}_i = \underset{\sim}{a}t + \underset{\sim}{b}$ $\quad \underset{\sim}{a}, \underset{\sim}{b}$ constant vectors

From O, the system centre of mass has a radius vector $\underset{\sim}{R}$, where

$$M \underset{\sim}{R} = \sum_{i=1}^{n} m_i \underset{\sim}{R}_i , \qquad M = \sum_{i=1}^{n} m_i ,$$

So $\underset{\sim}{R} = (\underset{\sim}{a}t + \underset{\sim}{b})/M; \qquad \dot{\underset{\sim}{R}} = \underset{\sim}{a}/M$.

So, by taking vector products of $\underset{\sim}{R}$, $\ddot{\underset{\sim}{R}}_i$ for each planet and summing:

$$\sum_{i=1}^{n} m_i \underset{\sim}{R}_i \times \ddot{\underset{\sim}{R}}_i = G \sum_{i=1}^{n} \sum_{j=i}^{n} \frac{m_i m_j}{r_{ij}^3} \underset{\sim}{R}_i \times \underset{\sim}{r}_{ij} \qquad i \neq j$$

and hence $\sum_{i=1}^{n} m_i \underset{\sim}{R}_i \times \ddot{\underset{\sim}{R}}_i = 0 \quad \sum_{i=1}^{n} m_i \underset{\sim}{R}_i \times \dot{\underset{\sim}{R}}_i = \underset{\sim}{C}$

where constant C defines the 'invariable plane' of Laplace.

Table 4.11

Relative contributions of planets

Planet	H	Planet	H
Mercury	0.000 000 06	Jupiter	0.005
Venus	0.000 001 8	Saturn	0.003
Earth	0.000 003 0	Uranus	0.009
Mars	0.000 000 5	Neptune	0.0016
		Pluto	~0.0001

Here, H = mass x mean distance from sun

where mass is in unit of the sun's mass

distance is in astronomical units.

4.3 Initial Examination

The heliocentric rectangular equatorial co-ordinates of the solar system centre of mass were calculated for the period JD 2378500.5 to JD 2451880.5 and were checked by comparison with those obtained by Eckert et al. (1950). It was decided to use the 'invariable plane' as the reference plane for the investigation, in order to minimize the z-component of motion, and thus permit 2-dimensional representation of the path of the sun with minimum distortion. The transformation equations used are tabled in Appendix II, together with elements for the invariable plane adopted from Astrophysical Quantities (1950).

The co-ordinates (X, Y, Z) of the sun with respect to the centre of gravity of the solar system were calculated for the 200 years of data available. As it was found that the Z co-ordinate was of order 10^{-5}, c.f. the X, Y co-ordinates of order 10^{-3}, projected distance D on the XY plane, and angle $\theta = \tan^{-1}(Y/X)$ were computed, and plots were drawn of the path of the sun in the invariable plane (figure 4.31). These spiral motion polar plots were found to be in good agreement with those reported previously (José, 1965; Dauvillier, 1977; 1978). It is seen that the distance D may vary from 0.01 $R_\odot$ to 2.19 $R_\odot$.

In order to investigate the spiral motion more fully, further parameters were considered:

Distance $R = \sqrt{X^2 + Y^2 + Z^2}$

and

Velocity $V = (\dot{X}^2 + \dot{Y}^2 + \dot{Z}^2)^{\frac{1}{2}}$;

The instantaneous radius of curvature of the sun's path;

$$\rho = V^3/\Delta$$

where $\Delta = \left[(\dot{Y}\ddot{Z} - \dot{Z}\ddot{Y})^2 + (\dot{Z}\ddot{X} - \dot{X}\ddot{Z})^2 + (\dot{X}\ddot{Y} - \dot{Y}\ddot{X})^2\right]^{\frac{1}{2}}$;

angular momentum L of the sun about the centre of mass:

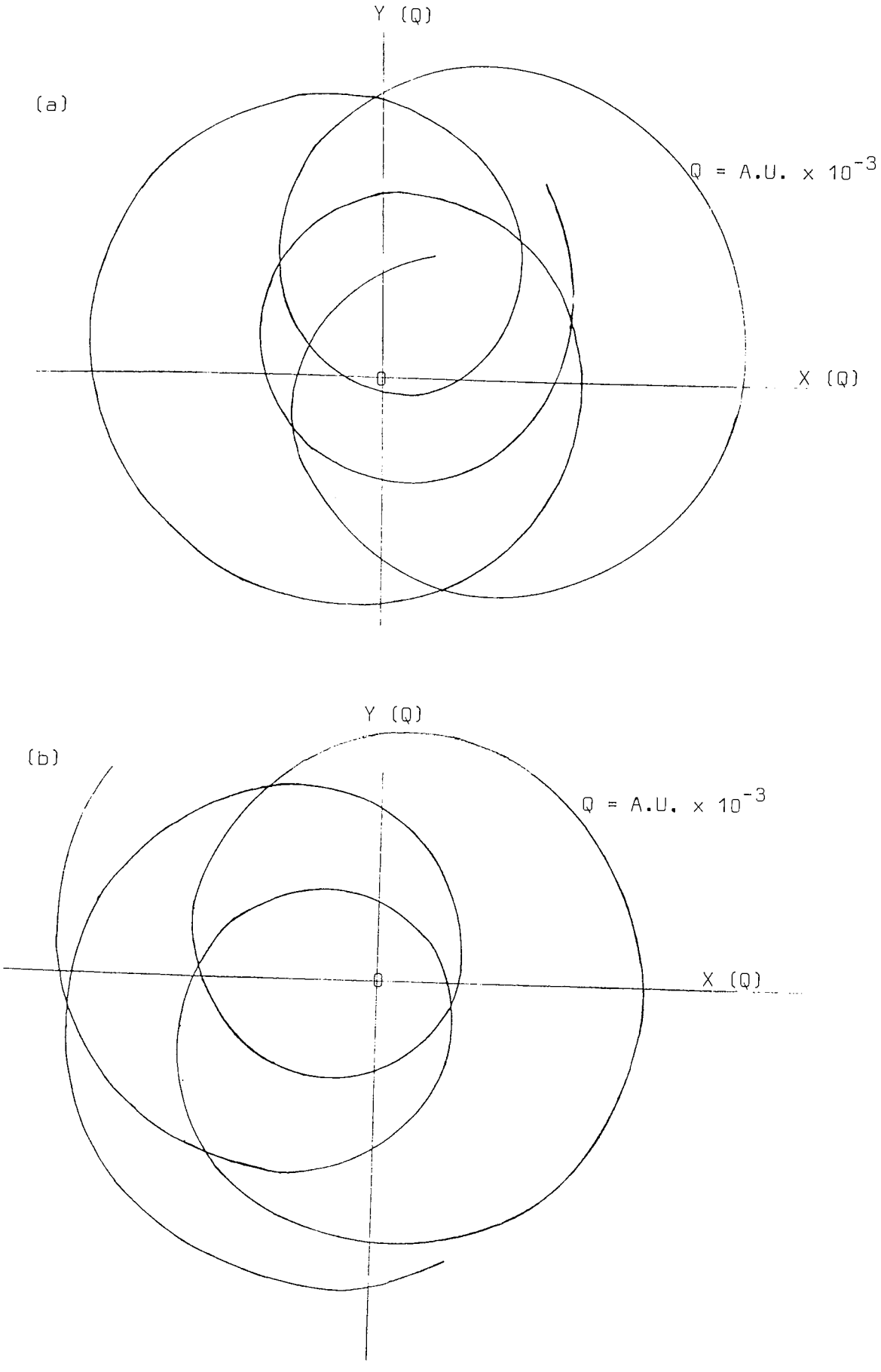

Figure 4.31 Path of Sun in Invariable Plane a) JD 2390820-2407200
b) JD 2407200-2423600

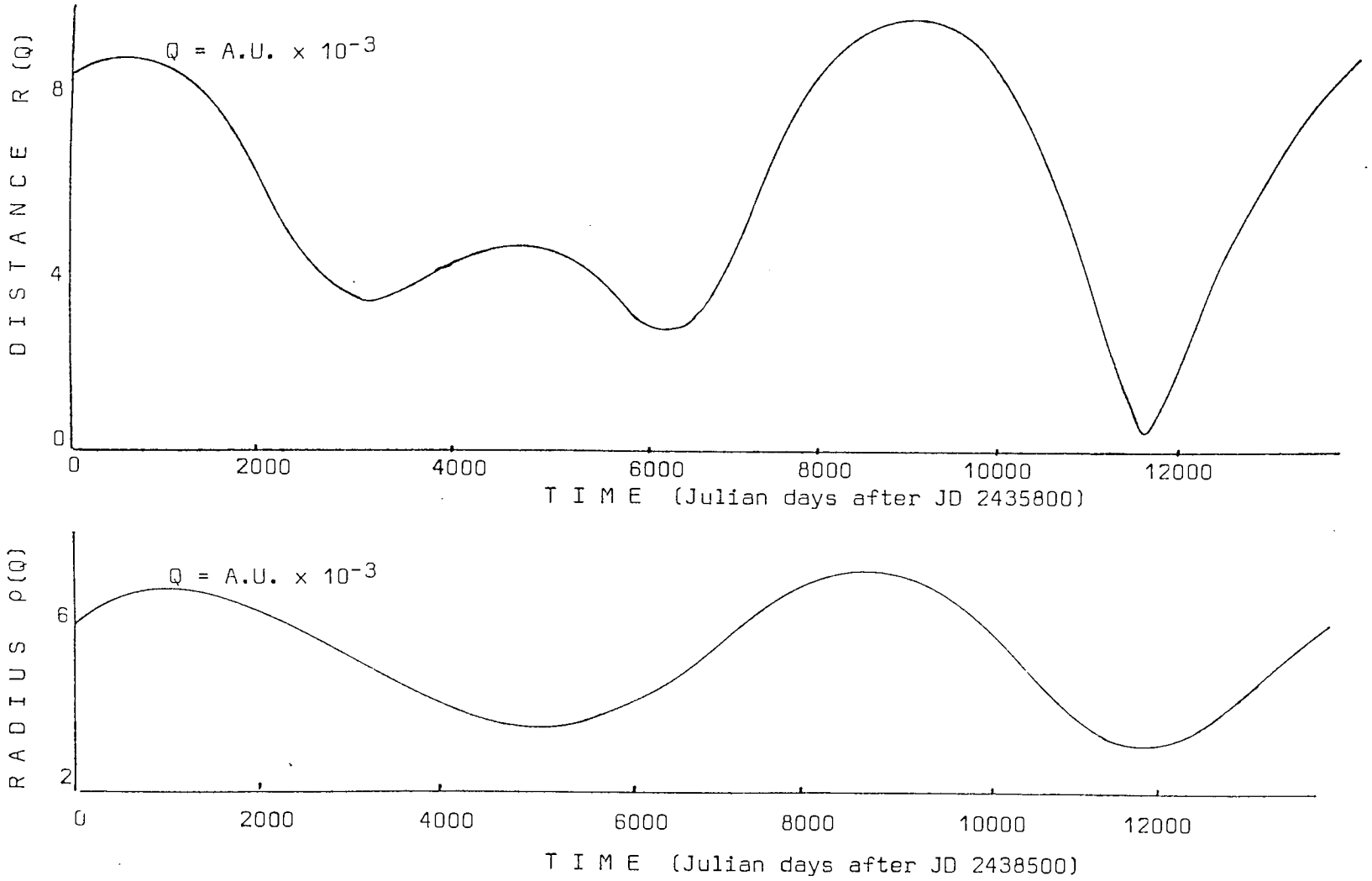

Figure 4.32 Variation with Time of Distance R and Radius of Curvature ρ in Interval JD 2435800-2450800

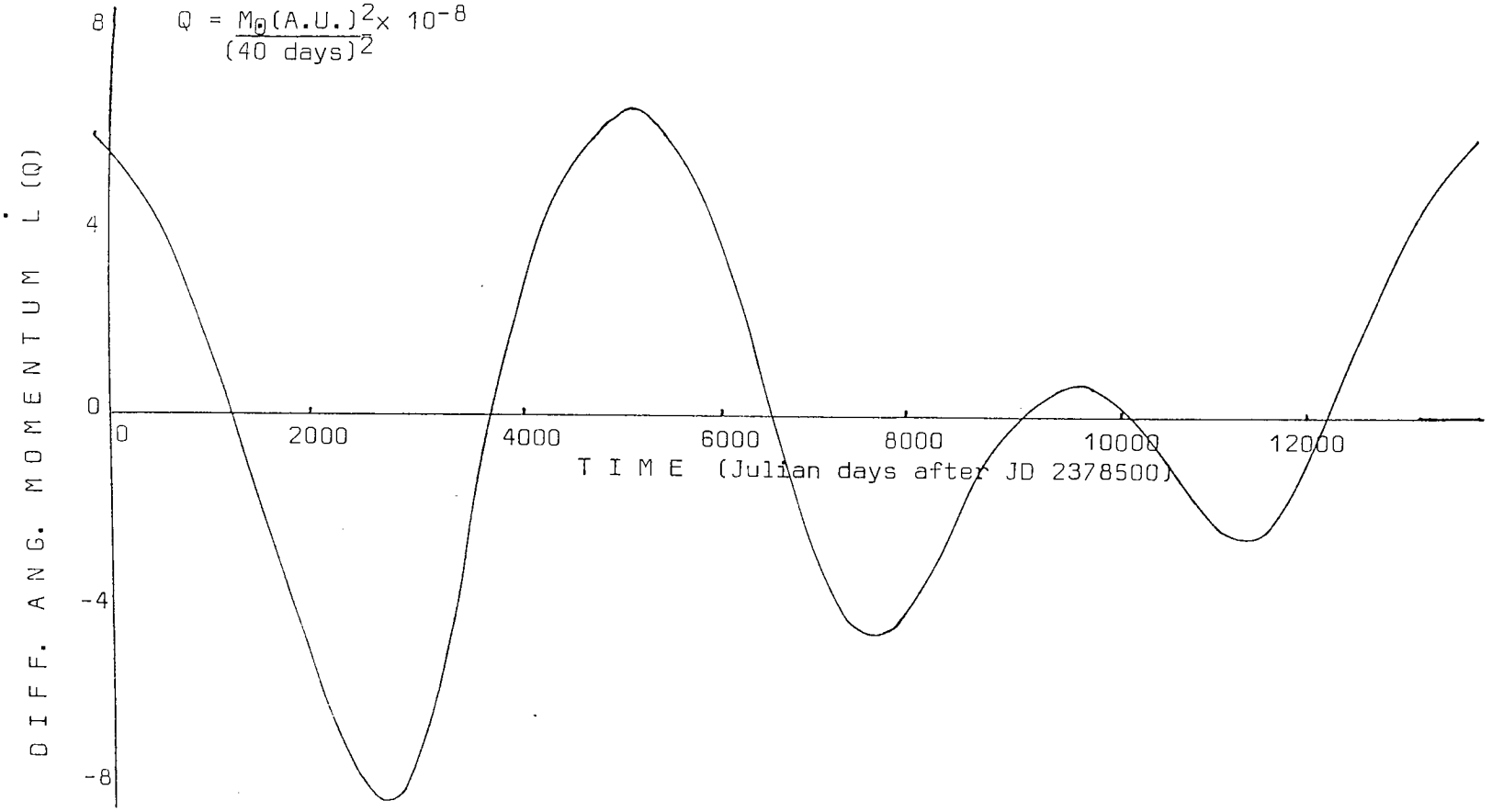

Figure 4.33 Variation with Time of Rate of Change of Angular Momentum $\dot{L}$, in the Period JD 2378500-2393600

$$L = \left[(Y\dot{Z} - Z\dot{Y})^2 + (Z\dot{X} - X\dot{Z})^2 + (X\dot{Y} - Y\dot{X})^2\right]^{\frac{1}{2}}$$

and the angular momentum about the instantaneous centre of curvature $P = \rho V$. The changes with time of P and L were also computed. Samples of the data obtained are plotted in figures 4.32 and 4.33 (with full 200 year plots of R and ρ graphed in Appendix III). It is clear from these graphs that quasi-periodic variations are present, but no single periodic effect can be isolated by eye from the data. Hence it was decided to examine the above parameters for an 'Ovenden' system, for comparison.

4.4 Motion of an 'Ovenden' System

Using the data previously obtained for an 'Ovenden' system (Section 3), co-ordinates for the centre of mass of this solar system relative to the 'sun and inner planets' were computed for a period of 100 years. Initially, the 'perihelion' set of data was used to calculated the distance R. As before, the z-component of motion was found to be small c.f. the x and y components; thus distance D and angle θ were calculated, and a polar plot for the 2-dimensional motion was drawn (figure 4.41). The resulting curve was found to be very similar to figure 4.31, the effect of planet 'A' being apparent as a slight distortion of the spiral pattern.

Reworking the above analysis for several other sets of 'Ovenden' data yielded co-ordinates for the system centre of mass not appreciably different from those previously obtained, and so only a single data set was retained for futher work. A graph of the variation of R with time was drawn (figure 4.42). Comparison with figures 4.32 shows that planet 'A' exerts an appreciable effect on the distance parameter D. This perihelion set of data, for a period of 100 years of coordinates

Figure 4.41 Path of the sun in the invariable plane for an 'Ovenden' system

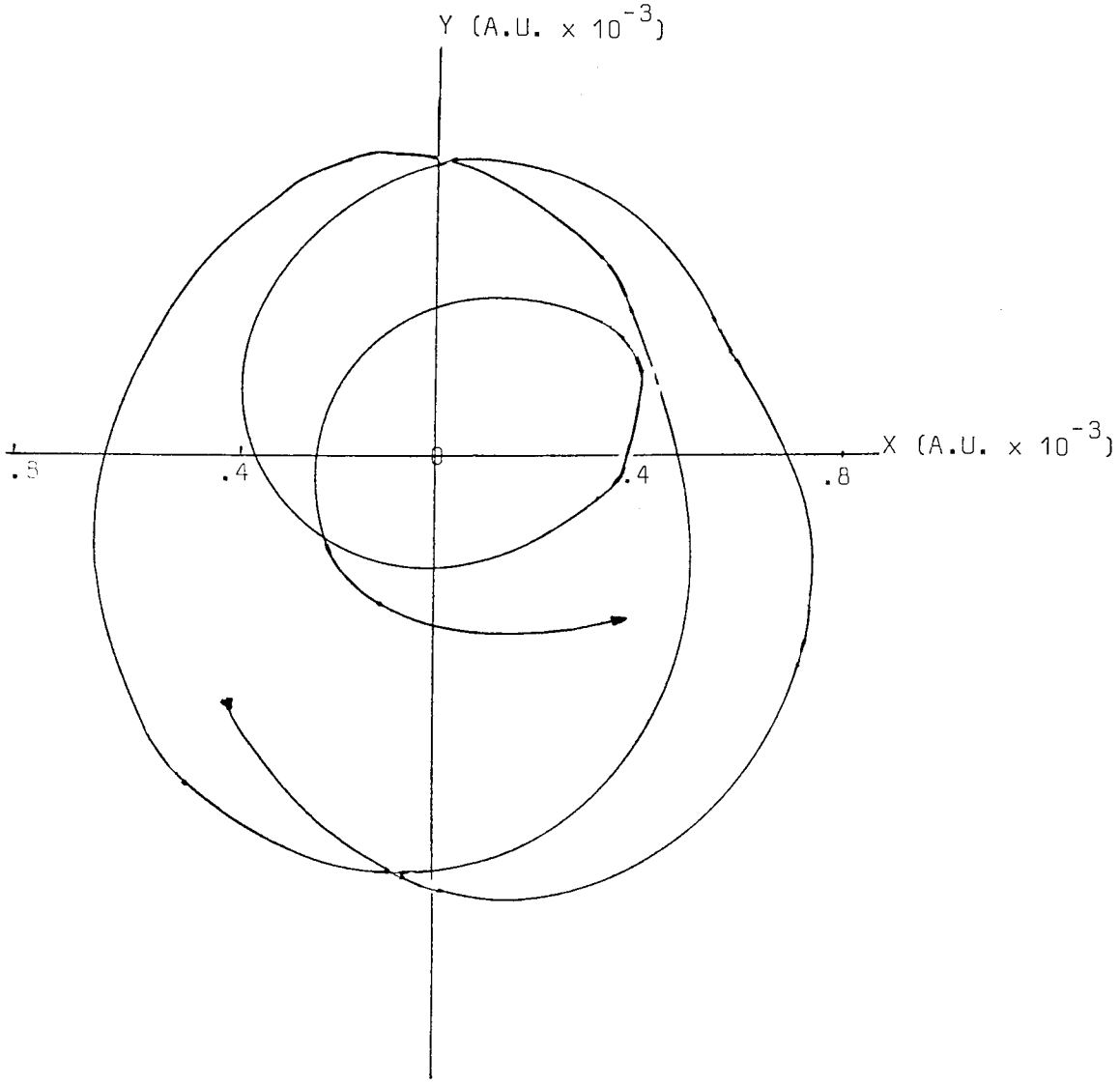

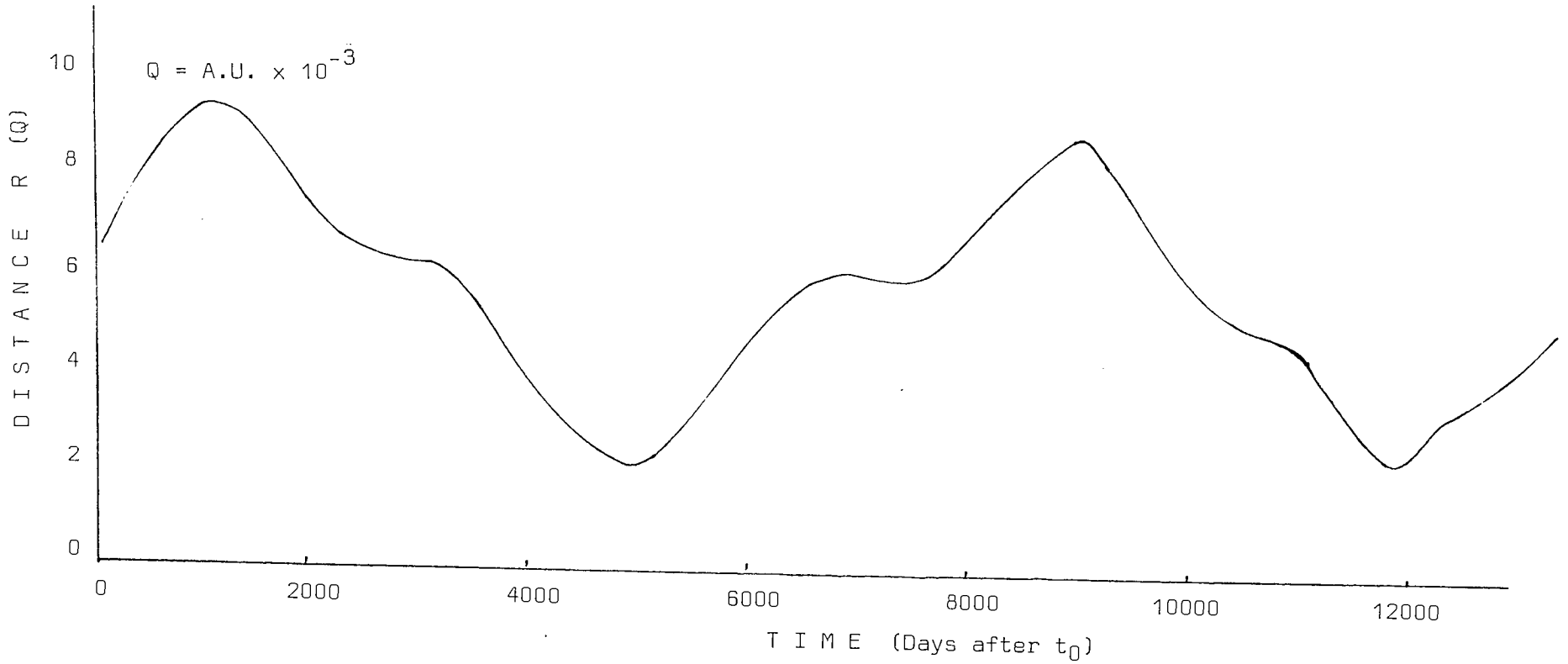

Figure 4.42 Variation with Time of distance R in an 'Ovenden' system, from Initial Epoch t_0

for the centre of mass of an 'Ovenden' system was thus retained for use as a control system.

4.5 Detailed Investigation

It was decided to conduct a thorough investigation into parameters of the sun's motion, including in the calculations the effect of the inner planets as previous researchers,(Wood and Wood, 1965; Dauvillier, 1977), had indicated that these might have an appreciable effect. Also, rather than use the subjective methods of data inspection previously employed (e.g. José, 1965; Wood and Wood, 1965; Dauvillier, 1977) it was decided to use power spectrum analysis to search for periodic effects.

The parameters previously studied were computed using all planets, for the hundred years of Mercury data available, at time interval 10 days. Samples of the resulting curves were compared with those previously obtained, and slight effects of the inclusion of the inner planets were observed (a sample of curves of R is given in figure 4.51). The other parameters studied showed similar slight oscillations. Recalculating all parameters, excluding Mercury, yielded curves with no discernable difference from those previously obtained, and so all parameters were recalculated for the interval 1800 January 4.5 to 2000 December 2.0, using planets Venus to Pluto.

Using a modification of the statistical technique previously outlined in Section 1, the variation in R was examined for the 39 year periodicity reported by Dauvillier (1976; 1977). Using a frequency spacing of .001 c/yr with lower frequency limit set at .01 c/yr, a power spectrum was generated from data sampled at 40 day intervals (figure 4.52). It is clear from this spectrum that two sharp peaks exist at $f = .050 \pm .001$ c/yr and $f = .078 \pm .001$ c/yr. A minor peak is observed at .072 c/yr.

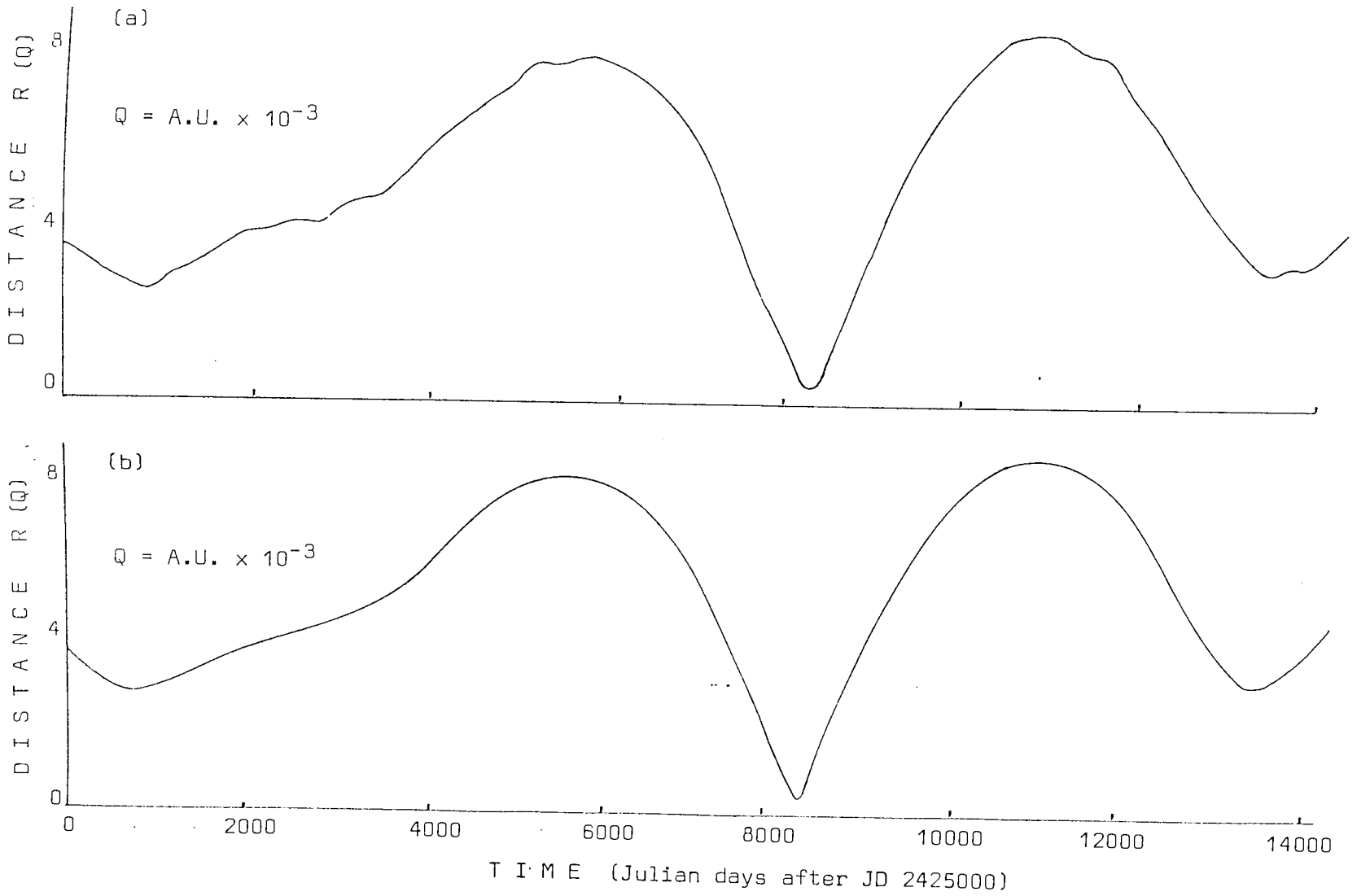

Figure 4.51 Variation with Time of Distance R in Interval JD 2425000-2440000 a) for all planets
b) outer planets only

Table 4.53

Synodic Periods of the Outer Planets

Planets	Frequency	Planets	Frequency
J - S	0.05035 c/yr	S - U	0.02204 c/yr
J - U	0.07240 c/yr	S - N	0.0279 c/yr
J - N	0.0782 c/yr	U - N	0.0058 c/yr

Here, J denotes Jupiter U denotes Uranus
S denotes Saturn N denotes Neptune

and - denotes alignment.

This almost completely deterministic data contains very little noise, the planet co-ordinates being highly accurate (Brouwer and Clemence, 1950). The regular sampling reduces the errors due to imperfect cancellation of cross terms (Ponman, 1981) and so the errors due to noise (eqn. 1.5(III) and variance (eqn. 1.5(IV) are small. An error bar for the lowest significant peak is drawn in figure 4.52, and it is seen that there are 3 peaks of interest.

Calculation of various planetary synodic periods yields the results in Table 4.53. From these figures it is clear that the appreciable power in the spectrum is contained in peaks which represent various synodic periods of the outer planets. It is noted that the J-N alignment exerts a stronger influence than the J-U alignment, a result indicated by Table 4.53.

No evidence is seen of the reported 39 year variation in R (Dauviller, 1976; 1977) and no periodicity compatible with that of the sunspot cycle is detected. Thus the preliminary analysis of Dauvillier (1977) and Sleeper (1972) are not borne out by more comprehensive examination.

Using the same frequency range, spectra were obtained for V, $\dot{L}$ and ρ (figures 4.54, 4.55, 4.56 respectively), error bars being given for the lowest peak of interest in each case. Peaks identified with planetary synodic or sidereal periods are so marked. It is seen that the spectra for V and ρ reveal only 1 significant peak, at the J-S synodic frequency. The distribution for $\dot{L}$ is more complex, with slightly broader peaks; however, the only appreciable peaks correspond to J-S, J-U, J-N synodic periods, with a marginal peak at .085 c/yr tentatively attributed to the sidereal period of Jupiter. Spectra were also obtained of $\dot{P}$ (figure 4.57) and L (figure 4.58). That of $\dot{P}$ indicates only the influence of the J-S synodic period; that of L has peaks at J-S, J-U, J-N synodic periods.

Figure 4.52 Power Spectrum for Distance R

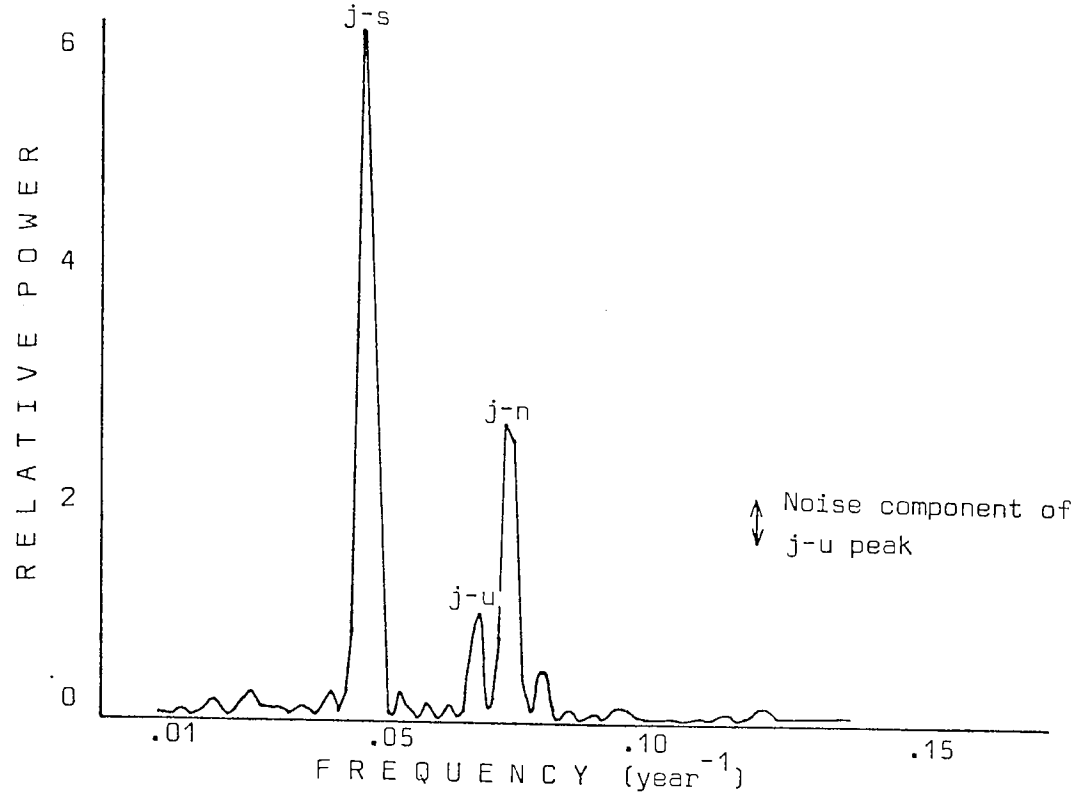

Figure 4.54 Power Spectrum for Velocity V

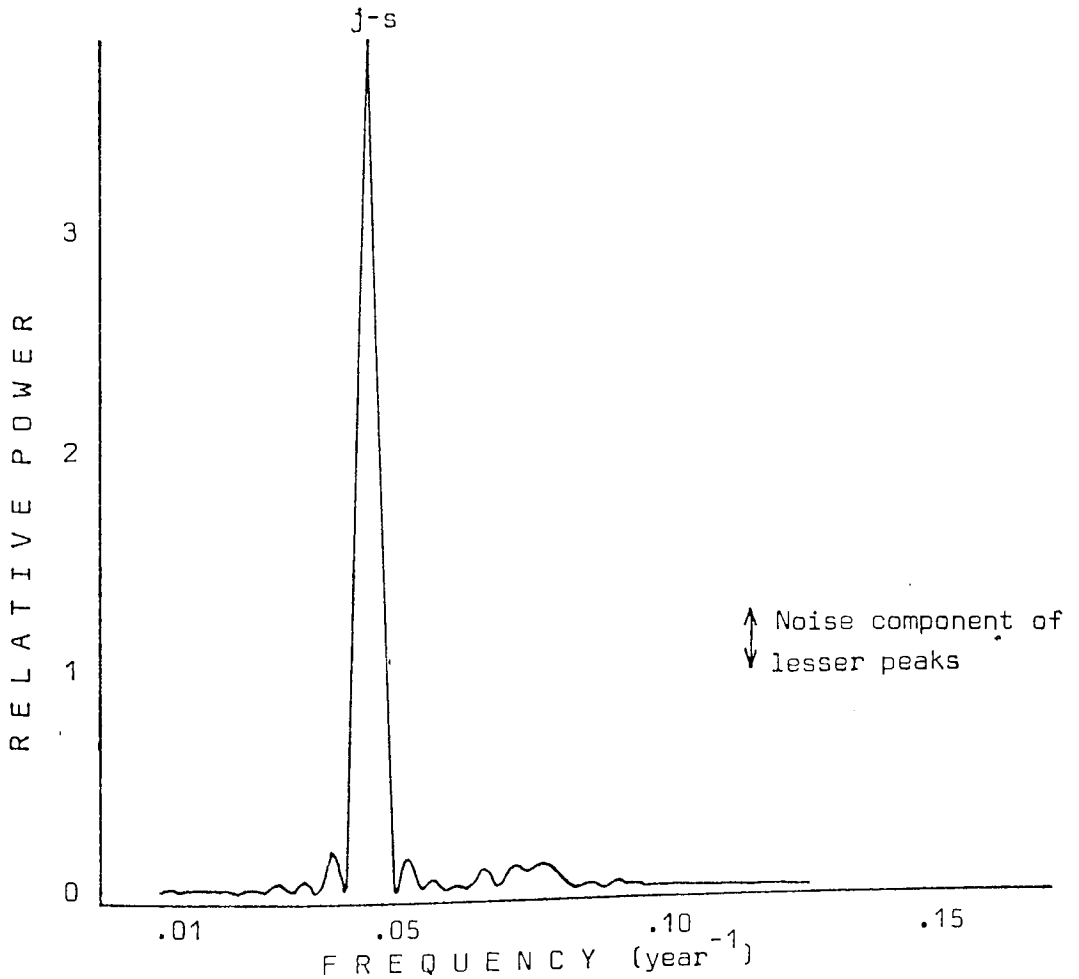

Figure 4.56 Power Spectrum for Radius of Curvature ρ

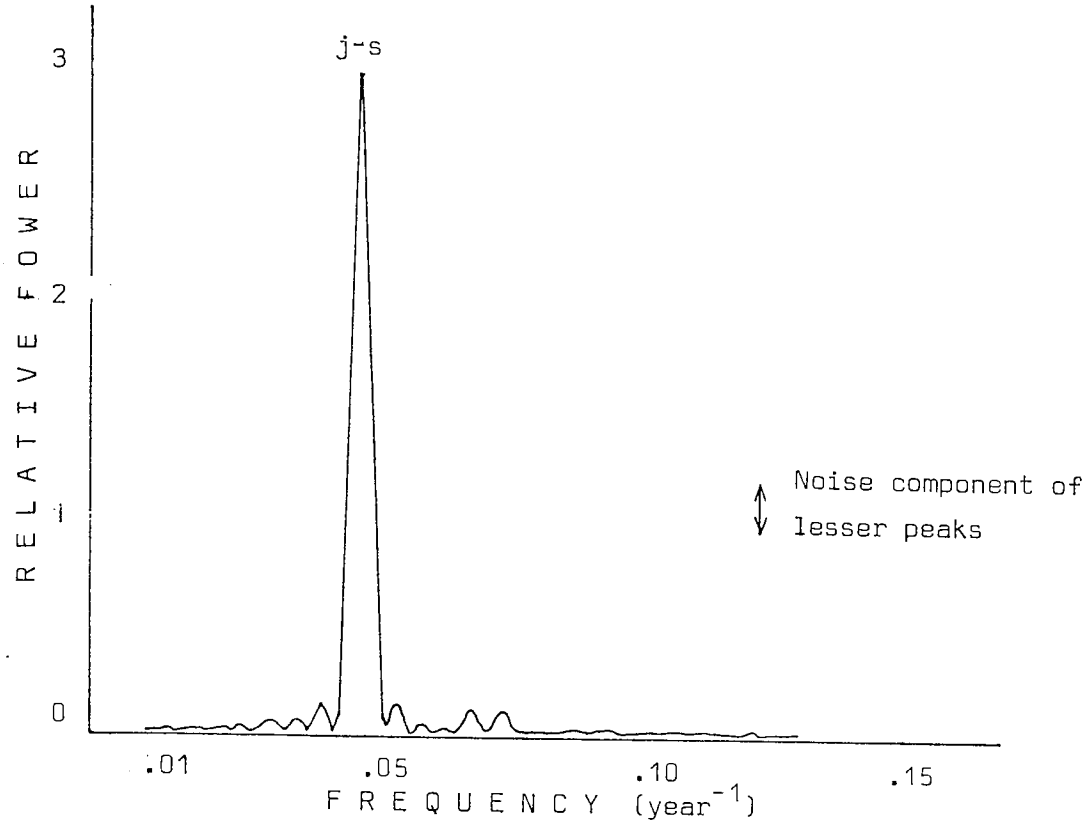

Figure 4.57 Power Spectrum for $\dot{P}$, Rate of Change of Angular Momentum P

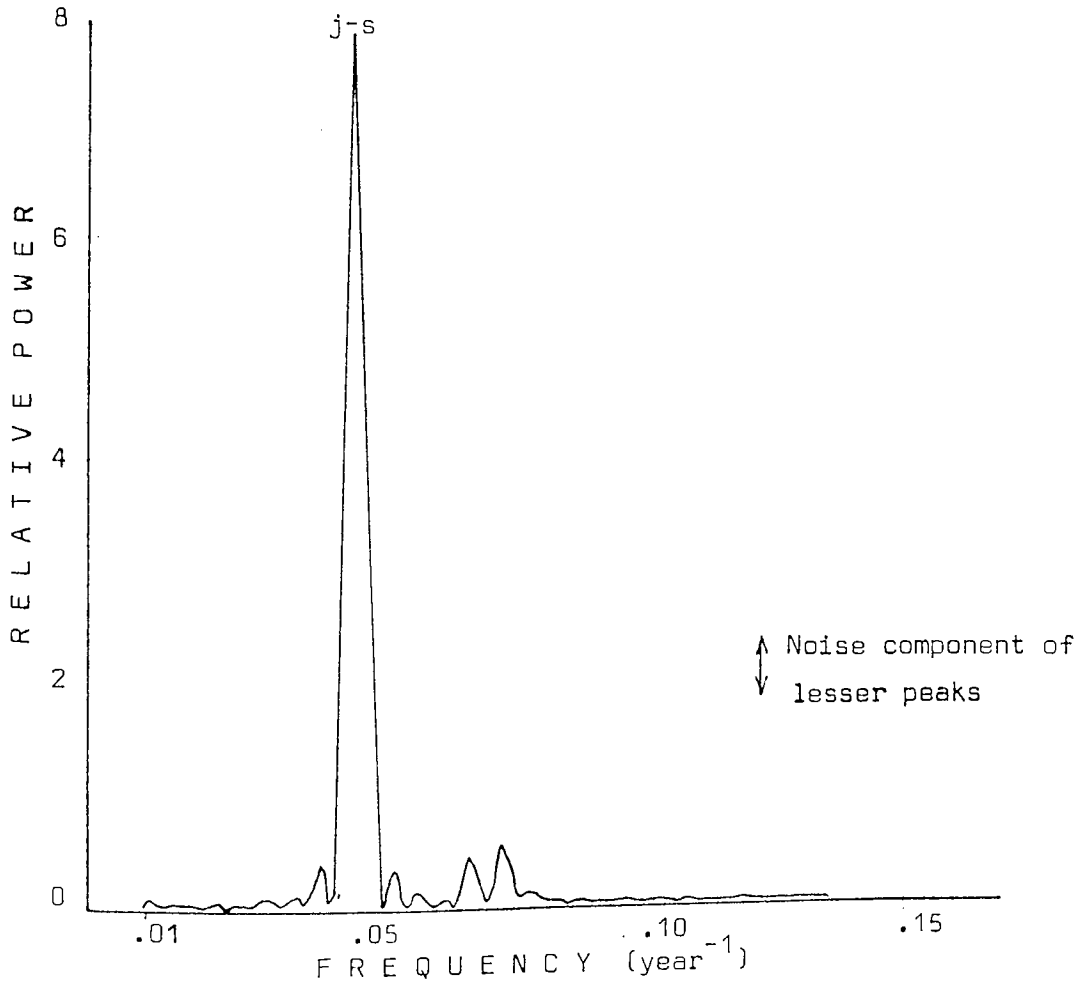

Figure 4.55 Power Spectrum of $\dot{L}$, rate of change of Angular Momentum

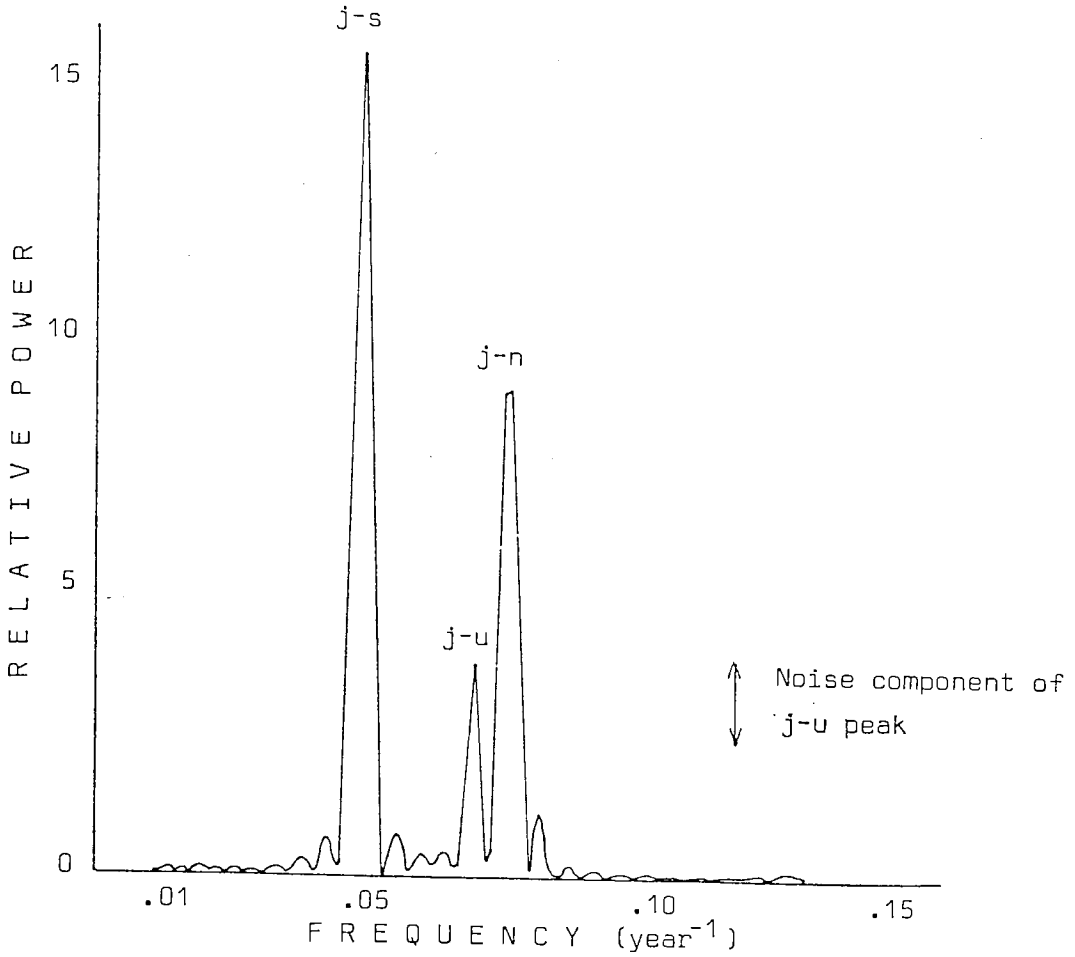

Figure 4.58 Power Spectrum of Angular Momentum L

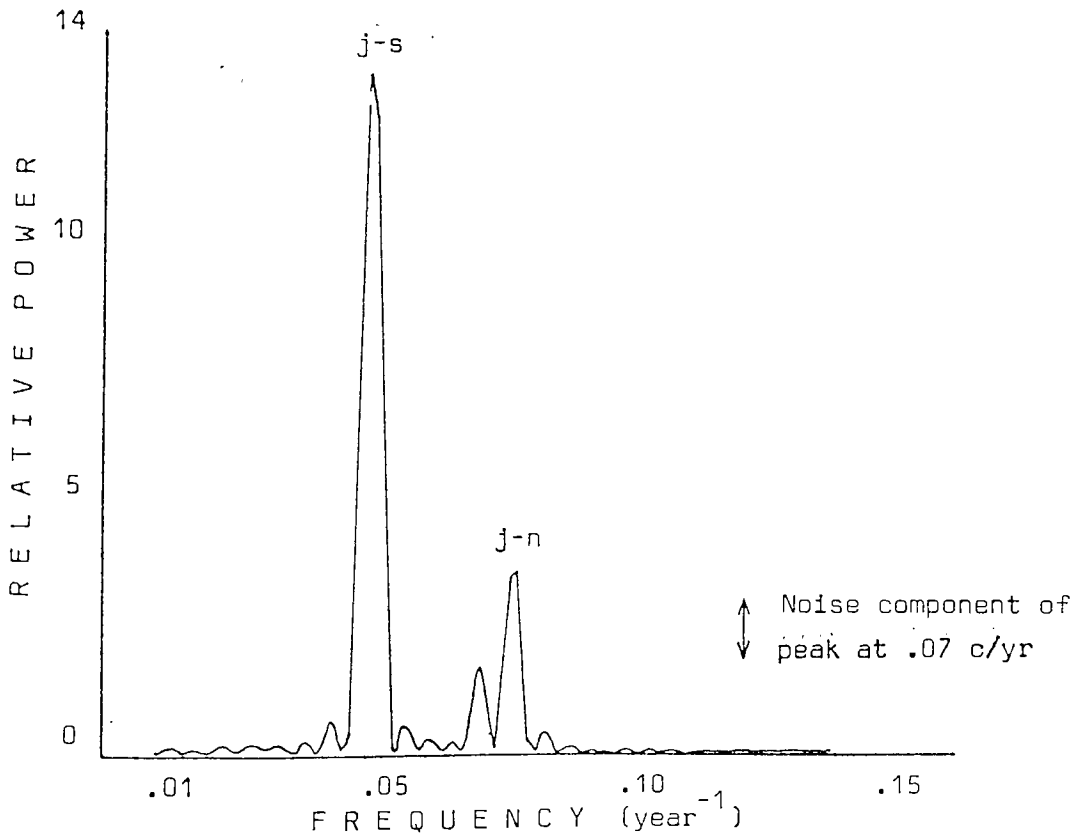

4.6 Further Analysis

It was decided to investigate further parameters of motion. Because motion at right angles to the invariable plane had been ignored previously, the variation of the Z co-ordinate of the sun's position was analysed, a sample of the curve being given in figure 4.61. The effect of Mercury on this co-ordinate was again found to be negligible, and so a spectrum of all 200 years of data was produced (figure 4.62). It is seen that the frequency distribution of this spectrum differs markedly from those previously obtained; the two high peaks may be identified with the sidereal period of Jupiter and Saturn. Some residual power is observed at the limiting low frequency .01 c/yr, indicating the presence of longer-period components, possibly corresponding to sidereal periods of Uranus and Neptune. Examination of the variation in Z for an Ovenden system (figure 4.64) revealed very little influence of A on parameter Z due to the choice of its plane of orbit.

The acceleration of the Sun with respect to the centre of gravity of the solar system was then computed. It was again found that Mercury had no observable effect, and so using data from AD 1800 to AD 2000, a spectrum was calculated for acceleration 'a', where

$$a = (\ddot{X}^2 + \ddot{Y}^2 + \ddot{Z}^2)^{\frac{1}{2}} .$$

The resulting frequency distribution (figure. 4.63) has 2 high peaks, identified with the J-S synodic period and the sideral period of Jupiter. No effect is discernible at or around a frequency of .09 c/yr, in contrast to the results of Wood and Wood (1965).

4.7 Constraints on Resolution

The components of acceleration 'a' were derived using numerical differencing; this process inevitably reduced the precision of the output data. When the small magnitude of the numbers concerned was considered ($\dot{L}$ and $\dot{P}$ are of order 10^{-8}) it was not thought practicable

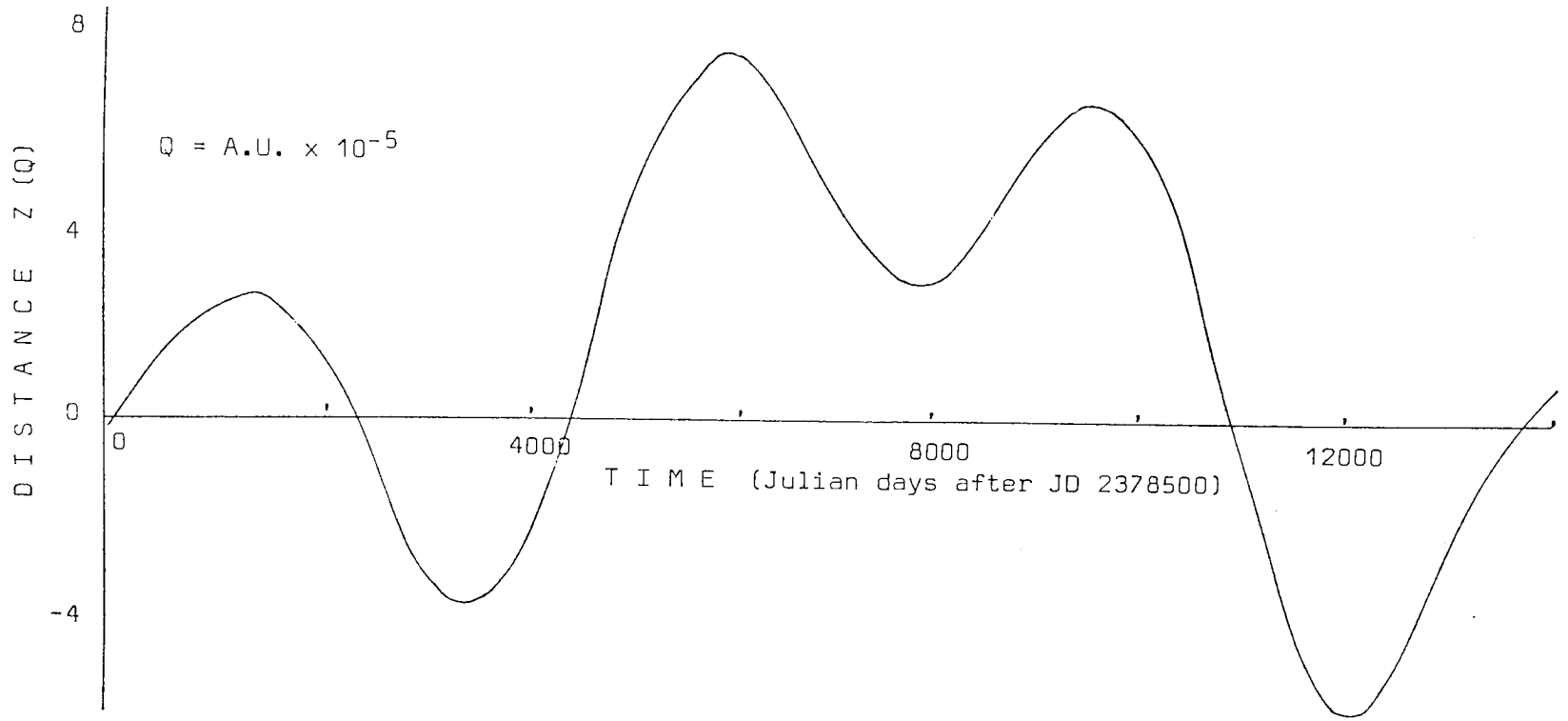

Figure 4.61 Variation with Time of Distance Z in Interval JD 2378520-2393520

Figure 4.62 Power Spectrum of Distance Z

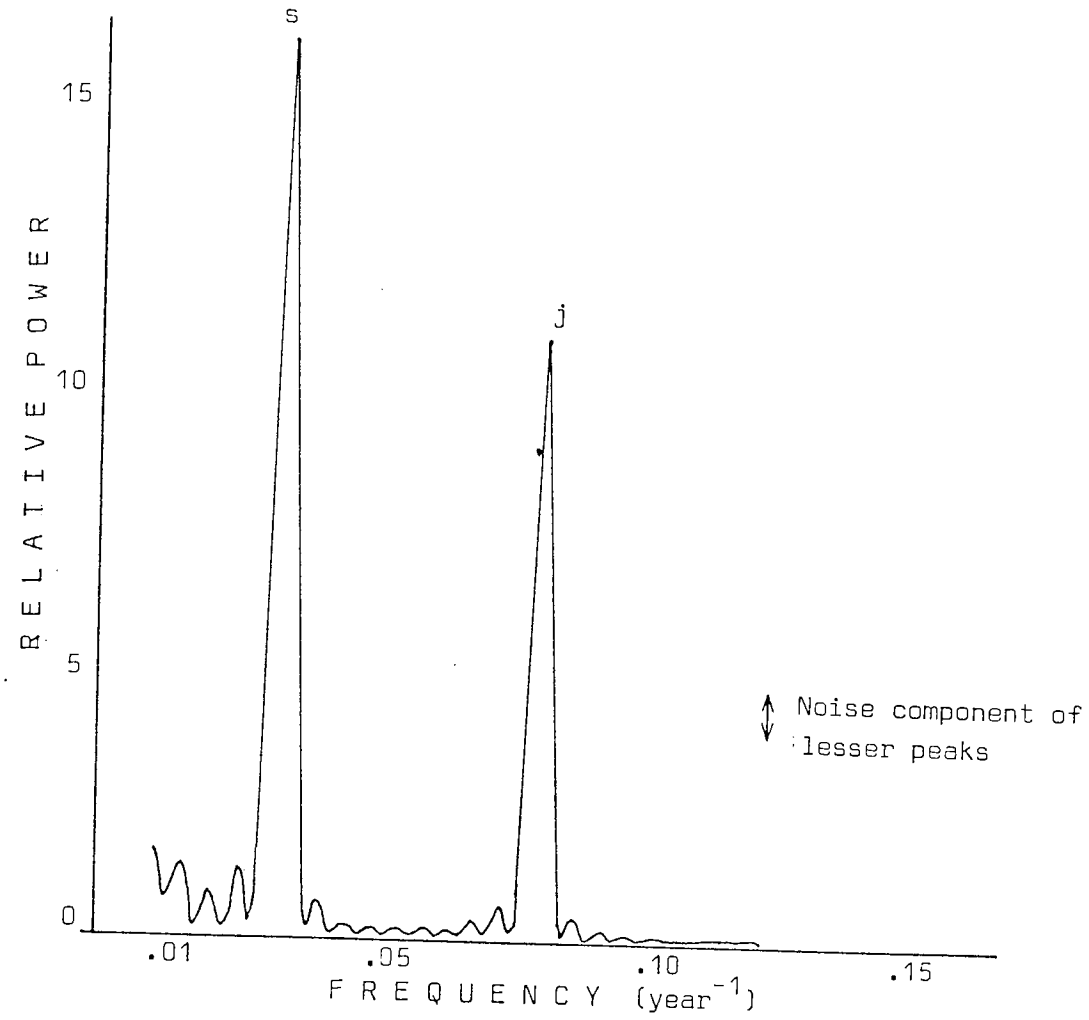

Figure 4.63 Power Spectrum of Acceleration a

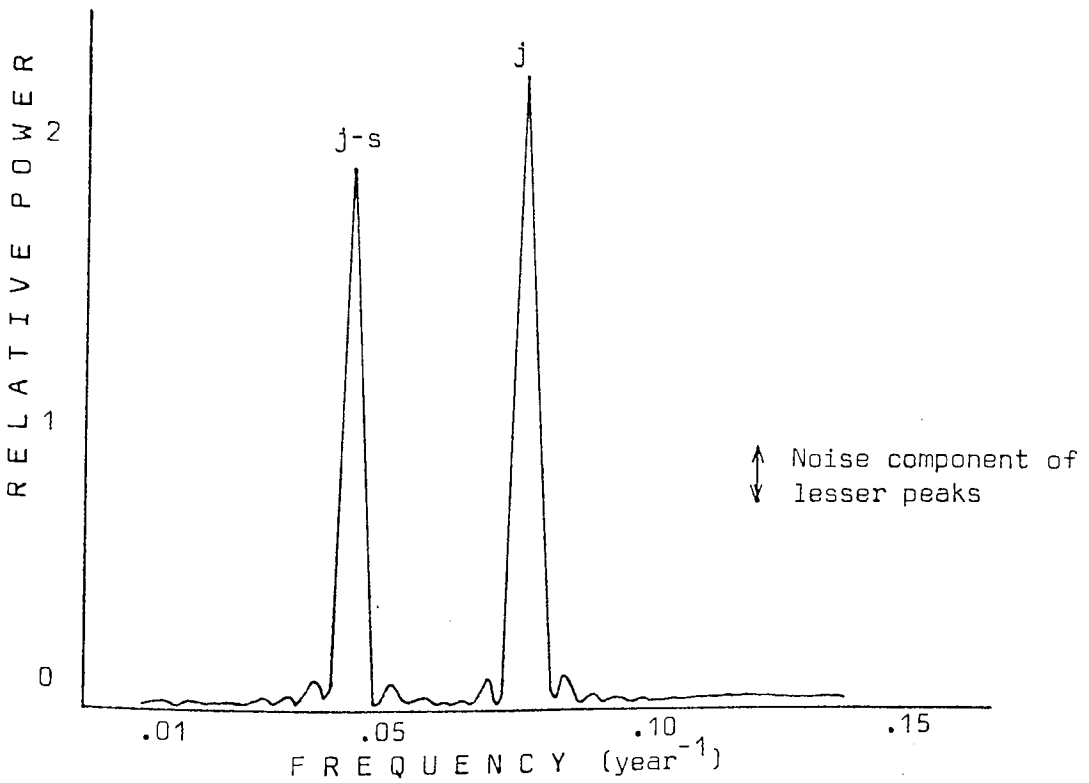

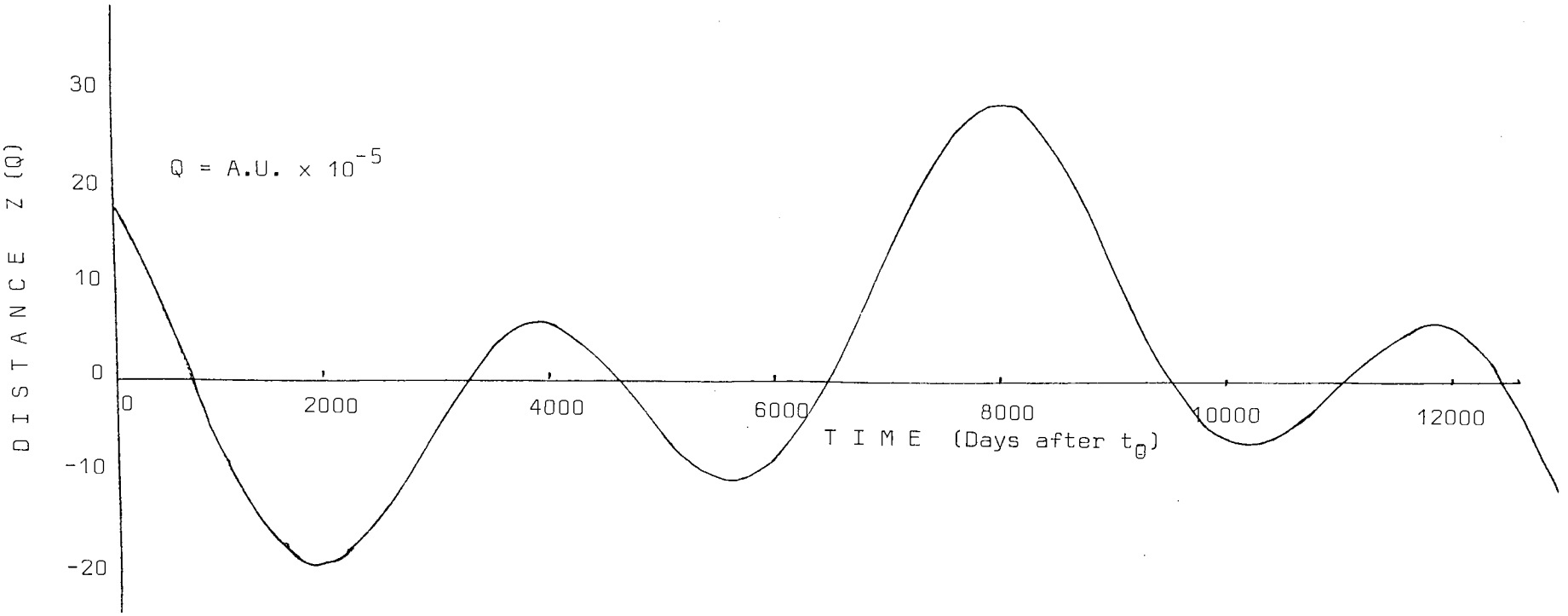

Figure 4.64 Variation with Time of Distance Z in an 'Ovenden' system, from Initial Epoch t_0

to difference yet again in order to examine directly parameters of the 'jerk force' investigated by Wood and Wood (1965), and defined as the change of acceleration. However, it is possible, using the power spectrum already obtained for acceleration A, to predict the structure of a power spectrum of 'jerk force' using the filter factor (section 2). Applying the difference filter

$$\psi_{\nabla}(Z) = 1 - Z$$

to input data is equivalent to a filter factor of

$$F_{\nabla}(\omega) = 2\ (1 - \cos\omega)$$

where ω is frequency and $Z = re^{i\theta}$.

The effect of passing data through this filter (figure 4.71) is to reduce the power at low frequencies. This effect may be observed in the spectra of angular momentum L, and that of $\dot{L}$ (see figure 4.56); in the spectrum of $\dot{L}$, where $\dot{L}$ was obtained by linear differencing from L, the relative power of J-U and J-N frequencies is boosted with respect to the power at the J-S frequency. The height of the J-N peak is also boosted with respect to the peak height at the J-U frequency.

This method permits prediction of information which is present in the spectrum of the 'jerk force' from the spectrum for acceleration a. However, it is found that although power at low frequencies is reduced c.f. higher frequencies, there is no peak at a frequency of 0.09 c/yr which could be 'amplified' by the differencing process. It was not considered practicable to attempt an evaluation of the 'rate of change of jerk force' considered by Wood and Wood (1965) for the reasons already stated.

4.8 Analysis of a Control System

As the influence of the inner planets on the motion of the solar system centre of mass was known to be small (section 4.5) it was

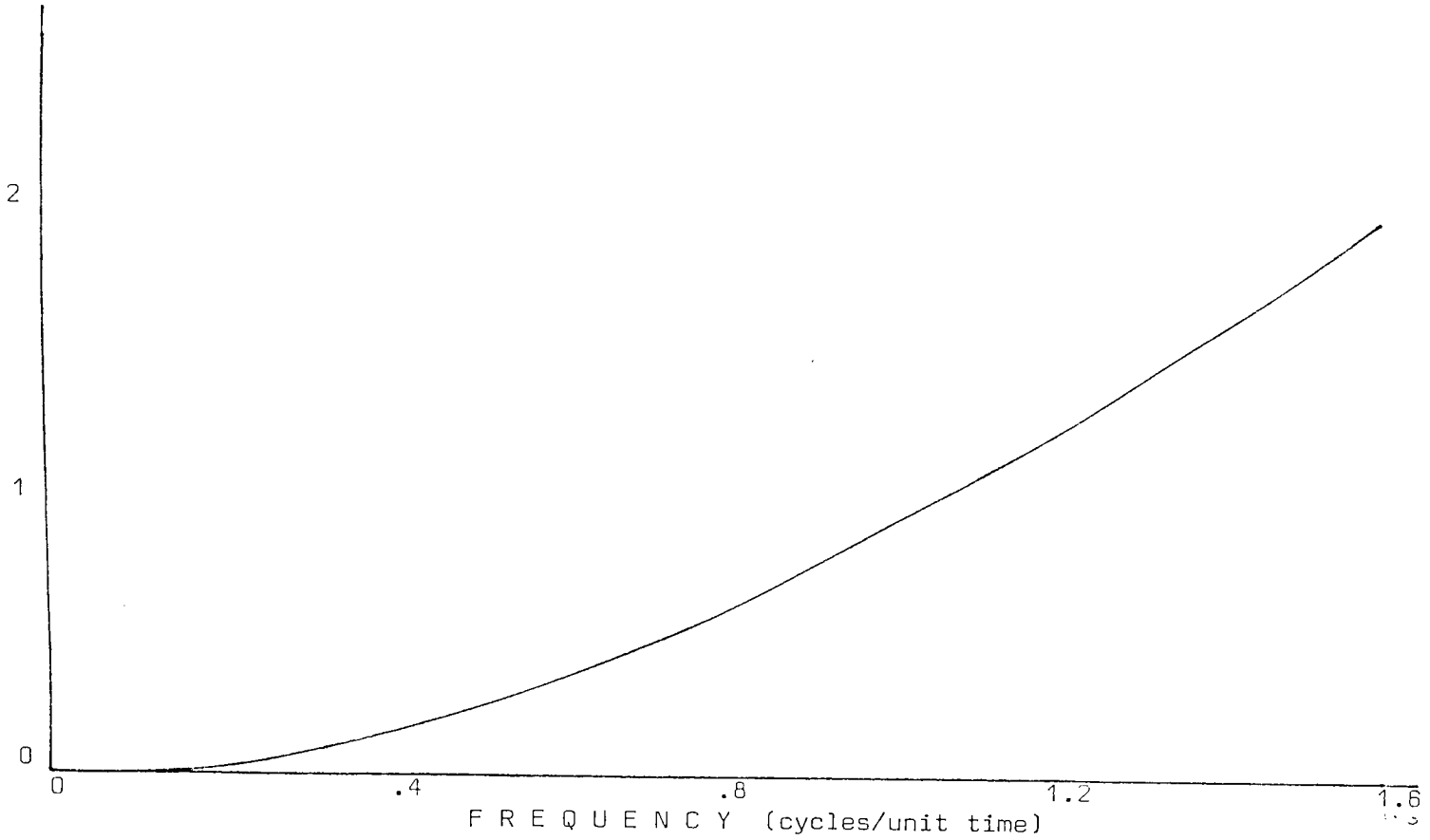

Figure 4.71 Power spectrum for linear difference filter

Table 4.81

Planetary Synodic Periods for an Ovenden System

Planets	Period	Planets	Period
A - J	7.69 years	J - U	13.81 years
A - S	5.55 years	J - N	12.84 years
A - U	4.94 years	S - U	44.54 years
A - N	4.81 years	S - N	35.81 years
J - S	20.01 years	U - N	182.7 years

decided that the result already obtained for motion of the outer planets in an 'Ovenden' system were adequate for analysis. Various synodic periods of the system were therefore calculated (table 4.81). With a lower frequency limit of 0.02 c/yr and a spacing of 0.001 c/yr, the variation in R with time was analysed. A sharp peak was observed at a frequency of 0.050 c/yr, identified with the J-S synodic period, with a smaller peak at 0.078 c/yr corresponding to the J-N alignment. Two marginal peaks were also observed, at the J-U and J-A synodic frequencies. No other synodic frequency of 'A' was found. An analysis of the Z co-ordinate motion of the centre of mass revealed only the sidereal periods of Jupiter and Saturn, as expected.

It was not considered relevant to continue with this analysis, as the power spectra for R and Z were so very similar to those obtained for our present solar system (figure 4.52) that the behaviour of other parameters of motion was predictable.

4.9 Discussion

It is apparent from the analyses in this section that the use of any arithmetic operator on input data can alter the character of the output information, for example by creating 'artificial' periodicities or suppressing those already present. Hence it is important to ensure that sufficient physical justification exists for any functions employed in such an analysis. For the 'jerk force' considered by Wood and Wood (1965), this condition would not appear to be met, as the authors themselves acknowledge.

From the analysis of the various parameters computed in this section, the importance of the sidereal periods of the outer planets in determining the motion of the sun around the centre of gravity of the solar system is evident. Thus it is not surprising that both José (1965)

and Petrova (1979) report a 179 year 'periodicity' in various parameters of the motion studied. Consideration of planetary orbits indicates that approximate 4-planet alignments occur at ~ 180 year intervals. Whilst this is a quasi-periodic effect rather than a true repeating pattern it is maintained over a considerable timescale. With the detection of an approximately 200 year variation in sunspot and auroral records (section 1), the possibility of a connection between the sunspot cycle and the motion of the sun around the centre of gravity of the solar system cannot be entirely excluded; however, no correlation is found between the eleven year sunspot cycle and any parameter of motion of the system centre of mass. With the limited amount of sunspot data available, it would seem to be more practicable to search for planetary effects on the sun which might be apparent over a shorter timescale, such as the tidal influence exerted by planets at the sun surface.

SECTION 5

Tidal Influence of Planets on the Sun

Several researchers seeking to connect planetary motion with the sunspot cycle have considered the motion of the inner planets, matching various synodic periods (Sleeper, 1972) and combinations of the inner and outer planet 'synodic resonances' (Romanchuk, 1981) to the 11 year sunspot period. Also, Bigg (1967) has examined the sunspot numbers for periods of inner planets. However, the majority of research involving the inner planets is directed towards the effect of tidal forces raised at the sun surface. Although the actual 'tidal heights' involved are of small amplitude, it has often been suggested (e.g. Wood, 1972; 1975; Dauvillier, 1976; 1977; Romanchuk, 1981) that a small periodic tidal component could act as a 'trigger' to sunspot activity, and several qualitative approaches, advancing general arguments (Brown, 1900; Anderson, 1954; Dauvillier, 1970; 1976; 1977; 1978; Prokudina, 1978; Krymsky, Petikhov and Nikolaev, 1978) have given widely differing opinions on the subject. Some authors have favoured a direct approach to the tidal problem, comparing heliocentric longitudes of two or three principal tide-raising planets with sunspot or flare appearances (e.g. Schuster, 1911; Dingle, van Hoven and Sturrock, 1973). Others have considered sequences of tidal planet conjunctions, with direct comparison to times of appearance of sunspots or flares (Blizard, 1968) or by matching periodic variations in tide amplitude raised at a series of planet conjunctions with the 11 year sunspot period (Wood, 1972; Condon and Schmidt, 1975; Wood and Wood, 1975). Several numerical

evaluations of functions of tidal height raised by three or four planets on the sun surface have been performed (Okal and Anderson, 1975; Smythe and Eddy, 1977; Krymsky, Petikhov and Nikolaev, 1978), and the results analysed for both the 11 year variation (Smythe and Eddy, 1977) and the multiple periodicities of Cohen and Lintz (1974) with negative results. However, direct comparisons of similar tidal height functions with active centre appearances (Trellis, 1966 A; B; C; Ambroz, 1971) yielded tentative positive results.

Of the approaches outlined above, there is naturally a degree of uncertainty about the validity of the simplest methods (e.g. Dingle et al.,1973). The planetary conjunction work of Wood (1972) and of Wood (1975) yields tidal functions with impressively close period matches to the sunspot cycle length (11.08 years, 11.14 years c.f. 11.08 ± .02 years). The negative results of Okal and Anderson (1975) and Smythe and Eddy (1977) are also of considerable interest, and it appears likely that any attempt to correlate 'solar tides' with the sunspot cycle must be able to explain these papers.

Since only four planets were considered by previous researchers, it was decided to utilize a full nine planet solar system model to calculate functions of the tidal height, and, as in the previous section, to employ statistical techniques of analysis to avoid the possibility of unconscious bias of results, and to search the tidal functions for periodicities.

Initially, it was decided to investigate the work of Wood (1972) and, if appropriate, to extend the scope of the analysis and seek a physical basis for the tidal function considered.

5.1 Tidal Equation

Consider the system of a sun, mass M, disturbed by one planet P. Taking P to be a point mass m, the undisturbed potential at some point C on the solar surface, radius r_0 from the sun centre, will be given, in spherical polar coordinates, origin sun centre, by

$V_1 (r, \theta, \phi) = - \frac{k^2 M}{r_0}$, where k^2 is the constant of gravitation.

The planet P effectively increases the sun radius by a tide height h; thus the new potential will be

$V_1 (R, \theta, \phi) + V_2 (R, \theta, \phi) = \text{constant}; \quad R = r_0 + h$.

Defining the polar system of reference such that θ is the heliocentric angle between P and C, the disturbing potential at C may be expressed in terms of the tidal height:

$$V_2 (R, \theta, \phi) = - \frac{k^2 m}{d} - \left(\frac{-k^2 m R \cos\theta}{r^2} \right) \quad \text{if } h << r_0$$

where r is the distance of P from the sun centre

and d is the distance of P from C.

Expanding in a series of Legendre polynomials, the tidal height at C due to planet P may be written as

$$h(\theta, \phi) \simeq \frac{k^2 m}{8g} \left[\frac{4R^2}{r^3} (3p^2 - 1) + \frac{4R^3}{r^4} (5p^3 - 3p) + \frac{R^4}{r^5} (35p^4 + 30p^2 + 3) + \ldots \right] \qquad 5.1(\text{I})$$

where $p = \cos\theta$ and $g = \frac{\partial V_1}{\partial r_0}$.

Truncating to first order, and setting $\theta = 0$ to evaluate the maximum contribution from planet P;

$$h(0) \simeq \frac{k^2 m R^2}{r^3 g} = \frac{k^2 R^2}{g} \left(\frac{m}{r^3} \right). \qquad 5.1(\text{II})$$

Denoting the maximum height by H_{tm}, the first order approximation to the tidal height at any time may be written as

$$h(0) = \tfrac{3}{2} H_{tm} (\cos^2 \theta - \tfrac{1}{3}) \quad . \qquad 5.1(\text{III})$$

5.2 Initial Evaluation

Using orbital elements taken from Astrophysical Quantities (1955), the maximum relative tidal 'height' H_{tm} was evaluated for each planet (Table 5.21) together with minimum and mean 'height'. It is evident that the major 'tide-raising' planets are Jupiter, Venus, Earth and Mercury; also that the greatest variation in tidal effect H_{tm} is that of Mercury, with a difference ratio of over 3:1 between highest and lowest possible values.

If it is assumed that planetary orbits are essentially coplanar, equation 5.1(iii) indicates that the tidal heights raised on the sun surface by two planets may be added numerically at all points on the surface when the planets are at conjunction or opposition. In the case of Earth and Venus, this combined tidal height H_{tm} is found to vary between successive alignments by a maximum of 6%. Thus, assuming this value to be a constant, $\bar{H}_{tm}$, the change in tidal height in the direction of Jupiter between successive alignments of Earth and Venus will be given by

$$\Delta H_t = \bar{H}_{tm} (\cos^2 \phi_{rc} - \cos^2 \phi_{ro}) \qquad 5.2(\text{I})$$

when $\phi_r = \phi_J - \phi_{EV}$ and ϕ_{rc} denotes E-V conjunction;

ϕ_{rc} denotes E-V opposition;

denoting the true longitude of Jupiter by ϕ_J and that of Earth and Venus at conjunction or opposition by ϕ_{EV}.

Hence a dimensionless tidal function may be defined (Wood, 1972) by

$$\Delta H'_t = \cos^2 \phi_{rc} - \cos^2 \phi_{ro} \quad . \qquad 5.2(\text{II})$$

It should be noted that this function has physical reality only at

Table 5.21

Relative Maximum Tidal Heights

Planet	H_{tm}	Planet	H_{tm}
Mercury	1.17 ± .66D	Jupiter	2.29 ± .33D
Venus	2.16 ± .05D	Saturn	0.07 ± .02D
Earth	1.00 ± .05D	Uranus	0.010 ± .008D
Mars	0.03 ± .01D	Neptune	0.00064 ± .00001D
		Pluto	0.00002 ± .00001D

where $D = \frac{k^2R^2}{g}$; units of H_{tm} are $M_{sun} \times (A.U.^{-3})$

times of Earth-Venus alignment, and that it is assumed implicitly that the tidal height equation 5.1(i) is still reasonably accurate when truncated to first order.

A basic solar system model was constructed to evaluate $\Delta H_t'$ for all dates of E-V alignment from AD 1800 to AD 2000. The results, together with the smoothed monthly sunspot numbers for the same period, are graphed in figures 5.21a, 5.22a and 5.23a. Good agreement is obtained with the results of Wood (1972), with an approximately eleven year variation present in $\Delta H_t'$. However, the calculations for $\Delta H_t'$ indicated that the value obtained was critically dependent on the precise time of E-V alignment; thus it was decided to compute the first order tidal height raised by the planets at the sub-Jupiter point (from equation 5.1(iii)) for times of E-V conjunction and opposition. The results were found to be similar to those already obtained (figures 5.21b, 5.22b, and 5.23b).

Because of the considerable tide-raising effect of Mercury, it was not thought valid to exclude the planet from calculations on the basis of its short period (c.f. Wood, 1972; Wood, 1975). The change in combined tidal heights between dates of E-V conjunction and opposition was thus recalculated for four planets; the results (figures 5.21c, 5.22c, 5.23c) indicate that the contribution of Mercury to this tidal function is considerable. For this reason, the combined tidal heights were calculated for series of times between those of E-V alignment. It was found that the tidal 'height' at the sub-Jupiter point varied widely between successive alignments and that the function 5.2(ii) did not describe in any meaningful sense the variation with time of the tidal effect of planets on the sun. However, the close agreement obtained between $\Delta H_t'$ and curves of sunspot activity (figures 5.21d, 5.22d, 5.23d) renders necessary

Figures 5.21 Tidal functions for period 1800-1850

5.22 Tidal functions for period 1850-1900

5.23 Tidal functions for period 1900-1950

Tidal function a) $\cos^2\phi_{rc} - \cos^2\phi_{ro}$

b) Tide $(JEV)_{EV_c}$ - Tide $(JEV)_{EV_o}$

c) Tide $(JEVM)_{EV_c}$ - Tide $(JEVM)_{EV_o}$

d) Smoothed monthly sunspot number $\overline{N}_{ss}$

Figure 5.21

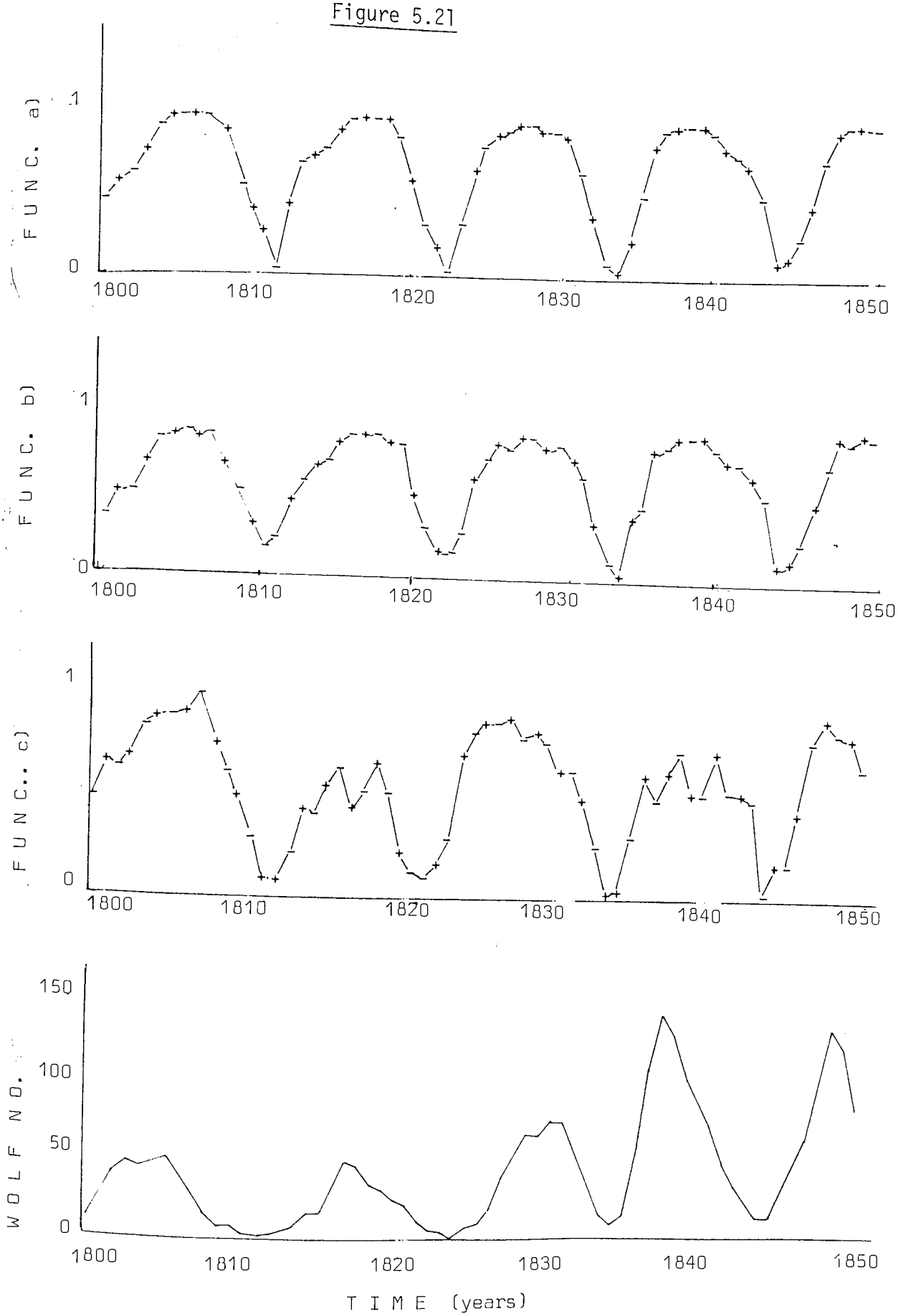
FUNC. a)
1
0
1800
1810
1820
1830
1840
1850
FUNC. b)
1
0
1800
1810
1820
1830
1840
1850
FUNC.. c)
1
0
1800
1810
1820
1830
1840
1850
WOLF NO.
150
100
50
0
1800
1810
1820
1830
1840
1850
T I M E (years)

Figure 5.22

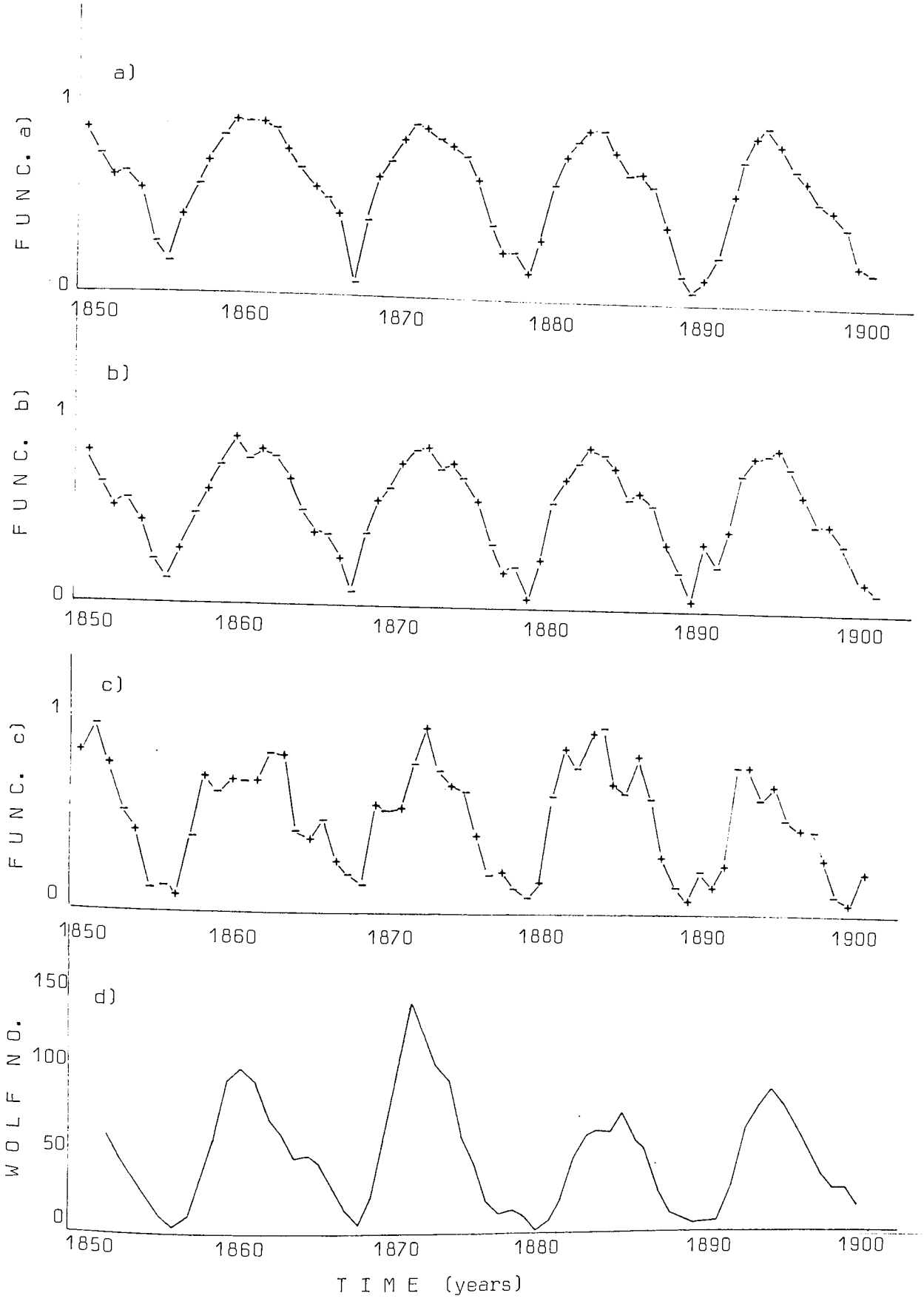
a)
FUNC. a)
1
0
1850
1860
1870
1880
1890
1900
b)
FUNC. b)
1
0
1850
1860
1870
1880
1890
1900
c)
FUNC. c)
1
0
1850
1860
1870
1880
1890
1900
d)
WOLF NO.
150
100
50
0
1850
1860
1870
1880
1890
1900
TIME (years)

Figure 5.23

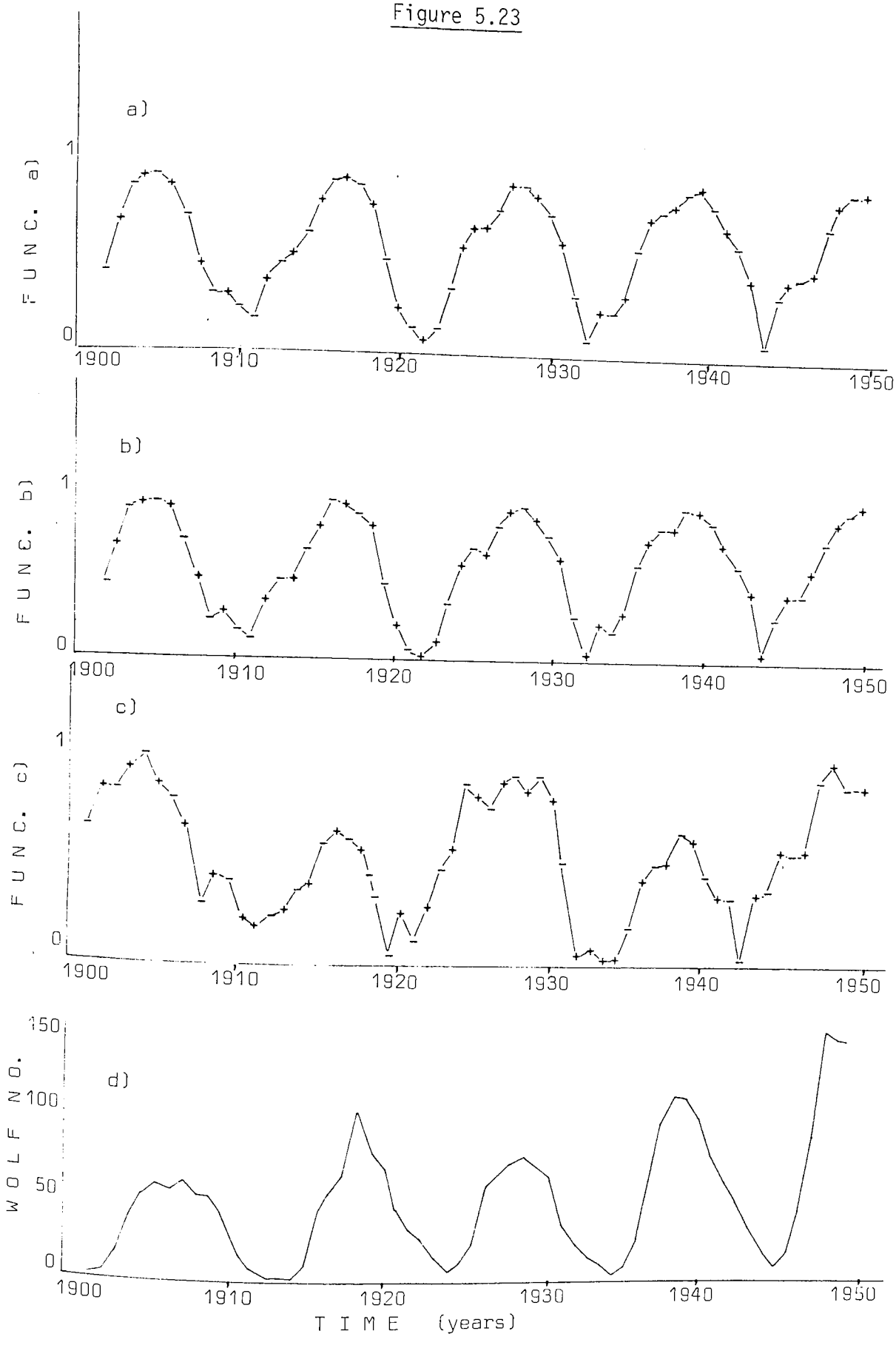
a)
FUNC. a)
1
0
1900
1910
1920
1930
1940
1950
b)
FUNC. b)
1
0
1900
1910
1920
1930
1940
1950
c)
FUNC. c)
1
0
1900
1910
1920
1930
1940
1950
d)
WOLF NO.
150
100
50
0
1900
1910
1920
1930
1940
1950
TIME (years)

some explanation of the presence of this eleven year 'tidal variation'.

5.3 Effects of Aliasing

The sampling interval utilized in the preceding work is effectively 0.8 years, an unusually large time interval to employ when searching for an eleven year variation. As the value of the tidal periodicity obtained (11.08 years) is very nearly an integral number of sampling intervals, it is possible that aliasing could be affecting the result.

Assuming planetary orbits to be circular and coplanar, V-E alignments will occur precisely at time $t = N\tau_a$, where τ_a is constant. Thus, equation 5.2(i) may be expressed more generally;

$$\Delta H_T = 1.5(H_{Mv} + H_{Me}) \{ \cos^2 \theta_{vJ} (t + \tau_a) - \cos^2\theta_{vJ}(t)\} \ .$$

For circular orbits, $\theta_{vJ}(t + \tau_a) = \theta_{vJ}(t) + \theta_{vJ}(\tau_a)$,

and substitution yields

$$\Delta H_T = -1.5 \ (H_{Mv} + H_{ME}) \sin (2\theta_{vJ}(t) + \theta_{vJ} (\tau_a)) \sin\theta_{vJ}(\tau_a) \quad \ldots \ 5.3(i)$$

As τ_d, H_{ME}, H_{Mv} are assumed constant, only one component is varying; thus the period of ΔH_T is that of $2\theta_{vJ}(t)$ ie. $2(\nu_v - \nu_J)$ where ν_v, ν_J are the frequencies of the orbits of Venus and Jupiter respectively.

The critical sampling frequency (Nyquist frequency) ν_c is here given by

$$\nu_c = (2 \ \tau_a)^{-1} \ .$$

Thus the actual periodicity obtained is a solution of

$$\nu_T' = |M(\nu_v - \mu_E) - 2(\nu_v - \nu_J)| \qquad M = \pm 1, \pm 3 \text{ etc.}$$

Smoothing selects the lowest frequency beat note, corresponding to $M = + 5$. This gives a value of $\nu_T' = .04519$ c/yr or a period of 22.13 years. Hence it is evident that undersampling (Bracewell, 1965) has artificially lengthened the periodicity of the tidal equation 5.2(i).

It is clearly possible to derive similar equations for other combinations of planets. As it is evident that the long period variation produced by equation 5.3(i) arises because the term '$\nu_V - \nu_E$' is small, it is of interest to examine the tidal height produced in the direction of Mercury by successive E-V alignments. The solution

$$\nu_T' = 10\nu_V - 8\nu_E - 2\nu_M$$

yields a periodicity of 20.4 years, indicating that short planetary periods are able to produce long period effects, and confirming that it is not valid to omit the contribution from Mercury on the grounds that its period is too short to exert appreciable long-term influence.

In an 'Ovenden' system, the tidal effect of A is dominant, its influence being twice as great as that of Jupiter; thus the three major tide-raising planets are A, Jupiter and Venus. A similar analysis for the tide at the sub-A point raised by Venus and Jupiter yields

$$\nu_T' = |M(\nu_V - \nu_J) - 2(\nu_V - \nu_A)|$$

with a lowest beat frequency of M = 2 corresponding to a period of 3.816 years. A longer periodicity of 20.4 years may be observed in the tidal function variation under Venus caused by alignments of J and A;

$$\nu_T' = |M(\nu_A - \nu_J) - 2(\nu_A - \nu_V)| \ .$$

The existence of a class of such functions with widely varying characteristic periods further reduces the significance of the low frequency variation of 5.2(i). It appears probable that the very good period match obtained between 'Wood's function' and the sunspot cycle is wholly due to the effects of aliasing. Whilst broadening the analysis to include the effects of elliptic orbits does produce a

variation in the resulting period comparable to that inherent in the eleven year sunspot cycle, there does not appear to be sufficient physical basis for this function to regard it as other than an interesting coincidence.

5.4 Further Investigation

It was decided to conduct a thorough three dimensional evaluation of the tidal effect of planets on the sun, including in the calculation all planets. Preliminary evaluation of the tidal height $h(\theta, \phi)$ for the four major tide-raising planets indicated that the truncation of the tidal equation to first order was not justifiable. It was subsequently determined that terms up to fifth order in $\cos(\theta)$ were necessary to obtain an accurate estimation of tidal height. Accordingly, a computer model was constructed to evaluate the 'relative tidal height' at a point on the sun surface due to all nine planets. Data for planet positions was taken from the Greenwich tapes previously used, and a point C was initially selected on the solar equator as close as possible to the sub-Jupiter point. However, there did not appear to be a valid physical reason for considering this point to be of special significance; the sub-Mercury point might be of more importance, since Mercury has the slowest rotation rate relative to a point on the surface of the rotating sun, and its orbit is inclined to within 1^{o} of the inclination of the solar equator. After some preliminary evaluations it was decided to examine the tidal effect at a point C rotating on and with the solar equator.

The tidal 'height' was calculated from JD 2415420.5 to JD 2451880.5, initially at 10 day intervals. As the variation between successive values was found to be considerable, it was found to be necessary to interpolate the planet co-ordinates to enable generation of daily

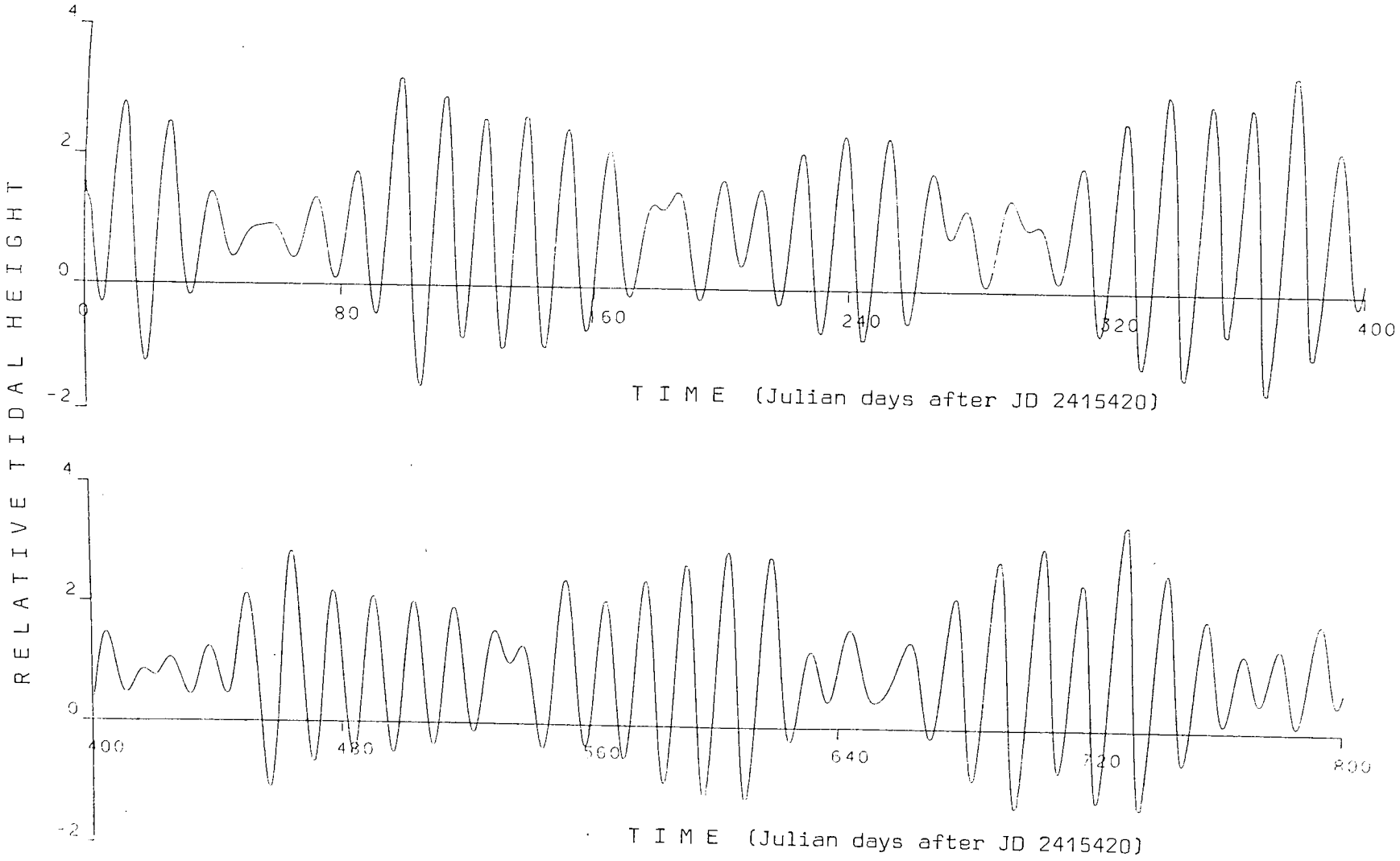

Figure 5.41 Sample of Equator Tidal Variation after JD 2415420

values of $h(\theta, \phi)$ in order to produce a smooth curve; with more data it became evident that sampling at two day intervals just sufficed to describe the variation. A sample of the tidal curve generated is given in figure 5.41.

5.5 Analysis of Tidal Effect at Sun Equator

Because of the large quantity of data involved, simple statistical methods were not found to be practicable. Some analyses were undertaken scanning the data for times of maximum/minimum tidal height, but these were not considered to be adequate. An attempt was made to use the spectral analysis techniques outlined in Section 2, as the input data is reduced to a correlation function, requiring less storage space in the computer. However, the correlation function did not damp out, indicating the presence of strong periodic components in the data, and attempts to filter the data were not successful. Consequently, although the volume of data involved rendered the calculations more tedious, a least-squares fit Fourier analysis technique was employed, similar to that used in Section 1.

Previous analyses of a 'tidal function' had detected sidereal and synodic planetary periods in the tidal data (Okal and Anderson, 1975; Smythe and Eddy, 1975). Accordingly, various synodic frequencies of tide-raising planets were calculated, and are given (Table 5.51) for reference. Because of the deterministic nature of the data, it was found to be practicable to analyse to the theoretical lower frequency limit, and so the data was initially analysed over the frequency range f = .02 c/yr to f = .50 c/yr. The resulting spectrum is shown in figure 5.52. It is evident that there exists no appreciable power at frequencies corresponding to synodic or sidereal planetary periods, and that a single significant peak is

Table 5.51

Synodic Frequencies of Principal
Tide-Raising Planets

Planet	Mercury	Venus	Earth
Venus	2.527 c/yr		
Earth	3.152 c/yr	0.625 c/yr	
Jupiter	4.068 c/yr	1.541 c/yr	0.916 c/yr

Figure 5.52 Power Spectrum of Equator Tidal Variation

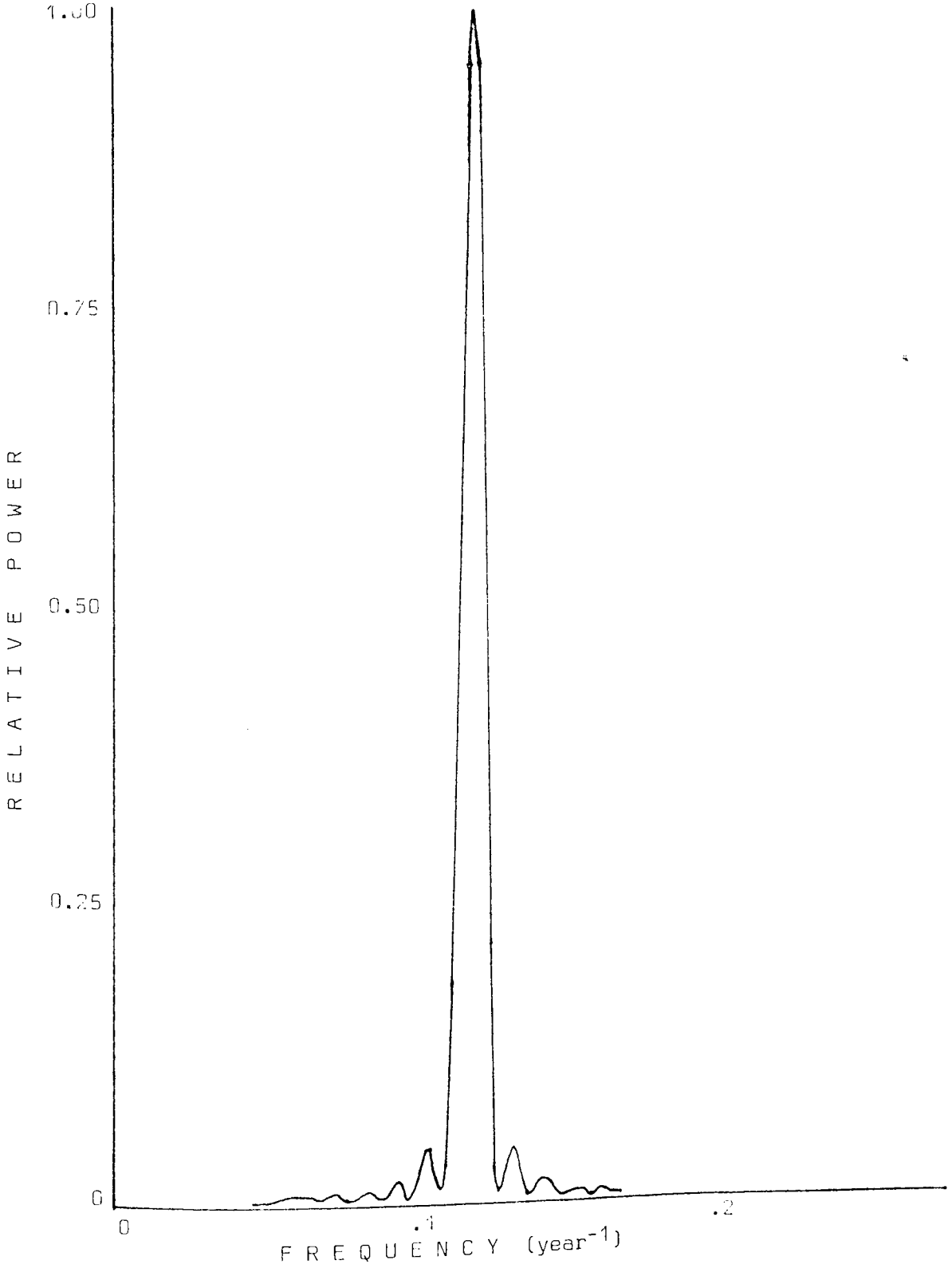

present at a frequency of .115 c/yr.

The spectrum was then calculated for frequencies up to 8 c/yr. No appreciable power was observed below 4 c/yr, but a high peak was detected at a frequency of 4.15 c/yr, corresponding to the sidereal period of Mercury. It is suggested that contributing to this large periodic effect is the 3:1 variation in tidal height raised by the planet, which is not distorted by the inclination of the orbital plane of the planet. No other peaks which could be attributed to planet periodicities were present in the spectrum, although the presence of residual power at low frequencies was noted.

5.6 Analysis of Tidal Effect for Control System

As previous research had indicated the presence of planet synodic and sidereal periods in the simple tidal functions considered (Okal and Anderson, 1975; Smythe and Eddy, 1977; Krymsky et al.,1978) it was decided to repeat the above analysis for a control system. Accordingly, a data set for an Ovenden system was generated at ten day intervals for a period of fifty years. The considerable contribution to the tidal effect of the inner planets necessitated their inclusion in the control system; for the intial evaluation actual coordinates for planets Mercury, Venus and Earth were arbitrarily chosen from epoch 1900.0, and the tidal effect at a point on the solar equator was calculated (a sample of the curve obtained is given in figure 5.61). A power spectrum was then generated for the frequency range 0.004c/yr to 4.0 c/yr, and a significant peak was observed at the low frequency end of the spectrum (figure 5.62), at a frequency of .43 ± .005 c/yr. A low, broad feature at ~ .17 c/yr was not found to be significant, and no effect was discernable at .115 c/yr. The reduced sample size is apparent from the 'ripple' on the spectral

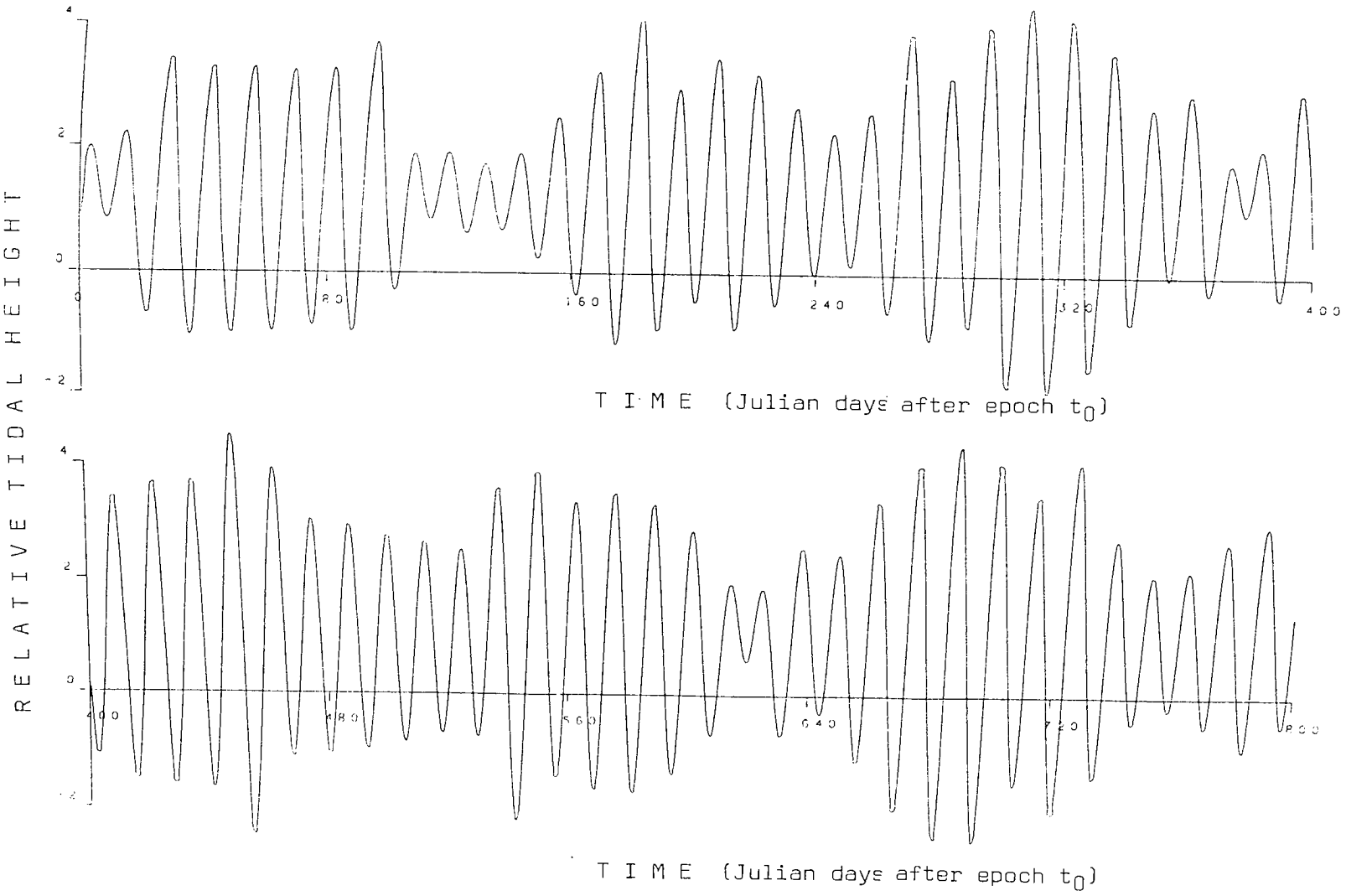

Figure 5.61 Sample of Ovenden Equator Tidal Variation (epoch t_0)

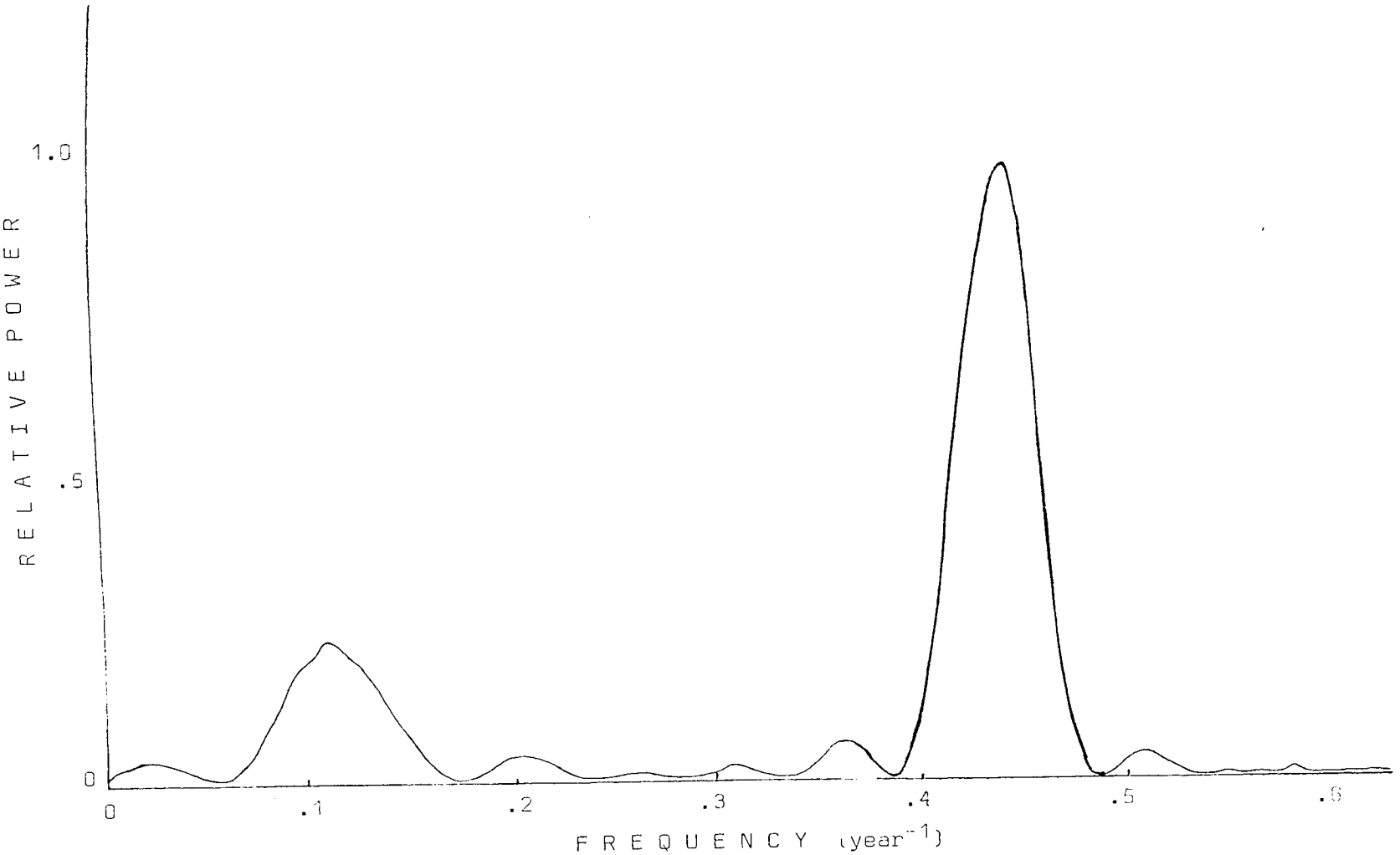

Figure 5.62 Power Spectrum of Equator Tidal Variation of an Ovenden System

curve. The peak at .43 c/yr was identified with the frequency $2\nu_A$, and the feature at ~ .17 c/yr was tentatively ascribed to the effect of Jupiter. Subsequent spectral analysis at frequencies up to 8 c/yr revealed a very high peak at the frequency of the orbit of Mercury.

The analysis was repeated using coordinates for the inner planets generated analytically from standard formulae, using values for semi-major axes given in Table 3.61, and with the eccentricity and plane of each orbit retaining their present values. The generated curves were found to have a similar character to those already obtained, and spectral analysis of the data yielded significant peaks at .43 c/yr and 4.15 c/yr, as before. However, it was observed that the noise in the high frequency range was somewhat lower than that in the spectrum previously obtained. Examination of both spectra in the high frequency range revealed only harmonics of the rotation frequency, with no significant effect at or around the frequency $2\nu_M$.

5.7 Effects of Smoothing

The rapidly changing value of the tidal effect at a point rotating on the solar equator invites the use of smoothing techniques to produce a more manageable set of data whilst retaining a good description of the overall variation. Calculation of monthly averaged values did not yield a smoothly varying function, and so it was determined to fit a series of moving average curves to the tidal data, and to assess the effect of this process on the tidal power spectra. It was realised that spectra for such smoothed data could be predicted analytically from the original spectral analysis results using the Filter Factor technique, thus avoiding the tedious computing otherwise required.

Consider the moving average tidal height averaged from fifteen 2-day interval values for each point.

Here, $\Psi(Z) = 1/15\ (1 + Z + Z^2 + Z^3 + Z^4 + ... + Z^{15})$

where $Z = e^{i\theta}$

yielding a filter factor $F(\omega)$

$$F(\omega) = 2/225\ (7.5 + \cos 14\omega + 2\cos 13\omega + 3\cos 12\omega$$
$$+ 4\cos 11\omega + 5\cos 10\omega + 6\cos 9\omega + 7\cos 8\omega + 8\cos 7\omega$$
$$+ 9\cos 6\omega + 10\cos 5\omega + 11\cos 4\omega + 12\cos 3\omega + 13\cos 2\omega + \cos 14\omega)$$

where ω is frequency.

This filter factor was calculated for values of ω from 0 to 2π, and the resulting spectrum is shown in figure 5.71. It is seen that there is a rapid fall to zero at just over .436 c/ unit time with much smaller ripples at higher frequencies. Since the new output system $g_{xx}(\omega)$ may be obtained from the relation

$$\ln g_{xx} = \ln F + \ln g_{uu}$$

where g_{uu} is the original spectrum, it is clear that the effect of this filter is to eliminate high frequency peaks in the original spectrum, allowing a little power through at some frequencies.

A type of smoothing often used to 'damp out' very short-term fluctuations is a Recentred Moving Average technique. A simple four point recentred M.A.,

$$\Psi(Z) = \tfrac{1}{8}(1 + 2Z + 2Z^2 + 2Z^3 + Z^4)$$

has a filter factor

$$F(\omega) = 1/32\ (7 + 12\cos\omega + 8\cos 2\omega + 4\cos 3\omega + \cos 4\omega)\ .$$

From figure 5.71, it is seen that the effect of this type of smoothing is greatly to reduce the 'ripple effects' of the standard M.A. process, and hence to eliminate high frequency response almost entirely.

Thus it is clear that the effect of prefiltering the tidal data, either simply by averaging over a time interval, or by using more sophisticated smoothing functions, is to eliminate high frequency peaks in the original spectrum, and selectively to boost those at lower

Figure 5.71 Power Spectra of Filter Factors For Moving Average Processes

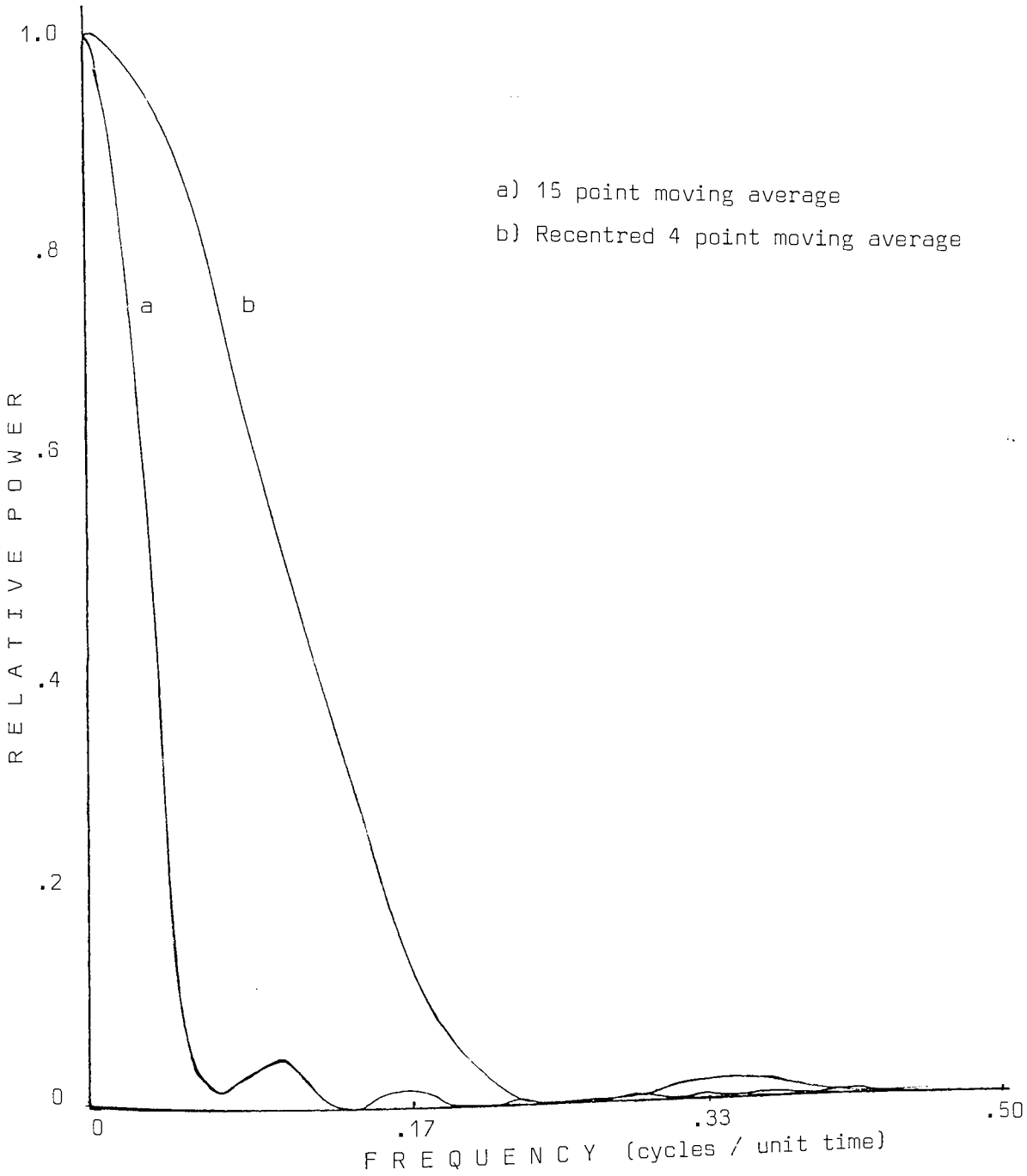

frequencies. Any of the above processes applied to the equator tidal data will yield a spectrum with only one significant peak, at ~8.7 years. However, it is also apparent that no new peaks will be created by the application to this data of such M.A. processes.

5.8 Discussion

It is evident that the tidal effect experienced by a 'sunspot' rotating on and with the solar equator alters on a timescale of days; thus functions evaluated only at times of planetary alignments (Blizard, 1968; Dingle et al.,1973; Dauvillier, 1976; 1977; Prokudina, 1978; Krymsky et.al.,1978; Romanchuk, 1981) are not able to trace the variation in a meaningful way. Some additional physical justification for the use of such functions is thus required. Also, the considerable periodic effect of Mercury on any parameter of tidal action implies that reults obtained from models which exclude the planet are inherently inaccurate.

The analyses previously undertaken of tidal height at a point on the solar surface (Okal and Anderson, 1975; Smythe and Eddy, 1977) have identified various planetary synodic and sidereal periods from power spectra of the tidal data, with no other periodic term detected. However, the results of this investigation are not in accord with previous research; no evidence is found for any periodic component of the motion of Venus or Earth being expressed in the overall tidal height at the solar surface. This is also found to be the case for the tidal forces within an 'Ovenden' system. Whilst the control system displays a possible slight influence of Jupiter, no such influence is observable in analysis of the 'actual' system, although it is feasible that a very slight effect of Jupiter could be present, masked by the residual low frequency power.

It appears probable that the principal reason for the recovery essentially of only input information in previous work, is the truncation of the tidal height equation to first order. In all the research papers considered, the tidal equation quoted is 5.1(iii); no consideration appears to have been given to the significance of higher order terms, although terms of up to order $(\cos\theta)^5$ are found to be significant for some values of θ.

The comparatively high tidal potential of A is apparent from figure 5.62. It is evident that the low eccentricity of the orbit assigned to the planet causes the frequency $2\nu_A$ to be expressed; it is seen that there is no discernible power at frequency ν_A. Contrasting this behaviour with that of Mercury in both actual and control systems, it is clear that the ellipticity of the planetary orbit is of critical importance in determining whether the fundamental frequency of orbit, or the first harmonic, is expressed in the tidal effect. It is, therefore, possible to predict the effect on the control system tidal variation of an increase in the ellipticity of orbit assigned to A. Of more immediate import, it is apparent from the behaviour of the control system that the dominant frequencies which would be observed in the tidal data, if Venus or Jupiter were exerting an appreciable periodic effect, would be $2\nu_V$ and $2\nu_J$ rather than the fundamental frequencies of orbit indicated by previous research (Smythe and Eddy, 1977; Krymsky et al., 1978). No higher harmonics of orbital frequencies are observed in any of the power spectra generated (c.f. Okal and Anderson, 1975).

The one unexpected, significant feature of the tidal variation at the solar equator is the periodic variation in tidal effect at a frequency of .115 c/yr. This effect is not identified with planetary synodic or sidereal periods, and examination of the tidal curve reveals

modulation of the amplitude of the short period tidal variation with a mean period of ~ 8.7 years. This intriguing long-period effect clearly merits further investigation.

Section 6

Latitude Distribution of Tidal Variation

Very little work has previously been undertaken to evaluate possible links between the distribution over the sun surface of sunspots and parameters of planetary motion, although a connection between sunspot births and a parameter of planetary tidal effect has been suggested (Trellis, 1966A, B, C). Series of planetary conjunctions of the four major tide-raising planets have also been correlated with short-term flare occurrence(Blizard, 1968), and occurence of calcium flocculi has been linked to the tidal effect of the six innermost planets (Ambroz, 1971).

On the basis of the results from Section 5, the results of Blizard are discounted, because of the use of planetary conjunctions as a tracer of tidal action. Whilst the general arguments of Trellis and Ambroz are of interest, their use of a first order approximation to the tidal function, together with the several averaging processes applied and the infrequent data sampling, greatly reduce the accuracy of the numerical calculations. Hence it is not possible to derive useful information about a possible tidal latitude effect from previous research.

6.1 Initial Investigation

It was decided to sample the instantaneous tidal effect encountered by a 'sunspot' rotating with the sun surface from a rest meridian at the initial epoch t_o, for a series of solar latitudes ϕ. A value of

$\phi = 4^o$ was initially selected, and the tidal effect calculated at two day intervals from JD 2415420 to JD 2451850. A sample of the variation with time is given in figure 6.11a. It is clear that the tidal effect encountered by a sunspot rotating at 4^o latitude has a short-term periodicity of ~ 12.5 days; this is ascribed to half the spot rotation period. The magnitude of the tidal effect at successive peaks is seen to vary greatly and non-randomly with time, with atypical features occurring at ~120 day intervals.

The tidal effect at $\phi = 12^o$ was then computed for the same 100 year period, and for a similar imaginary 'sunspot', set rotating from the same rest meridian at the initial epoch. A sample of the tidal variation is given in figure 6.11b. Comparison of curves 6.11a and 6.11b reveals the gradual shift out of phase of the short-period variations, due to solar differential rotation. It is evident that, as indicated from equation 5.1(i) the solar rotation frequency $2\nu_\theta$ is expressed in the tidal curve in preference to ν_θ.

Using a technique for generation of power spectra similar to that utilized in Section 5, an analysis was performed of the data set for $\phi = 4^o$. The lower frequency limit was set at .02 c/yr, with a frequency spacing of .001 c/yr. Two regions of interest were identified, the low frequency end of the spectrum (figure 6.12a) and the region ν = 1.4 c/yr to 1.6 c/yr (figure 6.12b). A single sharp peak is evident in figure 6.12a, at ν = .089 c/yr, close to the orbital frequency of Jupiter. However, as no effect was observed at or around the frequency ν = .19 c/yr, which the results of Section 5 would indicate as the predominate tidal frequency of Jupiter, no positive identification was made. However, the dominant peak in figure 6.12b, at ν = 4.15 c/yr, was identified with the orbital frequency of Mercury.

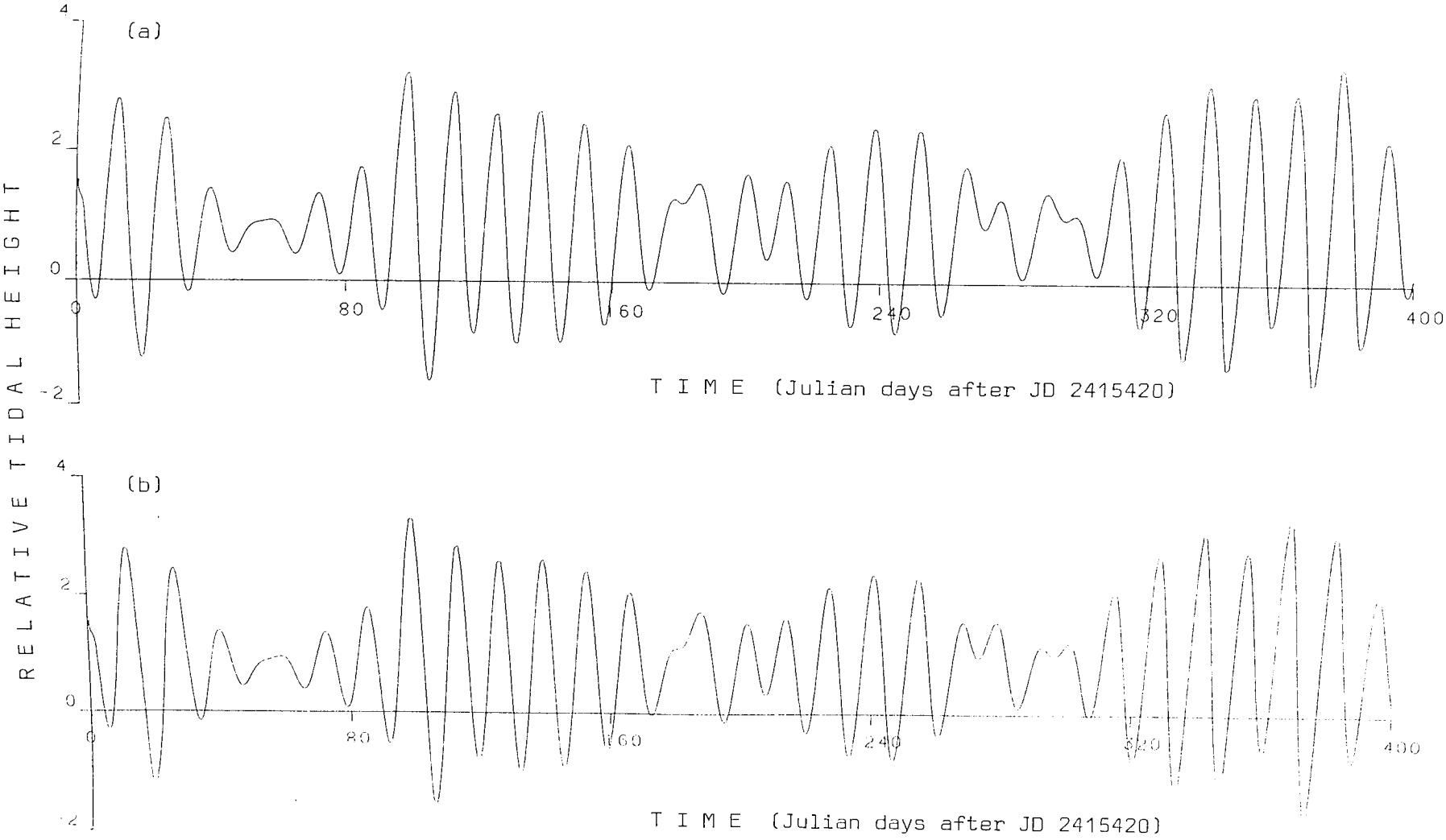

Figure 6.11 Samples of tidal variation at latitudes a) $\emptyset = 4^{o}$ b) $\emptyset = 12^{o}$

Figure 6.12 Power spectra for tidal effect at latitude $\emptyset = 4^{0}$

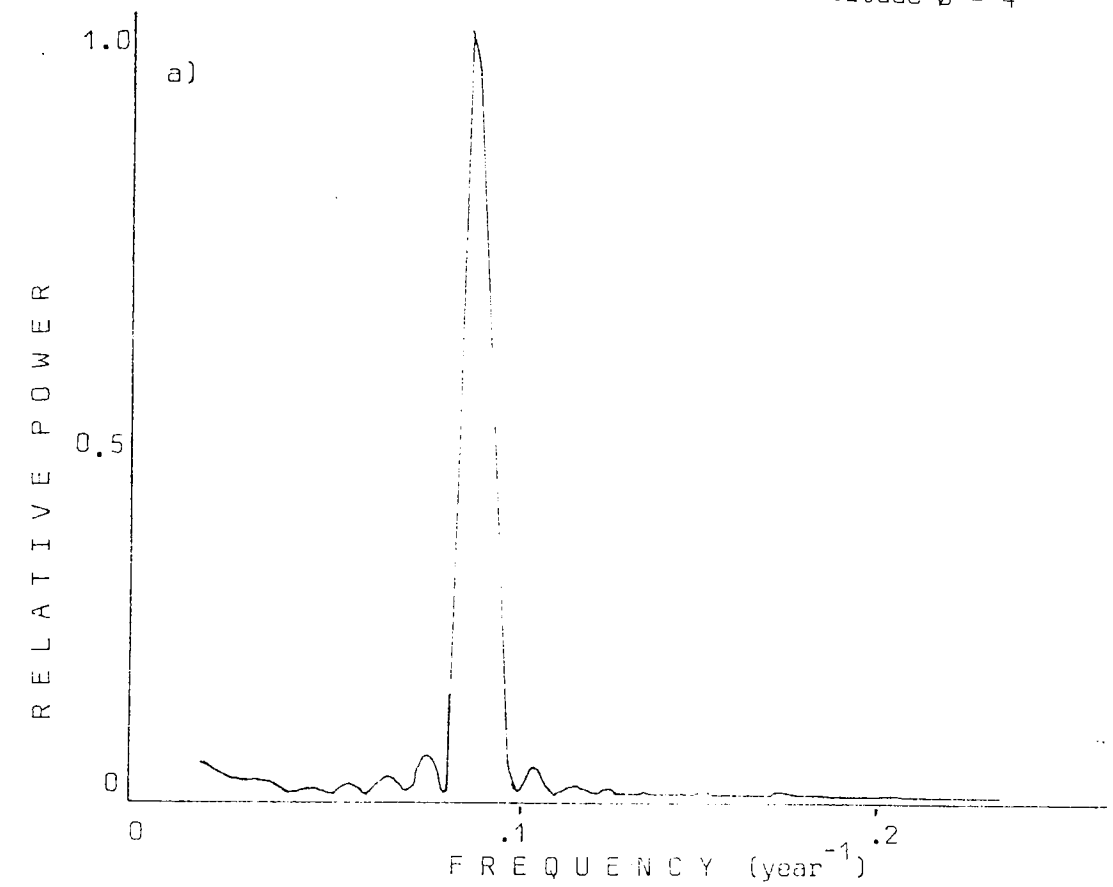

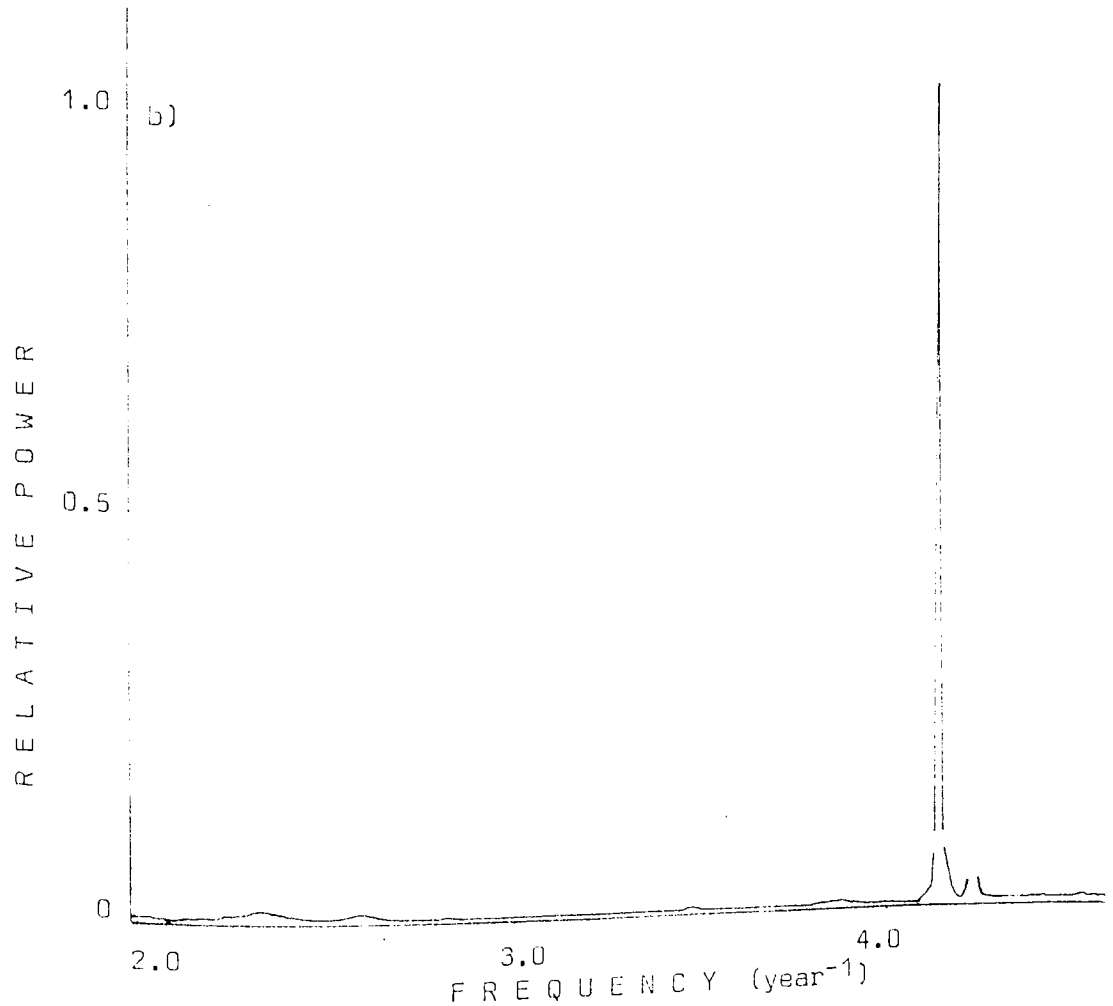

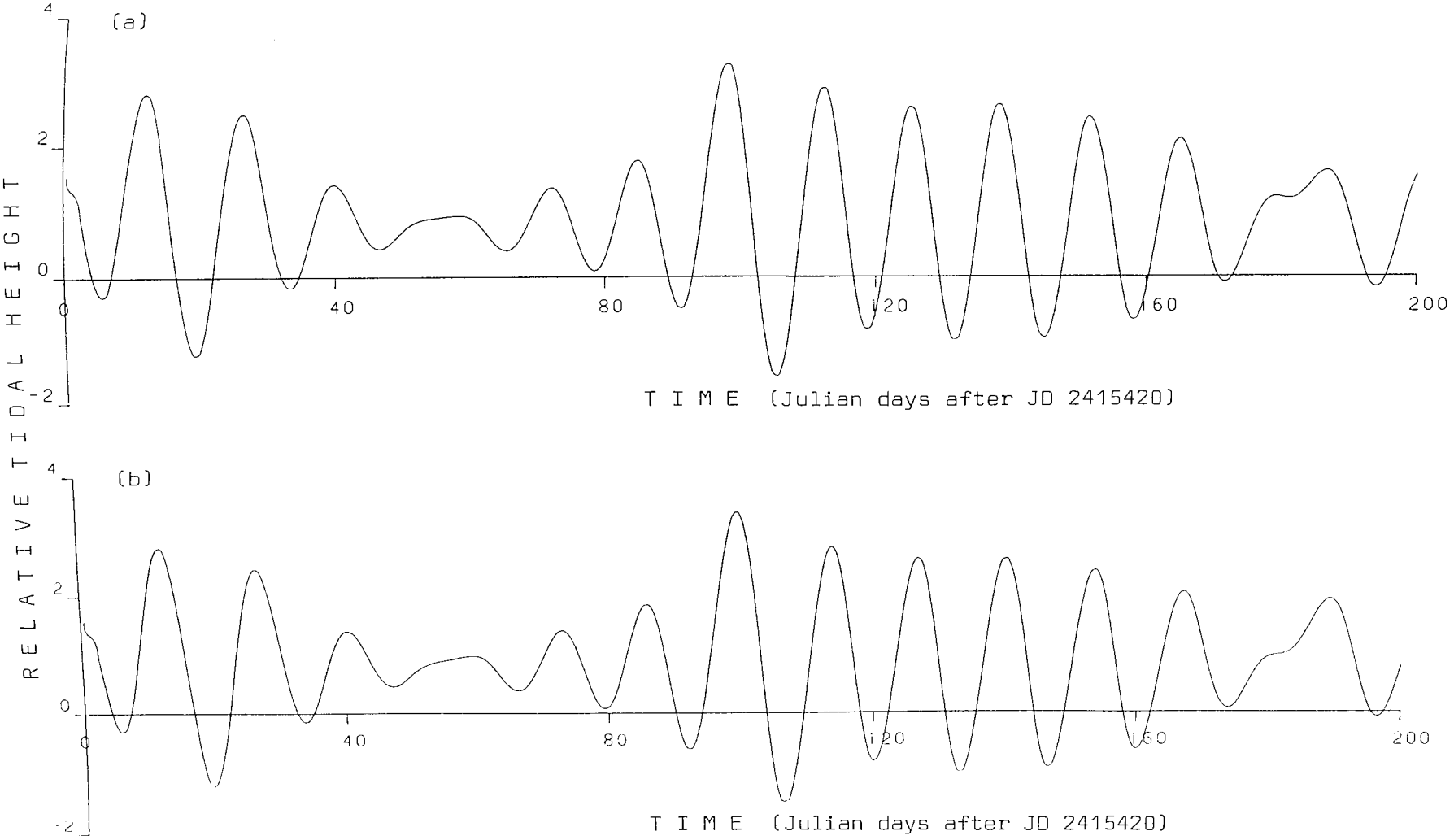

Figure 6.13 Samples of tidal variation at latitudes a) $\emptyset = 8^{o}$ b) $\emptyset = 16^{o}$

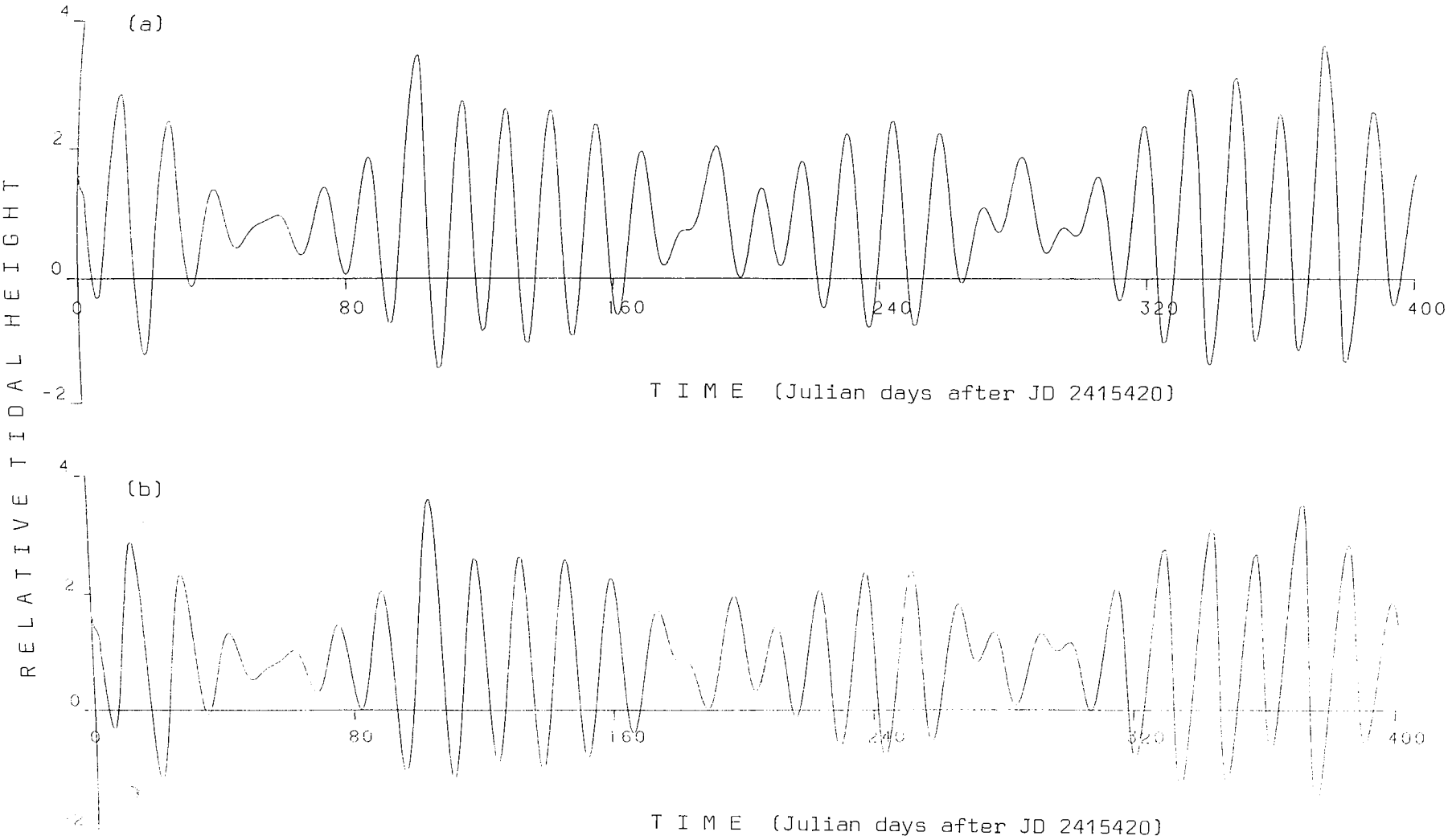

Figure 6.14 Samples of tidal variation at latitudes a) $\emptyset = 20^{o}$ b) $\emptyset = 30^{o}$

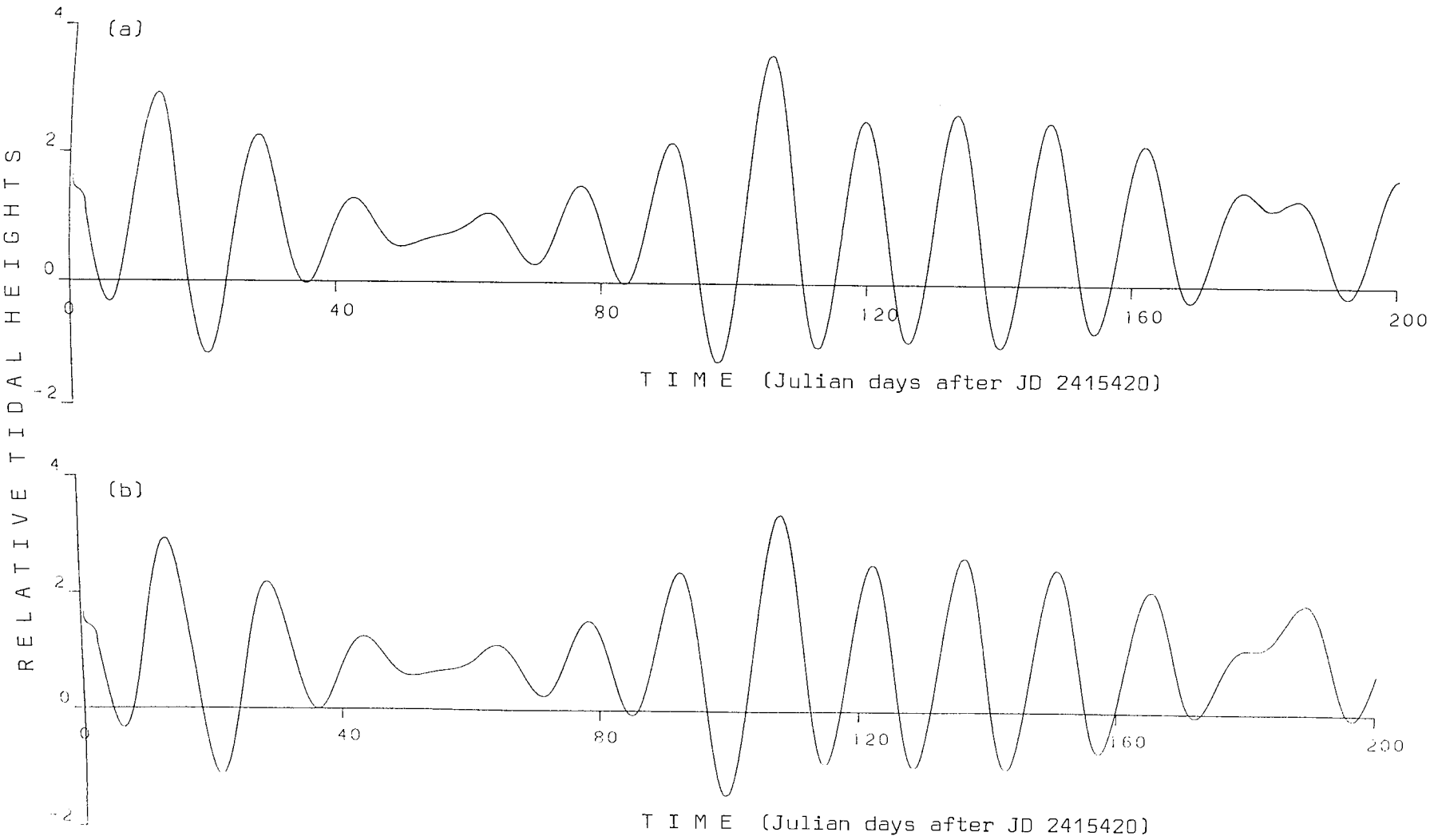

Figure 6.15 Samples of tidal variation at latitudes a) $\emptyset = 35^{o}$ b) $\emptyset = 40^{o}$

Analysis of the data set for $\phi = 12^0$ revealed a single sharp low-frequency peak at $\nu = .12$ c/yr. The frequency ν_M was also identified. Examination of very high frequencies above 6 c/yr indicated considerable power at frequencies associated with harmonics of the rotation frequency ν_0.

The tidal effect at latitudes $\phi = 8^0$ and $\phi = 16^0$ was generated; samples of the first section of the resulting curves are given in figures 6.13a and 6.13b respectively. Statistical analysis revealed sharp peaks at 4.15 c/yr as before. No low frequency peak was identified for $\phi = 8^0$, but for $\phi = 16^0$ a significant effect was observed at $\nu = 0.3$ c/yr. As no effect at these latitudes was apparent near $\nu \simeq .089$ c/yr, it was decided that the peak in figure 6.12a was not attributable to the effect of Jupiter.

The tidal variation encountered by a spot rotating with the sun surface was calculated for a series of latitudes. Samples of the variation at $\phi = 20^0$, 30^0, 35^0 and 40^0 are given in figures 6.14 and 6.15. Statistical analysis of the data indicated the presence of a strong periodic effect of Mercury at all latitudes considered. High frequency effects similar to those already detected in the $\phi = 4^0$ and $\phi = 12^0$ data, were also present. Also apparent in most data analysed was a single low-frequency peak.

6.2 Further Investigation

It was decided to compare the results with the behaviour of an 'Ovenden' system. Accordingly, tidal curves were generated at a series of latitudes for fifty years of planetary data, using the control

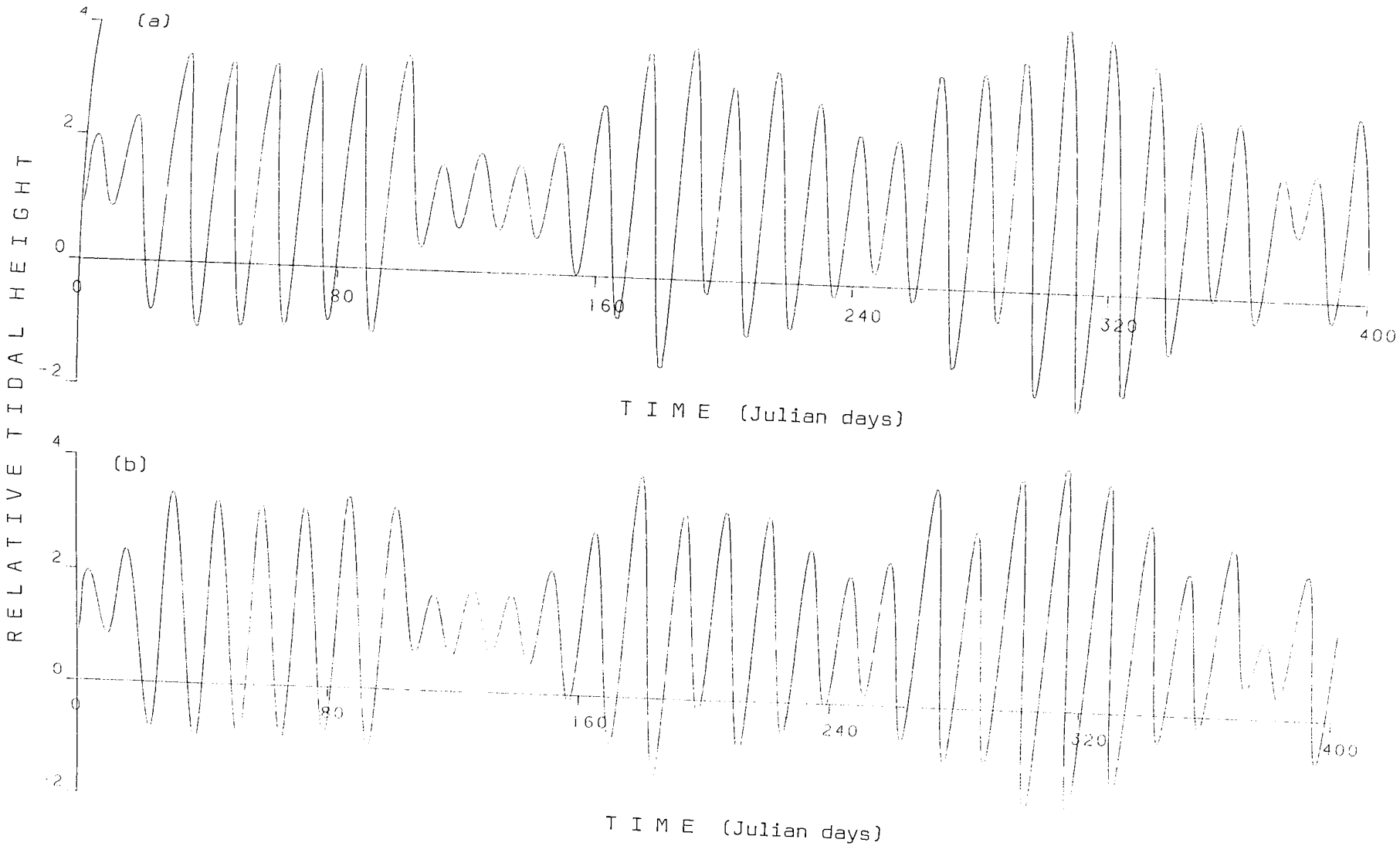

Figure 6.21 Samples of tidal variation for an 'Ovenden' system at latitudes a) $\emptyset = 8^{o}$ b) $\emptyset = 16^{o}$

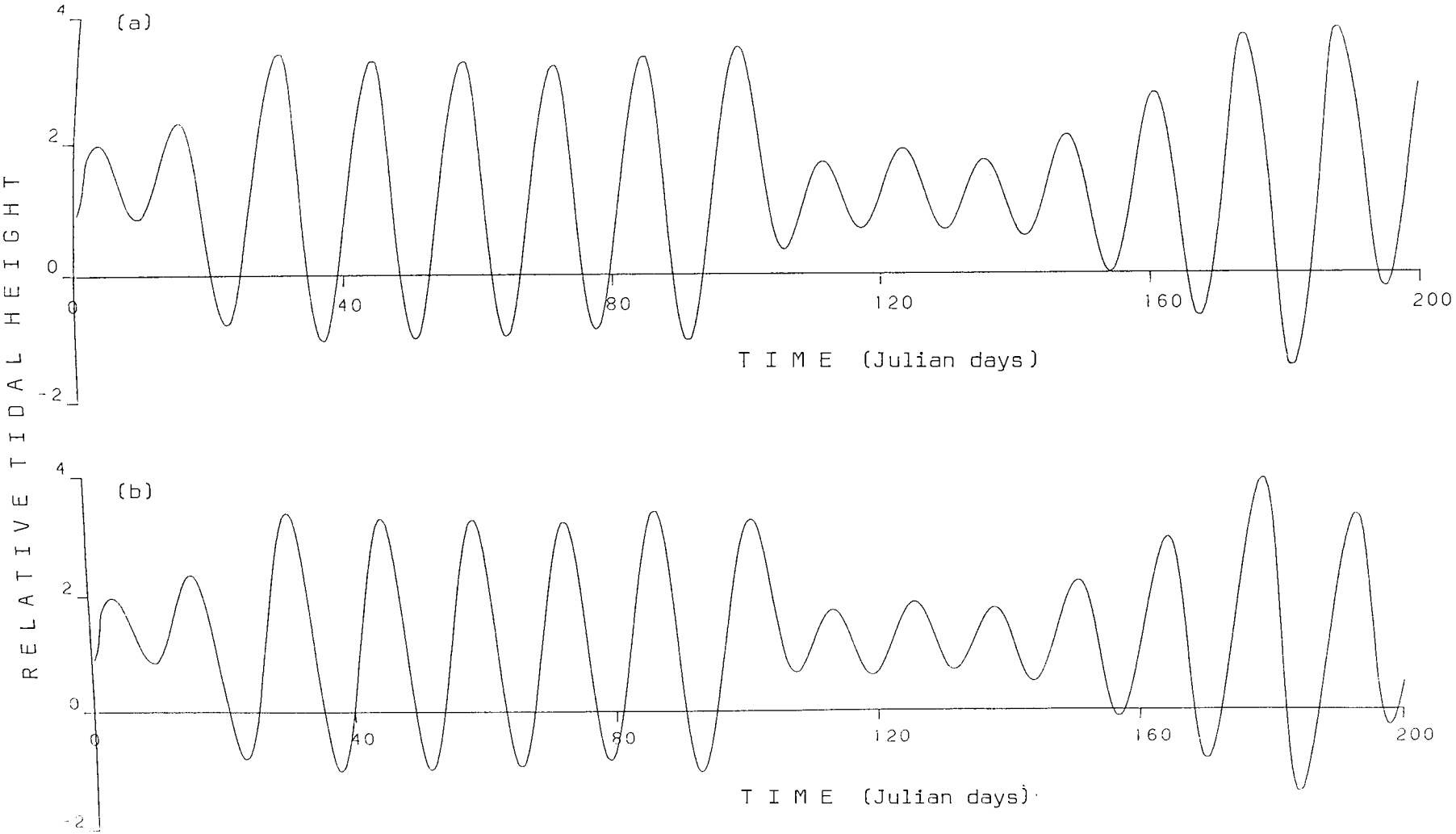

Figure 6.22 Samples of tidal variation for an 'Ovenden' system at latitudes a) $\emptyset = 24^{o}$ b) $\emptyset = 30^{o}$

system coordinates utilized in Section 5. Samples of the variation for $\phi = 8^o$, $\phi = 16^o$ are given in figure 6.21, and for higher latitudes $\phi = 24^o$ and $\phi = 30^o$, in figure 6.22. It is evident that the character of the variation is appreciably different from that in section 6.1.

Statistical analysis of the data at all latitudes revealed a high peak at around .43 c/yr, identified with the frequency $2\nu_A$. No effect was found at any latitude corresponding to the frequency ν_A, in accordance with the predictions from Section 5. A broad low peak of marginal significance was observed in all these spectra, similar to that in figure 5.62. As before, this feature of the spectrum was tentatively attributed to the effect of Jupiter. No low frequency effect comparable to that detected in 'our' solar system tidal effect was discernible at any solar latitude in the 'Ovenden' system.

6.3 Examination of Low Frequency Effect

It was decided to examine the variation with solar latitude of the low frequency effect, whose presence in the tidal data is manifest as a modulation of peak heights. Examination of the distribution of frequency with latitude (figure 6.31) revealed a considerable frequency span in the tidal data from latitudes $\phi = 0^o$ to $\phi = 40^o$. A graph was produced (figure 6.32) of the variation of period with latitude, and it was observed that the upper part of the resulting distribution exhibited marked similarity to the curve of distribution of sunspots over the sun surface during a typical cycle. If it were assumed that all the low frequency effects were in phase at some epoch t = 0, figure 6.32 would show for each latitude the time of the first subsequent maximum. Hence the upper portion of this distribution could be interpreted as indicating the progression, through successively lower latitudes, of a maximum in the planetary tidal effect at the sun surface.

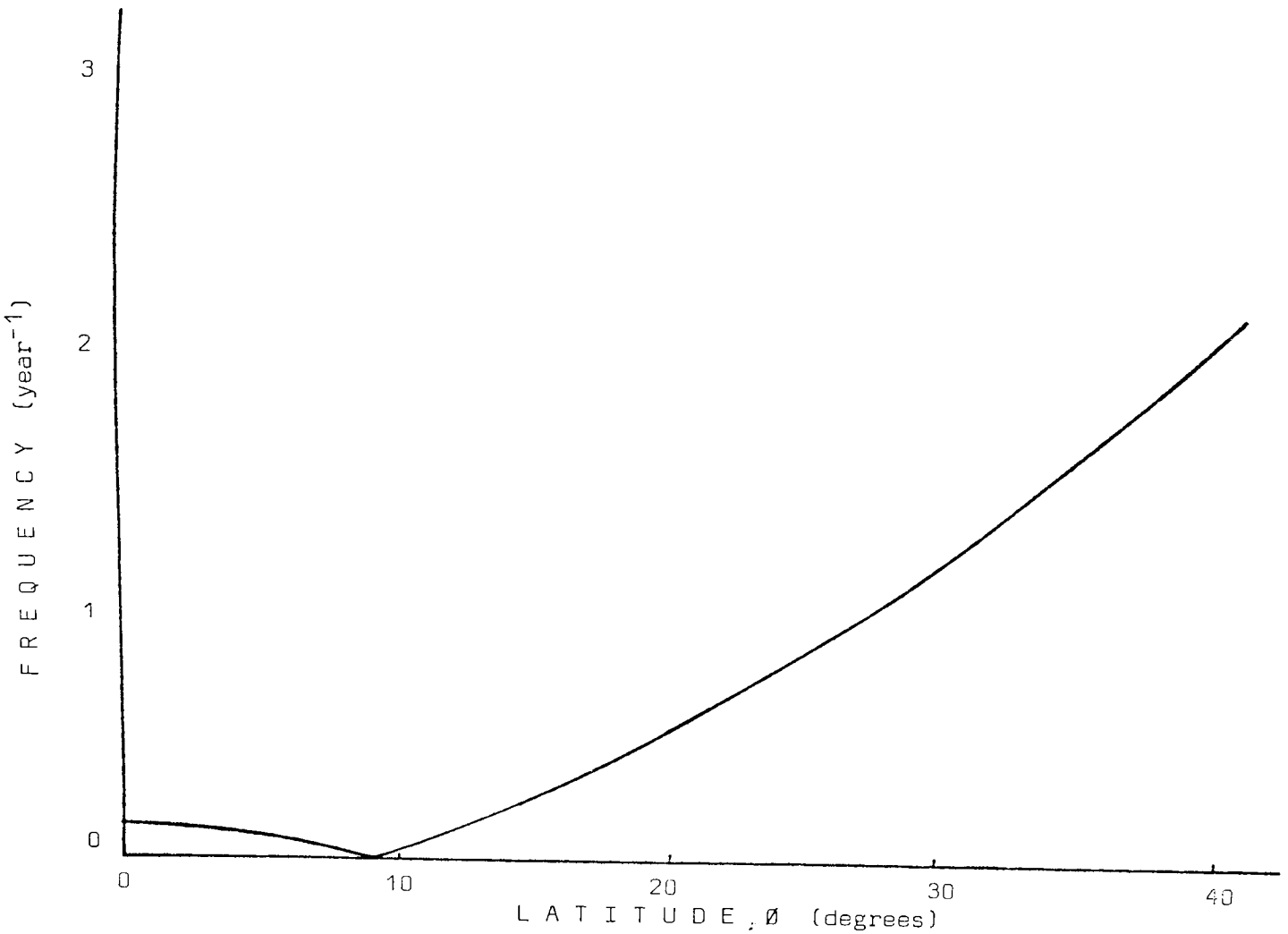

Figure 6.31 Distribution of Tidal Frequency with Latitude

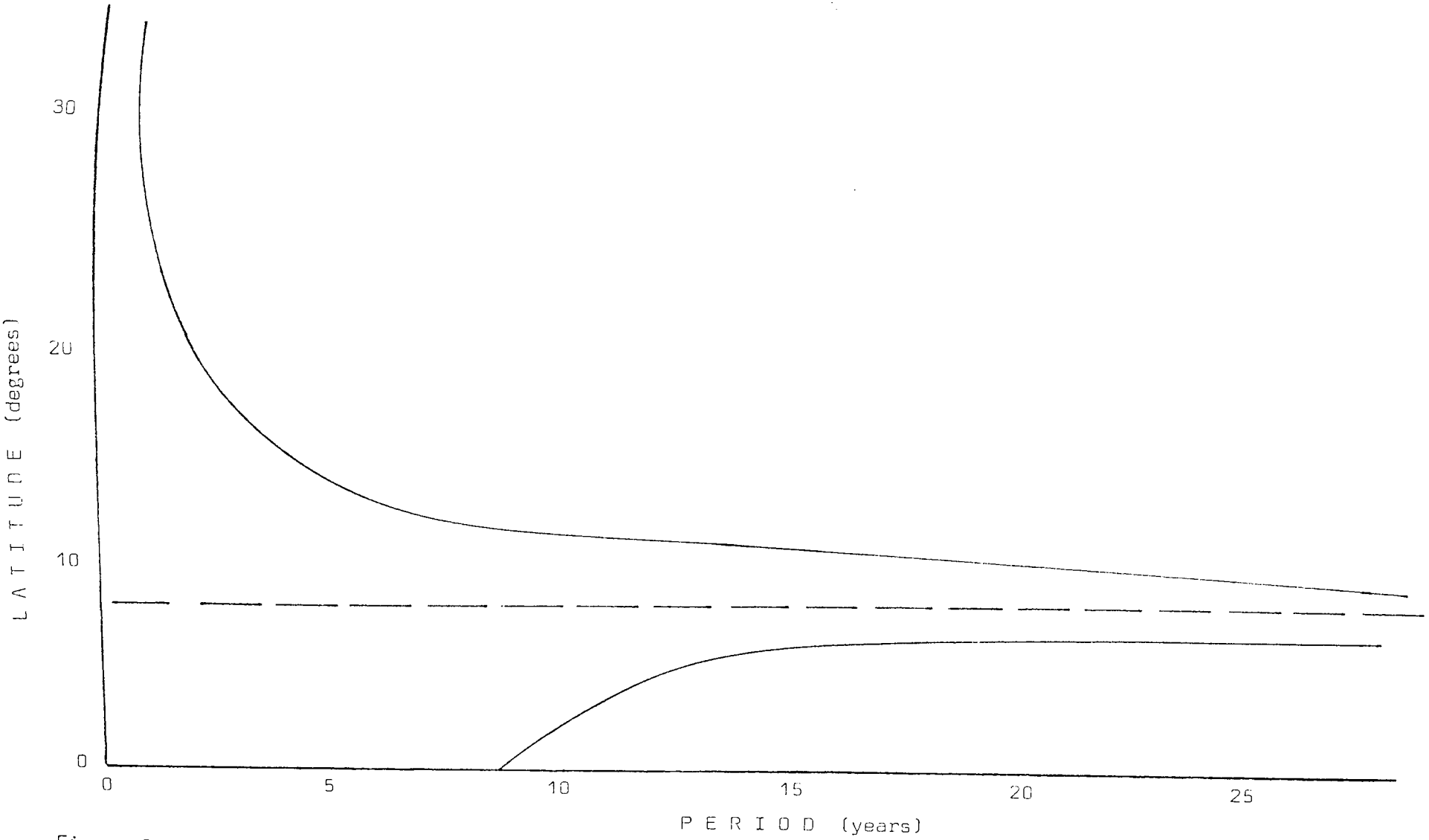

Figure 6.32 Distribution of Tidal Periodicity with Solar Latitude

6.4 Planetary tidal effect and Sunspot Distribution

The hypothesis was formulated that extreme tidal values occurring as a result of this long-period variation were acting as a 'trigger' to sunspot formation. A mechanism controlling the duration of sunspot cycles was envisaged as 'latching on' to the tidal effect at high latitudes at the commencement of each cycle, with sunspot formation triggered at successively lower latitudes as the cycle progressed. It was expected that there would be a time lag between sunspot formation and the subsequent appearance of spots on the solar disc, with some degree of scattering due to random convection effects in the solar photosphere.

6.5 Upper Latitude Bound

In such a model, it is reasonable to assume that some minimum period will exist, below which successive maxima and minima of the tidal effect follow one another so closely that sunspot formation is not triggered. Consideration of the frequency associated with the orbit of Mercury suggests a possible upper bound of ~ 4 c/yr on such a frequency; however, it has been suggested that the frequency of orbit of Mercury exists in the Waldmeier sunspot numbers (Bigg, 1967). Consideration of the diminishing power associated with the long period tidal effect with increasing latitude suggests a possible turning point in the region of 2 c/yr. This gives a maximum-minimum time of around three months, corresponding to a latitude of $\sim 40^{o}$. However, this tentative definition of a possible boundary by no means excludes the possibility of tidal triggering of active centres at higher latitudes.

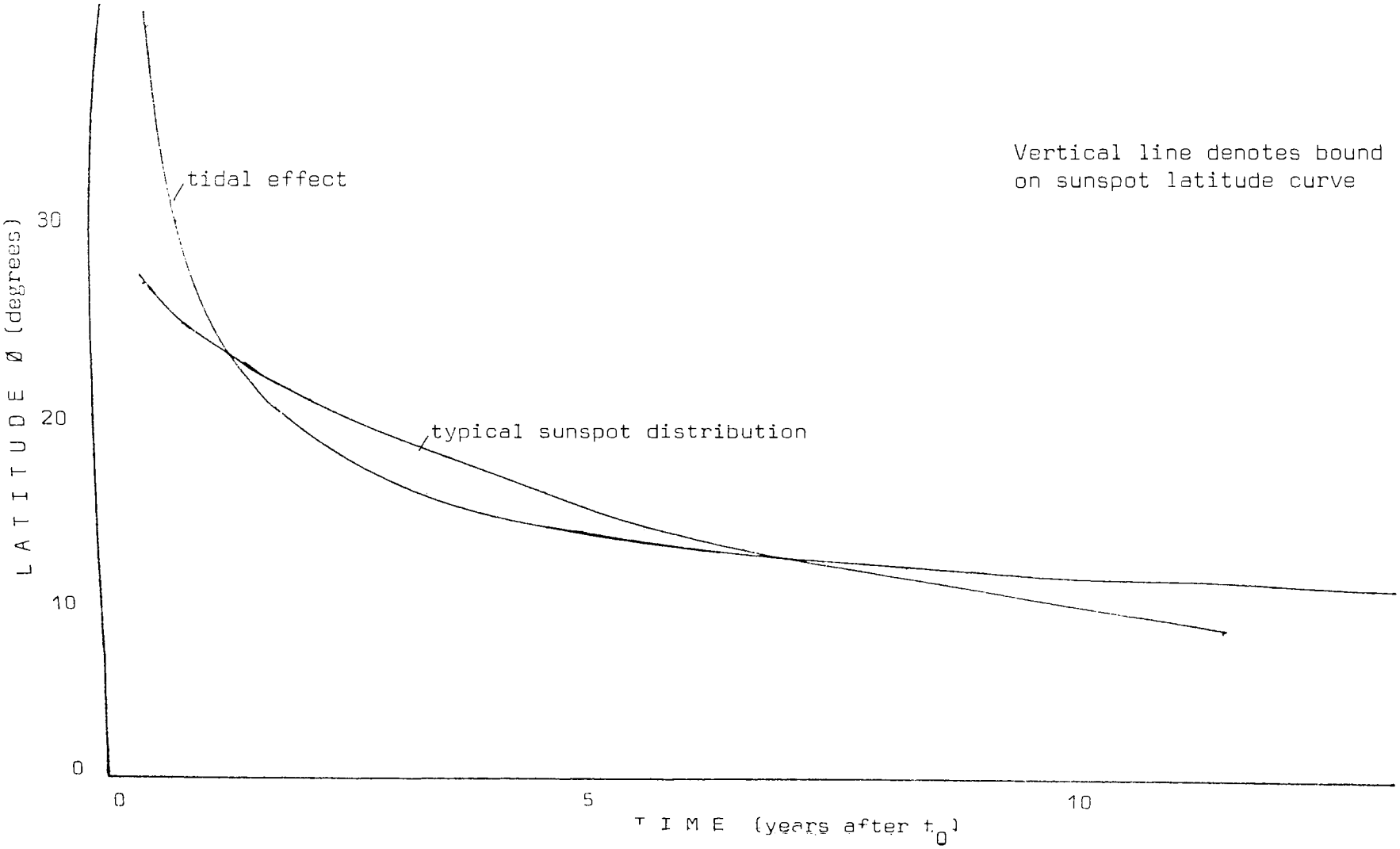

Figure 6.61 Comparison of Sunspot Latitude Distribution with Long Period Tidal Effect

6.6 Testing Model Against Observations

In view of the large random components inherent in the existing sunspot data, it was decided to utilize for comparison characteristics averaged over many solar cycles. Accordingly, the mean sunspot distribution with latitude over a typical sunspot cycle (taken from Allen, 1955) was plotted. Arbitrarily starting all 'tide cycles' in phase at time t_0, the distribution of tidal maxima was superimposed on the sunspot distribution (figure 6.61). It is clear that a close correlation may be drawn between the two phenomena.

In an attempt to assess the longer-term behaviour of the tidal function, the 'tide cycles' were set to run freely, and at time intervals t_i, corresponding to actual sunspot cycle lengths, a 'new' sunspot cycle was arbitrarily started. Typical curves are given in figure 6.62, and it is seen that the variations between curves are quite consistent with the actual variations observed between successive sunspot distributions.

The very good correlation observed between the two distributions led to the hypothesis of a planetary tidal trigger influencing sunspot genesis being accepted.

6.7 Further Consideration of Tidal Effect

Having determined a connection between the overall distribution of sunspots with latitude, and long period variation in the tidal effect of planets at the sun surface, it was decided to examine the fine structure of the tidal oscillations. From the data previously computed, an arbitrary relative high tide level of 6.0 was chosen, and the data was examined for times of high maxima, for a range of

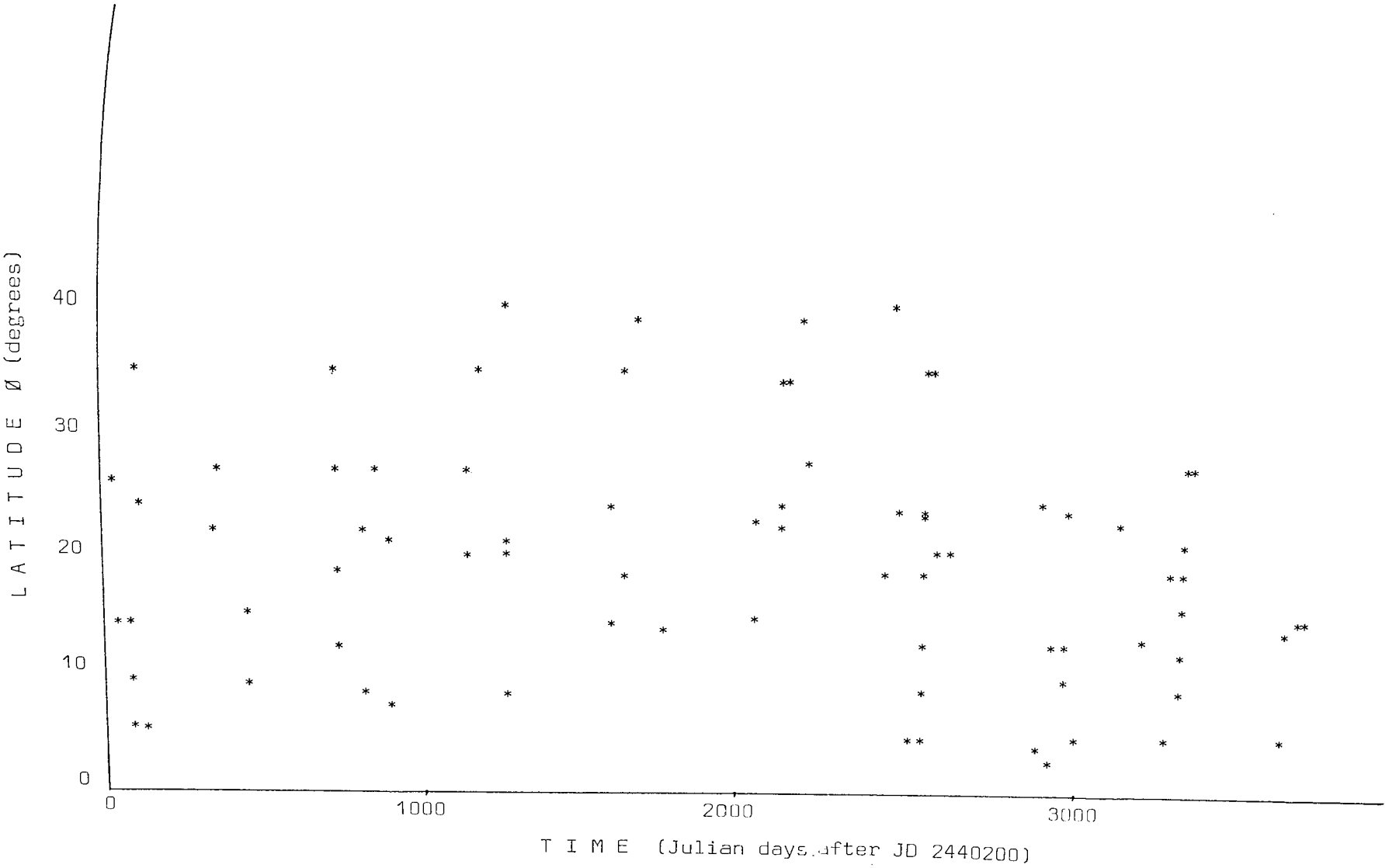

Figure 6.71 Sample distribution of tidal maxima after epoch JD 2440200

latitudes $0 \leq \phi \leq 60^{o}$ and for the period of time 1968-1980. The resulting distribution is given in figure 6.71. It is seen that there is a tendency for local maxima to occur simultaneously at different latitudes, and that two successive maxima sometimes occur at the same latitude with a separation of ~90 days; both these effects are attributed to the influence of Mercury. However, although it is found that higher numbers of maxima appeared in the data in the intervals 1969 to 1972, and 1976 to 1979, than in the period 1972 to 1975, no clear pattern is observed. Raising the limit for high maxima and repeating the procedure, led to a successively more random distribution. A similar series of results was obtained from examination of tidal minima.

Breaking the sample into 3 categories; single maxima, maxima sustained over 2 successive sample dates, and maxima recurring after 88 days, yielded some information; whilst the distribution of single and sustained maxima was found to be random, that of recurring maxima followed a distribution with latitude broadly similar to that of a sunspot distribution, with most recurring maxima occurring between $\phi = 16^{o}$ and $\phi = 22^{o}$.

It was realized from the above results that the sampling interval of 2 days employed in the data was too great to estimate the fine structure of the tidal variations accurately. In order to eliminate the selection effect of the sampling interval, which allows only those maxima or minima occurring at or near a sampling time to be detected, tidal data must be generated at intervals of about .1 day. Sustained maxima are clearly also randomly chosen by the sampling times, whilst recurring maxima are more likely to represent 'true' extremes of the tidal variation, especially as these recurrences are separated by unusually deep minima. However, the sampling interval will still

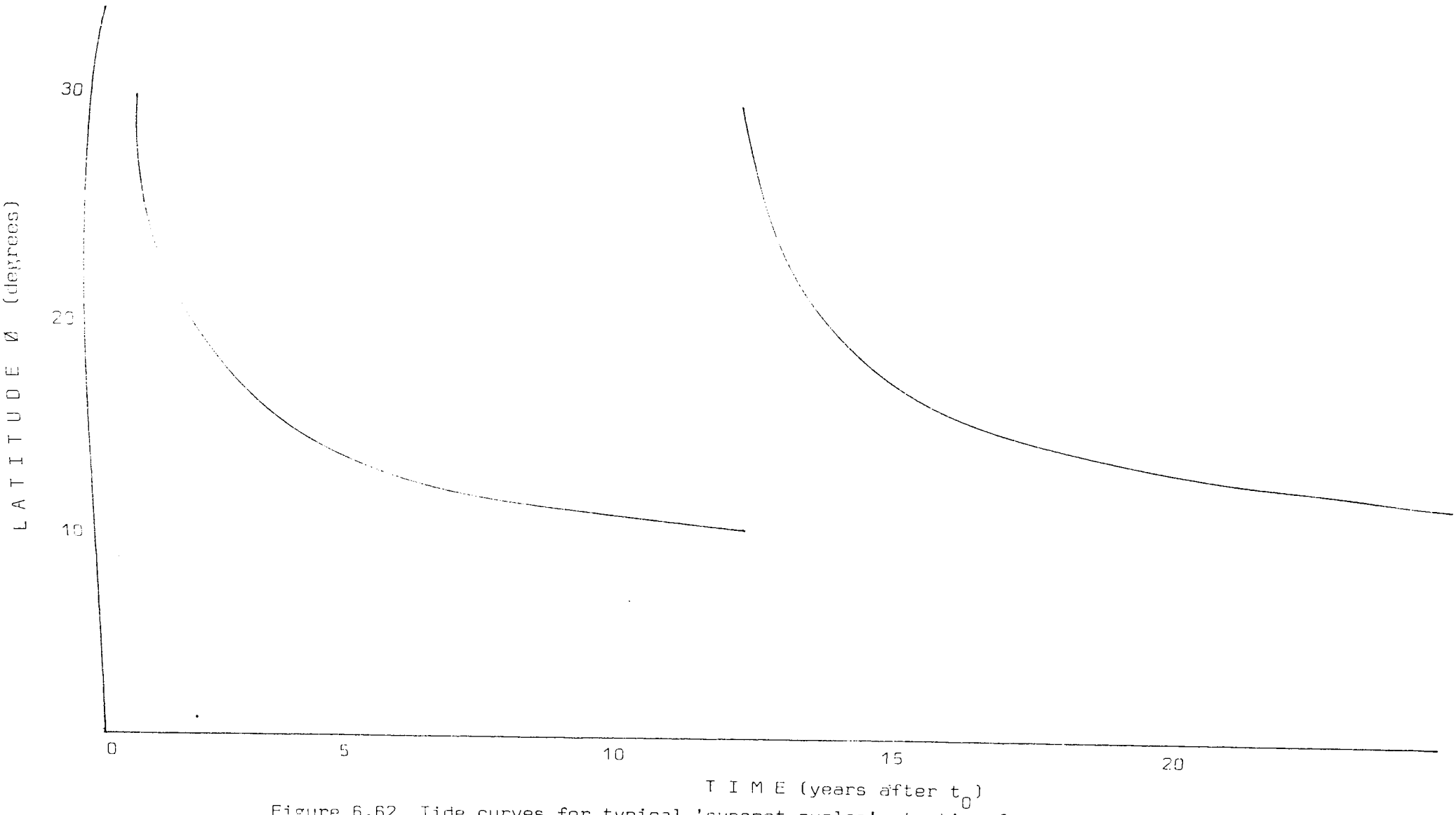

Figure 6.62 Tide curves for typical 'sunspot cycles' starting from initial epoch t_0

affect these preliminary results, causing many recurring maxima to be omitted from the above data.

6.8 Discussion

Comparison of the proposed model with observations was shown to give very favourable results, and it thus appears probable that the distribution of sunspots over the solar disc is influenced, and even possibly caused, by planetary tidal action. From the model, predictions can be made regarding several aspects of sunspot appearance. A fundamental consequence of the tidal equation 5.1(1) is that the formation of solar activity regions would be triggered simultaneously at longitudes 180^{o} apart.

In section 6.5, arguments have been examined relating to the cessation of the triggering effect at latitudes above ~ 40^{o}. Whilst a case can be made for this proposed cessation, firm evidence for the existence of such a turning point is not apparent. Therefore, it is suggested that a tidal hypothesis will favour the genesis of solar active regions at latitudes greater than 40^{o}; by inference, this suggests the appearance of high-latitude features prior to the commencement of the new cycle.

The report of a 12.2 day oscillation of the solar photosphere (Dicke, 1976A; B), later reinterpreted (Chapman, 1975; Hill and Stebbins, 1975) as a non-uniform brightness of the solar disc, together with a similar variation observed in Doppler line-of-sight velocity (Claverie et al.,1982) has recently generated interest in the short-term distribution of active centres on the sun surface as a possible cause of this apparent variation. Examination of recent solar data has led to confirmation of the existence of solar 'active longitudes' (Chapman, 1975; Bogart, 1982; Vitinsky, 1982),and to the discovery that

these centres of activity tend to develop simultaneously at longitudes 180^0 apart (Durrant and Schroter, 1983; Edmonds and Gough, 1983; Nyborg and Maltby, 1983). These 'active longitudes' are detected at all levels of solar activity, possibly longer-lived at times of high activity (Durrant and Schroter, 1983). In addition, research into polar 'wind holes' (Bohlin, 1978; Hundhausen, 1978; Broussard et al., 1978). Sime and Rickett, 1978; Simon, 1979) and of velocity patterns at the sun surface (Severny et al., 1976; Howard and LaBonte, 1980) has led to the suggestion that the basic physical process of each solar cycle begins a few years after the previous sunspot maximum, and at the time of formation it is a high latitude phenomenon (Legrand and Simon, 1981; Dimitrov, 1982; Howard and LaBonte, 1982 A; B; C). Two successive cycles with unrelated levels of activity are thus envisaged as evolving simultaneously at different latitudes and phases of development (Legrand and Simon, 1981).

Both these recent developments give strong support for the involvement of the planetary tidal trigger mechanism outlined in this section in the formation of solar active regions.

General Discussion

Many facets have been examined of the solar cycle and its possible planetary origin.

Statistical analysis of the auroral series of Schove (1955) and Bray (1980) reveals the existence of a periodicity of about 200 years in both data sets. Analysis does not show the 80 year period generally referred to in literature; it is suggested that whilst the eye tentatively traces a pattern over seven cycles, this pattern is too irregular to appear as a true periodicity in the data. The possible existence of such an effect over a few centuries is not excluded, but is not considered to be a strong influence on the level of sunspot activity as such.

From an examination of the available historical records for the period 1650-1715, it is concluded that the Maunder Minimum was indeed a time of exceptionally low solar activity, and that this interval does not represent a cessation of the solar activity cycle. This result gives additonal support to the results of Section 2, where comprehensive statistical analysis of the Waldmeier sunspot series have revealed differences in the overall character of the data between early and recent sunspot records, indicating that the 11 year cycle may be modulated in amplitude by long period effects. It is suggested that the mean period of the 'sunspot cycle' itself may vary in a non-random manner, oscillating between about 11.1 years (associated with times of high activity) and about 10.5 years at periods of unusually low activity.

The statistical analysis of the Waldmeier sunspot numbers has demonstrated the difficulties inherent in extracting information from

this limited amount of stochastic data. Many 'periodicities' detected by researchers in the sunspot series are demonstrated to arise from improper use of analytical techniques, often with cursory and conflicting interpretation of results, a lack of proper statistical tests for significance and the frequent use of unsuitable highly smoothed sunspot data. Thus, the various attempts to establish the existence of a link between planetary motion and solar activity on the basis of matching different synodic and sideral periods to these sets of data are not well founded.

The examination of parameters of planetary motion over an extended timescale requires a method for the generation of planetary co-ordinates. The Gauss-Jackson numerical integration process utilized for this purpose was found to be highly efficient and accurate for the integration of planetary equations of motion. However, the accuracy of the initial data was determined to be critical to the precision of the output information; thus the use of a high order starting procedure is advised if the Gauss-Jackson process is to be used for integrating equations of this type. It was also found practicable to use this numerical integrator for the generation of sets of planetary co-ordinates for an 'alternate' solar system using the approximate orbital parameters suggested in'Ovenden'(1972). This formed a basis for work in sub-sequent sections.

The possibility of a connection between the sunspot cycle and the motion of the sun around the centre of gravity of the solar system has been considered. However, none of the parameters examined is found to correlate in any way with the eleven year sunspot cycle. Statistical analysis of the data does not reveal any of the several periodicities previously reported (Wood and Wood, 1965; Dauvillier, 1977), although consideration of various synodic periods of the outer planets does

indicate the presence of a roughly 180 year quasi-periodic effect, in accordance with earlier work (Jose, 1965; Petrova, 1979). Both for the solar system and for the control system, various planetary sidereal and synodic frequencies of orbit were recovered from the output data. No effects attributable to the inner planets were observed; however, whilst a 200 year variation was found to exist in sunspot and auroral records (Section 1), it is difficult to associate this variation with the motion of the sun, relative to the mass centre of the solar system, in any meaningful way, bearing in mind that accuracy in determining such long sunspot periods is severly curtailed by the limited amount of reliable sunspot data.

The eleven year tidal functions of Wood (1972) and Wood (1975), although yielding an excellent period match with the sunspot cycle, are found to be affected by aliasing;the large sampling interval artificially lengthening the innate planetary synodic periods. It is found that a class of such functions exists with a wide range of output periodicities. Further, examination of the tidal variation reveals that it is not possible to trace the rapidly changing tidal effect in any meaningful way by the use of planetary alignments. The use of a first order approximation to the tidal height equation is shown greatly to reduce the accuracy of the result obtained, and it is found that terms to fifth order in $(\cos \theta)$ are required for some values of θ.

Analysis of the tide-raising effect of all planets encountered by a 'sunspot' rotating with the solar equator, revealed the previously unsuspected dominant planetary tidal influence of Mercury. No other planetary sidereal or synodic frequency is detected, in contrast to the results of previous researchers. Comparison with the behaviour of the control system, in which half the period of planet 'A' was detected in the tidal data in addition to the frequency ν_M, indicates

that those frequencies of orbit which would be expressed in the overall tidal effect (if Jupiter or Venus were exerting a strong periodic influence) would be $2\nu_J$ and $2\nu_V$ rather than the fundamental frequencies generally considered as dominant. This is a consequence of the critical dependence found to exist between the dominant orbital frequency, expressed in the tidal variation, and the eccentricity of the planetary orbit.

A latitude-dependent periodic variation was found to modulate the amplitude of the tidal effect encountered by a 'sunspot' rotating with the solar photosphere, over a period of 100 years. A solar model was discussed in which a mechanism governing the magnetic cycle began as a polar phenomenon, latching on to the tidal effect at high latitudes, sunspot formation being triggered at successively lower latitudes by the planetary tidal effect. The variation in period of this effect with latitude was found to correlate well with the time-latitude distribution of a typical sunspot cycle. A fundamental consequence of such a tidal mechanism is the tendency of centres of activity to develop simultaneously at longitudes 180^0 apart. The recent observational confirmation of this prediction gives support for a tidal mechanism.

The existence of global oscillations on the 'quiet sun' (Brookes, Isaac and van der Raay, 1976; Claverie et al., 1979; Grec et al., 1980; Scherrer et al., 1982) has called into question much accepted theory on the structure and stability of the solar interior (Deubner, 1981; Gough, 1981; Endel and Twigg, 1982). In particular, the possibility of a rapidly rotating solar core has affected many solar models (Hill, 1978; Christensen-Dalsgaard and Gough, 1981). One argument frequently advanced against hypotheses of planetary tidal action as an influence on the solar cycle, has been this perfect equilibrium of the sun (Smythe and Eddy, 1977; Eddy, 1978). With the detection of solar

oscillations, the possibility of a resonant response of the solar photosphere to a small but periodic tidal effect cannot be excluded (de Csada, 1981), although at present the timescale of observational work is an order of magnitude less than that required for detection of such long period solar oscillations (Deubner, 1981; Gough, 1981). In addition, the increasing amount of observational evidence in conflict with the classic dynamo models (Isaak, 1982) has focussed interest on the various flux-tube models available (Meyer et al., 1974; Piddington, 1978), these being inherently more favourable to the hypothesis of a tidal influence.

It is not suggested that a single, fundamental cause exists as the origin of the complex phenomenon of the 'sunspot cycle', in the form of a tidal influence of planets on the solar photosphere. It does, however, appear probable that the planets, particularly Mercury, have some influence on the birth and development of sunspots. In this context, the recent observation (de la Rosa, 1981) of two distinct spot group populations on the sun may be important. One possible explanation for this is the operation on flux-tube generated sunspot groups of a planetary tidal effect.

By modulating the small rising velocities of such groups (Schussler, 1977; Parker, 1979) such a trigger may affect the overall sunspot distribution on the sun surface, causing the appearance of transient 'active longitudes'.

A promising area for future research thus lies in the detailed examination of actual sunspot appearances, and a search for correlations both with local peaks in the rapidly varying tide function, and with the long period amplitude modification. It is suggested that the initial separation of sunspots into 'large and stable' and 'small and unstable' groups may be a useful initial step.

CONCLUSION

It is concluded that a 200 year periodicity exists in the long-term auroral and sunspot records. Statistical differences were shown to exist between early and more recent sunspot data, thereby confirming the suggestions of long term effects modulating the sunspot cycle. None of the short-term periodicities reported by researchers quoted in this thesis have been found to exist within the eleven year cycle. An alternate solar system model was established as a basis for later studies. A comparison was made between solar motion with respect to the centre of gravity of the solar system and sunspot cycle periodicities. No verifiable correlation between the two was found.

It has been shown that series of planetary alignments cannot be justified as tracers for tidal effects of planets at the solar surface. The use of a first order approximation to the tidal height equation has been demonstrated to involve significant inaccuracies. Whilst previous researchers have recovered many planetary synodic and sidereal planetary periods, examination of the daily tidal effect of all planets at the solar surface recovered only the sidereal period of Mercury. A latitude-dependent tidal effect, modulating the amplitude of the variation, was shown to have a distribution similar to the time-latitude curve of a typical sunspot cycle. It was found that results of recent observational work give support to a hypothesis of tidal action. The possibility thus exists that planetary tidal effects are an influence on the birth and/or development of sunspots.

APPENDICES

APPENDIX I

Reciprocals of planetary masses.

Planet	$Mass^{-1}$
Mercury	6000000
Venus	408000
Earth+Moon	329390
Mars	3093500
Jupiter	1047.35
Saturn	3501.6
Uranus	22869
Neptune	19314

APPENDIX II

Sets of starting values for numerical integration of an 'Ovenden' system.

	Planet	x	$\dot{x}$	y	$\dot{y}$	Z	$\dot{Z}$
PERIHELION	A	-1.783376941	-0.7940044523	-2.125345877	-0.6662488438	0.0	
	J	4.836128284	-0.1742318306	1.081792199	0.7718724535	-0.1130788314	0.010332554
	S	-0.1749786613	-0.5894463506	8.975657446	-0.0111090409	-0.1443071372	0.0238428756
	U	18.20612201	-0.0776446547	2.522260353	-0.4012976755	0.24884294	-0.0005351295
	N	21.23432323	-0.2204792879	20.387792	0.2296582539	-0.9130505291	0.0005435037
APHELION	A	1.808520222	-0.7829656624	2.155310471	0.6569861986	0.0	0.0
	J	-5.32759136	0.1580431131	-1.201766479	-0.7008234583	0.1245653635	-0.0009379759
	S	0.1956964336	0.572043500	-10.03727224	0.0099329612	0.1613933491	-0.0213187046
	U	19.98826942	0.0719482892	-3.939477736	0.365121172	-0.2733877849	0.0004870854
	N	-21.60704313	0.2166760366	-20.74565296	-0.2256966664	0.9290770392	-0.0005341283

APPENDIX III

Curves of Distance R and Radius

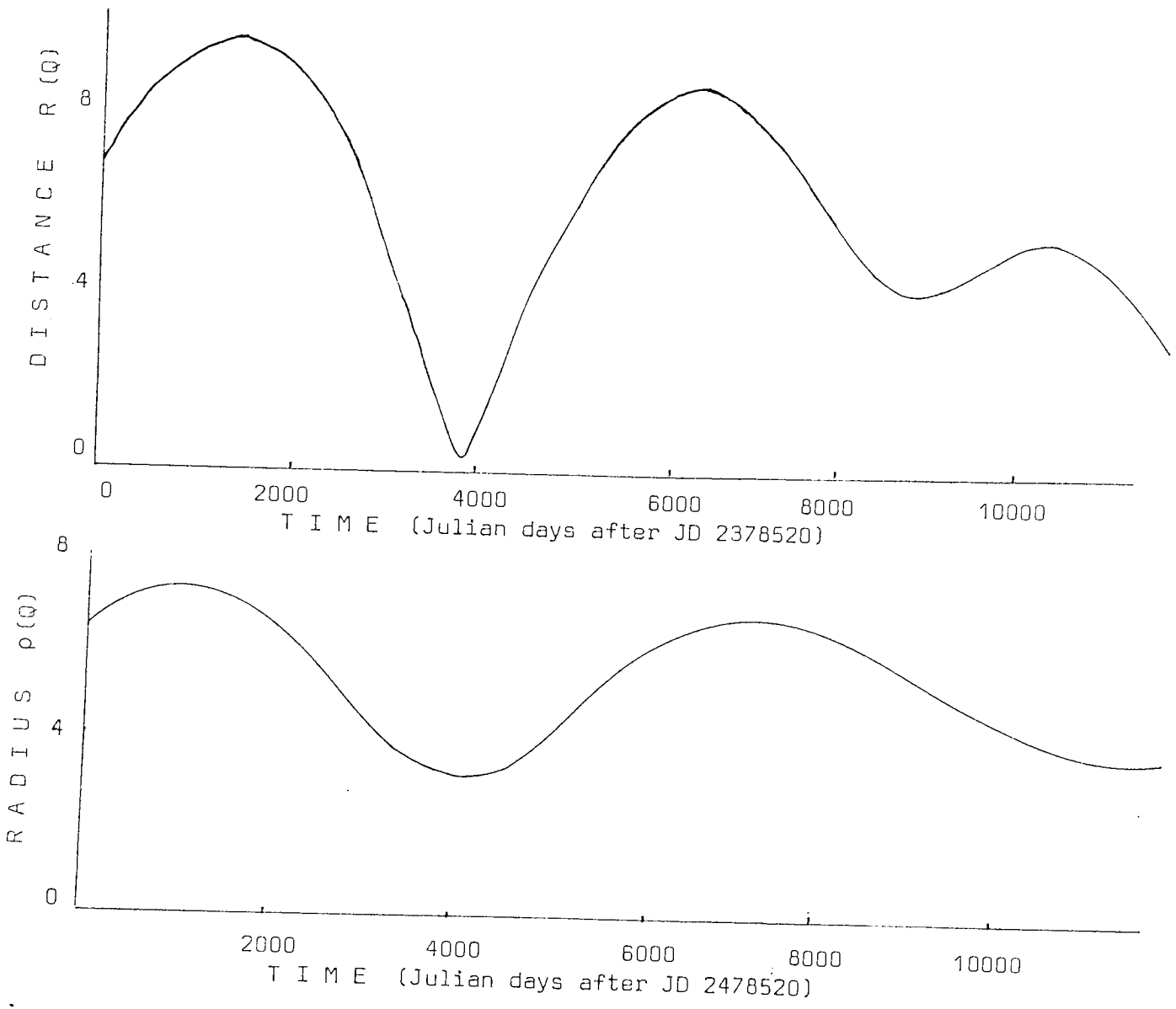
DISTANCE R(Q)
8
4
0
0
2000
4000
6000
8000
10000
TIME (Julian days after JD 2378520)
RADIUS ρ(Q)
8
4
0
2000
4000
6000
8000
10000
TIME (Julian days after JD 2478520)

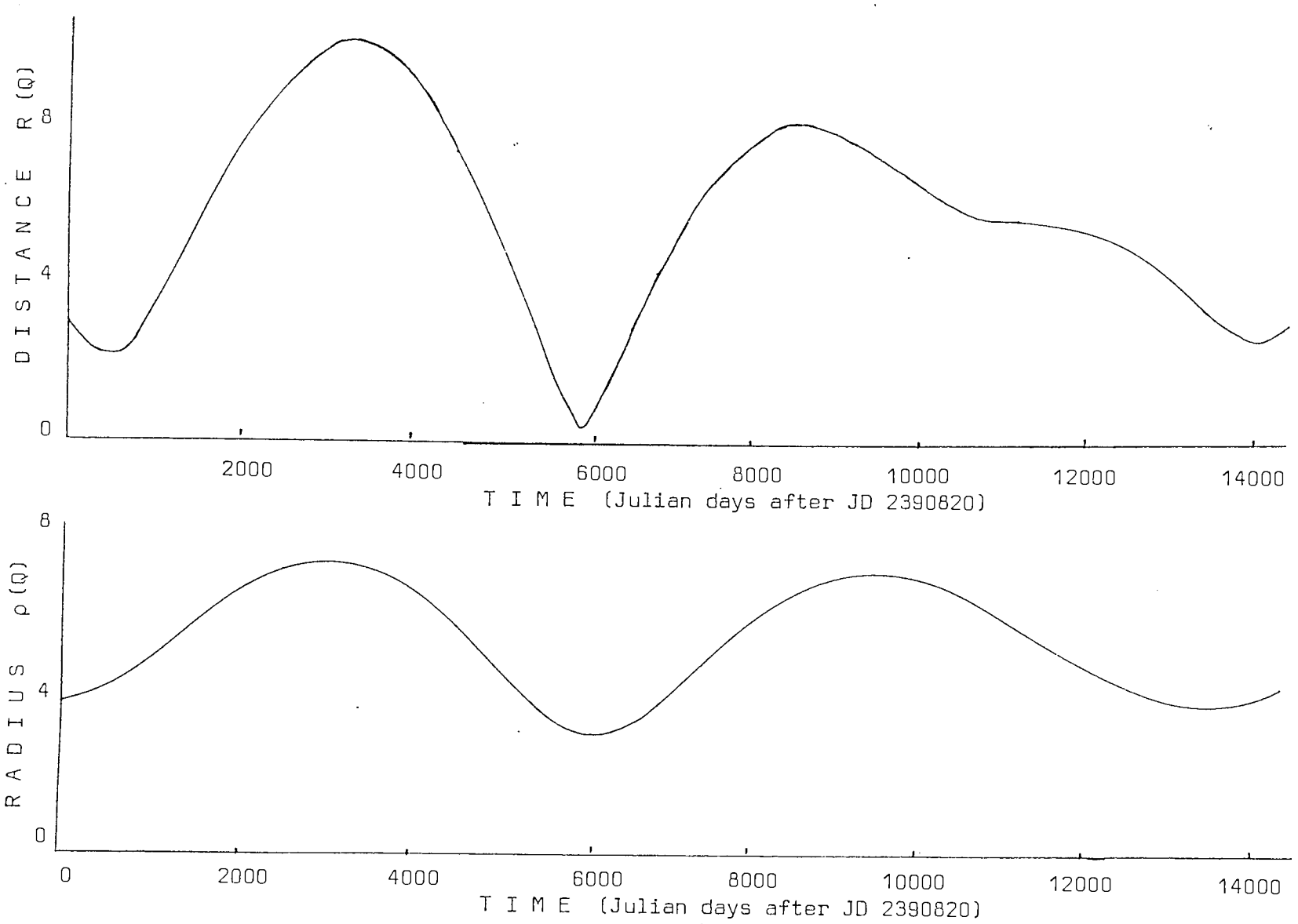
DISTANCE R(Q)
8
4
0
2000
4000
6000
8000
10000
12000
14000
T I M E (Julian days after JD 2390820)
RADIUS ρ(Q)
8
4
0
0
2000
4000
6000
8000
10000
12000
14000
T I M E (Julian days after JD 2390820)

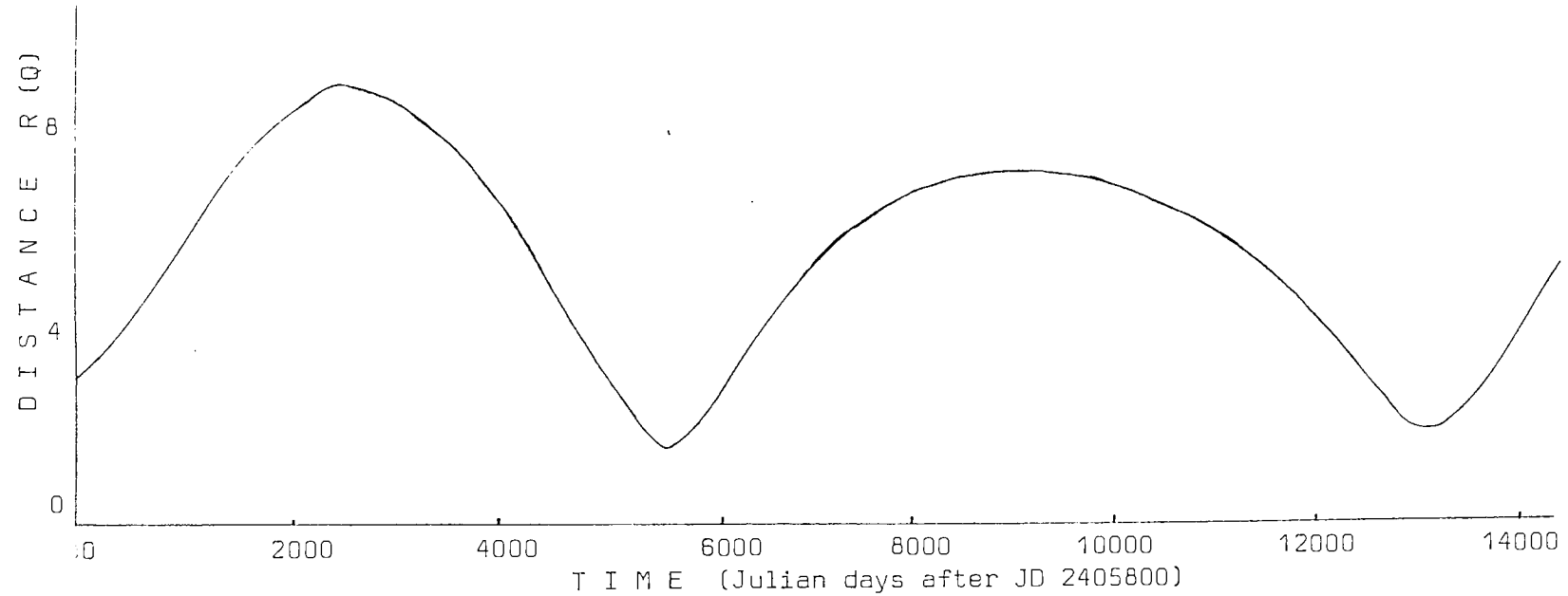
DISTANCE R(Q)
8
4
0
0
2000
4000
6000
8000
10000
12000
14000
T I M E (Julian days after JD 2405800)

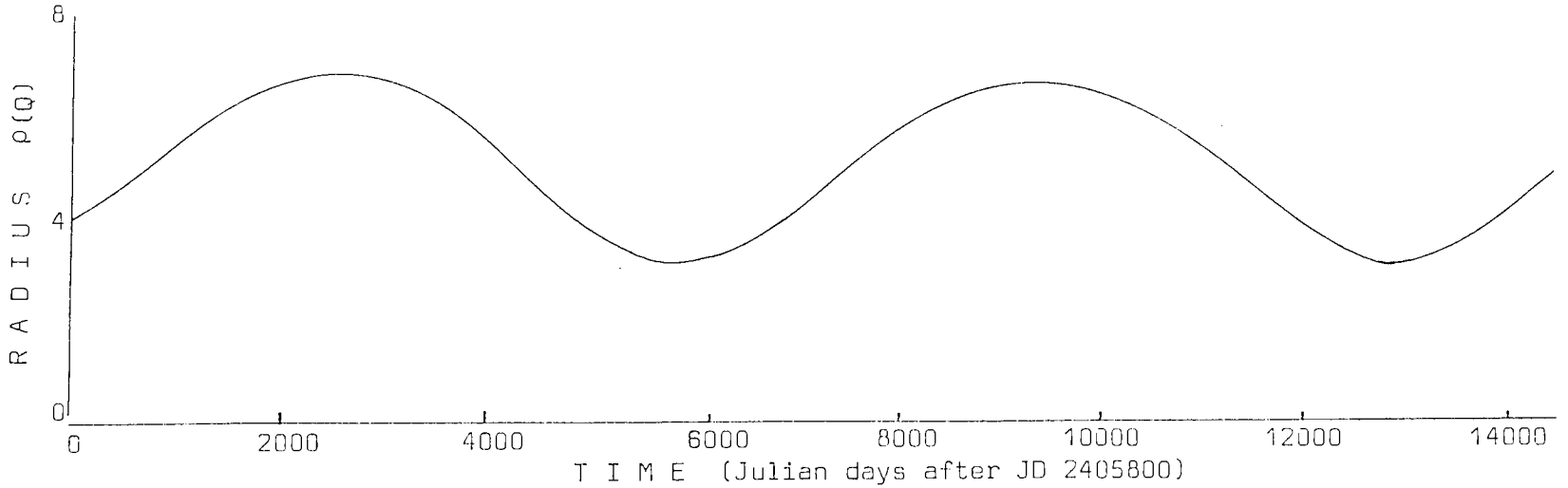
RADIUS ρ(Q)
8
4
0
0
2000
4000
6000
8000
10000
12000
14000
T I M E (Julian days after JD 2405800)

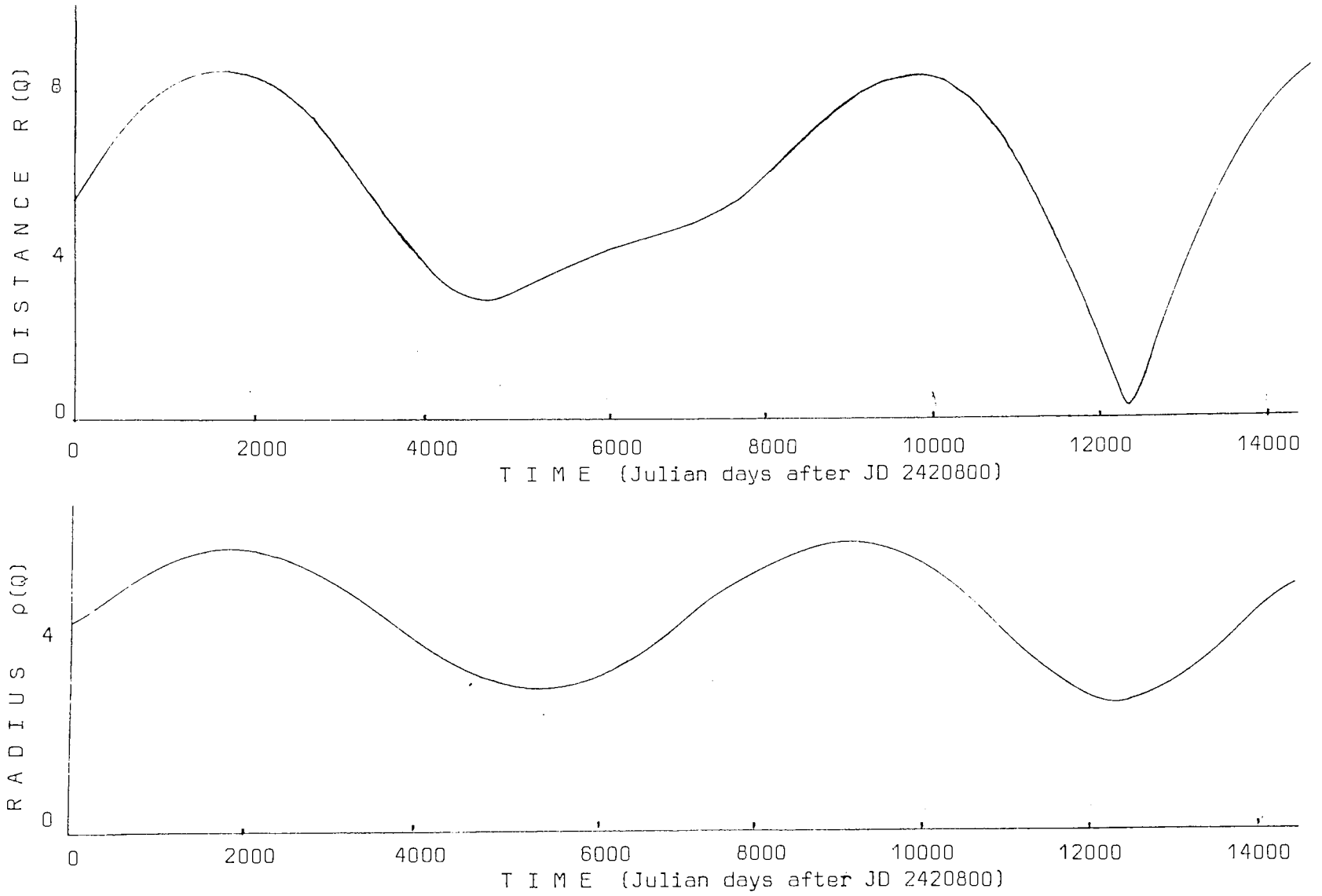
DISTANCE R(Q)
8
4
0
0
2000
4000
6000
8000
10000
12000
14000
TIME (Julian days after JD 2420800)
RADIUS ρ(Q)
4
0
0
2000
4000
6000
8000
10000
12000
14000
TIME (Julian days after JD 2420800)

APPENDIX 4

Derivation of $\tilde{\varepsilon}_p^2$ and upper bounds on possible variance, defined in Section I.

$$\tilde{\varepsilon}(\nu) = 2\sqrt{\frac{A^2(\nu)}{C_\nu} + \frac{B^2(\nu)}{S_\nu} - \frac{1}{2C_\nu^2} - \frac{1}{2S_\nu^2}}$$

When a reasonable amount of source power is present, the first two terms in the expression for $\tilde{\varepsilon}(\nu)$ dominate; hence

$$\tilde{\varepsilon}(\nu) \approx 2\sqrt{\frac{A^2(\nu)}{\sum_n c_n^2/\sigma_n^2} + \frac{B^2(\nu)}{\sum_n s_n^2/\sigma_n^2}}$$

Now $E[c_n^2] = E[s_n^2] = \frac{1}{2}$

and so

$$\tilde{\varepsilon}(\nu) \approx 2\sqrt{\frac{2A^2(\nu) + 2B^2(\nu)}{\sum_n 1/\sigma_n^2}} \quad .$$

Thus

$$\tilde{\varepsilon}_p^2(\nu) \approx \frac{8P(\nu)}{\sum_n 1/\sigma_n^2} \quad .$$

Throughout this derivation expectation values will be denoted by < > for simplicity.

For the case of unweighted data, the estimated cosine coefficient for a signal with a periodic component is given by

$$A(\nu) = \frac{1}{\sum_n c_n^2} \left[\sum_n c_n + \sum_n \alpha_1 c_n' c_n + \sum_n \alpha_2 c_n'' c_n \right.$$

$$\left. + \ldots + \sum_n \beta_1 s_n' c_n + \ldots \right]$$

For randomly distributed sampling times t_n, and if $\nu T >> 1$, the following approximations hold:

$$< c_n^{(\ell)} > = < s_n^{(\ell)} > = < c_n^{(\ell)} s_n^{(m)} > = 0$$

$$< c_n^{(\ell)} c_n^{(m)} > = < s_n^{(\ell)} s_n^{(m)} > = \frac{1}{2} \delta_{\ell m}$$

$$< c_n^{2(\ell)} c_n^{2(m)} > = < s_n^{2(\ell)} s_n^{2(m)} > = \frac{1}{4} + \frac{1}{8} \delta_{\ell m}$$

$$< s_n^{2(\ell)} c_n^{2(m)} > = 1/4 - 1/8 \, \delta_{\ell m}$$

It is clear by inspection that $< A(\nu) > = 0$ unless $\nu = \nu^{(m)}$, where $\nu^{(m)}$ is a frequency present in the data, when $< A(\nu) > = \alpha_m$.

Consider $A^2(\nu)$ evaluated at $\nu = \nu^{(m)}$. As $< \sum_n > = 0$,

$$< A^2(\nu^{(m)}) > = \left\langle \frac{1}{(\Sigma c_n^2)^2} \right\rangle \left[\frac{N}{2} \sigma_N^2 + \frac{N}{4} \sum_{i \neq m} (\alpha_i^2 + \beta_i^2) \right.$$

$$\left. + \alpha_m^2 \left\langle \left(\sum_n c_n^{2(m)} \right)^2 \right\rangle + \beta_m^2 \left\langle \left(\sum_n c_n^{(m)} s_n^{(m)} \right)^2 \right\rangle \right]$$

where σ_N^2 is the variation of the noise component;

$$\sigma_N^2 = \frac{1}{N} \sum_n^N n^2 .$$

Now $$\frac{1}{(\sum_n c_n^2)^2} = \frac{4}{N^2} - \frac{16}{N^4} \cdot O(N) + \ldots \simeq \frac{4}{N^2}$$

Using this approximation and evaluating the other two expectation values in the expression for $A^2(\nu^{(m)})$ yields

$$\langle A^2(\nu^{(m)})\rangle \simeq \frac{4}{N^2}\left\{\frac{N}{2}\sigma_N^2 + \frac{N}{4}\sum_{i\neq m} P_i + \alpha_m^2\left[\frac{N^2}{4} + \frac{N}{8}\right] + \beta_m^2\,\frac{N}{8}\right\}$$

$$= \alpha_m^2 + \frac{2}{N}\sigma_f^2 - \frac{P_m}{2N}$$

where $P_m = \alpha_m^2 + \beta_m^2$ and

$$\sigma_f^2 = \frac{1}{N}\sum_n f_n^2 = \sigma_N^2 + \frac{1}{2}\sum_i P_i$$

is the total data variance.

Evaluating $\langle B^2(\nu^{(m)})\rangle$ similarly and combining the two gives

$$\langle P(\nu^{(m)})\rangle = \langle A^2(\nu^{(m)})\rangle + \langle B^2(\nu^{(m)})\rangle$$

$$\approx P_m\left[1 - \frac{1}{N}\right] + \frac{4}{N}\sigma_f^2$$

i.e. a bias of $(4/N)\sigma_f^2 - (1/N)P_m$ is present in the spectral estimate of a peak at $\nu^{(m)}$. Elsewhere, the bias is $(4/N)\sigma_f^2$.

Evaluation of $\langle P^2(\nu)\rangle$ is necessary to evaluate the variance.

Clearly, however,

$0 \leq \text{var}(a + b) \leq 2(\text{var}(a) + \text{var}(b))$. Hence

$$0 \leq \sigma_p^2 \leq 2(\sigma^2_{A^2} + \sigma^2_{B^2}) = 8(A^2 \sigma_A^2 + B^2 \sigma_B^2)$$

Substitution yields the condition

$$0 \leq \frac{\sigma_p^2}{P} \leq \frac{16}{N} \left[\sigma_f^2 - \frac{1}{4} P_m\right] .$$

For the case of weighted data, a parallel analysis gives

$$0 \leq \frac{\sigma_p^2}{P} \leq \frac{16}{N^*} \left[\sigma_f^2 - \frac{1}{4} P_m\right]$$

where

$$N^* = \frac{(\sum_n 1/\sigma_n^2)^2}{\sum_n 1/\sigma_n^4} .$$

APPENDIX 5

Additional theoretical development of the spectral analysis technique of Section 2.

Appendix 5

Time Series Analysis

A time series can be described by an ordered set of random variables $X(t)$ $(-\infty \leq t \leq \infty)$; an observed time series $x(t)$ is regarded as one realization of an infinite ensemble of functions which might have been observed.

A5.1 Expectation Values

Given a random variable $X(k)$ in the range $-\infty$ to $+\infty$, the 'mean' or 'expected' value of $X(k)$ is obtained by an appropriate limiting operation when each value assumed by $X(k)$ is multiplied by its probability of occurrence, $p(X)$

$$\text{i.e.} \quad E[X(k)] = \int_{-\infty}^{\infty} X(k)p(X)dX = \mu_X$$

where $E[\ ]$ represents the expected value over the index k of the term within the brackets. Similarly the expected value of any real single-valued continuous function $g(X)$ is given by

$$E[g(X(k))] = \int_{-\infty}^{\infty} g(X)p(X)dX$$

where $p(X)$ is the probability density function associated with $X(k)$. In particular, for $g(X) = X^2$, the 'mean square value' of $X(k)$ is given by

$$E[X^2(k)] = \int_{-\infty}^{\infty} X^2\, p(X)dX = \Psi_X^2$$

and the variance of $X(k)$ is defined by the mean square value of $X(k)$ about its mean value μ_X:

$$E[(X(k) - \mu_X)^2] = \int_{-\infty}^{\infty} (X-\mu_X)^2\, p(X)dX$$

$$= \Psi_X^2 - \mu_X^2 = \sigma_X^2 \ .$$

For the case of two random variables X(k), Y(k), where k represents point in a suitable sample space,

$$E[g(X,Y)] = \int_{-\infty}^{\infty}\int g(X,Y)\, p(X,Y)\, dXdY$$

where $p(X,Y)\, dXdY = \text{Prob}[\, X < X(k) \leq X + dX \text{ and } Y < Y(k) \leq Y + dY]$.
If $g(X,Y) = (X(k) - \mu_X)(Y(k) - \mu_Y)$ where μ_X and μ_Y are the mean values of X(k) and Y(k), then the 'cross covariance function' γ_{XY} is defined by

$$\gamma_{XY} = E[(X(k) - \mu_X)(Y(k) - \mu_Y)]$$

$$= E[X(k)\, Y(k)] - E[X(k)]\, E[Y(k)]$$

$$= \int_{-\infty}^{\infty}\int (X - \mu_X)(Y - \mu_Y)\, p(X,Y)\, dXdY$$

If X(k) and Y(k) are independent random variables, then

$$E[X(k)\, Y(k)] = E[X(k)]\, E[Y(k)]$$

and so $\gamma_{XY} = 0$ and the variables are termed 'uncorrelated'.
Given a continuous series of random variables in time, the dependence between values at times t_1 and t_2 may be described using the autocovariance function γ_{XX}:

$$\gamma_{XX}(t_1,t_2) = E[(X(t_1) - \mu(t_1))(X(t_2) - \mu(t_2))]$$

where $\gamma_{XX}(t_1,t_2) = \sigma^2(t_1)$

To normalise γ_{XX}, the autocorrelation function

$$\rho_{XX}(t_1,t_2) = \frac{\gamma_{XX}(t_1, t_2)}{\sqrt{\sigma(t_1)\sigma(t_2)}}$$

is defined.
It is necessary to assume that the fundamental statistical properties of the time series, i.e. $\mu(t)$ and $\sigma^2(t)$ are approximately constant with time; this assumption of stationarity is true for most series over a

limited timespan.

Then

$$\gamma_{XX}(t_1,t_2) = E[(X(t_1) - \mu_X)(X(t_2) - \mu_X)]$$

$$= E[(X(t) - \mu_X)(X(t+u) - \mu_X)]$$

$$= \text{cov}[X(t), X(t+u)]$$

where $u = t_2 - t_1$ is termed the 'lag'.

For an observed time series $x(t)$, the theoretical autocovariance function $\gamma_{XX}(u)$ must be estimated; the most widely used estimator $c_{XX}(u)$ is given by

$$c_{XX}(u) = \frac{1}{T}\int_0^{T-|u|} (x(t) - \bar{x})(x(t+|u|) - \bar{x})dt \qquad 0 \leq |u| \leq T$$

$$= 0 \qquad |u| > T$$

where T is the length of the observed series.

If the observations $x(t)$ are taken from a discrete time series, $x_1, x_2, \ldots x_n$, the estimator will be expressed as

$$C_{XX}(k) = \frac{1}{N}\sum_{t=1}^{N=k} (x_t - \bar{x})(x_{t+k} - \bar{x}) \qquad k = 0,1, \ldots N-1$$

where

$$\bar{x} = \frac{1}{N}\sum_{t=1}^{N} x(t)$$

denotes the sample mean.

A5.2 The Spectrum

A stationary stochastic process is described by its autocovariance function. An equivalent description is found to be the 'power spectrum' of the process, which is the Fourier transform of the autocovariance function.

The variance of a signal $x(t)$ $(-T/2 \leq t \leq T/2)$ can be decomposed into contributions at harmonics $f_m = m/T$ of fundamental frequency $f_1 = 1/T$ according to

$$S_T^2 = \frac{1}{T}\int_{-T/2}^{T/2} x^2(t)\,dt = \sum_{m=-\infty}^{\infty} |C_m|^2 \qquad \ldots (1)$$

where C_m is the complex amplitude at frequency $f_m = m/T$;

$$C_m = \frac{1}{T}\int_{-T/2}^{T/2} x(t)\, e^{-i2\pi mt/T}\,dt \qquad \ldots (2)$$

and $x(t)$ may be written in Fourier form:

$$x(t) = \sum_{m=-\infty}^{\infty} C_m\, e^{+i2\pi mt/T} \quad .$$

Similar equations are found for a discrete signal.
The contribution $|C_m|^2$ to the average power at frequency f_m is termed the intensity at that frequency.

From (1), the variance of the infinite record is

$$\sigma^2 = \lim_{T\to\infty} \frac{1}{T}\int_{-T/2}^{T/2} x^2(t)\,dt = \lim_{T\to\infty} \sum_{m=-\infty}^{\infty} (T|C_m|^2) \cdot \frac{1}{T}$$

$$= \int_{-\infty}^{\infty} \Gamma(f)\,df$$

where $\Gamma(f) = \lim_{T\to\infty} T|\mathcal{X}_m|^2$ is the Fourier power spectrum of infinite time series $x(t)$.

From (2),

$$T|\mathcal{X}_m|^2 = C_{xx}(f) = \frac{1}{T}\left|\int_{-T/2}^{T/2} x(t)\, e^{-i2\pi ft}\, dt\right|^2 \qquad \ldots (3)$$

where $C_{xx}(f)$, defined for a continuous range of frequencies $-\infty \leq f \leq \infty$, is termed the 'sample spectrum'.

Using the definition of $c_{xx}(u)$ and equation (3),

$$C_{xx}(f) = \frac{1}{T}\int_{-T/2}^{T/2} x(t)e^{-i2\pi ft}\, dt \;.\; \int_{-T/2}^{T/2} x(t')e^{+i2\pi ft'}\, dt'$$

from 2.2(I).

Transforming with $u = t - t'$, $v = t'$ yields

$$C_{xx}(f) = \int_0^T \left[\frac{1}{T}\int_{-T/2}^{T/2-u} x(v)x(v+u)dv\right] e^{-i2\pi fu}\, du$$

$$+ \int_0^T \left[\frac{1}{T}\int_{-T/2-u}^{T/2} x(v)x(v+u)dv\right] e^{-i2\pi fu}\, du$$

Substituting for $c_{xx}(u)$,

$$C_{xx}(f) = \int_{-T}^{T} c_{xx}(u)e^{-i2\pi fu}\, du \qquad -\infty \leq f \leq \infty$$

and

$$c_{xx}(u) = \int_{-\infty}^{\infty} C_{xx}(f)e^{i2\pi fu}\, df \qquad -T \leq u \leq T$$

Now sample spectrum $C_{xx}(f)$ is a realization of random variable $C_{XX}(f)$;

$$E[\,C_{XX}(f)\,] = \int_{-T}^{T} E[\,c_{XX}(u)\,]e^{-i2\pi fu}\, du \;.$$

$$E[\, c_{XX}(u)\,] = E\left[\frac{1}{T}\int_0^{T-|u|} X(t)X(t+u)dt\right]$$

$$= \frac{1}{T}\int_0^{T-|u|} \gamma_{XX}(u)dt$$

$$= \begin{cases} \gamma_{XX}(u)\left(1 - \dfrac{|u|}{T}\right) & 0 \leqslant |u| \leqslant T \\ 0 & |u| > T \end{cases}$$

Hence

$$E[\, C_{XX}(f)\,] = \int_{-T}^{T} \gamma_{XX}(u)\left(1 - \frac{|u|}{T}\right)e^{-i2\pi fu}\, du$$

So

$$\Gamma_{XX}(f) = \lim_{T\to\infty} E[C_{XX}(f)] = \int_{-T}^{T} \gamma_{XX}(u)\, e^{-i2\pi fu}\, du \qquad \ldots (4)$$

and the mean of the sample spectrum estimator, $E[C_{XX}(f)]$, is seen to be the Fourier transform of the product of $\gamma_{XX}(u)$ and the 'window function' $w(u)$;

$$w(u) = \begin{cases} 1 - |u|/T & |u| \leqslant T \\ 0 & |u| > T \end{cases}$$

Hence

$$E[C_{XX}(f)] = \int_{-\infty}^{\infty} T\left(\frac{\sin \pi Tg}{\pi Tg}\right)^2 \cdot \Gamma_{XX}(f-g)\, dg \quad .$$

A5.3 Spectral Windows

Although $\lim_{T\to\infty} E[C_{XX}(f)] = \Gamma_{XX}(f)$, with finite record length, $C_{XX}(f)$ will have a bias

$$B(f) = E[C_{XX}(f)] - \Gamma_{XX}(f) \quad .$$

Dividing the finite time series into k sub-series each of length M yields estimates

$$C_{XX}^{(j)}(f) = \int_{-M}^{M} c_{XX}^{(j)}(u) e^{-i2\pi fu}\, du \qquad j = 1,2, \ldots k \ .$$

Thus the smoothed estimator

$$\bar{C}_{XX}(f) = \frac{1}{k} \sum_{j=1}^{k} C_{XX}^{(j)}(f) = \frac{1}{k} \sum_{j=1}^{k} \int_{-M}^{M} c_{XX}^{(j)}(u)\, e^{-i2\pi fu}\, du \ .$$

Setting

$$\bar{c}_{XX}(u) = \frac{1}{k} \sum_{j=1}^{k} c_{XX}^{(j)}(u)$$

$$= \frac{1}{k} \sum_{j=1}^{k} \left(\frac{1}{M} \int_{(j-1)M}^{jM-u} X(t)\, X(t+u)\, dt \right) \qquad u \geq 0$$

yields the result for $\bar{C}_{XX}(f)$:

$$\text{Smoothed estimator } \bar{C}_{XX}(f) = \int_{-M}^{M} \bar{c}_{XX}(u) e^{-i2\pi fu}\, du$$

Now

$$E\left[\bar{c}_{XX}(u) \right] = \gamma_{XX}(u) \left(1 - \frac{|u|}{M} \right)$$

and

$$E\left[\bar{C}_{XX}(f) \right] = \int_{-M}^{M} \left(1 - \frac{|u|}{M} \right) \gamma_{XX}(u) e^{-i2\pi fu}\, du$$

$$= \int_{-\infty}^{\infty} \Gamma_{XX}(f-g) \cdot M \left(\frac{\sin \pi gM}{\pi gM} \right)^2 dg \ .$$

i.e. the sample spectrum is smoothed by window

$$w(g) = M \left(\frac{\sin \pi gM}{\pi gM} \right)^2 \ .$$

A5.4 Variance and Bias

The bias of a time series will be given by

$$B(f) = E\left[\int_{-\infty}^{\infty} w(u)\, c_{XX}(u)\, e^{-i2\pi fu}\, du\right] - \int_{-\infty}^{\infty} \gamma_{XX}(u)\, e^{-i2\pi fu}\, du$$

$$\approx \int_{-\infty}^{\infty} (w(u)-1)\, \gamma_{XX}(u) e^{-i2\pi fu}\, du \,.$$

a) For Bartlett window, $w_B(u) = \begin{cases} 1 - \frac{|u|}{M} & |u| \le M \\ 0 & |u| > M \end{cases}$

$$\therefore B_B(f) \approx \frac{1}{M} \int_{-\infty}^{\infty} - |u|\, \gamma_{XX}(u) e^{-i2\pi fu}\, du$$

b) For Tukey window, $w_T(u) = \begin{cases} \frac{1}{2}\left(1 + \cos \frac{\pi u}{M}\right) & |u| < M \\ 0 & |u| > M \end{cases}$

$$B_T(f) \approx \frac{1}{2} \int_{-\infty}^{\infty} \left(\cos \frac{\pi u}{M} - 1\right) \gamma_{XX}(u) e^{-i2\pi fu}\, du$$

$$\approx \frac{\pi^2}{4M^2} \int_{-\infty}^{\infty} - u^2\, \gamma_{XX}(u) e^{-i2\pi fu}\, du + 0\left(\frac{1}{M^4}\right)$$

$$\text{Now } \Gamma_{XX}(f) = \int_{-\infty}^{\infty} \gamma_{XX}(u) e^{-i2\pi fu}\, du$$

$$\Gamma'_{XX}(f) = \frac{d}{df} \int_{-\infty}^{\infty} \gamma_{XX}(u) e^{-i2\pi fu}\, du$$

$$= \int_{-\infty}^{\infty} - i2\pi u \,.\, \gamma_{XX}(u) e^{-i2\pi fu}\, du$$

$$\Gamma''_{XX}(f) = \int_{-\infty}^{\infty} - 4\pi^2 u^2 \gamma_{XX}(u) e^{-i2\pi fu}\, du$$

$$\text{Thus } B_T(f) \approx \frac{\pi^2}{4M^2} \cdot \frac{1}{4\pi^2} \cdot \Gamma''_{XX}(f) + O\left(\frac{1}{M^4}\right)$$

$$= \frac{.0625}{M^2} \Gamma''_{XX}(f) + O\left(\frac{1}{M^4}\right)$$

c) For the Parzen window

$$B_p(f) \approx \frac{6}{M^2} \int_{-\infty}^{\infty} - u^2 \gamma_{XX}(u)\, e^{-i2\pi fu}\, du$$

$$= \frac{6}{4\pi^2 M^2} \cdot \Gamma_{XX}(f) + O\left(\frac{1}{M^3}\right)$$

$$= \frac{.152}{M^2} \cdot \Gamma_{XX}(f) + O\left(\frac{1}{M^3}\right)$$

$$\text{Now Var } (\bar{C}_{XX}(f)) \approx \frac{\Gamma^2_{XX}(f)}{T} \cdot \int_{-\infty}^{\infty} W^2(g)\, dg \qquad \text{(Box \& Jenkins, 1978)}$$

$$= \frac{\Gamma^2_{XX}(f)}{T} \cdot \int_{-\infty}^{\infty} w^2(u)\, du$$

$$= \Gamma^2_{XX}(f) \cdot \frac{I}{T}$$

For the Bartlett window,

$$I_B = \int_{-\infty}^{\infty} \left(1 - \frac{|u|}{M}\right)^2 du$$

$$= 2 \int_0^M \left(1 - \frac{2|u|}{M} + \frac{u^2}{M^2}\right) du = \frac{2}{3} M \quad .$$

For the Tukey window,

$$I_T = \int_{-M}^{M} \frac{1}{4}\left(1 + \cos\frac{\pi u}{M}\right)^2 du$$

$$= \frac{3}{4} M$$

For the Parzen window,

$$I_p = \int_{-\infty}^{\infty} w_p^{\,2}(u)\, du$$

$$= 2\int_0^{M/2} \left(1 - 6\frac{u^2}{M^2} + 6\frac{u^3}{M^3}\right)^2 du + 8\int_{M/2}^{M} \left(1 - \frac{u}{M}\right)^6 du$$

$$= 0.53\ M \quad .$$

The width of a spectral window is defined from the bandpass spectral window

$$w(f) = \frac{1}{h} \quad -\frac{h}{2} \leq f \leq \frac{h}{2}$$

and the variance of the corresponding smoothed spectral estimator is

$$\mathrm{Var}[C_{XX}(f)] \approx \frac{\Gamma_{XX}^2(f)}{T.b}$$

where bandwidth b is simply defined by $b = \frac{1}{I}$.

REFERENCES

AGTERBER, F.P.(1969). Stochastic model for deposition of varves in glacial lake Barlow.
Can. J. Earth. 6, 625-629.

ALLEN, C.W.(1955).(Ed.) 'Astrophysical Quantities'.
Athlone Press, University of London.

AMBROZ, P.(1971). Planetary influences on the large-scale distribution of solar activity.
Solar Phys. 19, 480-482.

ANCIENT SUNSPOT RECORDS RESEARCH GROUP (1976). An arrangement of records of sunspots in our past generations and an investigation of their active periods.
Acta. Astron. Sinica. 17, 217-227.

ANDERSON, C.N.(1954). Notes on the sunspot cycle.
J. Geoph. Res. 59, 455-457.

ANDERSON, T.W.(1971). 'The Statistical Analysis of Time Series'.
Wiley, New York.

BABCOCK, H.W.(1961). The topology of the sun's magnetic field and the 22 year cycle.
Astrophys. J. 133, 572-587.

BABCOCK, H.W. and BABCOCK, H.D.(1955). The sun's magnetic field and corpuscular emission.
Nature. 175, 296-298.

van BALLIGOOIJEN, A.A.(1982). The structure of the solar magnetic field below the photosphere.
Astron. Astr. 113, 99-112.

BARTLETT, M.S.(1946). On the theoretical specification and sampling properties of autocorrelated time series.
J. Roy. Sta. B. 8, 27-41.

BARTLETT, M.S.(1966). 'An Introduction to Stochastic Processes'.
University Press, Cambridge.

BERDICHEVSKAYA, V.S.(1976). Some long-period properties of solar activity.
Sov. Astron. 20, No.4.

BIGG, E.K.(1967). Influence of the planet Mercury on sunspots.
Astrophys. J. 72, 463-466.

BLACKMAN, R.B. and TUKEY, J.W.(1959). 'The Measurement of Power Spectra from the Point of View of Communications Engineering'.
Dover, New York.

BLIZARD, J.B.(1968). Solar activity and planetary positions.
B. Am. Phys. S. 13, 908.

BOGART, R.S.(1982). Recurrence of solar activity: evidence for active longitudes.
Solar. Phys. 76, 115-165.

BOHLIN, J.D.(1977). Extreme ultraviolet observations of coronal holes I.
Solar Phys. 51, 377-384.

BONOV, A.D.(1973). Characteristic features of secular and supersecular cycles of solar activity. A 180 year cycle.
Proc. First European Astron. Meeting, Athens, 83-86.

BOX, E.P. and JENKINS, G.M.(1978). 'Time Series Analysis, Forecasting and Control'.
Holden Day, San Francisco.

BRACEWELL, R.(1965). 'The Fourier Transform and its Applications'.
McGraw - Hill, New York.

BRAY, J.R.(1980). A sunspot auroral solar index from 522 BC to AD 1968.
N.Z. J. Sci. 23, 99-106.

BROOKES, J.R., ISAAK, G.R. and van der RAAY, H.B.(1976). Observation of free oscillations of the sun.
Nature. 259, 92-95.

BROUSSARD, S.M., SHEELEY, N.R., TOUSEY, N.R. and UNDERWOOD, J.H.(1978). Survey of coronal holes and their solar wind associations throughout sunspot cycle 20.
Solar Phys. 56, 161-183.

BROUWER, D. and CLEMENCE, G.M.(1961). 'Methods of Celestial Mechanics'.
Academic Press, London.

BROWN, E.W.(1900). A possible explanation of the sunspot period.
M. Not. R. Ast. 60, 599-606.

BROWN, G.M.(1976). What determines sunspot maximum?
M. Not. R. Ast. 174, 185-189.

BURKI, G. and RUFENER, F.(1930). An instructive case of period determination of the eclipsing spectroscopic binary star HR 9049.
Astron Astr. S. 39, 121-123.

BUREAU, R.A. and CRAINE, L.B.(1970). Sunspots and planetary orbits.
Nature. 228, 984.

BUTCHER, J.C.(1964). Implicit Runge-Kutta processes.
Math. Comput. 18, 50-56.

CHAPMAN, G.A.(1975). Recent measurements of flux excess from solar faculae and implication for solar oblateness.
Phys. Rev. Lett. 34, 755-758.

CHRISTENSEN-DALSGAARD, J. and GOUGH, D.O.(1981). Comparison of observed solar whole-disc oscillation frequencies with the predictions of a sequence of solar models.
Astron. Astr. 104, 173-176.

CLAVERIE, A., ISAAK, G.R., McLEOD, C.P., van der RAAY, H.B. and ROCA-CORTES, T.(1979). Solar core rotation.
Nature. 299, 704-706.

COHEN,T.J. and LINTZ, P.(1974). Long term periodicities in the sunspot cycle.
Nature. 250, 398-399.

COLE, H.P.(1975). Investigation of a possible relationship between height of low-latitude tropopause and sunspot number.
J. Atmos. Sci. 32, 998-1001.

COLE, T.W.(1973). Periodicities in solar activity.
Solar Phys. 30, 103-110.

CONDON, J.J. and SCHMIDT, R.R.(1975). Planetary tides and sunspot cycles.
Solar Phys. 42, 529-532.

CRADDOCK, J.M.(1967). An experiment in the analysis and prediction of time series.
The Statistician. 17, 257-268.

de CSADA, I.K.(1981). On the non-symmetric solar dynamo.
Solar Phys. 74, 103-105.

CULLEN, C.(1980). Was there a Maunder minimum ?
Nature. 283, 427-428.

CURRIE, R.G.(1973). Fine structure in the sunspot spectrum - 2 to 70 years.
Astro. Sp. Sc. 20, 509-512.

DAUVILLIER, A.(1970). Sur les marées excercées par les planètes sur le soleil et la prévision de l'activité solaire.
Comptes Rendus. Acad. Sci. Paris, Ser. B. 270, 1119-1121.

DAUVILLIER, A.(1975). On the variation of planetary orbits and the solar activity period.
Bull. Soc. R. Liège. 44, 161-164.

DAUVILLIER, A.(1976). Maunder's paradox and the tidal theory of solar activity.
Bull. Soc. R. Liege. 45, 211-221.

DAUVILLIER, A.(1977). Physique solaire: interprétation mechanique de l'activité solaire.
Ciel. Terre. 93, 204-214.

DAUVILLIER, A.(1978). Au sujet de la théorie planètaire de l'activité solaire.
Ciel. Terre. 94, 372-377.

DEUBNER, F-L.(1981). Detection of low order p-modes in brightness fluctuations of the sun.
Nature. 290, 682-683.

DICKE, R.H.(1976A). Evidence for a solar distortion rotating with a period of 12.2 days.
Solar Phys. 47, 475-515.

DICKE, R.H.(1976B). New solar rotational period, solar oblateness, and solar faculae.
Phys. Rev. L. 37, 1240-1242.

DICKE, R.H.(1978). Is there a chronometer hidden deep in the sun ?
Nature. 276, 676-680.

DICKE, R.H.(1979). The clock inside the sun.
New Scientist. 83, 12-14.

DIMITROV, D.L.(1982). A new look on the solar activity.
Rise hvezd. 63, 89-92.

DING, You-Ji. and CHANG, Zu-Wen.(1978). Continuity of the eleven year cycle of solar activity.
Kexue Tongbau (China). 23, no. 2, 107-111.

DINGLE, R.A., van HOVEN, G. and STURROCK, P.A.(1973). Test for planetary influence on solar activity.
Solar Phys. 31, 243-246.

DODSON, H.W. and HEDEMAN, E.R.(1968). Comments on related flares.
I.A.U. Symposium 35. 56-59.

DURRANT, C.J. and SCHROTER, E.H.(1982). Solar global velocity oscillations and active region rotation.
Nature. 301, 589-591.

ECKERT, W.S., BROUWER, D. and CLEMENCE, G.M.(1953). Coordinates of the five outer planets 1653-2060.
A. P. Vol. XII, part III.

EDDY,J.A.(1977). The case of the missing sunspots.
Sci. Am. 236, 80-89.

EDDY, J.A.(1978).(Ed.) 'The New Solar Physics'.
Praeger, Westview Press, Boulder, Colorado.

EDDY, J.A., GILMAN, P.A. and TROTTER, D.E.(1976). Solar rotation during the Maunder minimum.
Solar Phys. 46, 3-14.

EDDY, J.A., GILMAN, P.A. and TROTTER, D.E.(1977). Anomalous solar rotation in the early 17th century.
Science. 198, 824-828.

EDMONDS, M.G. and GOUGH, D.O.(1983). Solar atmosphere temperature inhomogeneities induce a 13 day oscillation in full-disc Doppler measurements.
Nature. 302, 810-812.

EMERSON, B.(1981). Approximate coordinates of Jupiter and Saturn.
N. A. O. Tech. Note. no. 56.

ENDEL, A.S. and TWIGG, L.W.(1982). The effect of perturbation of convective energy transport on the luminosity and radius of the sun.
Astrophys. J. 260, 342-346.

EPSTEIN, S. and YAPP, C.J.(1976). Climatic implications of D-H ratio of hydrogen in C-H groups in tree cellulose.
Earth Plan. 30, 252-261.

FAIRBRIDGE, R.W. and HILLAIRE-MARCEL, C.(1977). An 8000 year paleoclimatic record of the 'double-Hale' 45 year cycle.
Nature. 268, 413-416.

FERNS, G.A.J.(1969). Planetary influences on sunspots.
J. Br. Astron. Assoc. 79, 385-388.

FRITTS, H.C.(1972). Tree rings and climate.
Sci. Am. 226, 92-98.

FRITTS, H.C.(1976). 'Tree Rings and Climate'.
Academic Press, London.

FRITZ, H.(1928). The periods of solar and terrestrial phenomena.
Monthly Weather Review. 56, 401-407.

GLEISSBERG, W.(1944). Predictions for the coming sunspot cycle.
Terr. Magn. Atmos. Elect. 48, 243-244.

GLEISSBERG, W.(1962). Investigation of three 80 year cycles of solar activity.
Z. Astrophys. 55, 153-160.

GLEISSBERG, W.(1973). The 80 year solar cycle and its use for solar activity forecasting.
J. Interdisc. Cycle. Res. 3, 391-394

GLEISSBERG, W. and DAMBOLT, T.(1979). Reflections on the Maunder minimum of sunspots.
J. British Astron. Assoc. 89, 440-449.

GOUGH, D.O.(1981). Problems with solar oscillations.
Nature. 293, 703-704.

GREC, G., FOSSAT, E. and POMERANTZ, M.(1980). Solar oscillations - full disc observations from the geographic South Pole.
Nature. 288, 541-544.

HANTZCHE, E.(1978). On the tidal theory of solar activity.
Astron. Nachr. Band. 299, 259-276.

HENKEL, R.(1972). Evidence for an ultralong cycle of solar activity.
Solar Phys. 25, 489-499.

HERRICK, S.(1972). 'Astrodynamics', Vol. II.
Van Nostrand Reinhold, London.

HIBLER, W.D.(1979). Twenty year cycle in Greenland ice-core records.
Nature. 280, 481-488.

HILL, H.A.(1978). Seismic sounding of the sun.
In 'The New Solar Physics' (Eddy, J.A., Ed.), 22-47. Praeger,
Westview Press, Boulder, Colorado.

HILL, H.A., ROSENWALD, R.D. and CAUDELL, T.P.(1978). Solar oscillations-
influence of sun's outer layers on their detection.
Astrophys. J. 225, 304-317.

HILL, J.R.(1977). Long term solar activity forecasting using high-
resolution time spectral analysis.
Nature. 266, 151-153.

HINDLEY, K.(1977). The long years of the quiet sun.
New Scientist. 75, 468-470.

HOWARD, R. and LaBONTE, B.J.(1980). The sun is observed to be a torsional
oscillator with a period of 11 years.
Astrophys. J. 239, L33-L34.

HOWARD, R. and LaBONTE, B.J.(1982A). Torsional waves on the sun and the
activity cycle.
Solar Phys. 75, 161-178.

HOWARD, R. and LaBONTE, B.J.(1982B). Solar rotation measurements at Mt.
Wilson III: meridional flow and limbshift.
Solar Phys. 80, 361-372.

HOWARD, R. and LaBONTE, B.J.(1982C). Are the high latitude torsional
oscillations of the sun real ?
Solar Phys. 80, 373-378.

HUNDHAUSEN, A.J.(1977). A study of coronal holes.
In 'Coronal Holes and High Speed Wind Streams' (Zirker, J.B., Ed.),
225-261. Colorado Univ. Press, Boulder, Colorado.

ISAAK, J.(1982). Is the sun an oblique magnetic rotator ?
Nature. 296, 13-15

IZENMAN, A.J. (1983). J.R. Wolf and H.A. Wolfer: an historical note on
the Zurich relative sunspot number.
J. Roy. Sta. A. 146, 311-318.

JACKSON, J.(1924). Note on numerical integration of $d^2x/dt^2=f(x,t)$
M. Not. R. Ast. 84, 602-608.

JENKINS, G.M. and WATTS, D.G.(1978). 'Spectral Analysis and its applications'.
Holden-Day, New York.

JOHNSON, L.W.(1982). 'Numerical Analysis'.
Addison-Wesley, U.S.A.

JOSE, P.D.(1965). Sun's motion and sunspots.
Astrophys. J. 70, 193.

KANDA, S.(1933). Ancient records of sunspots and aurorae in the Far East and the variation of the period of solar activity.
Proc. Imp. Acad. Tokyo. 9, 293-296.

KEIMATSU, M.(1976). A sunspot and auroral record from 687 BC.
Annals of Science, Kanazawa University. 13,1-32.

KOPECKY, M.(1978). La periode de 80 ans de taches solaires.
Astronomie. 92, 369-371.

KOPECKY, M.(1980). What will the level of solar activity be in future decades ?
Bull. Astron. Inst. Czeckoslovakia. 31,1-6.

KOPECKY, M., KUKLIN, G.V. and RUZICKOVA-TOPOLOVA, R.(1980). On the relative inhomogeneity of long-term series of sunspot indices.
Bull. Astron. Inst. Czeckoslovakia. 31, 267-283.

KOZHEVNIKOV, N.I.(1976A). On the influence of planets on solar activity.I.
Astron. Tsirk. 915, 2-3.

KOZHEVNIKOV, N.I.(1976B). On the influence of planets on solar activity.II.
Astron. Tsirk. 915, 5-7.

KOZHEVNIKOV, N.I.(1976C). On the influence of planets on solar activity.III.
Astron. Tsirk. 919, 5-6.

KRYMSKY, G.F., PETIKHOV, S.I. and NIKOLAEV, N.S.(1978). Search for the tidal effects of planets on some features of solar activity.
Byull NTI. Yakutsk. fil. Sib. otd. AN SSSR. Apr. 7-9.

LARSON, M.F. and KELLY, M.C.(1978). Available potential energy in the middle atmosphere as it relates to the sun-weather effect.
In 'Solar-Terrestrial Influences on Weather and Climate' (McCormack, B.M. and Seliga, T.A., Eds.),125-134. Reidel, Dordrecht, Holland.

LEGRAND, J.P. and SIMON, P.A.(1981). Ten cycles of solar and geomagnetic activity.
Solar Phys. 70, 173-195.

LEIGHTON, R.B.(1969). A magneto-kinematic model of the solar cycle.
Astrophys. J. 156, 1-9.

LINK, F.(1962). Early solar cycles.
Prace Geofysikalniho Ustavo Ceskoslovenske Akademie Ved, Geofysikalni Sbornik. 173, 297-387.

LINK, F.(1964). Manifestations of solar activity in the historical past.
Planet. Space Sci. 12, No. 5, 333-348.

LINK, F.(1977A). Solar activity during the 17th century.
Astron. Astr. 54, 859-861.

LINK, F.(1977B). Historical evidence of solar activity.
Astronomie. 91, 857-858.

LINK, F.(1978). Solar cycles between 1540 and 1700.
Solar Phys. 59, 175.

LO, Pao-Yung. and LI, Wei-Pao.(1978). To investigate the stability of the sunspot period by means of the periodic analysis of the aurorae and earthquake records in ancient China.
Kexue Tongbau. (China). 23, no.6, 362-366.

LOMB, N.R. and ANDERSON, A.P.(1980). The analysis and forecasting of the Wolf sunspot numbers.
M. Not. R. Ast. 190, 723-732.

LUST, R.(1965).(Ed.) 'Stellar and Solar Magnetic Fields'.
Max-Planck-Institut für Physik und Astrophysik, München, Germany.

MAUNDER, A.S.D.(1907). Terrestrial influence on sunspots during 1889-1901.
M. Not. R. Ast. 67, 451-476.

MAYAUD, P.N.(1977). On the reliability of the Wolf number series for estimating long-term periodicities.
J. Geoph. Res. 82, 1271-1272.

McNISH, A.G. and LINCOLN, J.V.(1949). Prediction of sunspot numbers.
Trans. Am. Geophys. Union. 30, no.5, 673-685.

MEEUS, J.(1978). Planetes et activité solaire.
Ciel. Terre. 94, 19-27.

MEISEL, D.D.(1978). Fourier-transforms of data sampled at unequal observational intervals.
Astronom. J. 83, 538-545.

MERSON, R.H.(1972). 'An Improved Fourth Order Runge-Kutta Process for Starting Near Circular Orbits'.
M. O. D. Tech. Report. 72118.

MERSON, R.H.(1975). 'Numerical Integration of the Differential Equations of Celestial Mechanics'.
M. O. D. Tech. Report. 74184.

MEYER, F., SCHMIDT, H.U., WEISS, N.O. and WILSON, P.R.(1974). The growth and decay of sunspots.
M. Not. R. Ast. 169, 35-54.

de MEYER, F. G. (1981). Mathematical modelling of the sunspot cycle.
Solar Phys. 70, 259-272.

MITCHELL, J.M., STOCKTON, C.W. and MEKO, D.M.(1978). Evidence of a 22 year rhythm of drought in the western Unites States related to the Hale cycle since the 17th century.
In 'Solar-Terrestrial Influences on Weather and Climate'(McCormack, B.M. and Seliga, T.A., Eds.), 125-143. Reidel, Dordrecht, Holland.

MOCK, S.J.(1976). Twenty year oscillation in eastern North-American temperature records.
Nature. 261, 484-486.

MORRIS, M.J.(1977). Forecasting the sunspot cycle.
J. Roy. Sta. A. 140, 437-468

MORTH, H.T. and SCHLAMMINGER, L.(1978). Planetary motion, sunspots and climate.
In 'Solar-Terrestrial Influences on Weather and Climate' (McCormack, B.M. and Seliga, T.A., Eds.), 193-199. Reidel, Dordrecht, Holland.

NYBORG, B. and MALTBY, P.(1983). Has rapid solar core rotation been observed ?
Nature. 302, 808-810.

OESTERWINTER, C. and COHEN, C.J.(1972). New orbital elements for moon and planets.
Celest. Mech. 5, 261-281.

OKAL, E. and ANDERSON, D.L.(1975). On the planetary theory of sunspots.
Nature. 253, 511-513.

OVENDEN, M.W.(1972). Bode's law and the missing planet.
Nature. 239, 508-509

PARKER, E.N.(1976). Basic mechanisms of solar activity.
In 'Proceedings of IAU Symposium 71' (Bumba, V. and Kleczek, J., Eds.), 3-13. Reidel, Dordrecht, Holland.

PARKER, E.N.(1979). 'Cosmical Magnetic Fields' .
Clarendon Press, Oxford.

PARZEN, E.(1961). Mathematical considerations in the estimation of spectra.
Technometrics.3, 167-178.

PERCY, J.R.(1977). Application of maximum entropy spectral analysis to study of short-period variable stars.
M. Not. R. Ast. 181 , 647-656.

PETROVA, N.S., SHPITAL'NAYA, A.A. and VASIL'EVA, G. Ya.(1979). A comparison between the time-spatial position of the centre of mass of the solar system and the solar activity.
Soln. Dannye. Byull. no. 12, 89-94.

PIDDINGTON, J.H.(1971). Theory of the solar 22-year cycle.
Proc. Astron. Soc. Australia. 2, 7-10.

PIDDINGTON, J.H.(1982). Dynamo action in cosmic bodies.
Astro. Sp. Sc. 87, 89-104.

PITTOCK, A.B.(1978). Solar cycles and the weather - successful experiments in autosuggestion ?
In ' Solar-Terrestrial Influences on Weather and Climate' (McCormack, B.M. and Seliga, T.A., Eds.), 181-192. Reidel Dordrecht, Holland.

POCOCK, R.J.(1918). Relative numbers and areas of sunspots east and west of the central meridian, 1902-1907.
M. Not. R. Ast. 79, 54-58.

PONMAN, T.(1981). The analysis of periodicities in irregularly sampled data.
M. Not. R. Ast. 196, 583-591.

PONMAN, T.(1982A). Evidence for periodicity in GX349+2 and GX17+2.
M. Not. R. Ast. 200, 351-358.

PONMAN, T.(1982B). A survey of the bright galactic bulge X-ray sources.
M. Not. R. Ast. 201, 769-778.

POVINETS, P.(1977). Investigation of solar activity in the past by means of cosmogenic isotopes.
IZV. AN. SSSR. Ser. fiz. 41,383-389.

PROKUDINA, V.S.(1978). Some dynamical parameters of the motion of planets and the solar activity cycle.
Soobshch. Gos. Astron. Inst. Shternberga. 196, 44-52.

ROBERTS, W.O.(1978). Review of solar-terrestrial weather and climate relationships.
In 'Solar-Terrestrial Influences on Weather and Climate'(McCormack, B.M. and Seliga, T.A., Eds.),29-34. Reidel, Dordrecht, Holland.

ROMANCHUK, I.(1981). Origin of solar activity cycle recurrence.
Astronom. Zh. 58, 158-173.

ROMANCHUK, P.R.(1975A). On the question of the n-s asymmetry of solar activity.
Astron. Obs. Kiev. Preprint no. 8, 11pp.

ROMANCHUK, P.R.(1975B). The nature of solar cycles.
Astron. Obs. Kiev. Preprint no. 10, 15pp.

ROMANCHUK, P.R.(1976). The nature of solar cyclicity. I.
Vestn. Kiev. Univ. no. 18, ser. Astron.,3-10.

ROMANCHUK, P.R.(1977). The nature of solar cyclicity. II.
Vestn. Kiev. Univ. no. 19, ser. Astron., 3-14.

de la ROSA, G.(1981). Sunspot populations and their relation with the solar cycle.
Solar Phys. 74, 117-123.

SCHAERF, M.C.(1964). Estimation of the covariance and auroregressive structure of a stationary time series.
Tech. Rept., Dept. of Statistics, Stanford University, Stanford.

SCHERRER, P.H., WILSON, J.M., CHRISTENSEN-DALSGAARD, J. and GOUGH, D.O. (1982). Observations of additional low-degree 5-minute modes of solar oscillation.
Nature. 297, 312-313.

SCHOVE, D.J.(1955). The sunspot cycle 649 BC to AD 2000.
J. Geoph. Res. 60, 127-146.

SCHOVE, D.J.(1962). Auroral numbers since 500 BC.
J. Br. Astron. Assoc. 72, 30-35.

SCHRODER, W.(1979). Auroral frequency in the 17th and 18th centuries. and the Maunder minimum.
J. Atm. Terr. P. 41, 445-446.

SCHUBART, J. and STUMPFF, P.(1966). On an n-body program of high accuracy for the computation of ephemerides of minor planets and comets.
Veroffentlichungen des Astronomischen Rechen-Instituts, Heidelberg, nr. 18.

SCHUSSLER, M.(1977). Sunspot dynamics: gravitational draining.
Astron. Astr. 56, 439-442.

SCHUSSLER, M.(1981). The solar torsional oscillation and dynamo models of the solar cycle.
Astron. Astr. 94, L17-L18.

SCHUSTER, A.(1911). Planetary influence on sunspot formation.
Roy. Soc; Proc. Ser. A. 85, 309-323.

SCHWABE, H.(1844). Sonnen-beobachtungen in Jahre 1843.
Astronomische Nachrichten. 21, 233-236.

SEVERNY A.B., KOTOV, V.A. and TSAPP, T.T.(1976). Observations of solar pulsations.
Nature. 259, 37-89.

SEYDL, O.(1954).
Prace Geofisikalniho ustavu Ceskoslovenske. Academie Ved., Geofysikalni Sbornik 17, 159-189.

SIME, D.G. and RICKETT, B.J.(1978). Latitude and longitude structure of solar-wind speed from IPS observations: note.
J. Geo.R.-S.P. 83, 5757-5762.

SIMON, P.(1979). Polar coronal holes and solar cycles.
Solar Phys. 63, 399-410.

SLEEPER, H.P.(1972).'Planetary resonances, bi-stable oscillation modes and solar activity cycles.'
NASA Rept. CR-2035.

SLUTZ, R.J.(1970). 'Solar Activity Prediction'.
NASA Rept. H-54409A, NOAA.

SMITH, H.J. and SMITH, E.V.P.(1963). 'Solar Flares'.
Macmillan, New York.

SMYTHE, C.M. and EDDY, J.A.(1977). Planetary tides during the Maunder minimum.
Nature. 266, 434-435.

SONETT, C.P. and SUESS, H.E.(1984). Correlation of bristlecone pine tree widths with atmospheric ^{14}C variations; a climate-Sun relation.
Nature. 307,141-143.

STEWART, J.Q. and EGGLESTON, F.C.(1940). The mathematical characteristics of sunspot variations II.
Astrophys. J. 91, 72-82.

STIX, M.(1981). Theory of the solar cycle.
Solar Phys. 74, 79-101.

TRELLIS, M.M.(1966A). Marees solaires d'origine planetaire.
C. R. Acad. Sci. Paris. 262, 221-223.

TRELLIS, M.M.(1966B). Sur un relation possible entre l'aire des taches solaires et la position des planetes.
C. R. Acad. Sci. Paris. 262, 312-315.

TRELLIS, M.M.(1966C). Influence de la configuration du systeme solaire sur la naissance des centres d'activite.
C. R. Acad. Sci. Paris. 262, 376-378.

VASSILYEVA, G. Ya., KUZNETSOV, D.A. and SHPITAL'NAYA, A.A.(1971). On the nature of solar activity.
Solnechnye Danne. Byull. no. 8, 96-100.

VITINSKY, Yu. I.(1962). 'Solar Activity Forecasting'.
U.S. Dept. of Commerce, NASA TTF, 289.

VITINSKY, Yu. I.(1978). Comments on the so-called Maunder minimum.
Solar Phys. 57, 475-478.

VITINSKY, Yu. I.(1979). On relative inhomogeneities of various series of sunspot indices.
Soln. Dannye. Byull. no. 3, 96-101.

VITINSKY, Yu. I.(1982). On active longitudes of sunspot groups.
Soln. Dannye. Byull. no.2, 113-119.

WALDMEIER, M.(1961).'The Sunspot Activity in the Years 1610-1960'.
Technische Hoschule, Zurich.

WARD, F.(1965). The general circulation of the solar atmosphere and the maintenance of the equilibrium acceleration.
Astrophys. J. 141, 534-547.

WEISS, J.E. and WEISS, N.O.(1979). Andrew Marvell and the Maunder minimum.
Q. Jl. Roy. Ast.20, 115-118.

WHITE, O.R.(1977).(Ed.) 'The Solar Output and its Variation'.
Colorado Press, Boulder, Colorado.

WILLIS, D.M.(1976). Energetics of sun-weather relationships - magnetospheric processes.
J. Am. Terr. Phys. 38, 685-698.

WITTMANN, A.(1978). The sunspot cycle before the Maunder minimum.
Astron. Astr. 66, 93-97.

WOLF, R.(1868). Mittheilungen uber die Sonnenflecken.
Astron. Mitt. Zurich. 24, 110-116.

WOLF, R.(1883). Neue Untersuchungen uber die Periode der Sonnenflecken und ihre Bedeutung.
Astron. Mitt. Zurich.,73, 88-94.

WOLFF, C.L.(1976). Timing of solar cycles by rigid internal rotations.
Astrophys. J. 205, 612-621.

WOOD, K.D.(1972). Sunspots and planets.
Nature. 240, L91- 93.

WOOD, R.M.(1975). Comparison of sunspot periods with planetary synodic period resonances.
Nature. 255, 312-313.

WOOD, R.M. and WOOD, K.D.(1965). Solar motion and sunspot comparison.
Nature. 208, 129-131.

XANTHAKIS, J.(1965). 'Solar Physics'.
Wiley Interscience, New York.

XANTHAKIS, J.(1973). Comparison of Wolf number series with others.
In 'Solar Activity and Related Interplanetary and Terrestrial Phenomena'.(Xanthakis,J. Ed.),25-37. Springer, New York.

YULE, G. U.(1927). On the method of investigating periodicities in disturbed series, with special reference to Wolfer's sunspot series.
Phil. Trans. Roy. A., 226,267-298.